

Calhoun: The NPS Institutional Archive DSpace Repository

Theses and Dissertations

1. Thesis and Dissertation Collection, all items

1955

Design of strip transmission line systems and antennas.

Butler, John E.

Monterey, California: U.S. Naval Postgraduate School

<http://hdl.handle.net/10945/14049>

Downloaded from NPS Archive: Calhoun



<http://www.nps.edu/library>

Calhoun is the Naval Postgraduate School's public access digital repository for research materials and institutional publications created by the NPS community.

Calhoun is named for Professor of Mathematics Guy K. Calhoun, NPS's first appointed -- and published -- scholarly author.

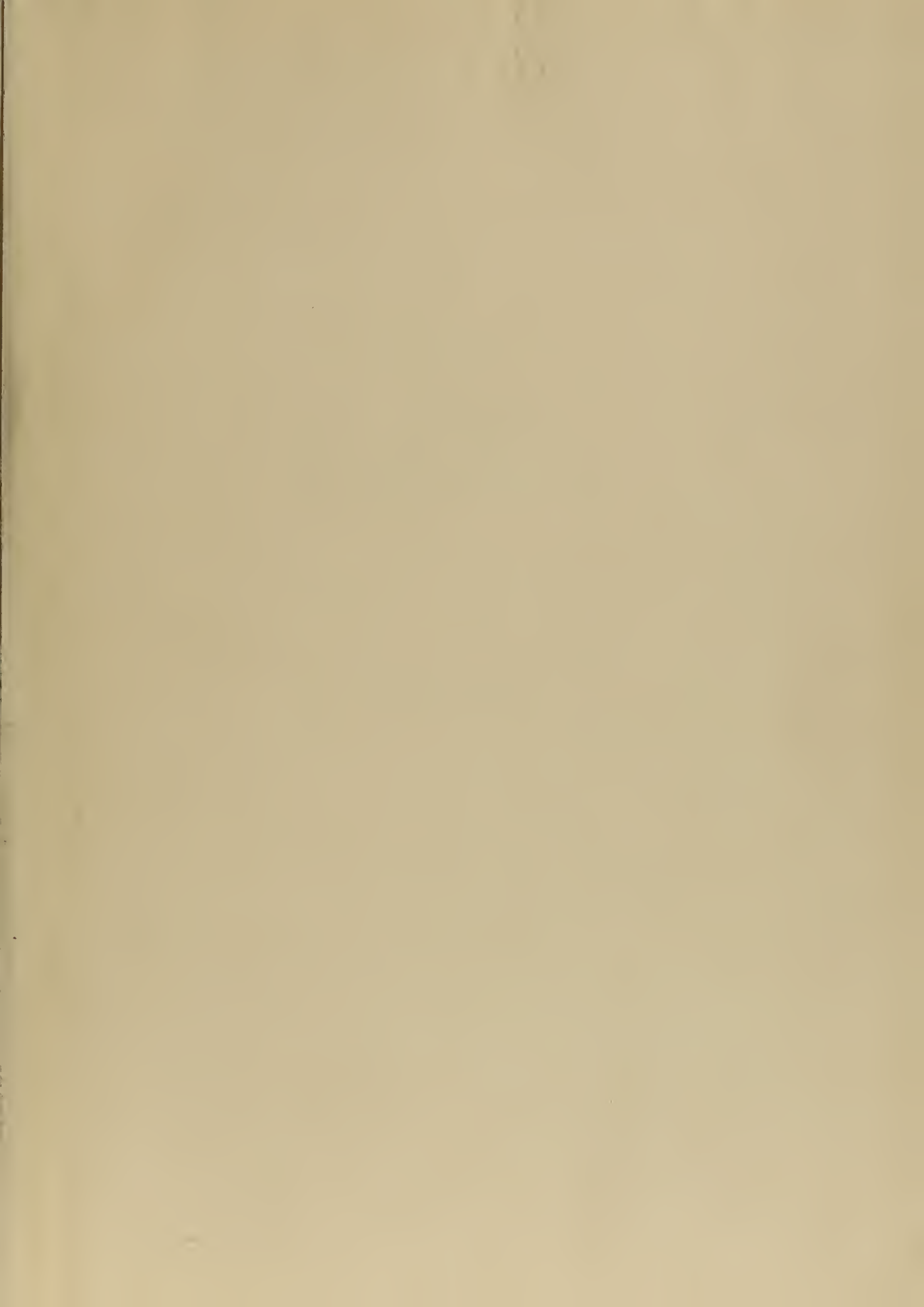
Dudley Knox Library / Naval Postgraduate School
411 Dyer Road / 1 University Circle
Monterey, California USA 93943

100-8011-AD

DESIGN OF STRIP TRANSMISSION
LINE SYSTEMS AND ANTENNAS

—
JOHN E. BUTLER

Library
U. S. Naval Postgraduate School
Monterey, California

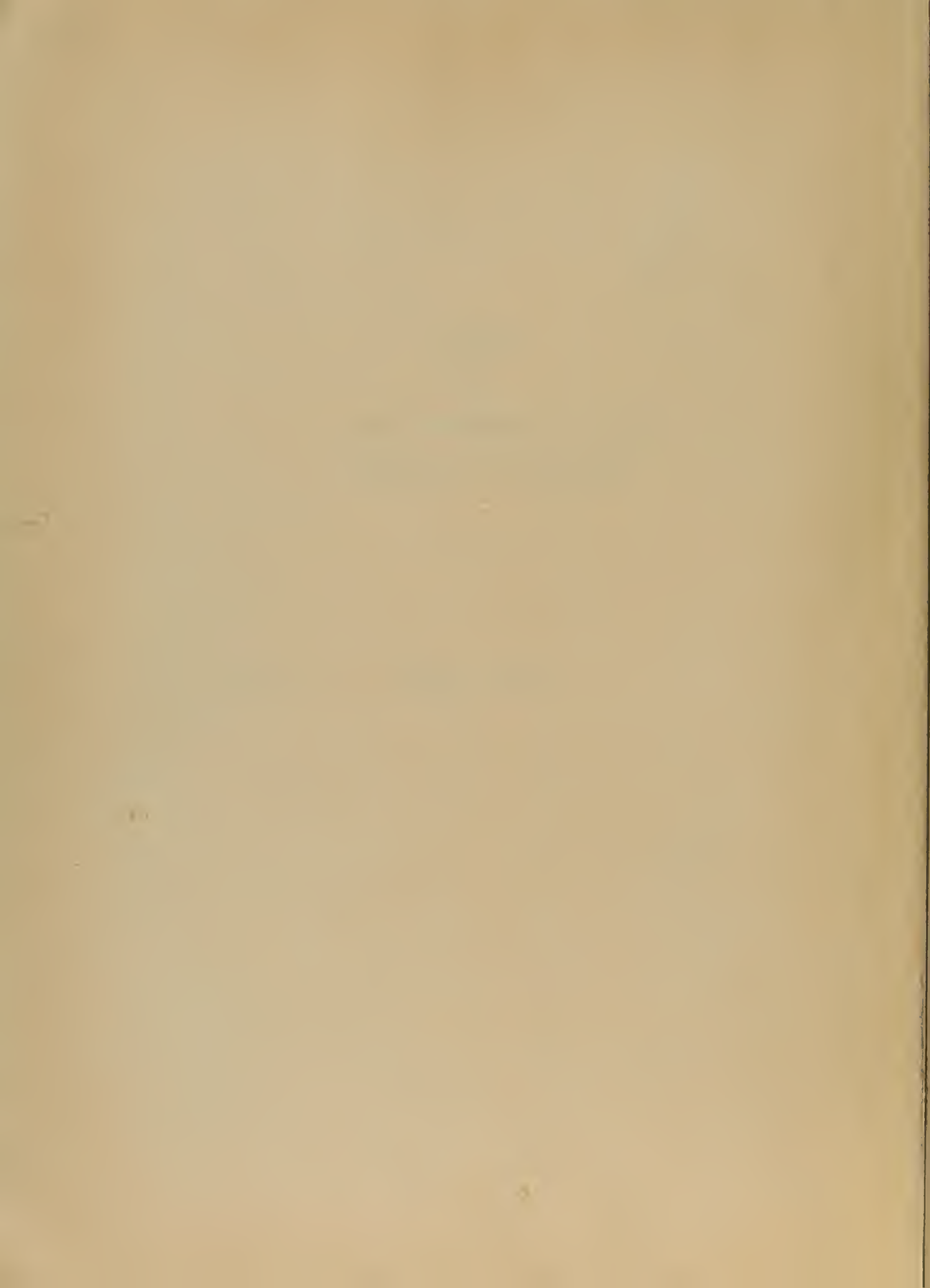




DESIGN
OF
STRIP TRANSMISSION LINE
SYSTEMS AND ANTENNAS

* * * *

John E. Butler



**DESIGN OF STRIP TRANSMISSION LINE
SYSTEMS AND ANTENNAS**

by

John Edward Butler

Lieutenant, United States Navy

Submitted in partial fulfillment
of the requirements
for the degree of
MASTER OF SCIENCE
IN
ENGINEERING ELECTRONICS

**United States Naval Postgraduate School
Monterey, California**

1955

Tesis
B 946

This work is accepted as fulfilling
the thesis requirements for the degree of

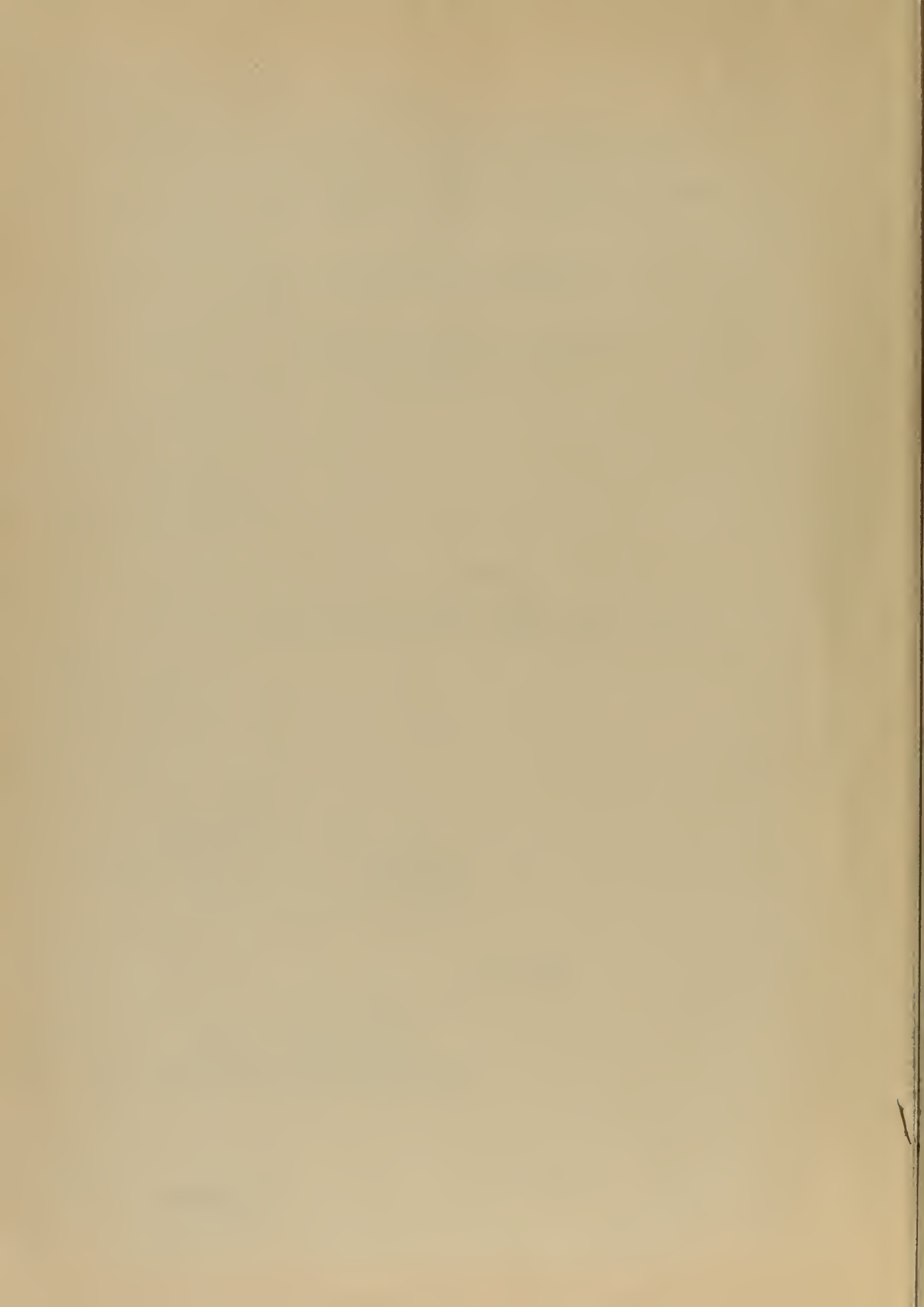
MASTER OF SCIENCE

IN

ENGINEERING ELECTRONICS

from the

United States Naval Postgraduate School



PREFACE

LITERATURE
AND POSTGRADUATE COURSES

This thesis is written in an effort to compile, for the first time, all the information that is available and necessary for the design and construction of strip transmission line systems. Data for this work has been accumulated through study and experimentation at the U. S. Naval Postgraduate School from 1953 to 1955, and while affiliated with the Airborne Instruments Laboratory as a junior engineer from 1 January to 15 March 1955.

The author is indebted to Dr. Eugene Fubini and Mr. Winfield Fromm whose foresight and perseverance have greatly advanced the state of the art; and to Messers Henry Keen, Warren Offutt, Robert Maleck, James McDonough and the others at the Airborne Instruments Laboratory who freely gave the author the benefit of their knowledge and wide practical experience in the field. He also wishes to thank Professors Donald A. Stentz and Jesse G. Chaney for reading the manuscript and for valuable discussions.

The photographs and many of the illustrations are presented through the courtesy of the Airborne Instruments Laboratory.

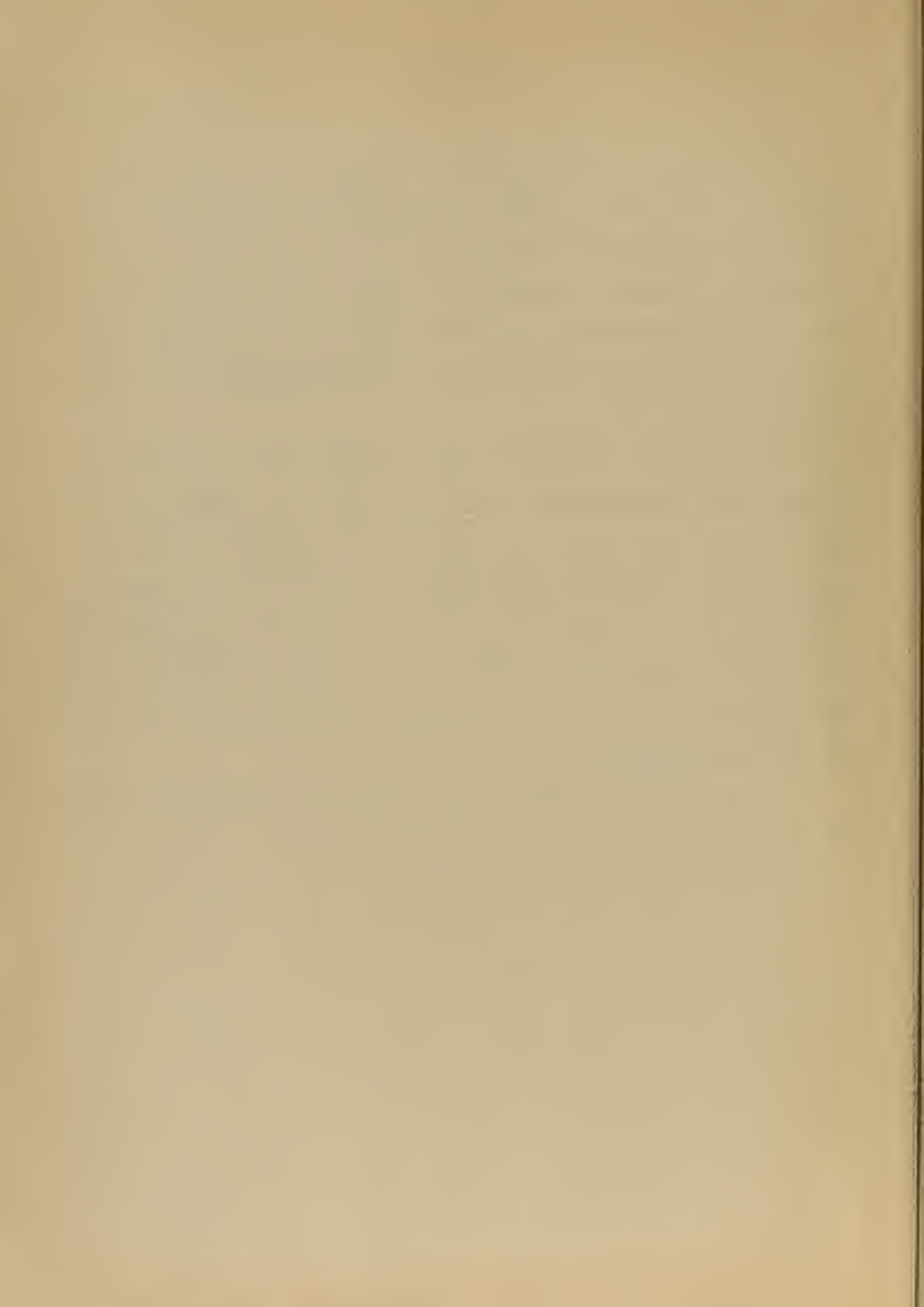
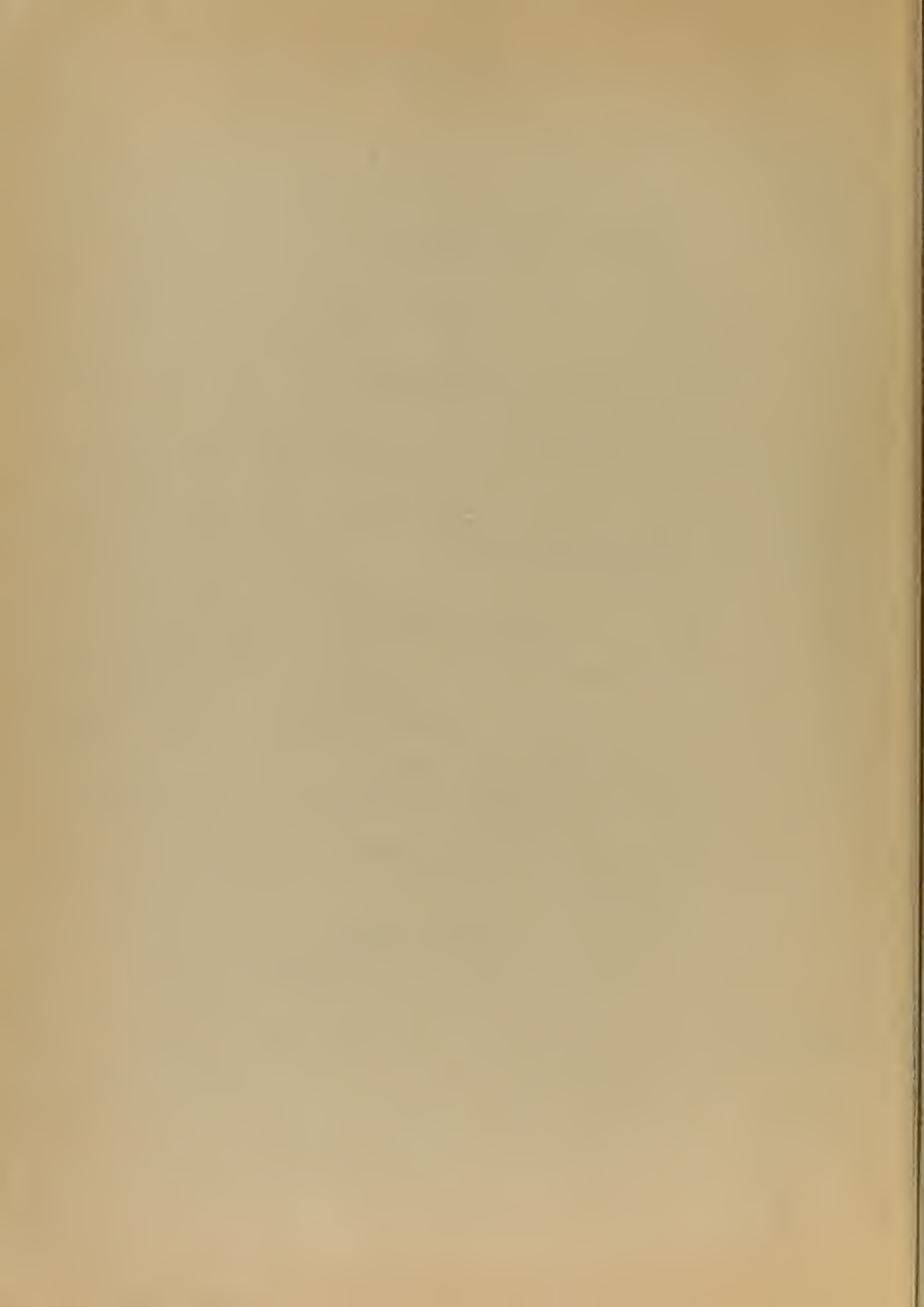
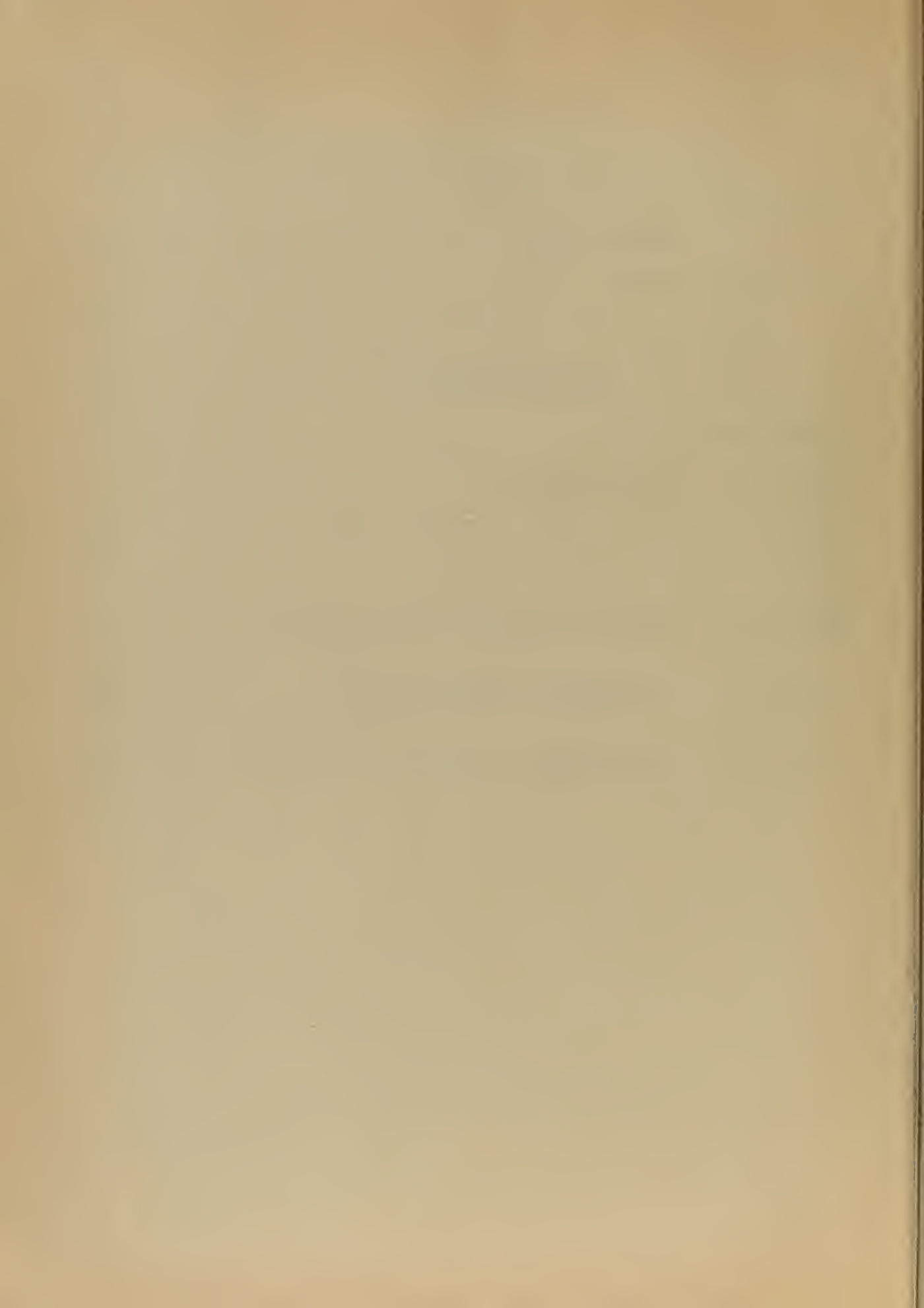


TABLE OF CONTENTS

Item	Title	Page
Chapter I	Introduction	1
Chapter II	General Strip Transmission Line Considerations	
	1. Types of Strip Transmission Lines	3
	2. Characteristic Impedance and Frequency Limitations	8
	3. Attenuation	17
	4. Velocity of Propagation	18
	5. Design and Construction	22
Chapter III	Design and Construction of Components	
	1. Transitions to Coaxial Line and Waveguide	26
	2. Matched Loads and Attenuation . . .	31
	3. Bends in the Center Conductor . . .	36
	4. Tees and Power Dividers	37
	5. Line Impedance Transformers . . .	39
	6. Stub and Capacitive Tuners	41
	7. Slotted Sections	43
	8. Low and High Pass Filters	49
	9. Band Pass Filters with Resonant Elements	58
Chapter IV	The Hybrid Junction	
	1. Introduction	77
	2. Characteristics of the Shunt	



Item	Title	Page
	Hybrid Junction	77
	3. Practical Applications for the Hybrid Junction	86
Chapter V	Strip Transmission Line Systems	89
Chapter VI	Printed Antennas	
	1. Basic Concepts	97
	2. Characteristics and Design of Printed Antennas	98
Bibliography	119
Appendix A	Layout and Construction of Center Conductors	
	1. The Photo etching Process	124
	2. The Hand Process	125
Appendix B	Polyiron Attenuation Characteristics and Detailed Curing Instructions	128
Appendix C	Tchebyscheff Design for Series of Quarterwave Transformers	130
Appendix D	The Behavior of the Hybrid Junction Over a Wide Frequency Range	135



LIST OF ILLUSTRATIONS

Figure		Page
1.	Strip Line	4
2.	Balanced Strip Transmission Line Field Configuration	4
3.	Sandwich Line	5
4.	Stripline	6
5.	Microstrip	7
6.	The Field Configuration of Unbalanced Strip Transmission Line	7
7.	Comparison of Calculated and Measured Strip Transmission Impedances	10
8.	Nomograph for Determination of Characteristic Impedance of Strip Transmission Lines	11
9.	Cut-off Wavelength of First Higher Mode in Stripline	13
10.	Calculated Maximum Frequency for Various Ground Plane Spacings	14
11.	Propagation Between Ground Planes	16
12.	Attenuation of Various Strip Transmission Lines as a Function of Characteristic Impedance	20
13.	Attenuation Change with Ground Plane Spacing	21
14.	Hand Scribing Center Conductor Configuration by Use of the Height Gauge	24
15.	Transition from Strip Transmission Line to Coaxial Line	26
16.	Waveguide to Strip Line Transition	28
17.	SWR Vs Frequency of Strip Line to Waveguide Transition	29

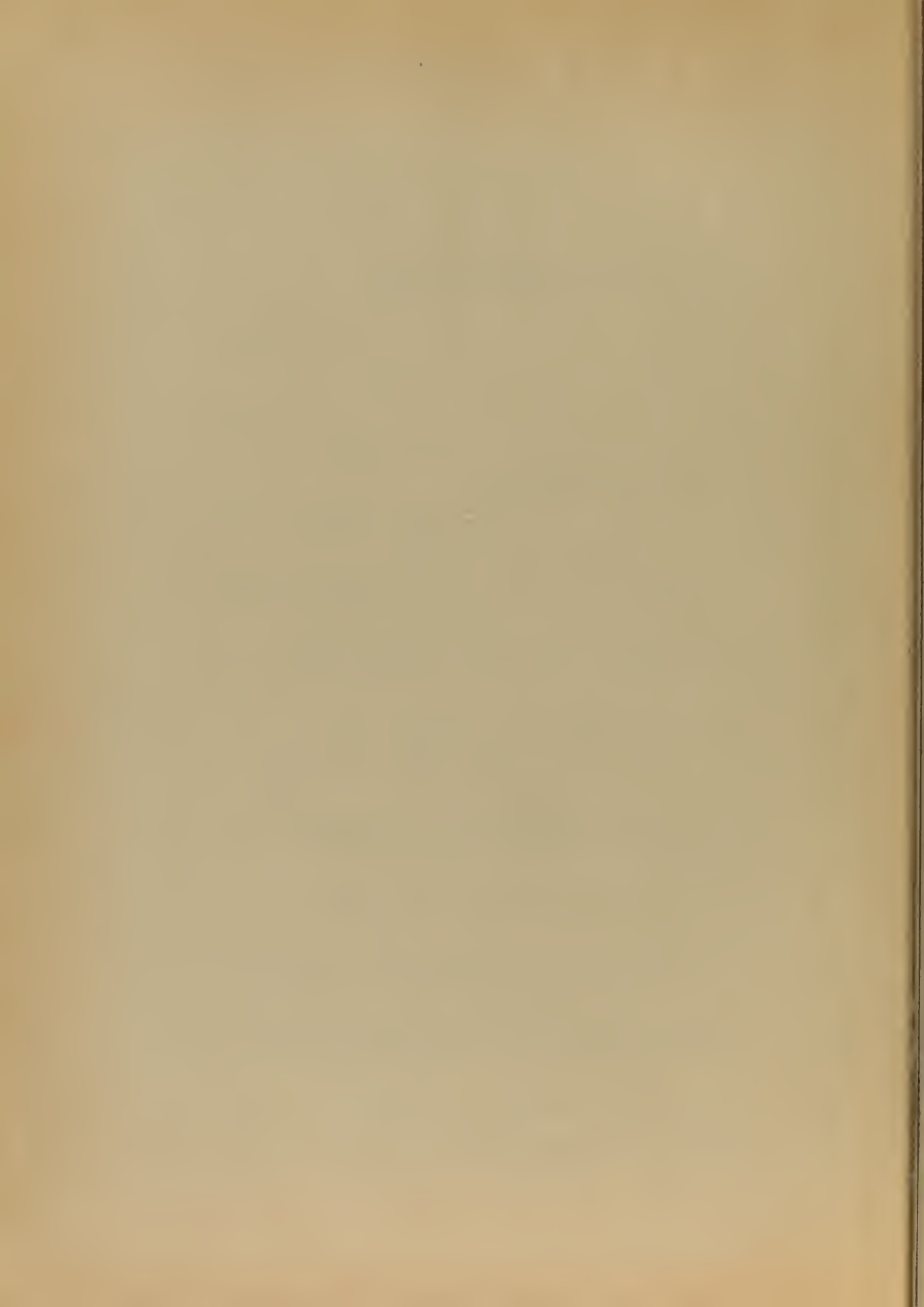
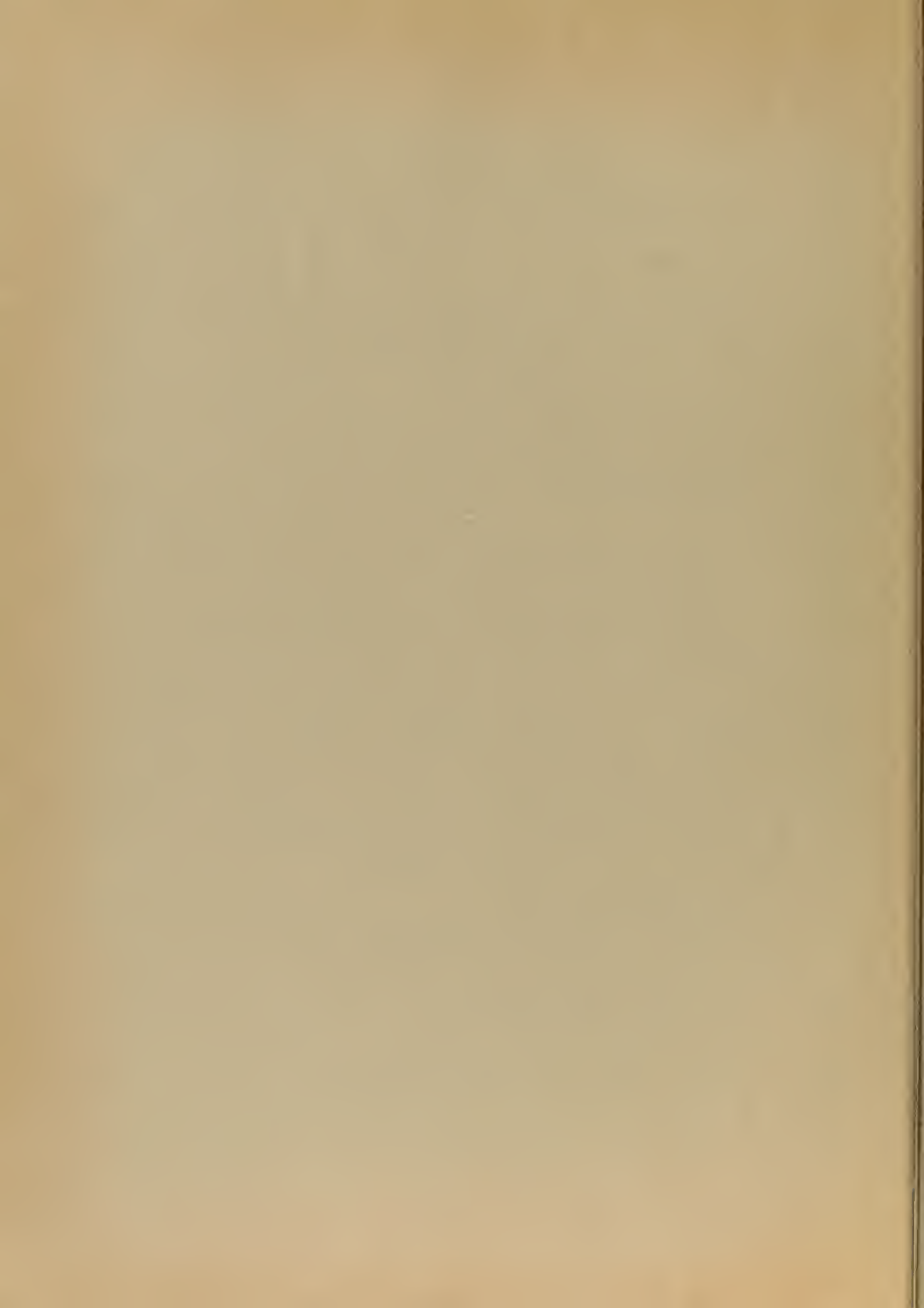


Figure		Page
18.	Coaxial to Strip Line Transition	32
19.	SWR of Coaxial to Strip Line Transition	33
20.	A Polyiron Load	34
21.	A Compensated Tee Junction	38
22.	Tchebyscheff Design of a Series of Quarter-wave Transformers	40
23.	Series Inductance of Round Hole in the Center Conductor	44
24.	Shunt Capacitance of Round Hole in the Center Conductor	45
25.	End Probe Slotted Section	47
26.	Slotted Ground Plane Slotted Section	48
27.	Prototype Section for Strip Transmission Line Low Pass Filter	52
28.	The Center Conductor of a Low Pass Filter . .	54
29.	Input Impedance and Reactance of a Low Pass C Band Filter	55
30.	Twelve-Section Low Pass Filter	56
31.	Tests of Preliminary Low Pass Filter Designs .	57
32.	Stripline High Pass Filter with Fixed Capacitive Elements	59
33.	Construction of Stripline High Pass Filter with Fixed Capacitive Elements	60
34.	Response of Stripline High Pass Filter with Fixed Capacitive Elements . .	61
35.	Construction of Compact Stripline Low Pass Filter with Fixed Capacitive Elements	62
36.	Response of Compact Strip Low Pass Filter . .	63



37.	A Full Wave Resonant Element Narrow Band Pass Filter for KU Band Frequencies	65
38.	Product of Gap Capacitance and Z_0 as a Function of Relative Gap Width	66
39.	Product of Fringing Capacitance and Z_0 as a Function of Relative Gap Width	67
40.	Response of a Resonant Element at Half Wavelength and Full Wavelength Frequencies	68
- 41.	Voltage Distribution in Two and Three Element Filters	69
42.	Comparison of the Computed and Measured Q . .	71
43.	A Single Resonant Element Filter with Top Ground Plane Removed	72
44.	Response of Three Element Filter	75
45.	Schematic Representation of a Resonant Element Filter	76
46.	An Arbitrary Four Arm Junction	78
47.	An Actual Size Center Conductor for a C Band Strip Transmission Line Hybrid Junction	79
48.	Two Hybrid Junctions with Identical Electrical Characteristics	83
49.	Hybrid Junction with Different Arm Admittances	85
50.	Hybrid Transformer Radar Antenna Coupling Unit	87
51.	Hybrid Junction Balanced Mixer	87
52.	Prototype C Band Receiver Front End	90
53.	Prototype C Band Receiver Front End, Opened to Expose stripline Circuitry	91
54.	Conventional Waveguide and Microstrip Receivers	93

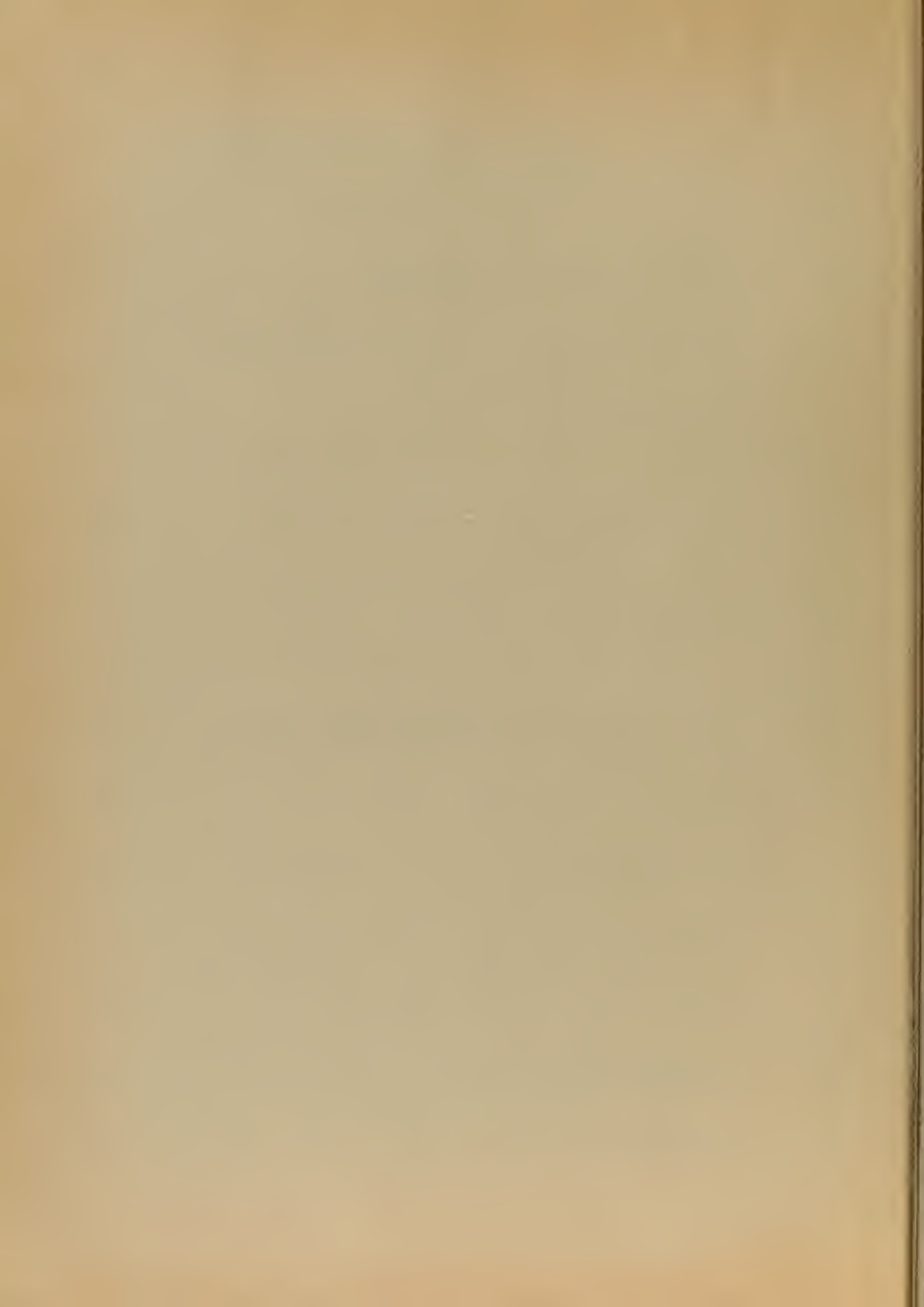


Figure		Page
55.	Hybrid Junction Test Arrangement	96
56.	Impedance Measurement Arrangement	100
57.	Radiation Intensity Pattern in XY Plane for Folded Half-wave Dipole	102
58.	Colinear Array with Unbalanced Feed	103
59.	Radiation Intensity in XY Plane	104
60.	Twelve Element 3000 MC Yagi Array	105
61.	Radiation Intensity Pattern 3° Above the XZ Plane for Twelve Element Yagi Array	106
62.	Radiation Intensity Pattern in XY Plane for Twelve Element Yagi Array	107
63.	Forty Element Coplanar Array	108
64.	Forty Element Coplanar Array.	109
65.	Forty Element Coplanar Array with Double Stub Balun	110
66.	Radiation Intensity Pattern in XY Plane for Forty Element Coplanar Array	111
67.	Radiation Intensity Pattern in YZ Plane for Forty Element Coplanar Array	112
68.	Thirty Element Coplanar Array with Hybrid Junction Balun	115
69.	Radiation Intensity Pattern in XY Plane for Thirty Element Coplanar Array	116
70.	Radiation Intensity Pattern in YZ Plane for Thirty Element Coplanar Array	117
71.	Printed Chereix-Mesny Array	118

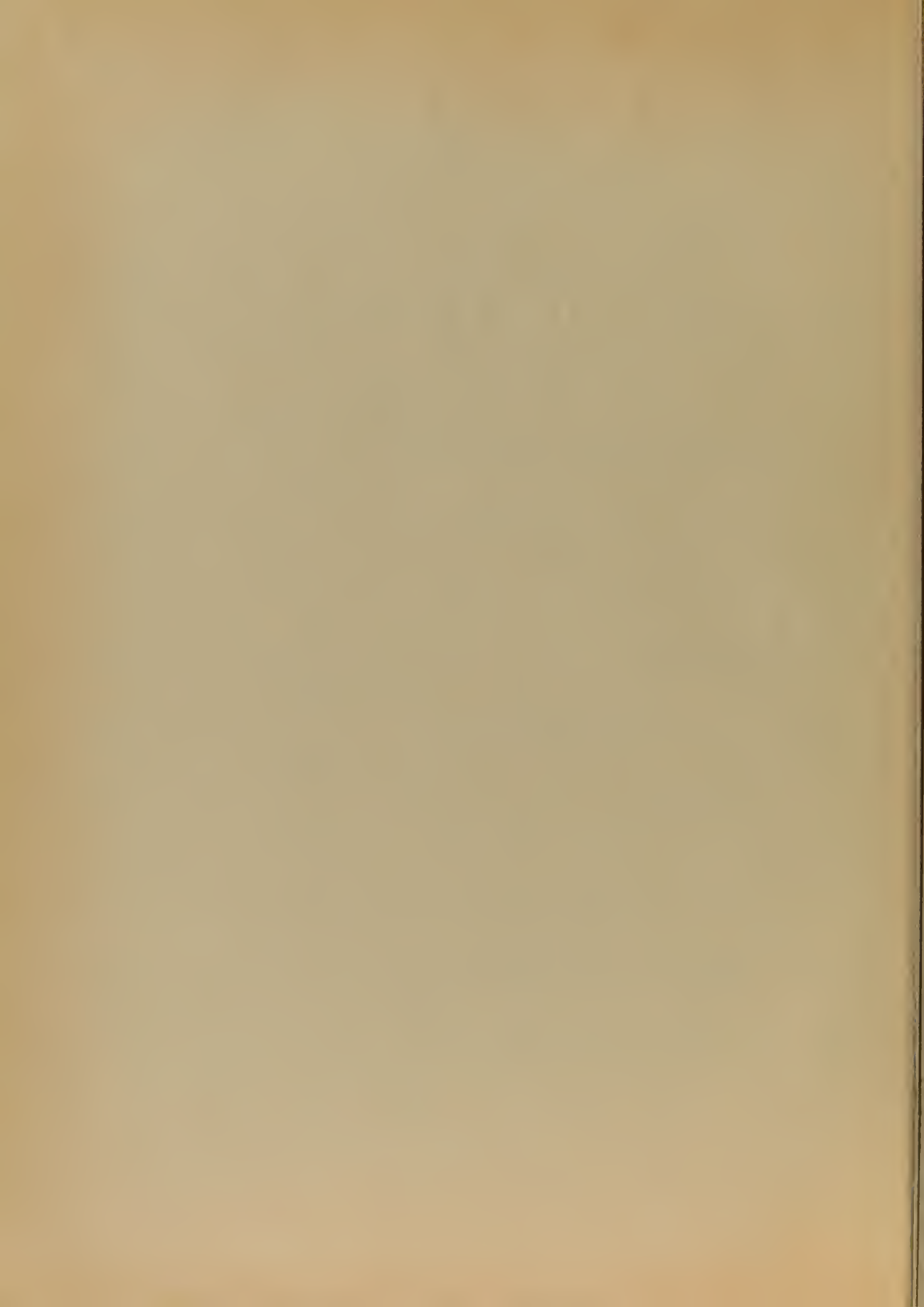
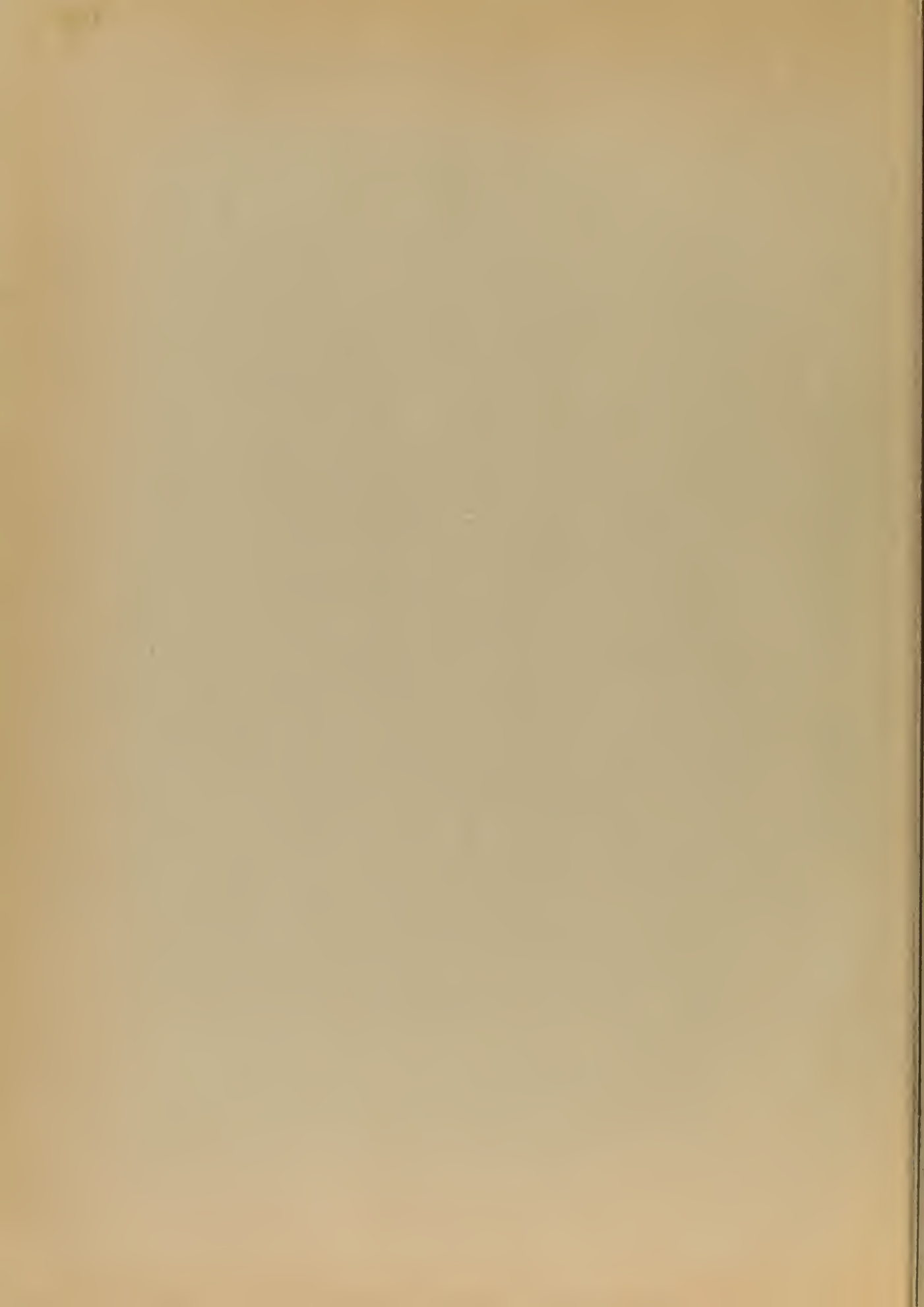


TABLE OF SYMBOLS AND ABBREVIATIONS

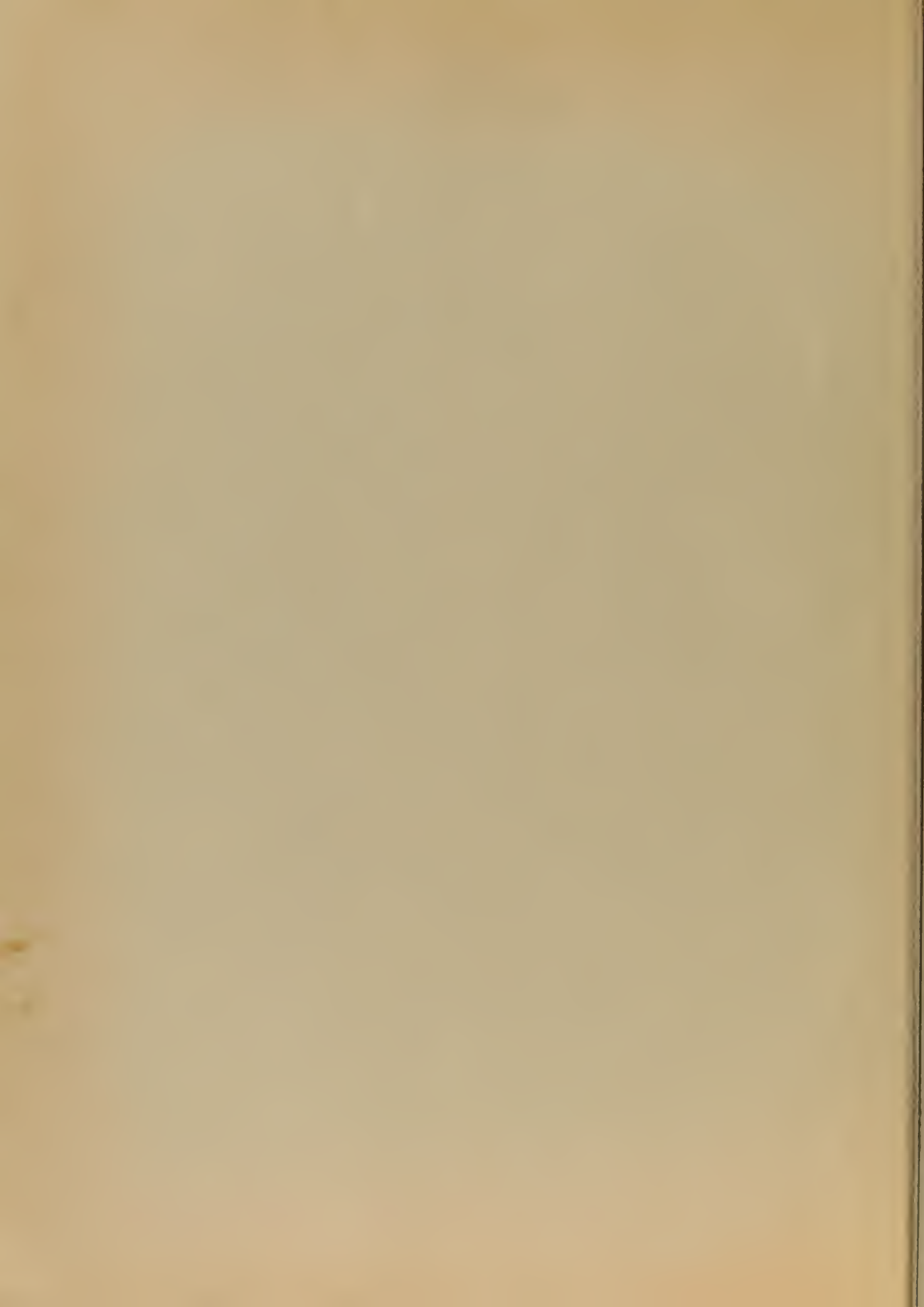
A	Angstrom
A. F. C.	Automatic Frequency Control
A. I. L.	Airborne Instruments Laboratory
ATR	Anti-Transmit-Receive
Δ	Cofactor of Determinant
DB	Decibels
DC	Direct Current
\emptyset	Electrical Length
f_c	Frequency of Cutoff
IF	Intermediate Frequency
I. R. C.	International Resistance Company
IRE	Institute of Radio Engineers
KMC	Kilomegacycles
L	Length
MC	Megacycles
Q	Merit of a Circuit
SWR	Standing Wave Ratio
T	Transmission Ratio
TEM	Transverse Electromagnetic Waves
TR	Transmit-Receive
VSWR	Voltage Standing Wave Ratio
λ	Wavelength
Y_o	Characteristic Admittance
Z_o	Characteristic Impedance



CHAPTER I

INTRODUCTION

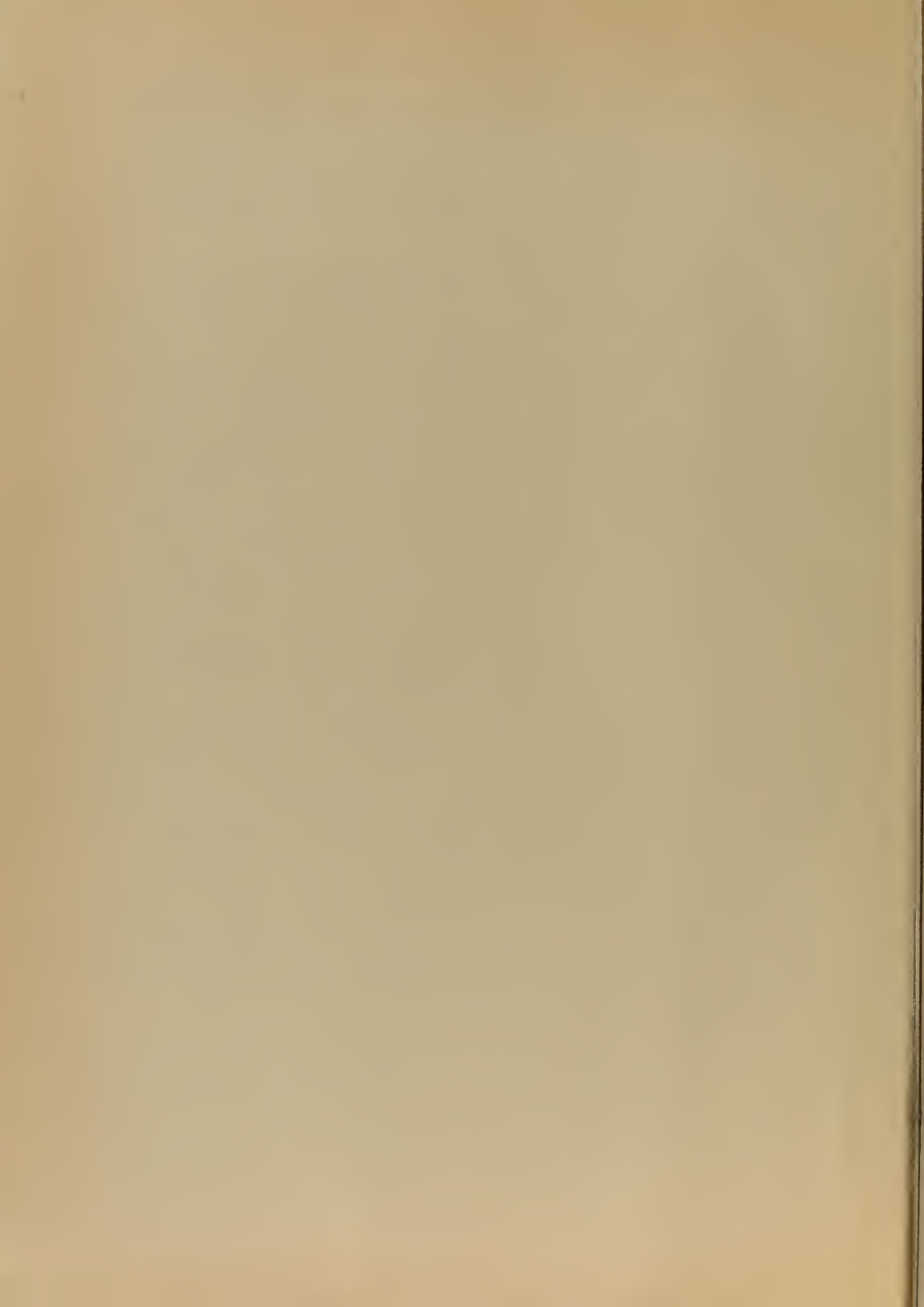
The strip transmission line is a new and remarkable means of transferring electromagnetic energy at microwave frequencies. It was first conceived, according to the best available information, by V. H. Rumsey and H. W. Jamieson during World War II as a power divider for an antenna system [37]. In 1949, interest was revived in the field of strip transmission lines when R. M. Barrett showed that this technique could be used to replace many types of microwave components [2]. Since that time, it has been studied and developed, both theoretically and experimentally, by many educational institutions and commercial companies. An overwhelming number of papers from these sources have been published reporting their individual findings. Each paper covers a specific facet of the field and from this myriad of information, much that is necessary to design and construct a strip transmission system can be gleaned. However, due to the nature of these papers, this would represent a formidable task. The author has extracted the information necessary from these reports, has filled in the gaps between the unrelated reports, has utilized his own experimentation and discussions with the authors of some of the reports, and herein presents a complete picture of the work that has been done on the strip transmission line. Included with this information is the first presentation of an original analysis of the hybrid junction. This thesis has been prepared in a form that will allow an engineer, familiar with basic microwave technique,



to design and construct a complete strip transmission line system.

Lengthy mathematical derivations have not been included in this report when they are available in other works. However, the results and conclusions have been noted and the source of the complete derivations is available in the Bibliography.

The opening section of Chapter II is a general discussion of the types of strip transmission lines. The balanced strip transmission line is covered in more detail due to its inherently wider application. Unbalanced microstrip is discussed briefly with numerous references in the Bibliography for those primarily interested in microstrip. In a logical manner, the author then provides design information concerning the characteristic impedance, attenuation, velocity of propagation, and environmental considerations. The components required for complete systems are covered individually in detail in Chapter III: transitions from coaxial line or waveguide, slotted sections, bends, tees and power dividers, loads and attenuators, tuning devices, impedance transformers, low and high pass filters, and band pass filters utilizing resonant elements. In Chapter IV, the hybrid junction is analyzed through the use of an equivalent circuit, and the results attained are applicable to coaxial lines, H plane waveguide, and strip transmission lines. Complete strip line and microstrip systems are discussed and illustrated in Chapter V. Printed antennas, an extension of the strip transmission line concept, are discussed in Chapter VI.



CHAPTER II

GENERAL STRIP TRANSMISSION LINE CONSIDERATION

1. Types of Strip Transmission Lines

Since this is the first paper that has been written integrating all forms of strip transmission lines, there is no exactly defined terminology available to discuss the field. Therefore, definitions of the terms to be used in this thesis are needed. The following definitions have been generally accepted through common usage.

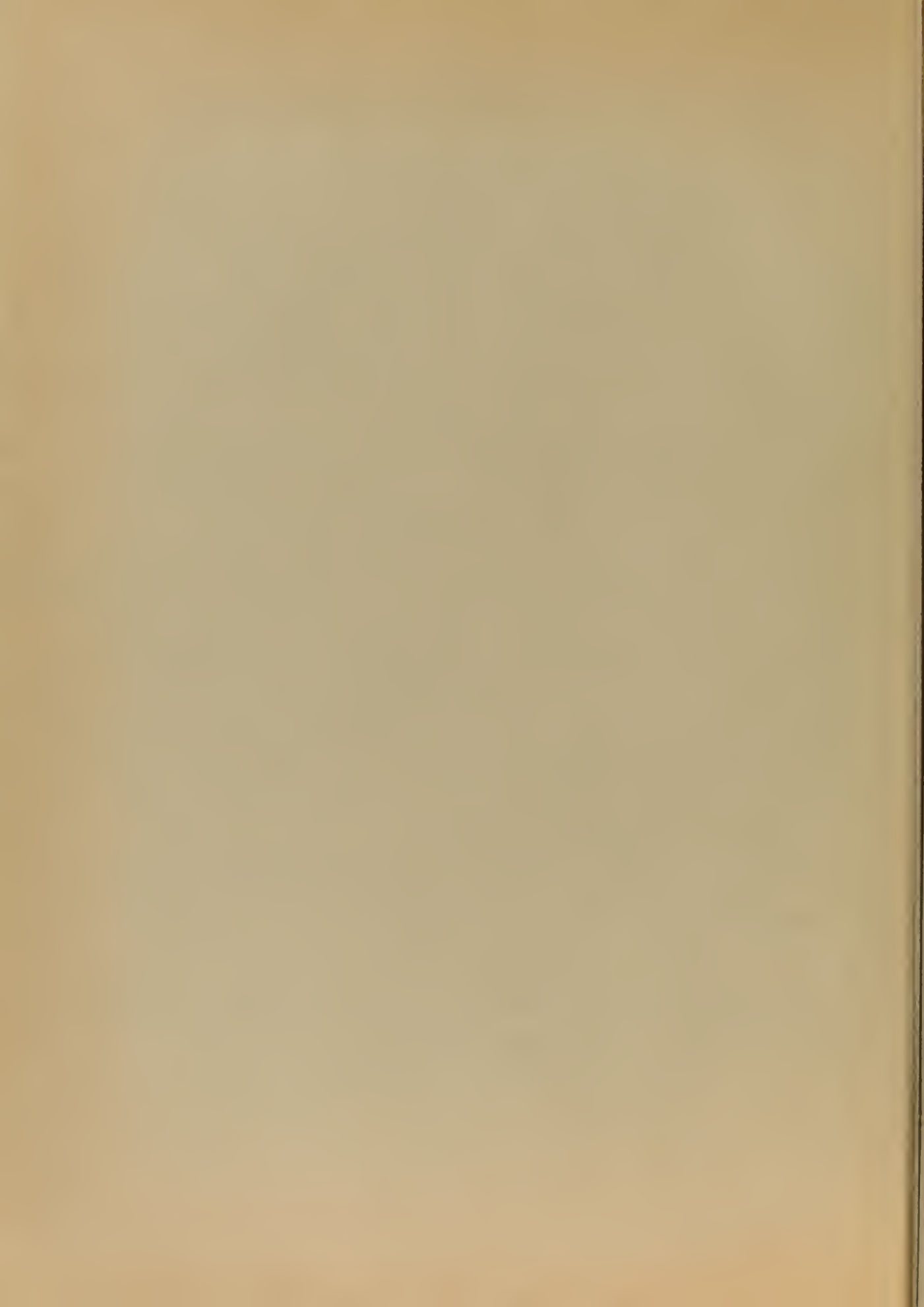
Strip Transmission Line -- A general term referring to all transmission lines composed of a rectangular strip over an effectively infinite ground plane or between two effectively infinite ground planes.

Balanced Strip Transmission Line -- That group of strip transmission lines which have the strip, or center conductor, placed between two effectively infinite ground planes. It is considered balanced due to the identical field configuration above and below the center conductor.

Unbalanced Strip Transmission Line -- The strip transmission line that has the strip over an effectively infinite ground plane. It is unbalanced since the fields above and below the strip are not the same.

The general catagories may be further divided into the four types of strip transmission lines that are known to be in use at the present time.

Strip Line -- A balanced strip transmission line with a solid center conductor centered between two ground planes.



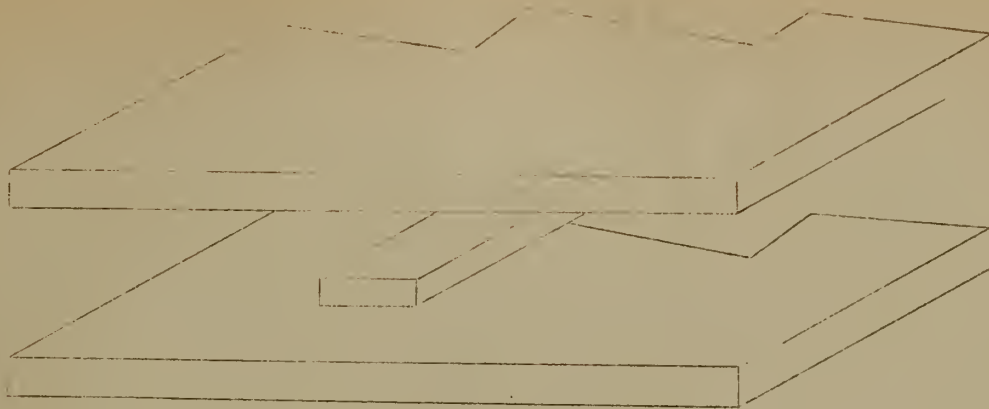


Figure 1. Strip Line

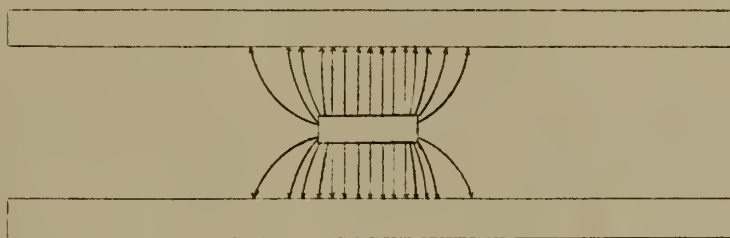


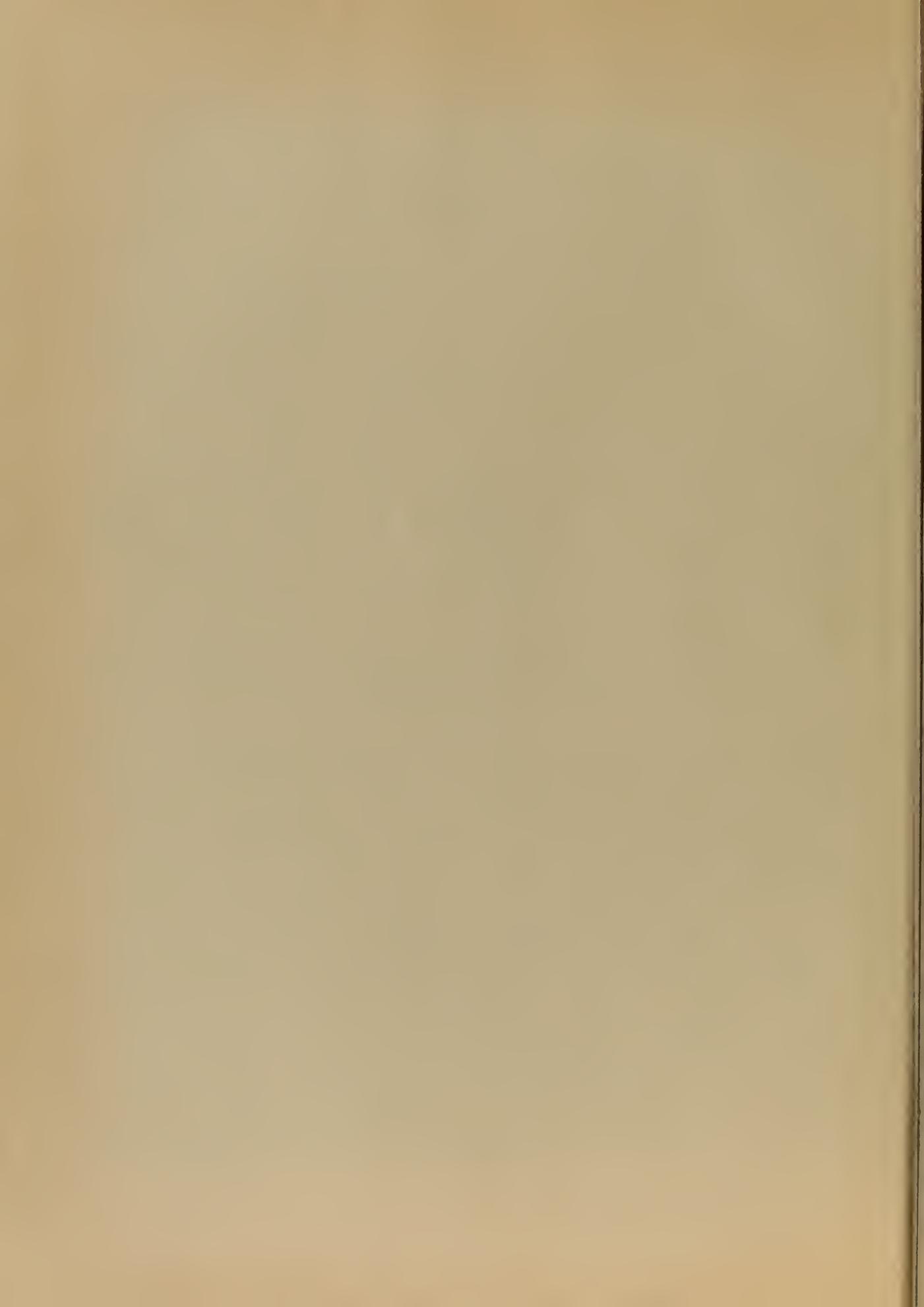
Figure 2. Balanced Strip Transmission Line

Field Configuration

Figure 1 is a simplified sketch of the strip line configuration.

Figure 53 is an excellent example of a complete system constructed of strip line. The field configuration of all the balanced strip transmission lines to be discussed in this paper is shown in Figure 2. An examination of this field configuration will show that it operates in the dominant or TEM mode, and bears a close resemblance to that of a coaxial line.

Strip line in low powered, complex networks has many advantages over conventional coaxial line or waveguide. The entire network, including components, may be etched on a single strip center conductor and enclosed between two ground planes with considerable saving in size,



weight, cost and time consumed in manufacturing. It is essentially a low loss device, since the center conductor is supported in air. With silver-plated ground planes and center conductor, a theoretical and measured "Q" in excess of 5,000 may be obtained. The one disadvantage of the strip line is mechanical. The strip must be supported by beads or edge supports, involving special design and construction problems.

Sandwich Line -- A balanced strip transmission line with a solid center conductor supported rigidly between the ground planes by dielectric.

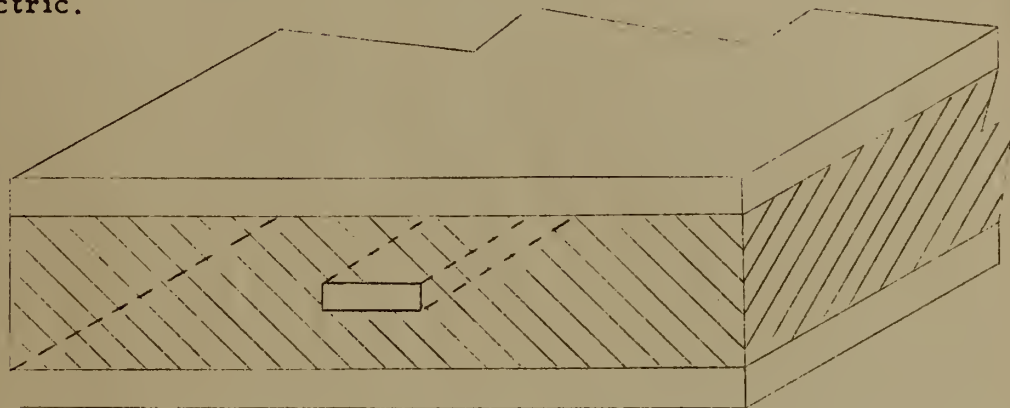
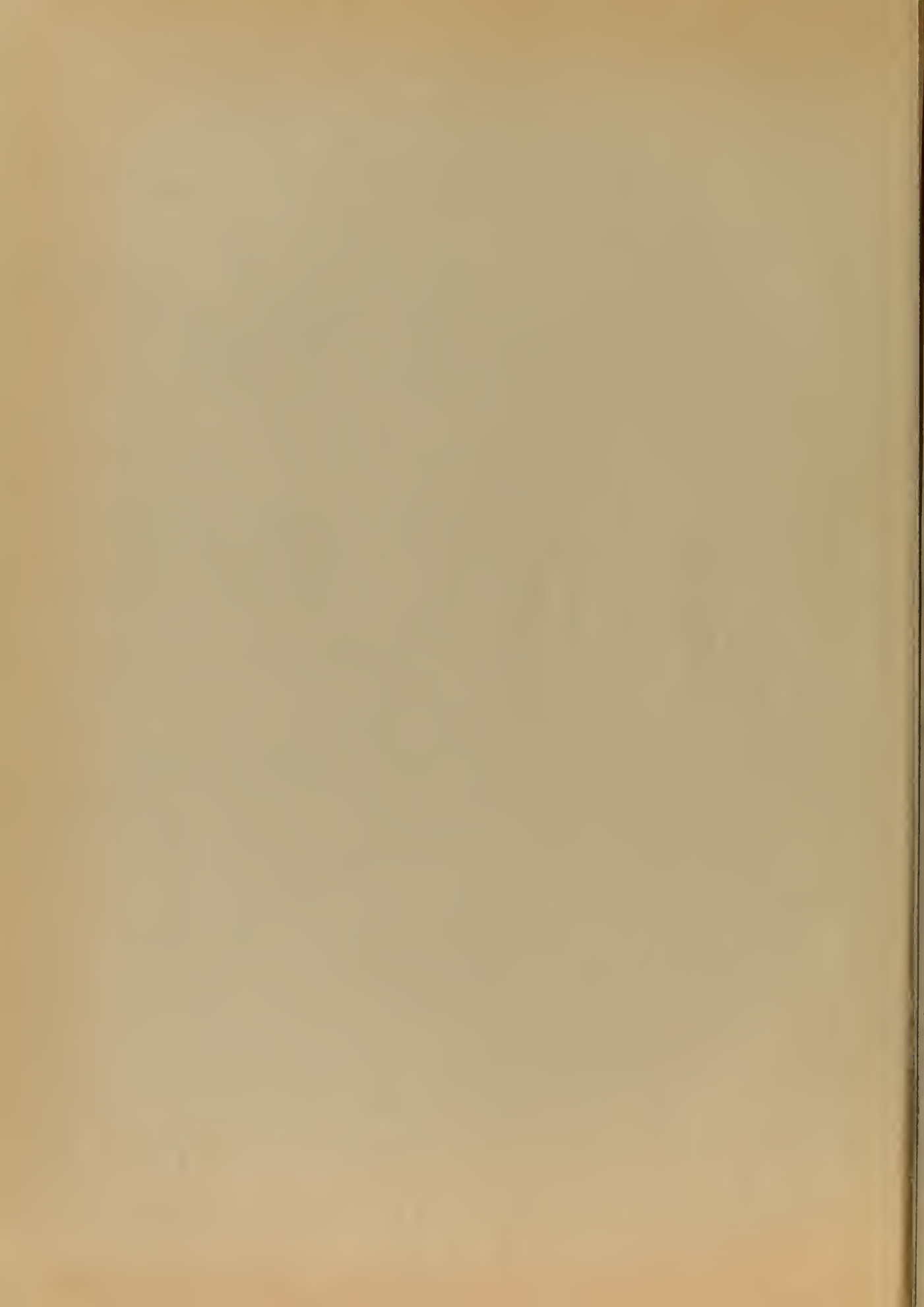


Figure 3. Sandwich Line

Sandwich line has the same advantage over coaxial line and waveguide as strip line. It may be made physically smaller than a strip line with the same electrical characteristics due to the reduction of the wavelength because of the dielectric constant of the supporting media. A sandwich line may be constructed very inexpensively by the juxtaposition of two sections of copper clad dielectric. The center conductor is etched on one side of the dielectric and the copper on the other side is retained as a ground plane, resembling microstrip which is discussed later in this section. Then, a second section of dielectric with the copper only on one side, serving as the second ground plane, is placed



over the center conductor forming the sandwich line. The disadvantage of the sandwich line is that it has a lower "Q" than strip line due to the loss inherent in all common dielectrics.

Stripline -- A balanced strip transmission line that is essentially the same as strip line except that the center conductor is composed of etched, copper-clad strips on opposite sides of a thin dielectric sheet, as shown in Figure 4.

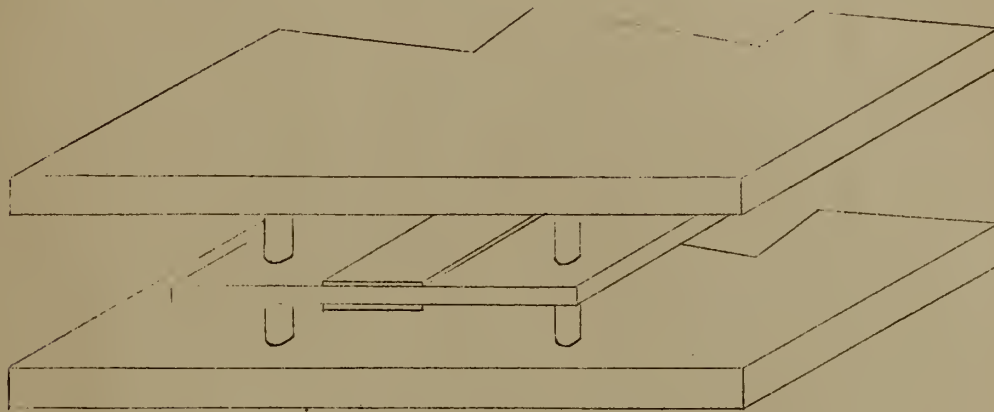
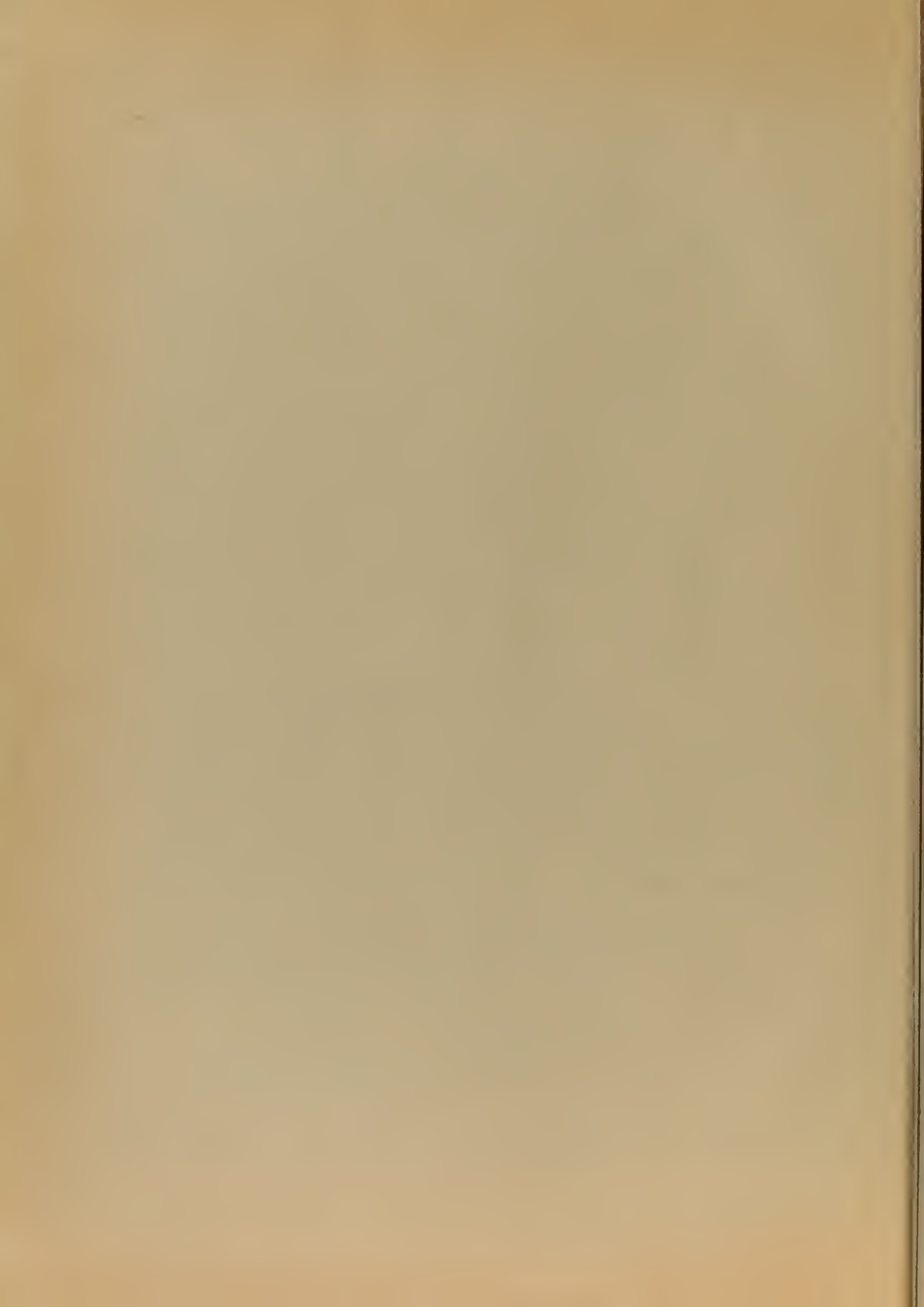


Figure 4. Stripline

The dielectric sheet serves as a convenient means of support for the center conductor. There is some loss caused by the dielectric sheet, but it is small, because the sheet lies in the fringing fields between the strip and the ground planes. There is a slight reduction in the wavelength along the line due to the dielectric. The effect of the dielectric has not been satisfactorily determined analytically as yet, but it has been determined experimentally that there is a reduction in wavelength of from two to eight percent. The amount depending on the extent of the fringing fields, and the thickness of the dielectric sheet.

Microstrip -- An unbalanced strip transmission line composed of a thin strip conductor supported over a ground plane by a uniform die-



lectric sheet, as shown in Figure 5. A complete microstrip system is shown in Figure 54.

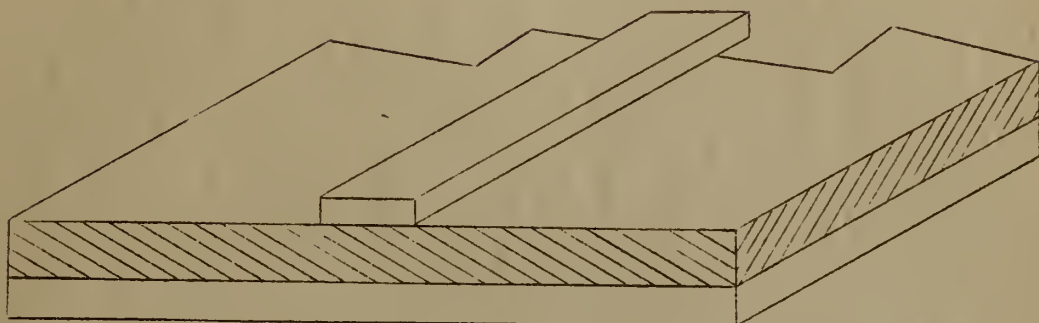


Figure 5. Microstrip

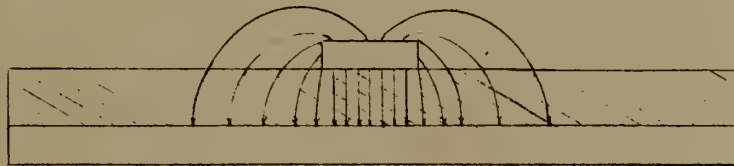
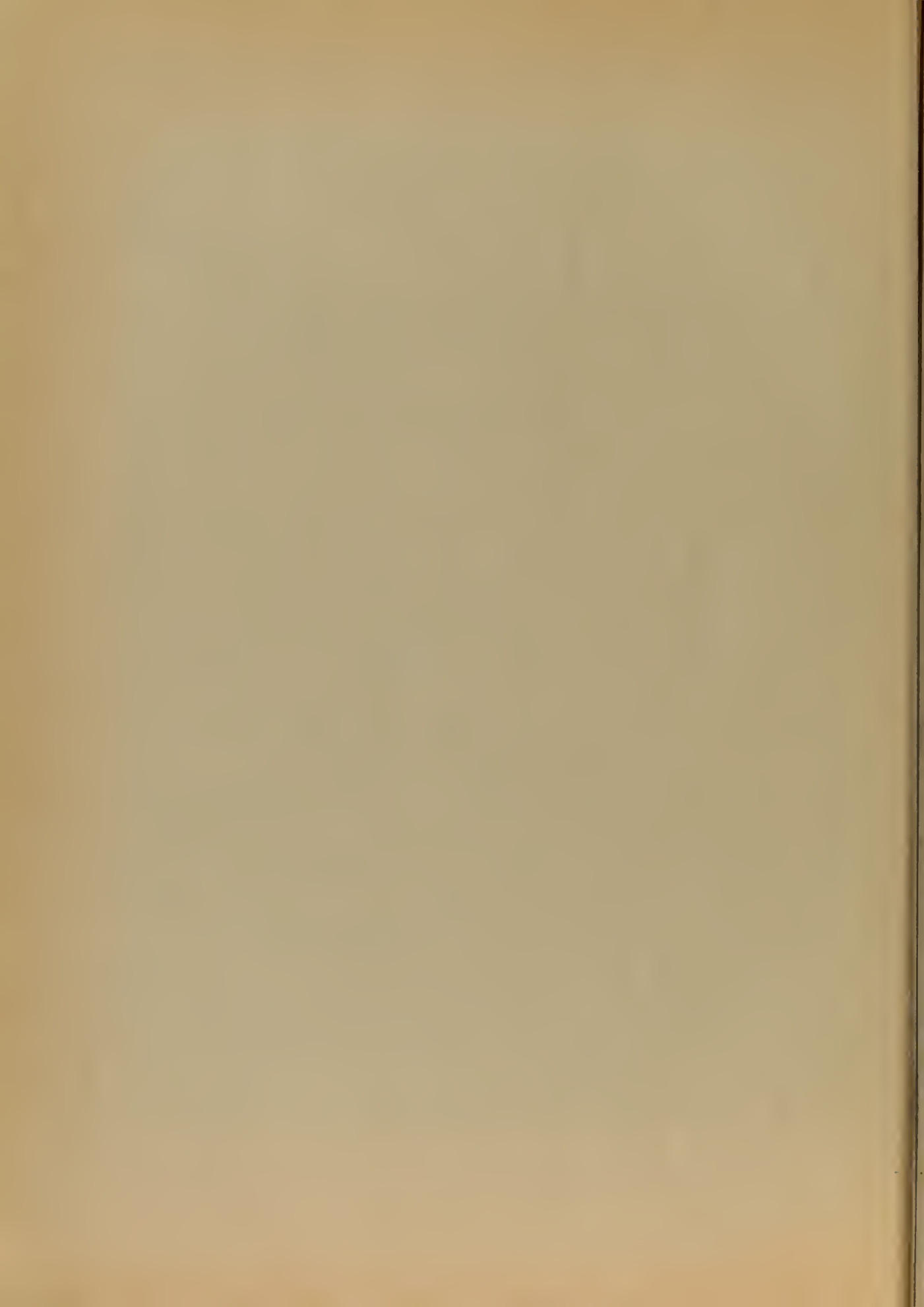


Figure 6. The Field Configuration of Unbalanced Strip Transmission Line

Figure 6 is a sketch of the field configuration of unbalanced strip transmission line. An examination of this field configuration will show that it bears close resemblance to a two strip transmission line with a conducting plane, placed at the zero voltage line midway between the two strips, replacing the second strip. The fields are the same above the ground plane as they would be if the conducting plane was removed and the second strip replaced.

Microstrip is smaller and simpler to construct than any of the bal-



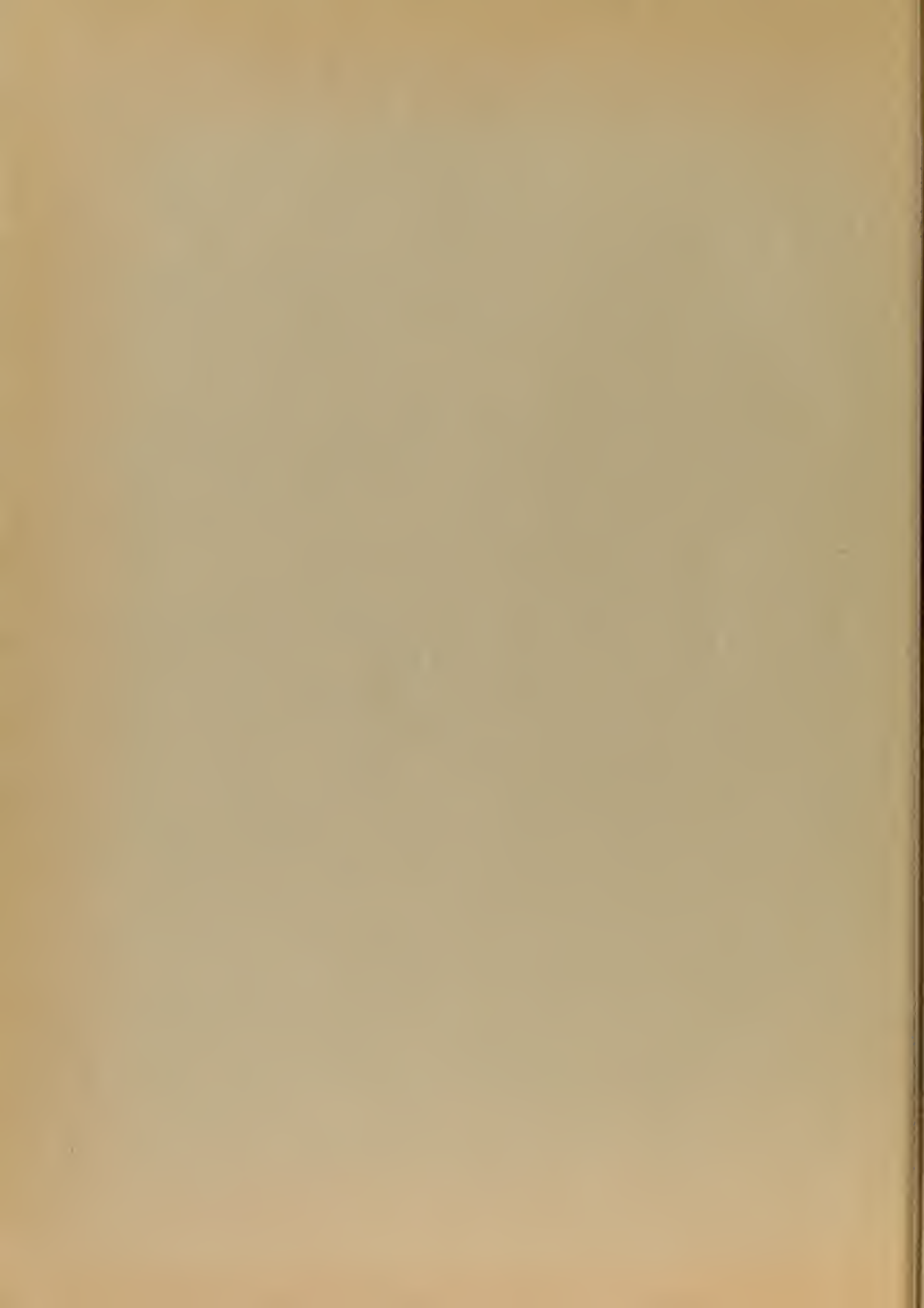
anced strip transmission lines. The simplicity of the construction is due mainly to unbalance of the system. Connections may be made directly to the strip through the ground plane without the special precautions that are necessary to maintain balance when making the same type of connection with balanced strip transmission line.

Reference [1] is an excellent paper with numerous illustrations discussing most of the theoretical and experimental work that has been done on microstrip.

Strip line and sandwich line are results of the original work of R. M. Barrett and his predecessors. Microstrip was developed by the Federal Telecommunications Laboratories. Stripline was developed by the Airborne Instruments Laboratories.

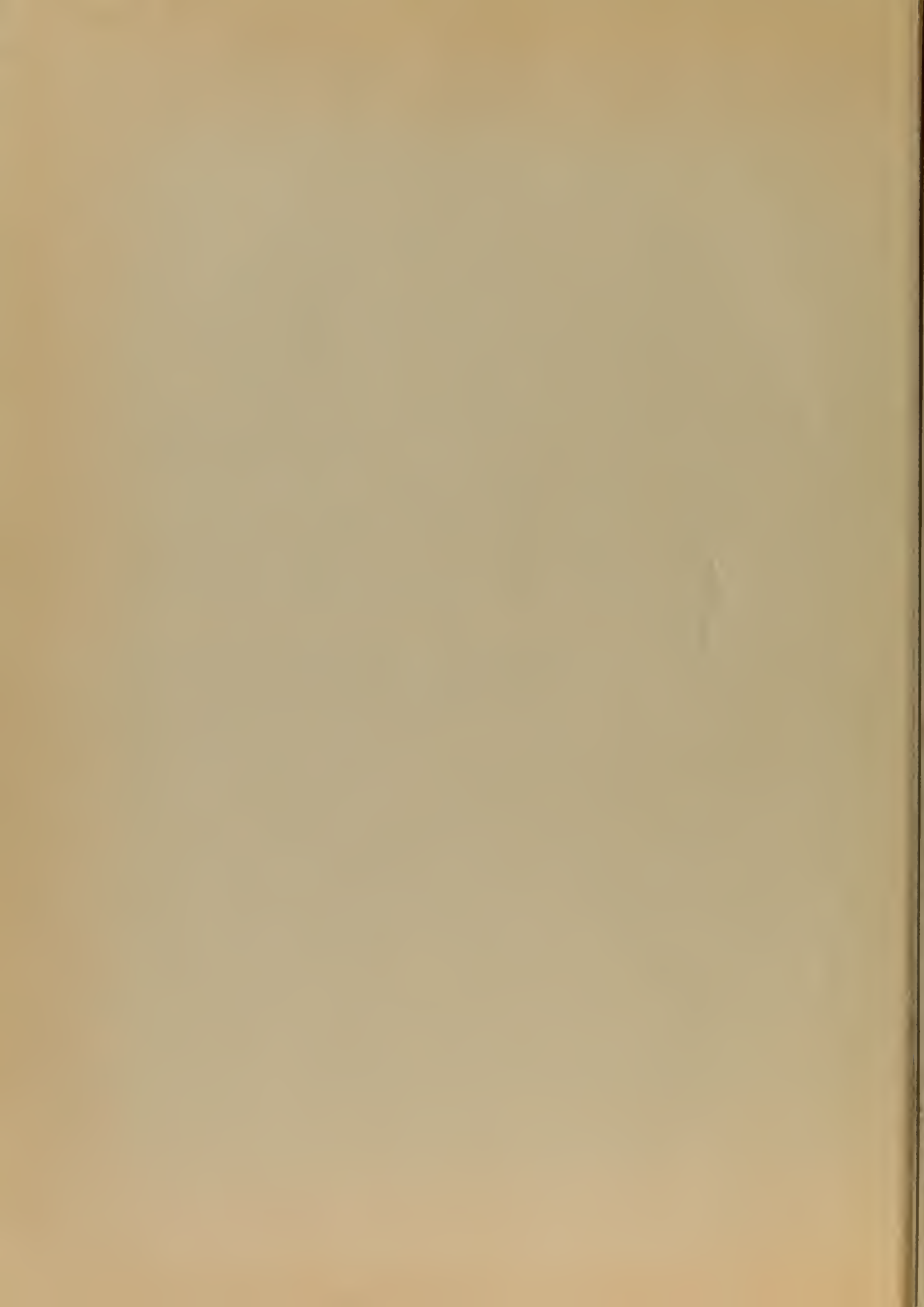
2. Characteristic Impedance and Frequency Limitations

The geometrical configuration of the balanced strip transmission line is not one that leads to a straightforward mathematical analysis. The determination of the characteristic impedance is, therefore, a complex problem that is virtually impossible to solve rigorously for all practical applications. The problem has been independently solved by several people with varying degrees of success depending on the approximations used, and is still under study to provide a more accurate solution. The solutions obtained during the early years of the strip transmission line investigation provided a reasonable approximation for the characteristic impedance [2] [4]. Recently S. B. Cohn completed his solution of the problem with a calculated maximum error of 1.24%, and has published the result in useful, graphical form [12]. His solution has been verified within the limits of measurement accuracy at



A. I. L. Figure 7 is a comparison of the computed and measured characteristic impedances at several arbitrarily selected points. Figure 8 is a nomograph based on Mr. Cohn's work, that was prepared by Elio Sion at A. I. L. The nomograph provides a rapid means of determining the parameters that govern the characteristic impedance. However it is not as accurate as the original graphs. Should the reader require precise values for the characteristic impedance, the original graph has been reprinted in the following references [14] [15] [22]. Two later solutions of the characteristic impedance problem have been published that are somewhat more precise than Mr. Cohn's [3] [35]. However, since Mr. Cohn's solution is theoretically as accurate as necessary for practical work and has been experimentally proven to be reliable, it will be used as the means of determining characteristic impedance throughout this paper.

All of the solutions of the characteristic impedance problem have been computed for a solid center conductor. The results have been successfully used as an excellent approximation for the determination of the characteristic impedance of stripline with the overall thickness of copper clad dielectric considered as the strip thickness. When the data for the characteristic impedance is used for the design of a strip transmission line network, the ground plane spacing, center conductor thickness, and characteristic impedance are normally fixed, and the width of the center conductor is made to correspond with the other parameters. The designer should not fail to consider the possibility of changing the center conductor thickness in sections requiring a change of impedance. The ring of the hybrid junction, that has a changing



<u>READING</u>	<u>W/D</u>	<u>t/D</u>	<u>(CALCULATED BY COHN)</u>	<u>(MEASURED BY AIL)</u>
1	.25	.25	87.8	87.0
2	.25	.25	87.8	86.0
3	.34	.044	109.0	109.5
4	.49	.044	92.0	95.5
5	.525	.044	89.0	91.0
6	.525	.044	89.0	89.0
7	.85	.044	67.0	69.5
8	1.0	.25	45.2	45.4
9	4.0	.044	20.0	20.0
10	4.0	.25	15.5	15.3

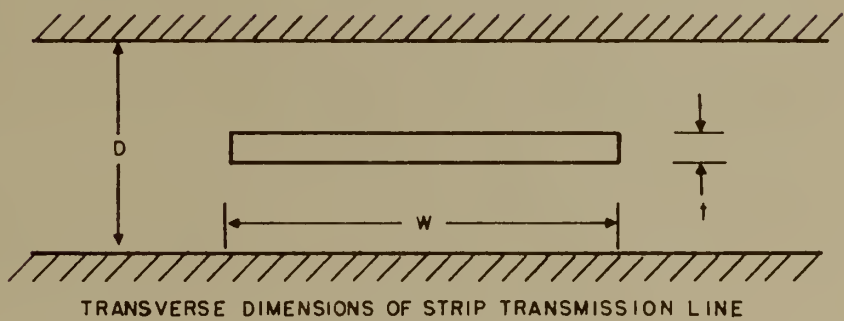
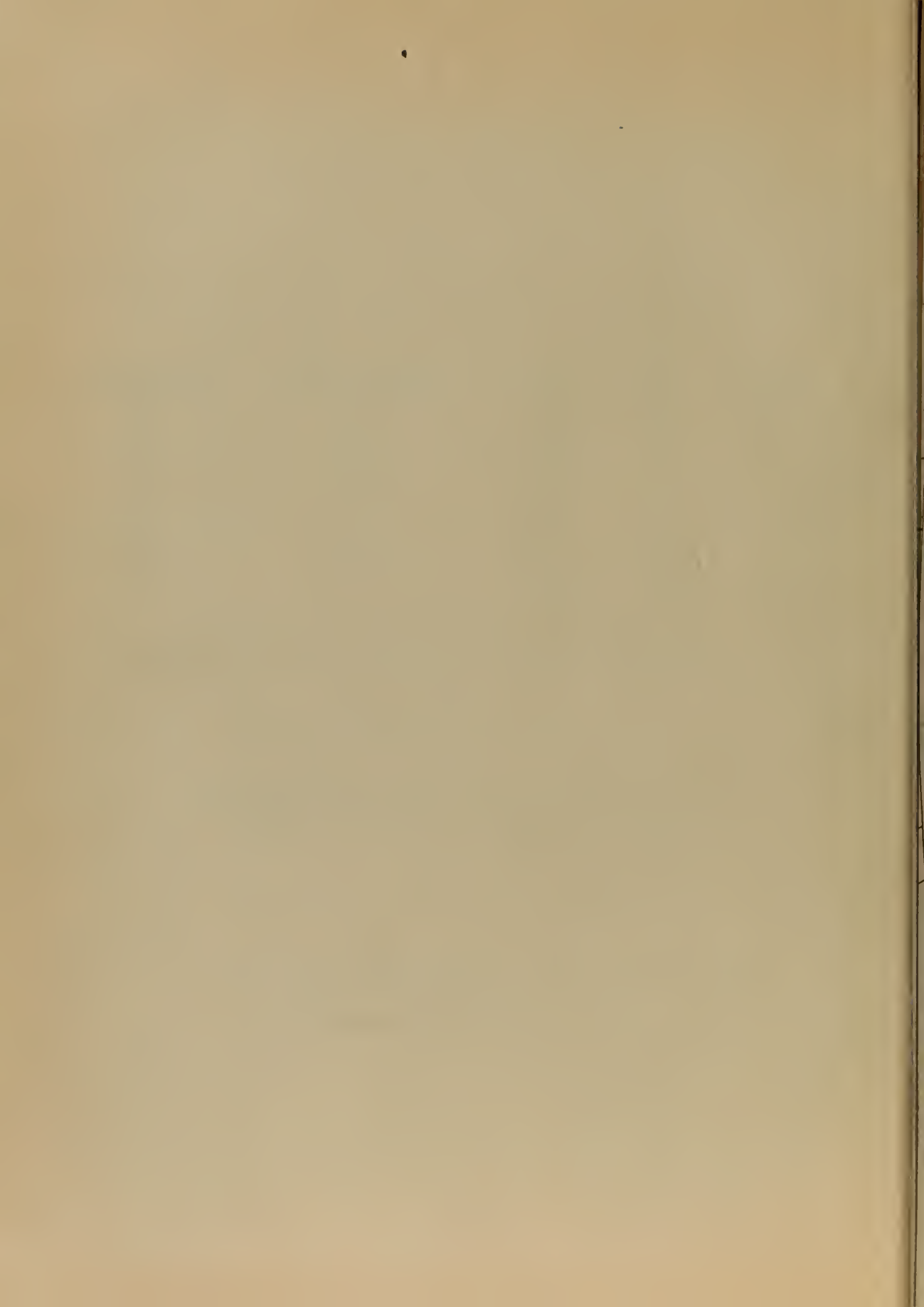
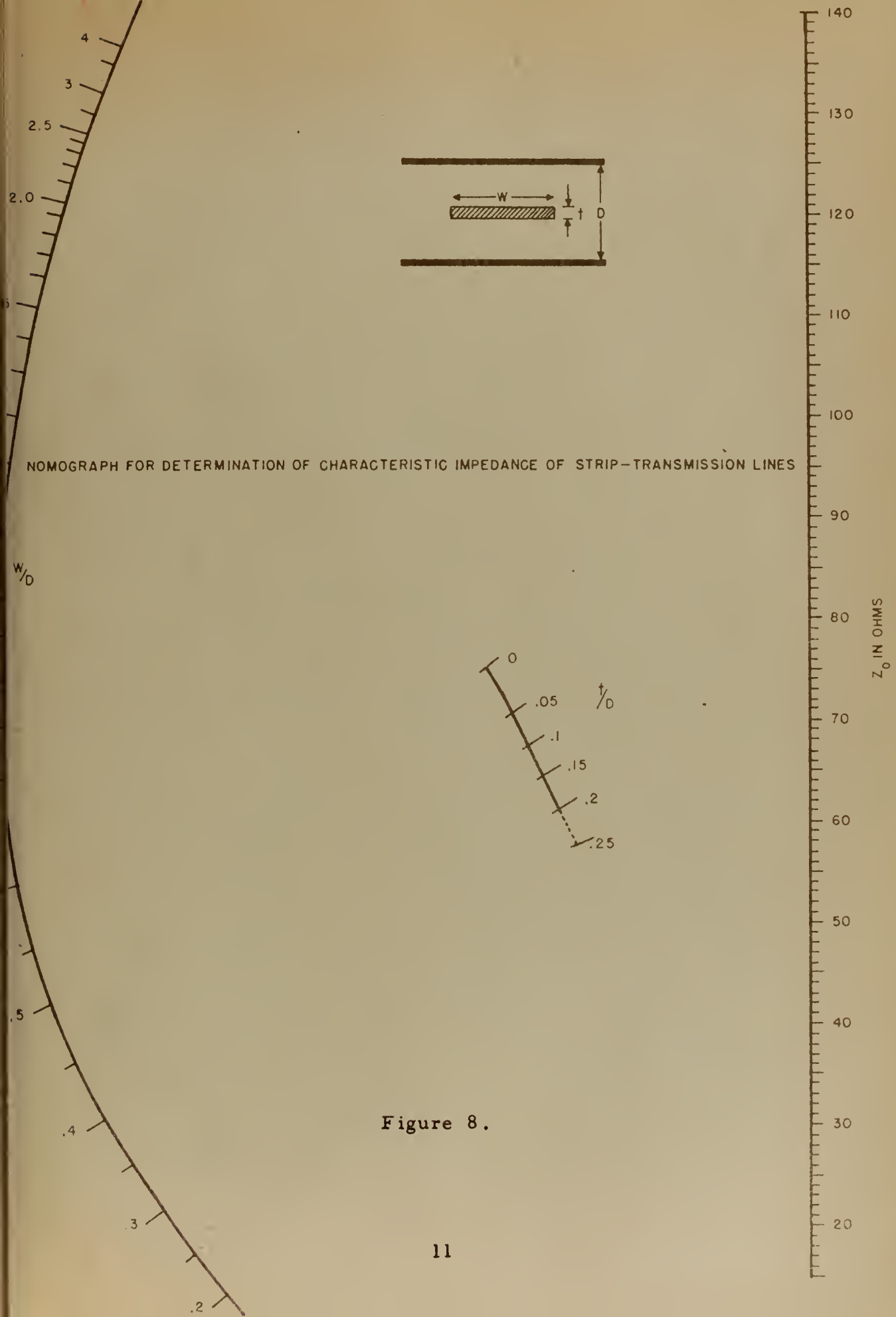
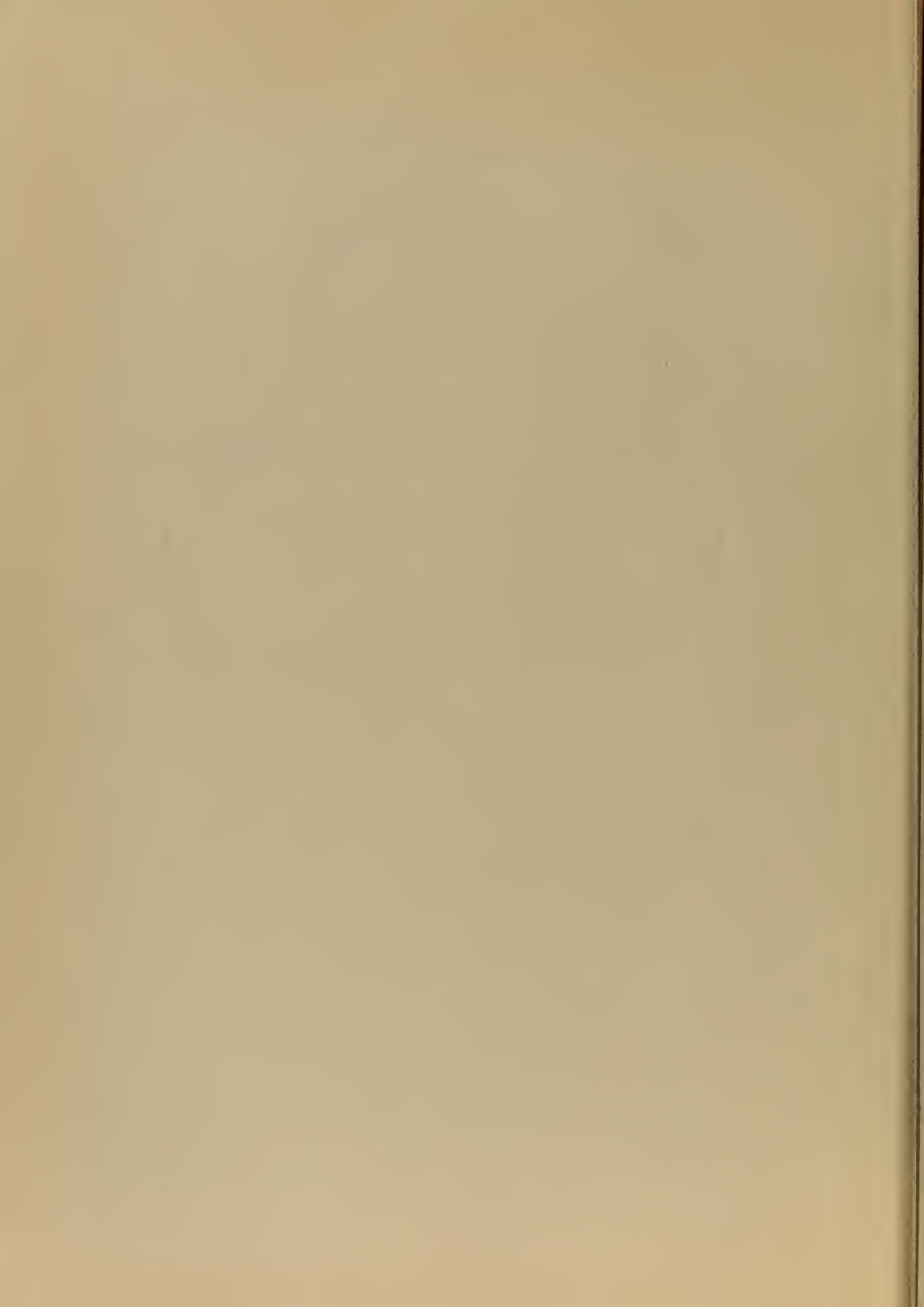


Figure 7. Comparison of Calculated and Measured
Strip Transmission Line Impedances







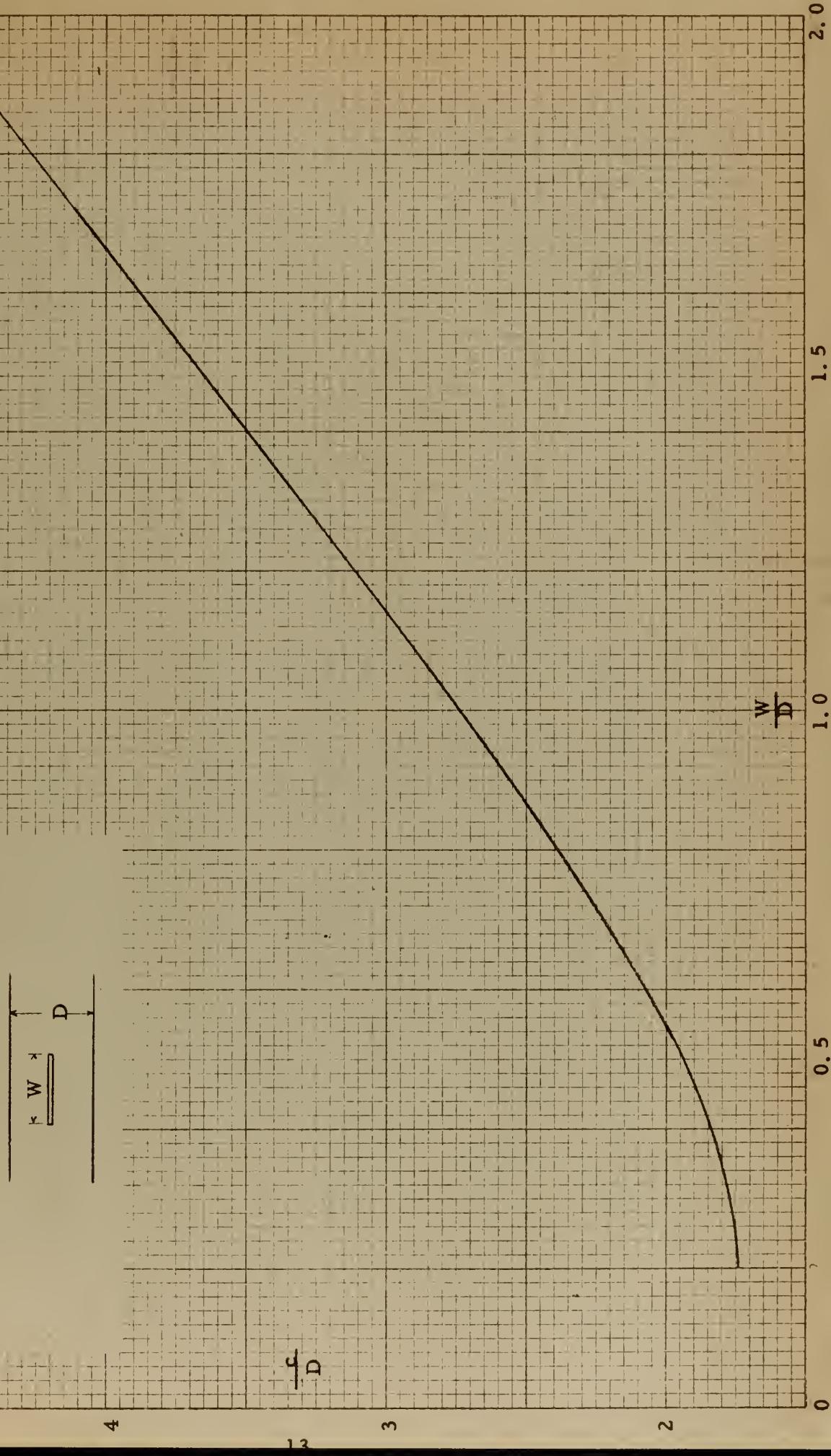
impedance, (see Chapter III,) serves to illustrate where this philosophy may well be employed.

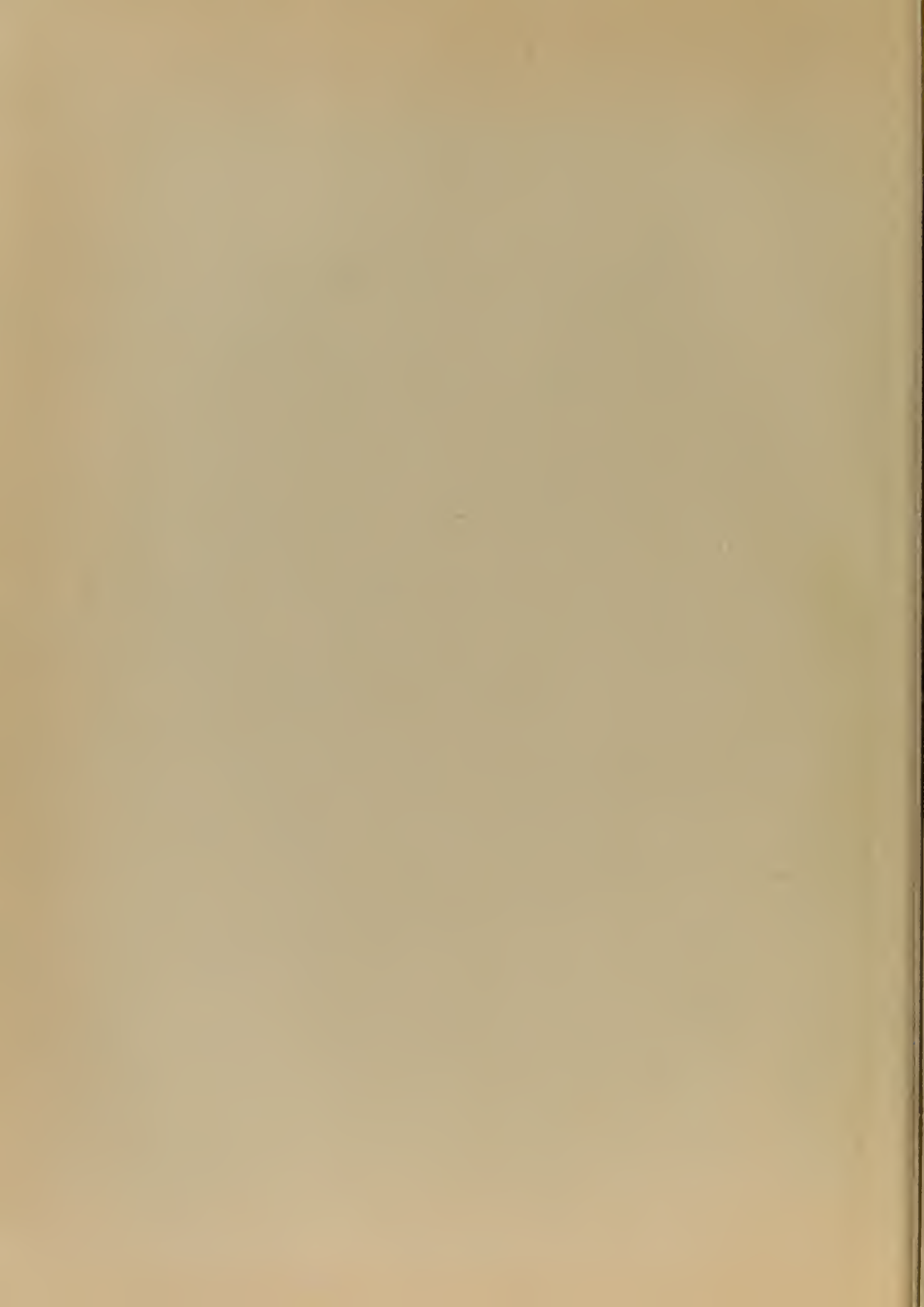
The characteristic impedance of the balanced strip transmission line has been computed assuming that the center conductor is located precisely midway between the ground planes. In practice it may prove difficult to fix exactly the position of the center conductor. Because of this difficulty, the effect of a slight offset in the center conductor was checked experimentally at A. I. L. and found to be negligible. Actually an offset of 53% of the distance from the center position to the ground planes caused only a 22% reduction in the characteristic impedance. The test was made for one particular configuration but is considered to be generally applicable.

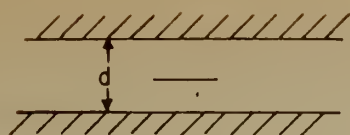
A lower limit of the characteristic impedance that can be used for a given balanced strip transmission line geometric configuration and frequency is imposed because of the excitation of higher order modes. This phenomenon is analogous to the limiting condition of coaxial line where the mean circumference between the center conductor and outer shield must be less than a wavelength to maintain propagation in the TEM mode. The exact determination of the limiting condition in balanced strip transmission line is complicated again by the geometry and fringing capacitance, but a first order approximation may be obtained by considering the mean circumference about the strip. The cut-off frequencies of the higher order modes have been determined by computing the effective width of the strip considering the fringing capacitance as additional strip width [28] [34]. The limiting frequency is the one at which the effective strip width equals one half the wavelength.



Figure 9. Cut-off Wavelength c of
the First Higher Mode in Strip Line







ABOVE 97.5 OHMS, GROUND-PLANE SPACING BECOMES THE LIMITING FACTOR

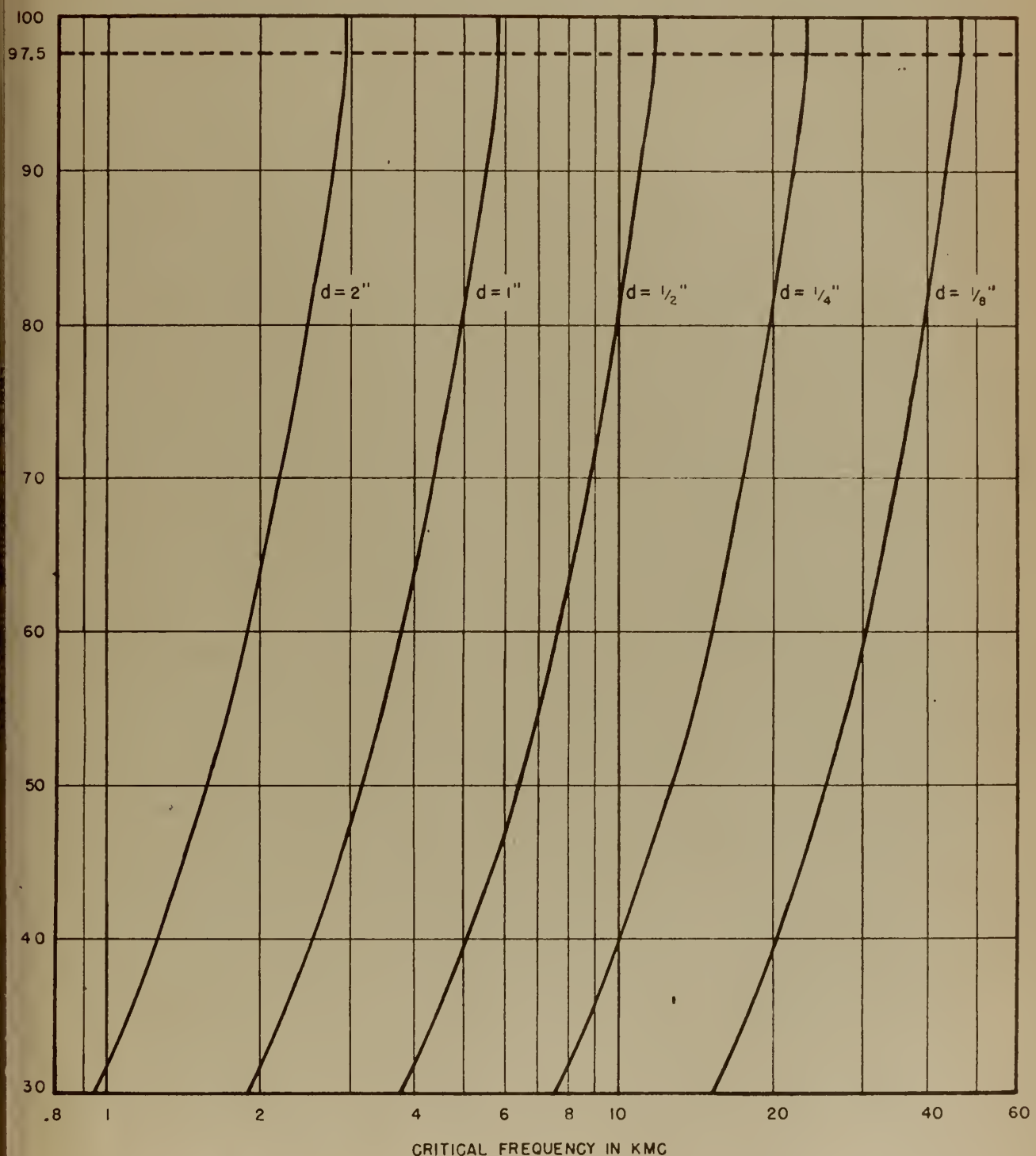


Figure 10. Calculated Maximum Freq. for Various Ground Plane Spacings

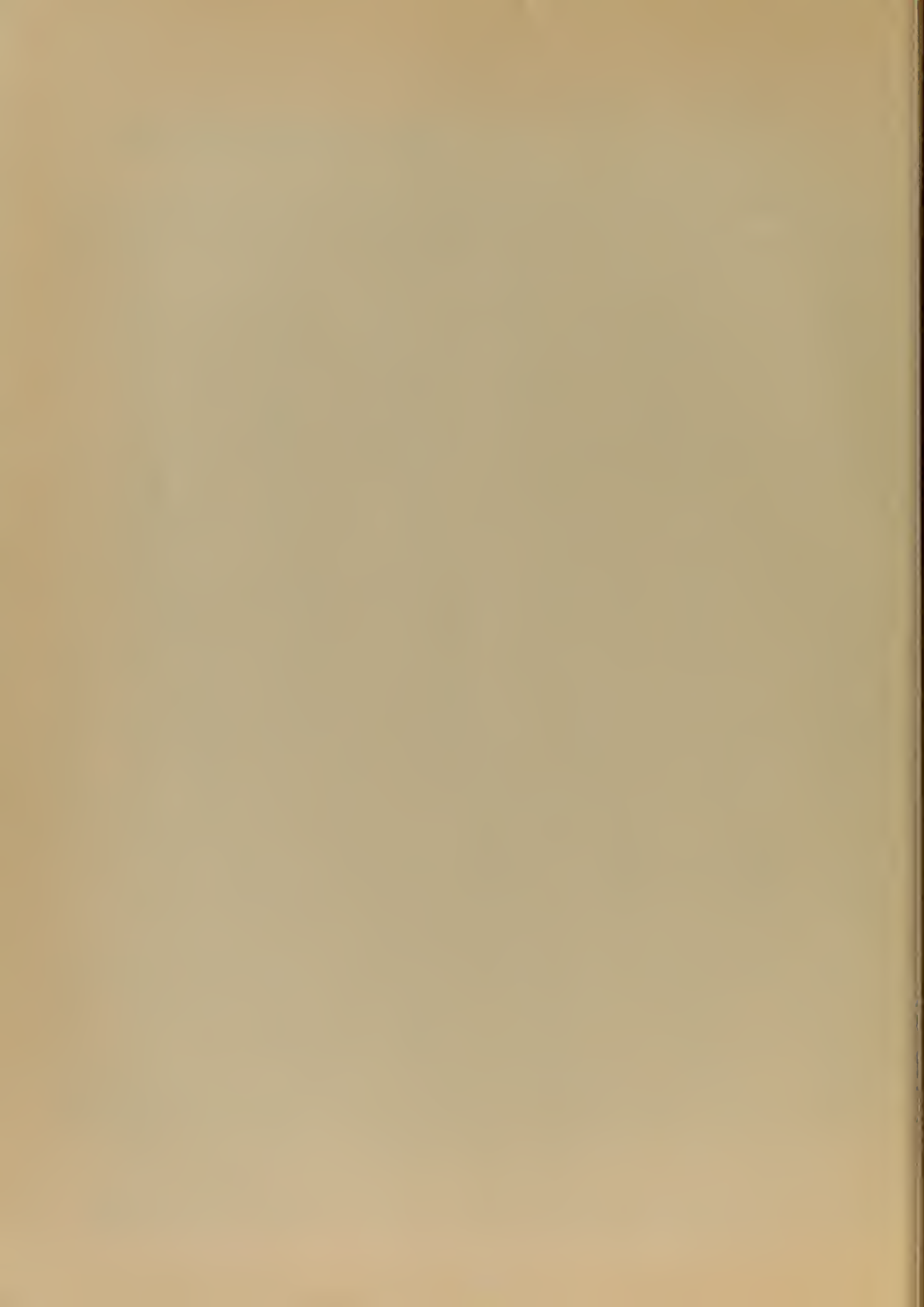


Figure 9, a curve showing the cut-off wavelength of higher order modes as a function of strip width and ground plane spacing, is a result of the computation of Prof. Oliner of Brooklyn Polytechnic Institute. Points falling above the line indicate that the line in question can operate only in the dominant TEM mode and cannot excite higher order modes.

Figure 10 provides the same information as Figure 9, but is presented in terms of maximum frequency, characteristic impedance, and ground plane spacing. The curve was computed at A. I. L. based on the work of Mr. Jasik [28]

The ground plane spacing is limited to less than one half wavelength regardless of the characteristic impedance, because spacings one half wavelength or greater will allow parasitic TEM parallel plate radiation.

Figure 11 shows the results of an experimental test of the effect of parallel plate radiation. The test was conducted with a pair of ground planes with no center conductor and fixed spacing that had a signal of varying frequency impressed between them. From the curve of the insertion loss, it can be seen that there is essentially no propagation until the ground plane spacing approaches one half wavelength. In the example, the ground plane spacing is one half wavelength at 5900 MC.



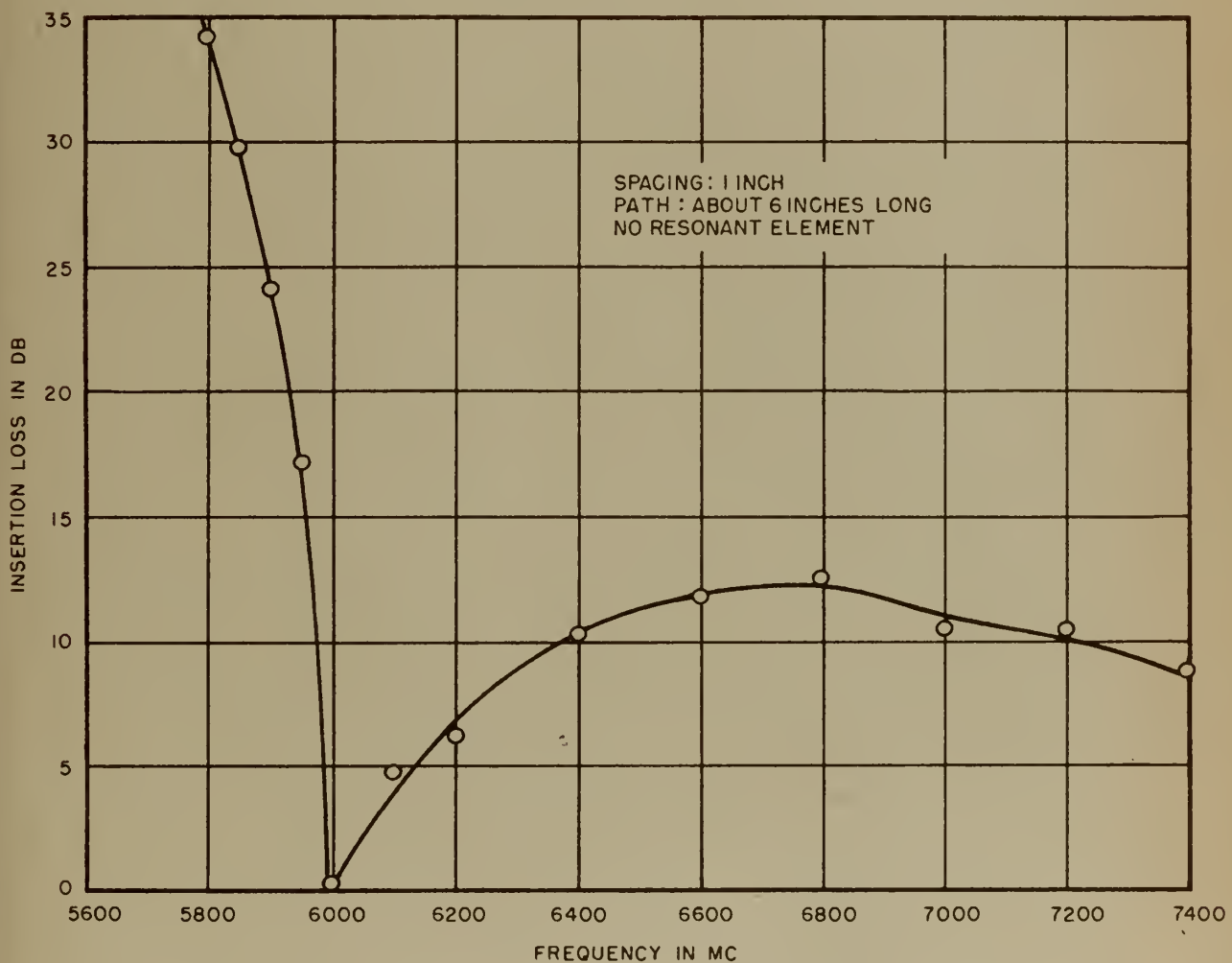
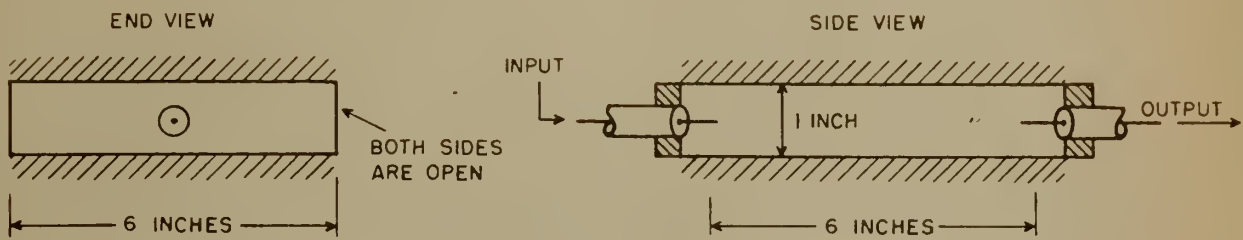
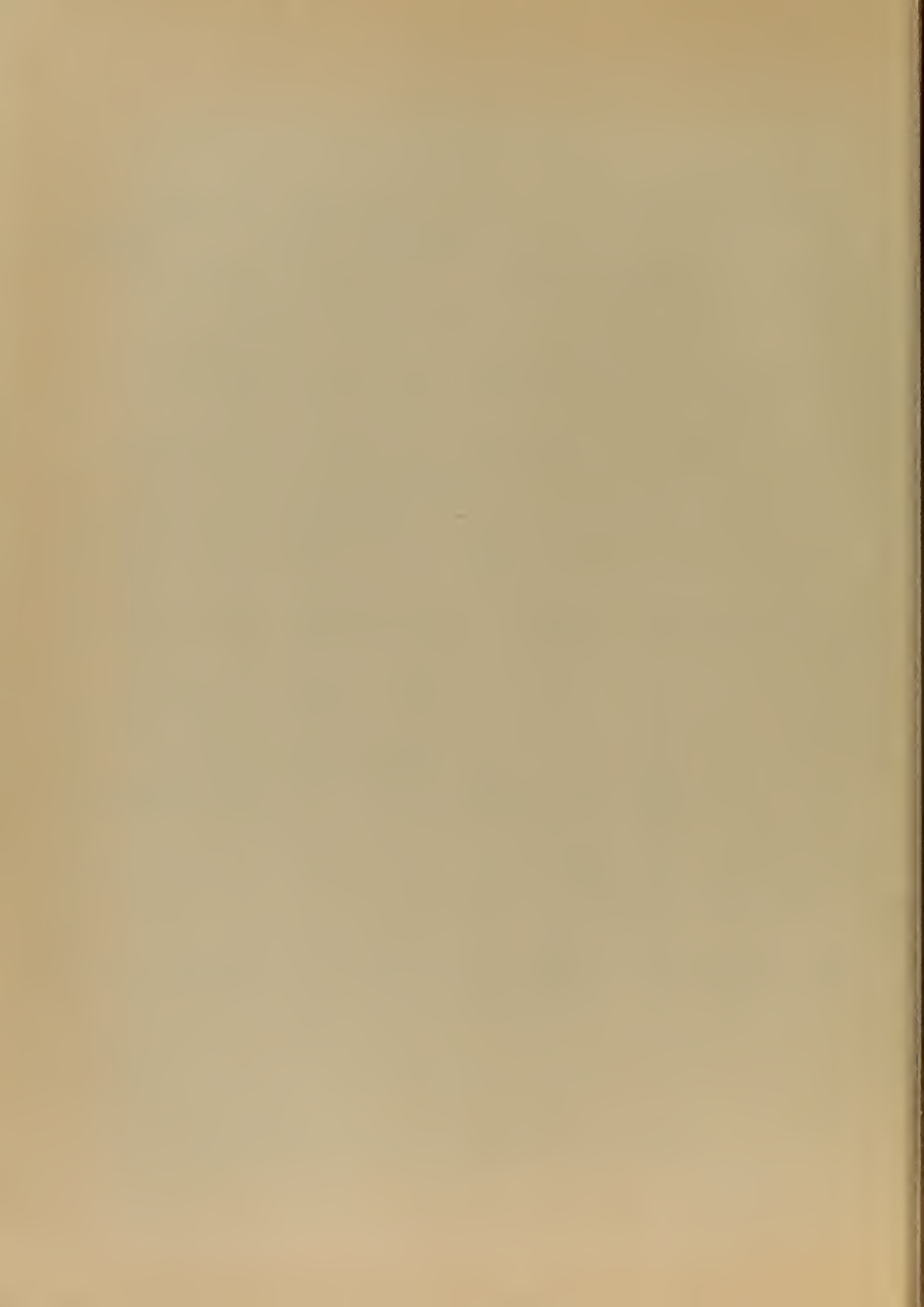


Figure 11. Propogation Between Ground Planes



3. Attenuation.

The attenuation in a strip transmission line results from losses of two types. The dissipation of the center conductor and ground planes due to the surface resistivity of the metal, and the dissipation of the dielectric medium surrounding the center conductor due to the conductance of the dielectric material. The reduction of attenuation is of prime importance in any system designed to transfer energy. Considering the factors that result in the attenuation of a strip transmission line, it should be obvious that the attenuation may be minimized as follows:

1. Select a dielectric material with the lowest possible conductance. This information is given as the loss tangent in the common properties of material tables.
2. Select metals with low surface resistivity for the ground planes and center conductor. The center conductor material is more important due to the higher current density over its surface particularly at the corners. The entire system may be silver plated to insure minimum loss due to the conductor.
3. The center conductor should be made as large as possible, commensurate with the factors that determine its width and thickness, to reduce the loss by increasing the surface area. Thus, reducing the current density at the corners of the strip.
4. The ground plane spacing should be as large as possible within its limits to spread the fields at the surfaces of the ground planes and, thereby, reduce the current density and thus the loss in the ground planes.

The analytic determination of the attenuation is a complex problem



due to the non-uniform current density in the center conductor. However, an elaborate calculation of the attenuation in strip line and sandwich line has been completed by S. B. Cohn. The results, are estimated to be accurate within ten percent for strip line or sandwich line and provide a somewhat optimistic estimate for stripline, and are available in convenient graphical form [14] [15]. The parameters of the graph are characteristic impedance, dielectric constant, thickness of center conductor, ground plane spacing, and frequency. The graph is computed for copper conductors, but may be scaled proportionally to the specific resistivity of any conductor. As an example of the attenuation that may be expected from strip line, a typical value is taken from the graph. The attenuation is 0.0065 DB per foot with a characteristic impedance of 50 ohms, a ground plane spacing of one inch, a center conductor thickness of 0.030 inches and a frequency of 1000 MC.

The validity of the impedance graph has been confirmed by measurement of the Q of resonant elements at A. I. L. and the results are shown in Figure 42. The measurement procedure and relationship between Q and attenuation are discussed in section 9 of Chapter III. Figures 12 and 13 show the measured attenuation of various types of balanced strip transmission lines as a function of characteristic impedance.

4. Velocity of Propagation

Signals are transmitted along a balanced strip transmission line, as they are with any device operating in the TEM or dominant mode, at a velocity equal to the velocity of light in the medium. This is based on the usual assumption that conductors are perfect and the medium in which the wave is transmitted has no conductance. This assumption is valid,



to a close approximation, in normal strip transmission lines, since the conductors employed have been selected mainly for their high conductivity, and the dielectrics have been chosen for low loss. The materials that are generally used for the center conductor are copper and brass. The ground planes are normally made from aluminum. Copper, aluminum, and brass have conductivities that are high enough for most applications, but should a still higher conductivity be required, the system may be silver plated. The materials used to support the center conductor are teflon impregnated fiberglass, expanded polystyrene, and polystyrene since these materials have almost negligible losses.

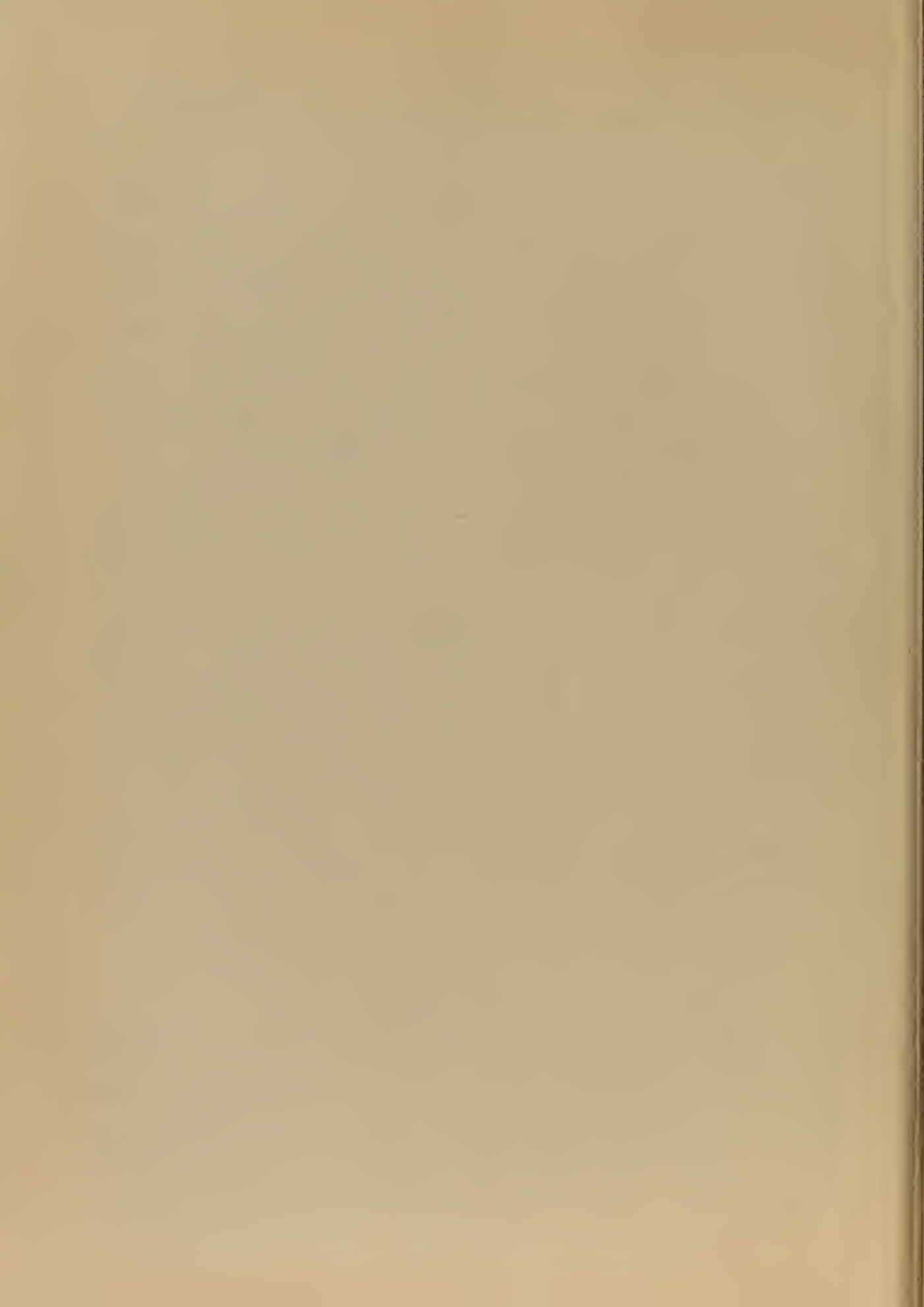
Each type of balanced strip transmission line has special features that effect the velocity of propagation, therefore, they will be discussed individually as follows:

Strip Line. The velocity of propagation along a strip line is for all practical purposes equal to the velocity of light in free space, because it has an air dielectric throughout most of its length. The occasional supports that are required are as small as possible, and are made from low loss materials such as expanded or regular polystyrene

Sandwich Line The velocity of propagation along a sandwich line is equal to the velocity of light in the medium. It is simply derived from the following basic relationship:

$$V = \frac{1}{\sqrt{\mu e}} = \frac{c}{\sqrt{\epsilon_0 \epsilon_r}}$$

Stripline The velocity of propagation along stripline is somewhat less than the velocity of light in free space. An exact analytic determination of the velocity of propagation is complicated due to the indefinite



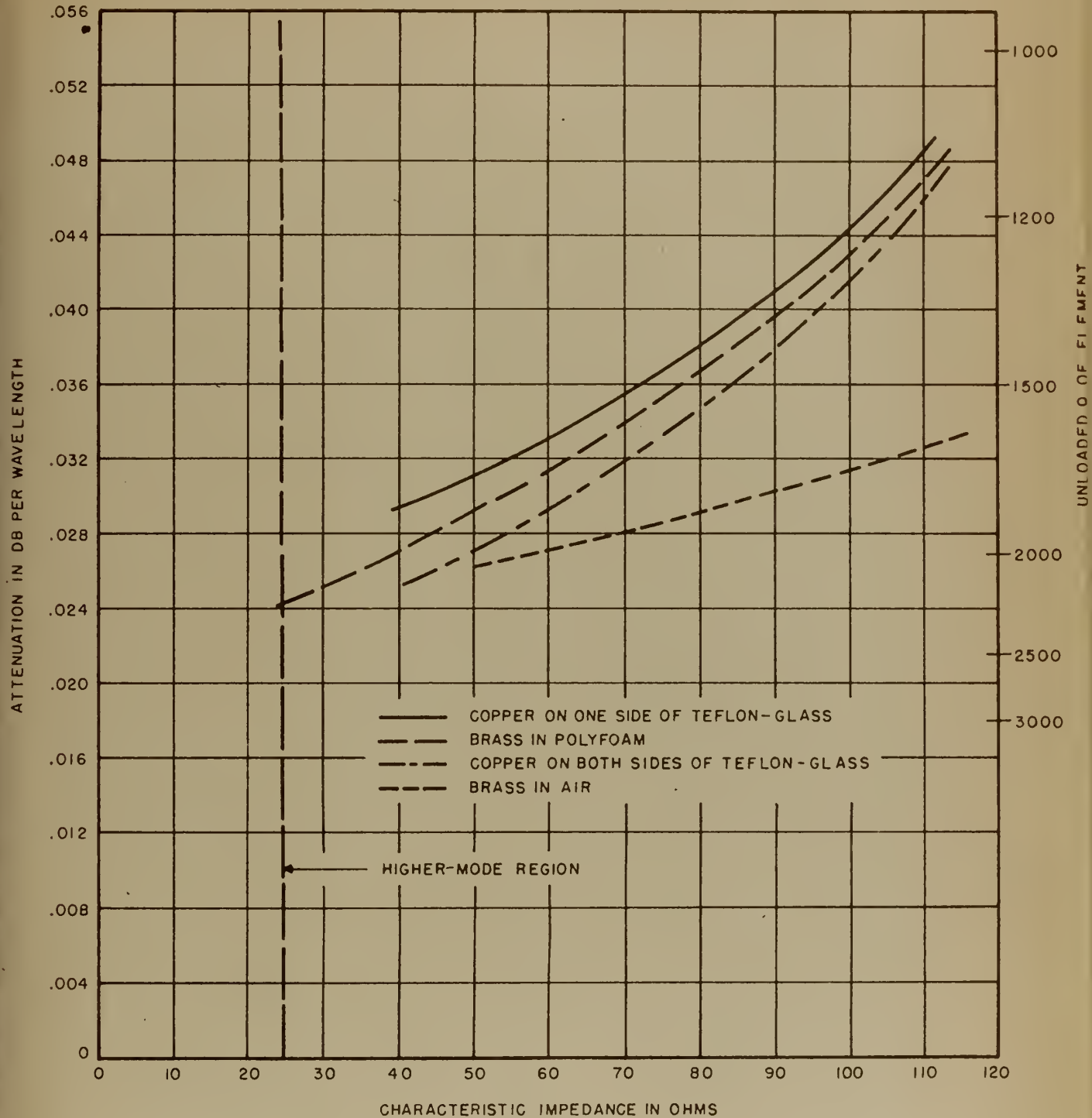
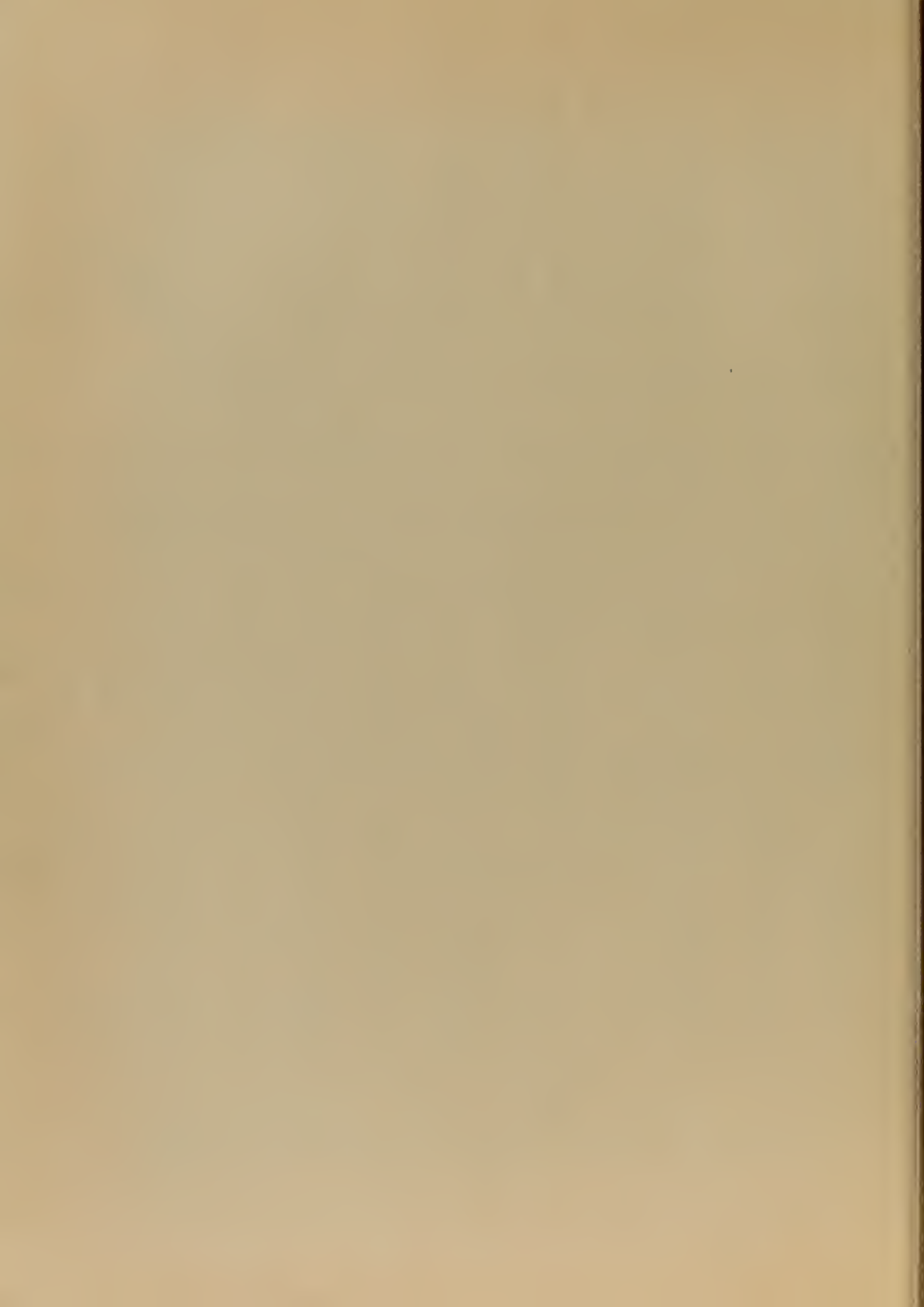


Figure 12. Attenuation of Various Strip Transmission Lines



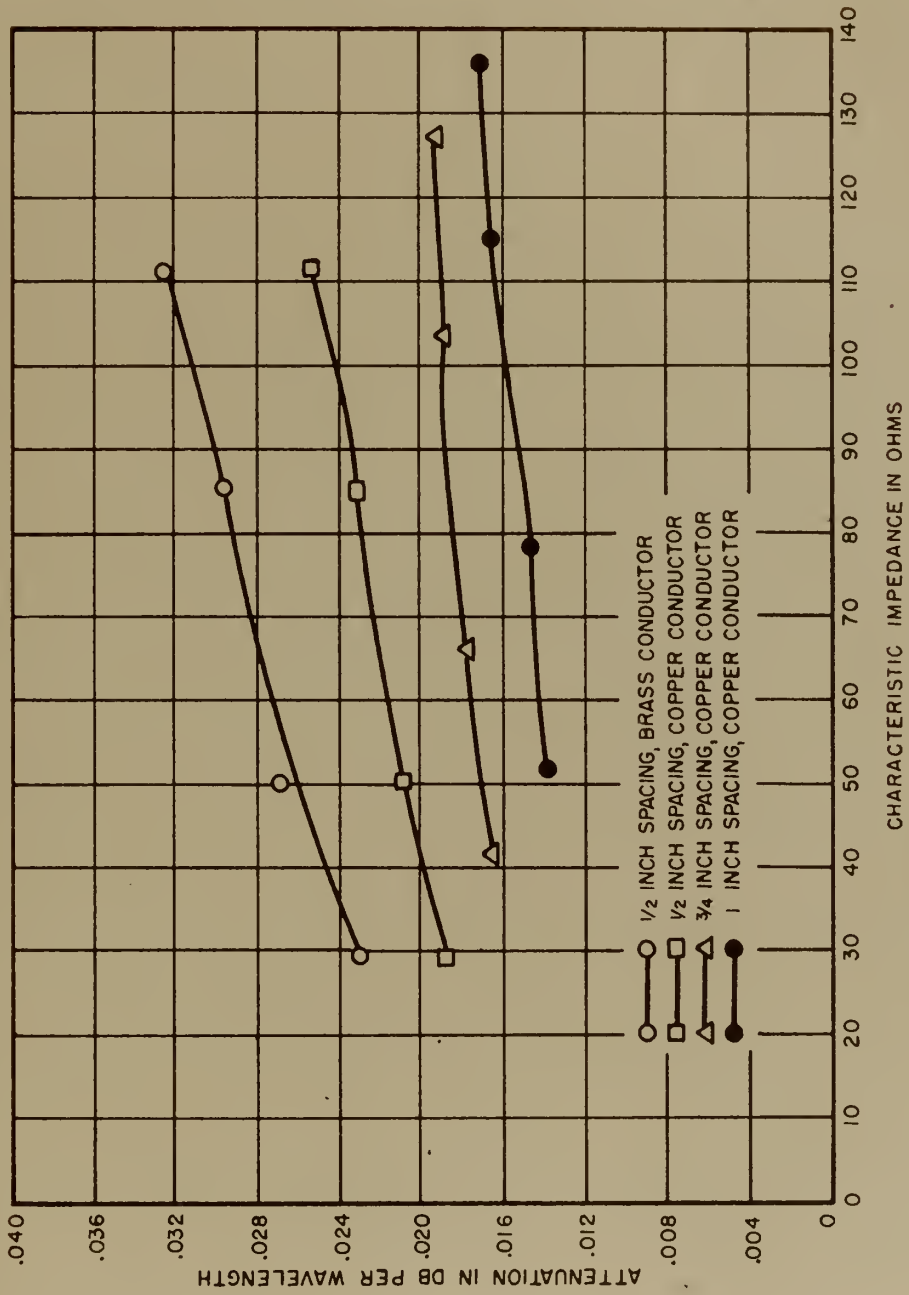
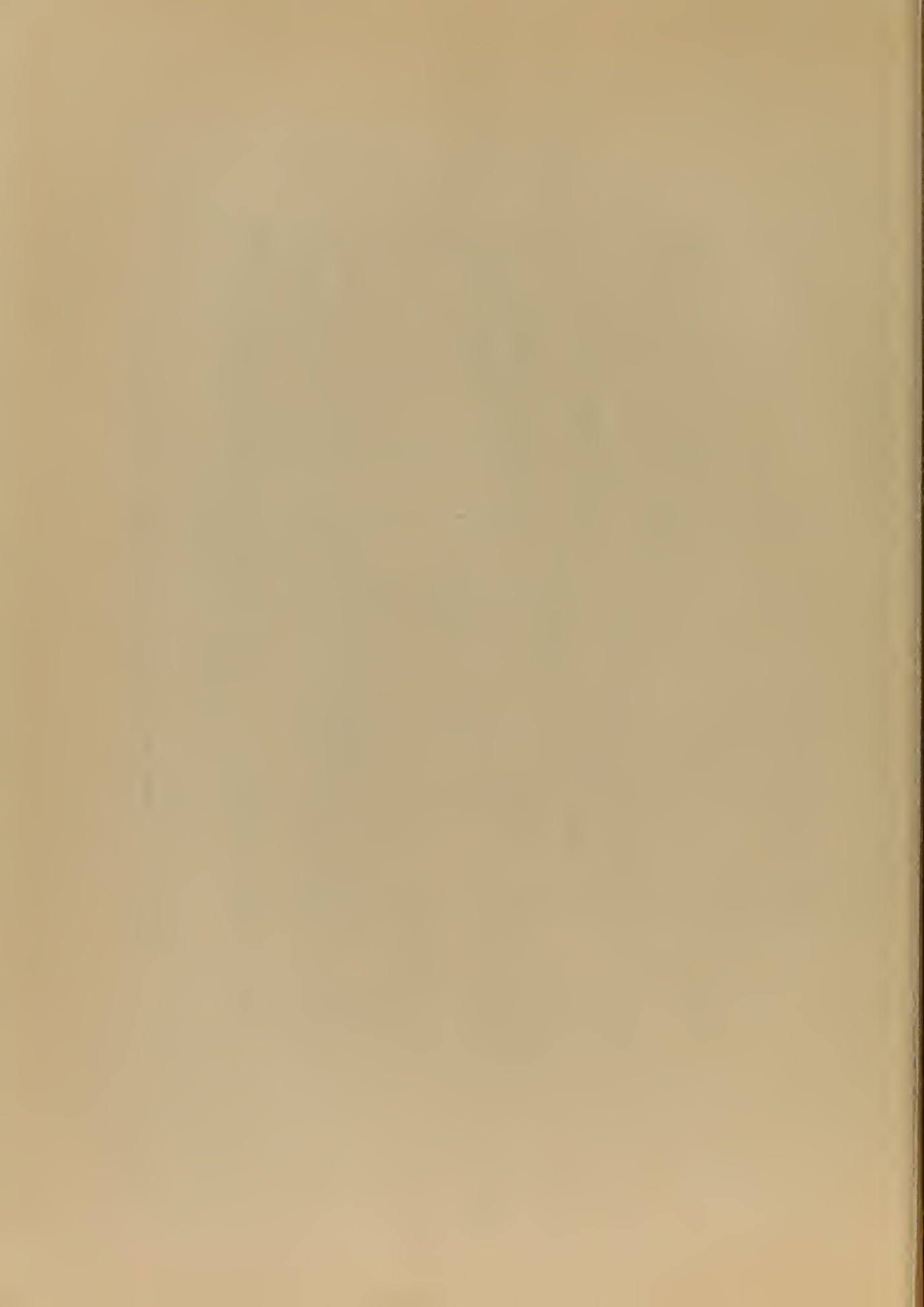


Figure 13. Attenuation Change with Ground Plane Spacing



effect of the thin dielectric that is located in the fringing field of the strip, and since there are other problems of greater importance, the calculation has not yet been made. The velocity of propagation may be readily determined experimentally, however, by measuring the wavelength along the line at a particular frequency. The velocity of propagation is then given by:

$$V = \lambda f$$

The velocity, determined in this manner, has been found to be from two to eight percent less than the speed of light, the exact amount depending on ground plane spacing, characteristic impedance, and thickness of the dielectric sheet. The author made a velocity of propagation measurement in conjunction with the work on the hybrid junction. The condition and results are included here as an example of the effect of the dielectric sheet. With a ground plane spacing of three eighths of an inch, characteristic impedance of 70 ohms, dielectric sheet thickness of 0.020 inches, and a frequency of 5500 MC, the velocity of propagation along the line was four percent less than the velocity of light in free space.

5. Design and Construction

The center conductor is the heart of a balanced strip transmission line. The overall performance of a system depends to a large degree on the accuracy of the layout and the precision of the construction of the center conductor. The techniques to be discussed in this section are applicable to both the solid strip, and the strip made from copper-clad dielectric, i.e., strip line, sandwich line, stripline, and with slight modification of viewpoint, to microstrip.

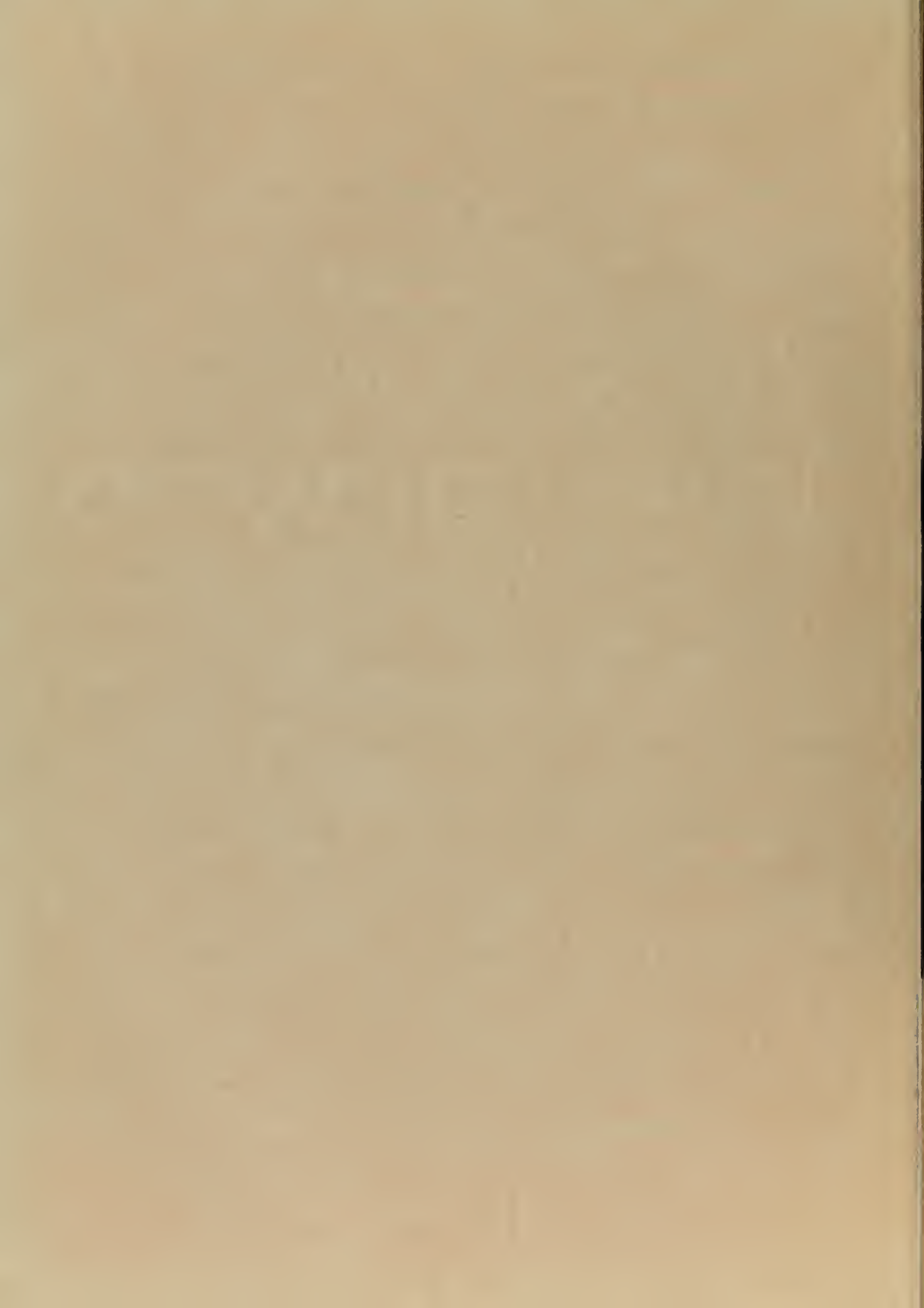
The technique to be employed in forming the center conductor de-



pends on the quantity to be produced. For large quantity production, a photo etching process, identical with that used to produce conventional printed circuit boards, would normally be used. For the production of a few items, or for development work, the center conductor may be produced by hand. Figure 14 illustrates the use of the height gauge to accurately layout a center conductor to be finished by hand. Appendix A contains a brief discussion of the photo etching process, since the technique has become fairly well known, and a detailed discussion of the construction of the center conductor by hand, because the reader probably is not familiar with the technique and it is not published in the literature.

The ground planes used with strip line, stripline, and some forms of sandwich line are usually made from aluminum plate due to its high conductivity and light weight. Plate thickness of from one-eighth to three sixteenths of an inch are normally used to insure sufficient strength to maintain constant spacing throughout the ground plane area.

The support of the center conductor of strip line and stripline may be accomplished by various means. For experimental purposes, where the center conductor is frequently changed, strips of polyfoam cut to fill the space between the center conductor and the ground planes provides a simple support. Figure 26 shows polyfoam supporting a stripline center conductor; the polyfoam used between the upper ground plane and the center conductor has been removed to show the construction of the center conductor. Figure 25 shows a polyfoam support for the strip line center conductor. In this example, a slot was cut in the polyfoam to hold the strip. The strip was not completely encased in the polyfoam, reducing somewhat the effective loss of the system.



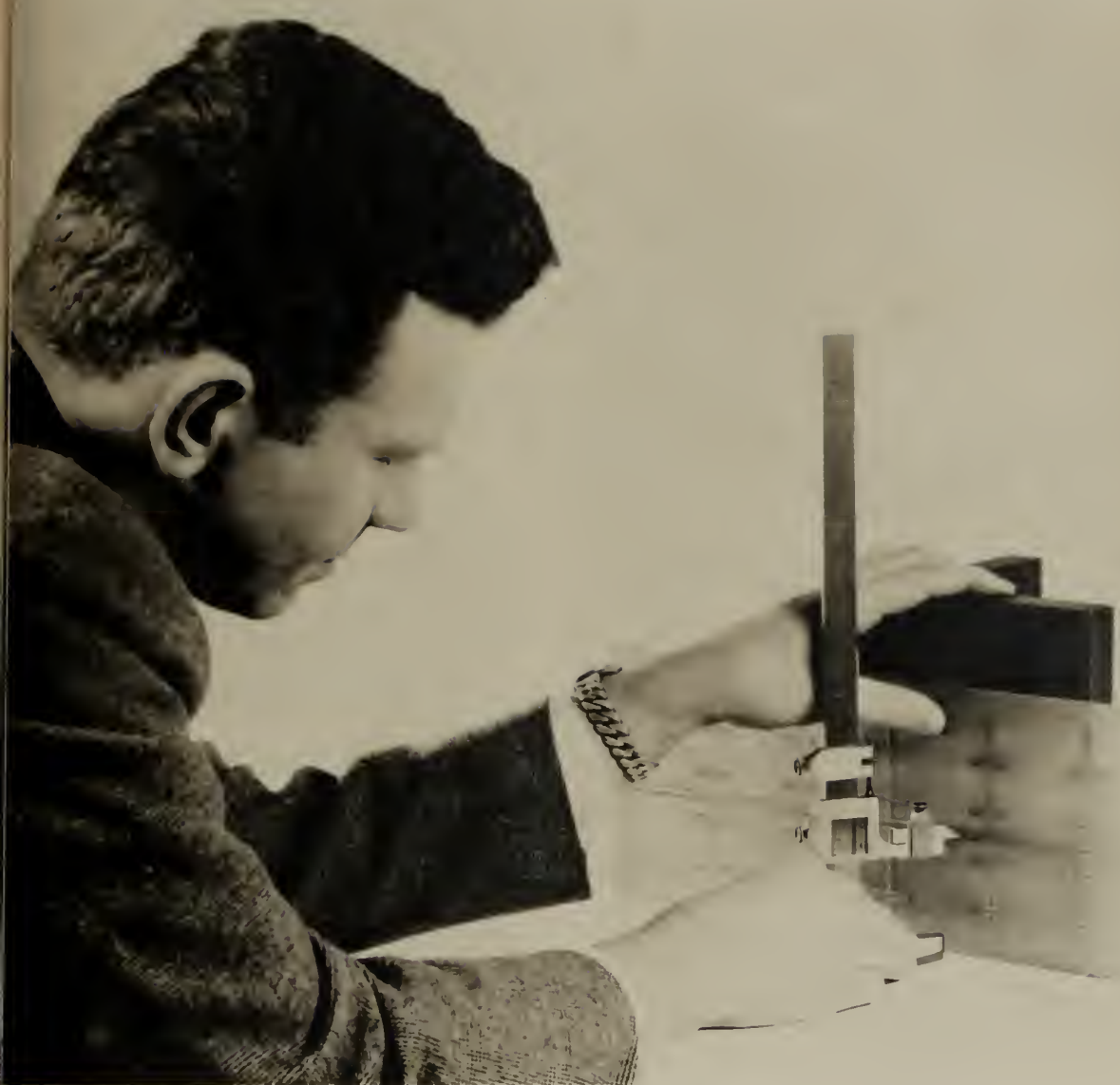


Figure 14. Hand Scribing Center Conductor Configuration
by Use Of Height Gauge



Polyfoam is the almost perfect dielectric. The dielectric constant has been measured as 1.05, and the loss is much lower than that of solid polystyrene. Since polyfoam is in sponge form, it is mainly composed of air with some polystyrene spaced throughout its volume to provide body for the material.

Polyfoam is not suitable for the construction of operational equipment unless special precautions are taken. Since it does not have the strength of the solid dielectrics, it will deform if subjected to shock. The porous structure of polyfoam tends to collect moisture if subjected to high humidity, therefore to preserve the dielectric and loss properties of the entire system, a moisture proof shield is required. Polyfoam is inexpensive and readily available from florists and department stores as well as through standard sources.

More solid permanent supports may be made for strip line from expanded polystyrene or other suitable dielectrics. These supports may be made as solid beads as shown in Figure 37 or as edge supports as shown in Figure 53. To compensate for the change in characteristic impedance due to the dielectric constant of bead supports, the strip may be undercut at the bead. The effect of the supports may also be reduced by using them in pairs with a quarter-wavelength spacing.

Stripline supports are an almost trivial matter. The supports will not effect the operation of the line if they are placed two ground plane spacings from the strip. Therefore, either metal or dielectric blocks of any convenient shape may be used to support the dielectric sheet provided they are located out of the field surrounding the strip.



CHAPTER III

DESIGN AND CONSTRUCTION OF COMPONENTS

1. Transition to Coaxial Line and Waveguide

The transitions to coaxial line and waveguide to be discussed in this section were devised by experimentation after a thorough investigation of the basic principles involved. The method of attack was determined from field configuration, stray capacitance, impedance etc., then the optimum configuration was attained through experimentation by systematically varying the parameters in accordance with expected behavior.

The most common transition is that used to convert from coaxial line to balanced strip transmission line of the same characteristic impedance as shown in Figure 15.

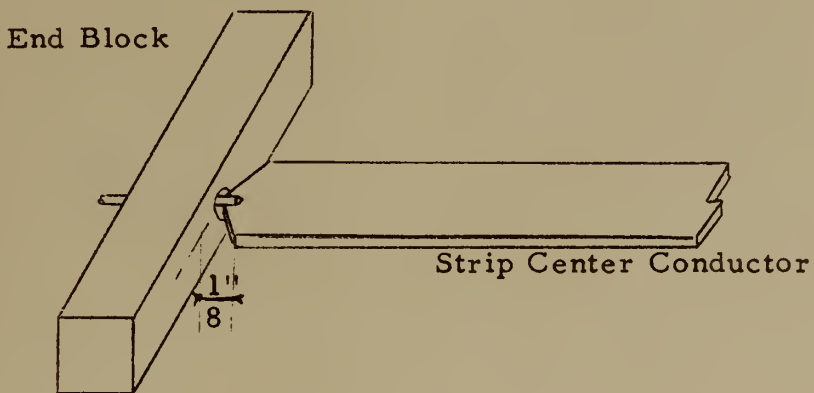


Figure 15. Transition from Strip Transmission Line
to Coaxial Line

This transition had a measured VSWR of 1.05 in the range of impedances 50 to 75 ohms with ground plane spacings of three-eighths to one-half inch frequency 1.8 to 6 KMC. Therefore, this transition may be



used without further consideration within this region or for any non-critical application. However, if precise information is required for a specific transition, the measurement procedure that was used for the above design is given as follows. The required angle of the taper, introduced to reduce the capacitance at the discontinuity, is determined by the method of Deschamps [17] [39]. A sliding load was moved along the coaxial line and impedance measurements were made by probing the fields about the strip. Section 7 discusses slotted lines applicable to this measurement.

S. B Cohn has independently determined and reported [15] that the transition of Figure 15 provides a good impedance match. However, he has determined that the disturbed fields set up by the transition extend along the strip line a distance of approximately twice the ground plane spacing. A more squared off transition has a shorter disturbed field approximately equal to ground plane spacing, but does not provide as good impedance match. The method used by Cohn to make this measurement is novel and is included here for possible use in other situations where the disturbed fields about a discontinuity may be of interest.

An audio signal is applied at the input of the strip transmission line. The field is probed with a strip slotted section whose output detector is tuned to the audio signal. The disturbed field region is indicated by a low output from the detector. The area where the fields are undisturbed is indicated by a high constant output at the detector.

The waveguide to strip line transition shown in Figure 16 was designed in a manner analogous to that of a current loop for power output in waveguide. The pertinent design considerations are:



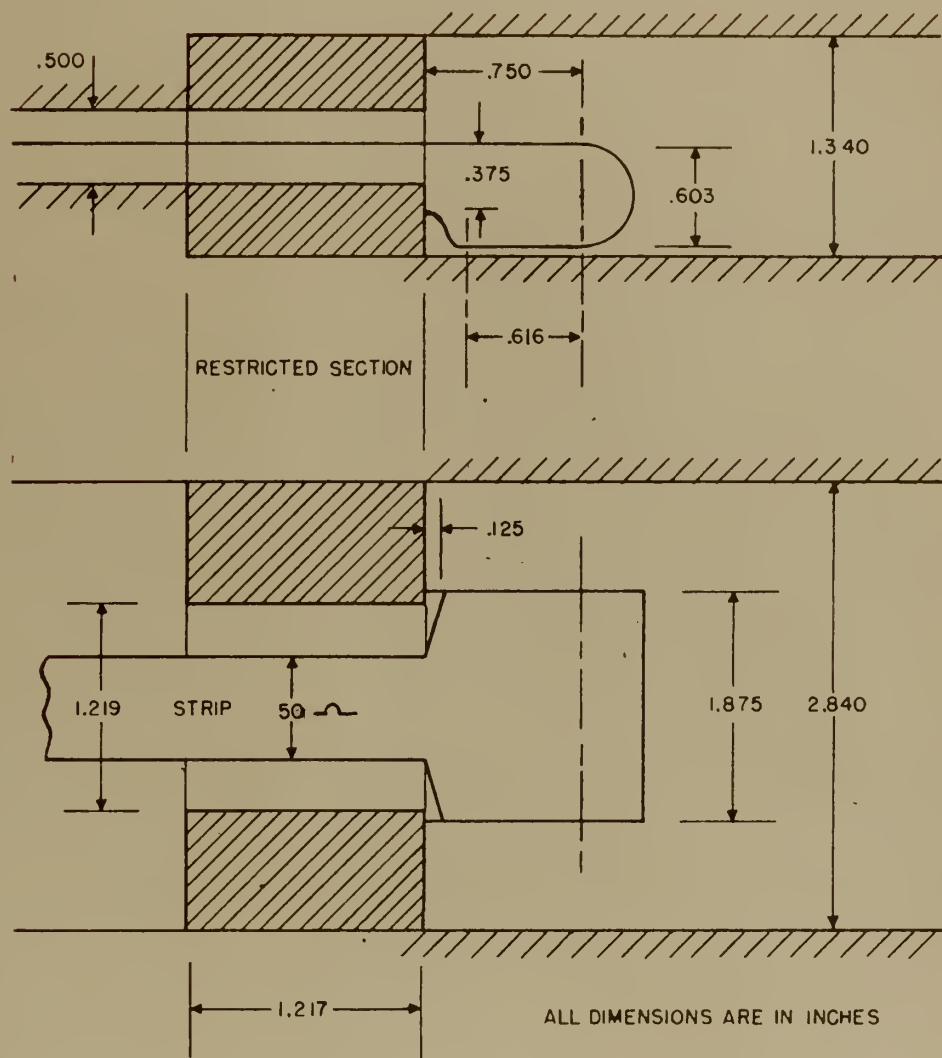
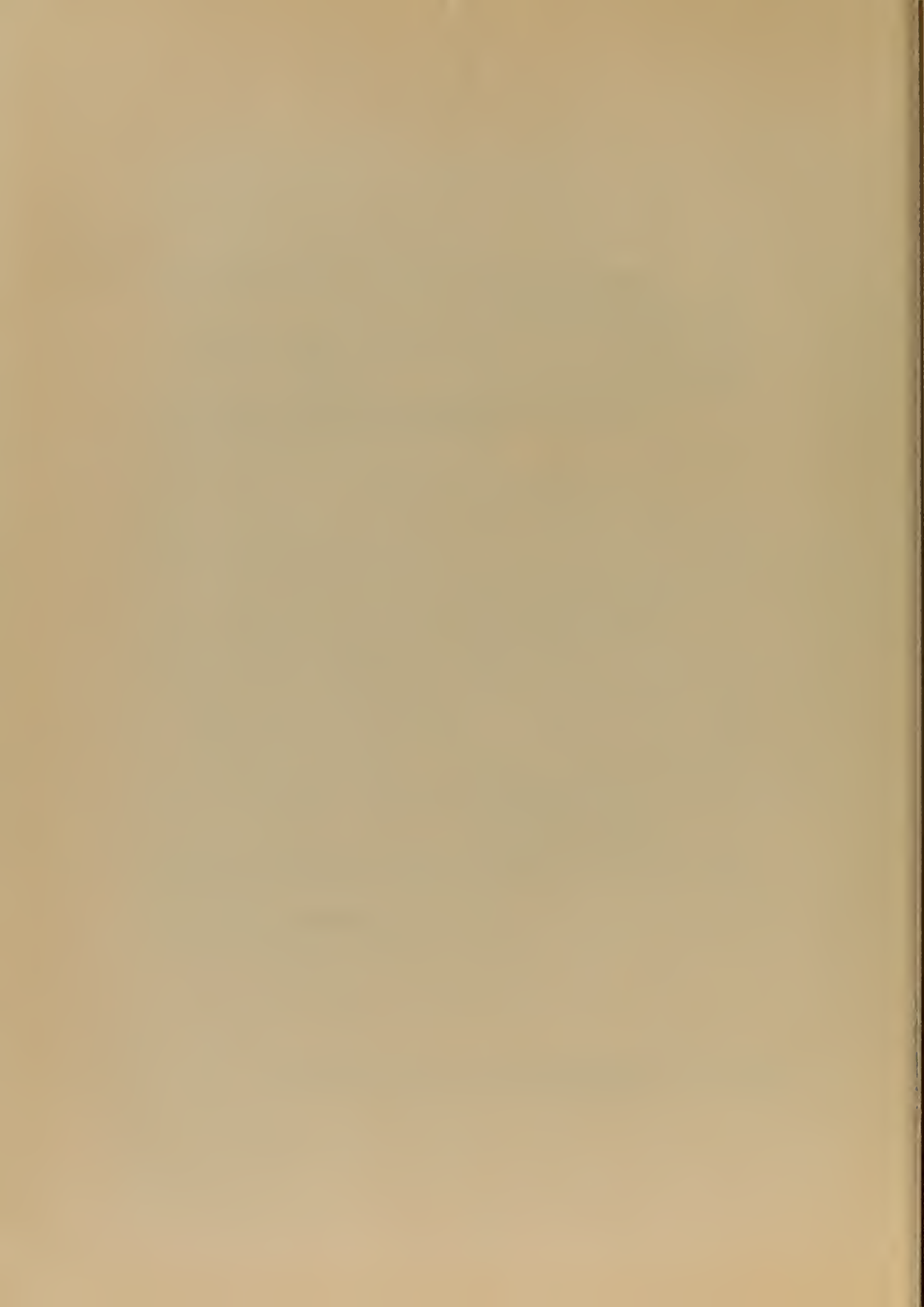


Figure 16. Waveguide to Strip Line Transition



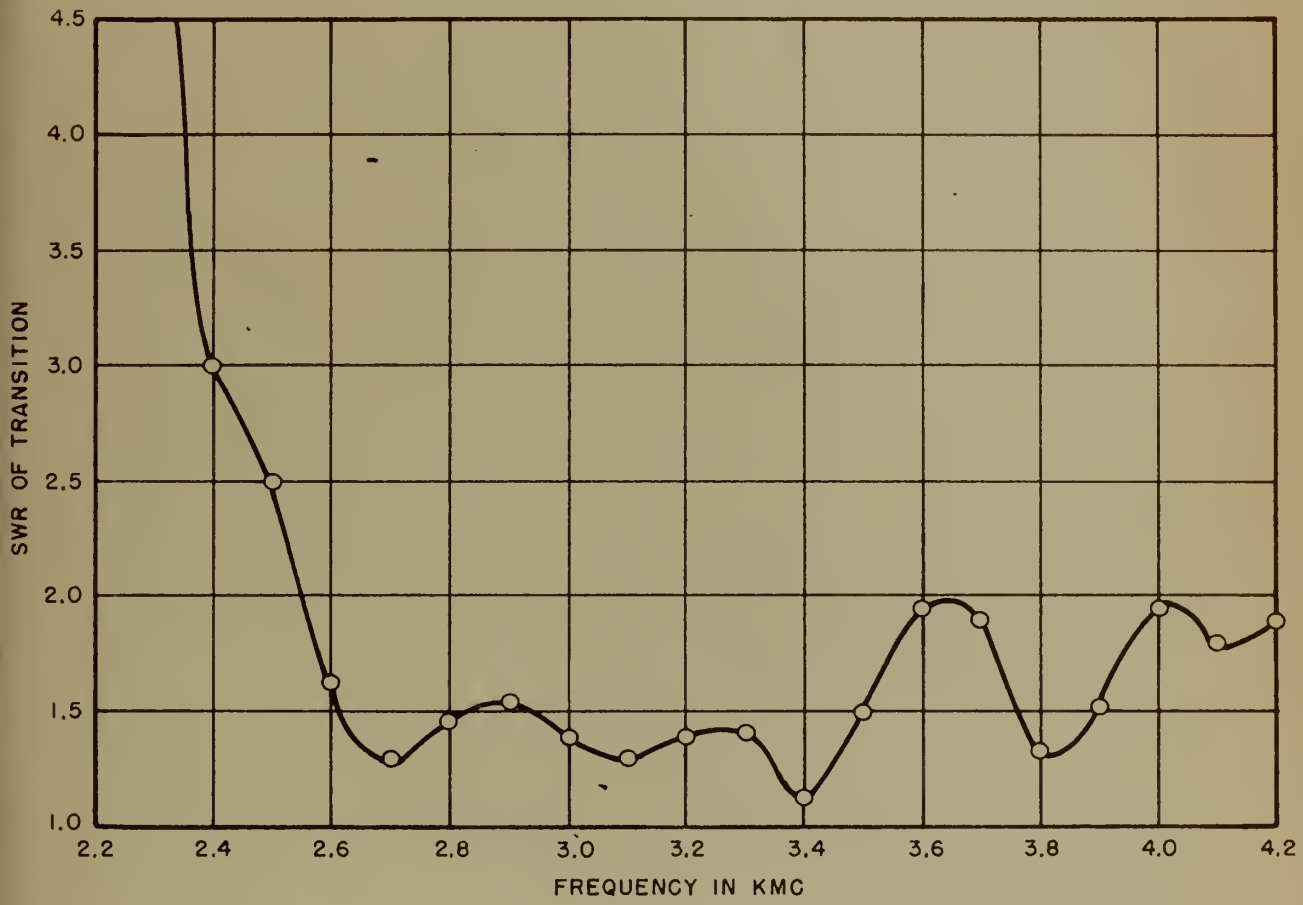


Figure 17. SWR Vs Frequency of Strip Line to
Waveguide Transition



1. to maintain the characteristic impedance of the strip transmission line at 50 ohms. Note the wider section in the waveguide due to the greater ground plane spacing. (Here the top and bottom of the waveguide are considered the ground planes).
2. to prevent propagation of the waveguide mode into the strip line by means of the restricted section which acts both as the strip line transition and a waveguide beyond cutoff for the waveguide mode.
3. to facilitate the removal of the strip line assembly from the waveguide by returning the loop to the removable restricted section. Electrically the loop could have been fastened to the top or bottom walls of the waveguide. This incidentally provides an integral DC return required for crystals etc

The VSWR of the junction with a matched load on the strip line and the measurement made with a conventional slotted section in the waveguide, shown in Figure 17 is seen to be about 1.5 from 2.6 to 3.5 KMC.

Strip transmission line also may be coupled to waveguide by means of the coaxial transition discussed earlier in the section and a conventional waveguide to coaxial transition (usually a probe in the waveguide). This type of transition is shown in Figure 37.

All the previously mentioned transitions were coupled to the edge of the strip transmission line, so that electrical balance of the system was maintained. Often it is convenient to couple power through the ground planes to permit effective use of the outer surfaces of the ground planes for mounting tubes, components etc. Figure 52 illustrates the effective use of one outer surface of a pair of ground planes for mounting the



equipment associated with a strip line system. A coaxial connection through the ground planes may be made directly by passing the coax center conductor through the ground plane and connecting it to the strip line at a right angle as shown in Figure 18, or by placing a strip line to coaxial transition in the proper position between the ground planes, then coupling through one of the ground planes with a coaxial right angled bend. The direct connection, although simple to construct, induces a special problem. The lead from one side of the strip destroys the balance of the strip line and tends to propagate parallel plate modes between the ground planes. This undesired propagation may be reduced by the use of mode suppressors, i.e., the 1/4 diameter spacers shown in Figure 18. The mode suppressors form short waveguides beyond cut-off and thus reduce the spurious radiation. Figure 19 shows the SWR in the coax with a matched strip line load as a function of frequency.

2. Matched Loads and Attenuators

At microwave frequencies, loads and attenuators perform the functions of resistors and potentiometers which cannot be used unless special precautions are observed. The large physical size of a resistor or potentiometer compared to the wavelength introduces an unknown reactance and thus prohibits, for all practical purpose, the use of conventional resistances or potentiometers in microwave networks.

An attenuator, like a resistor, is used to dissipate the incident energy, but due to the characteristics of a high frequency network, care must also be taken to insure that there is little or no reflection. Loads and attenuators may be readily constructed for use with balanced strip transmission line after considering the following basic requirements.



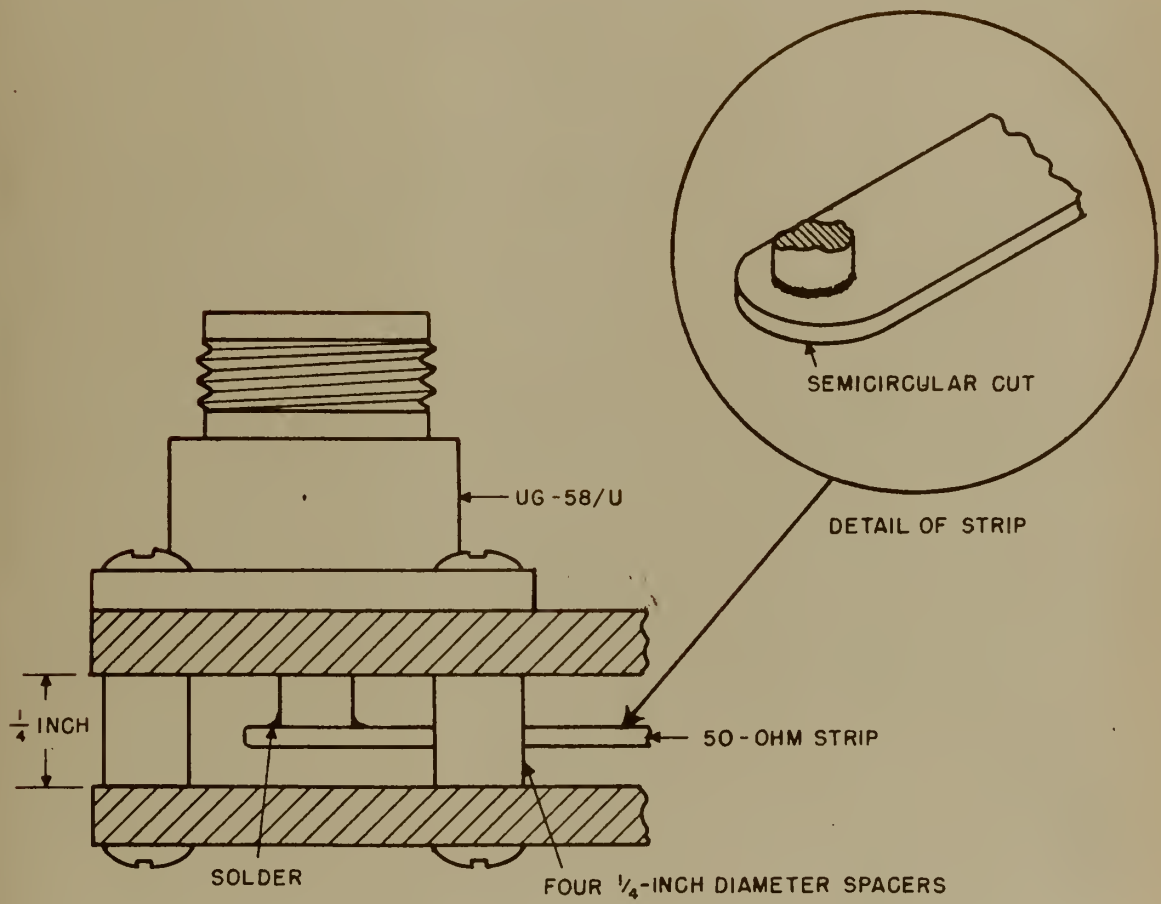
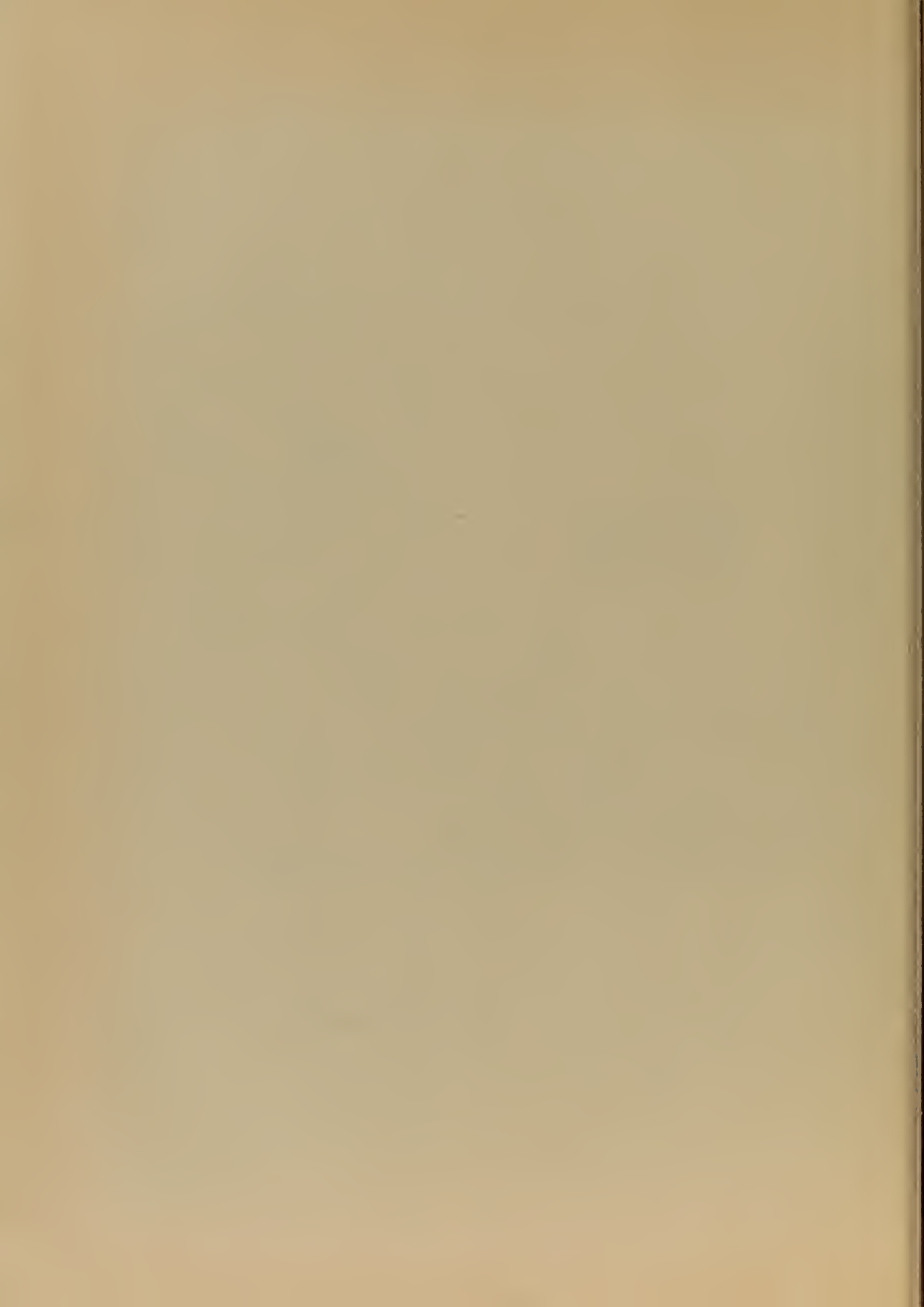


Figure 18. Coaxial to Strip Line Transition



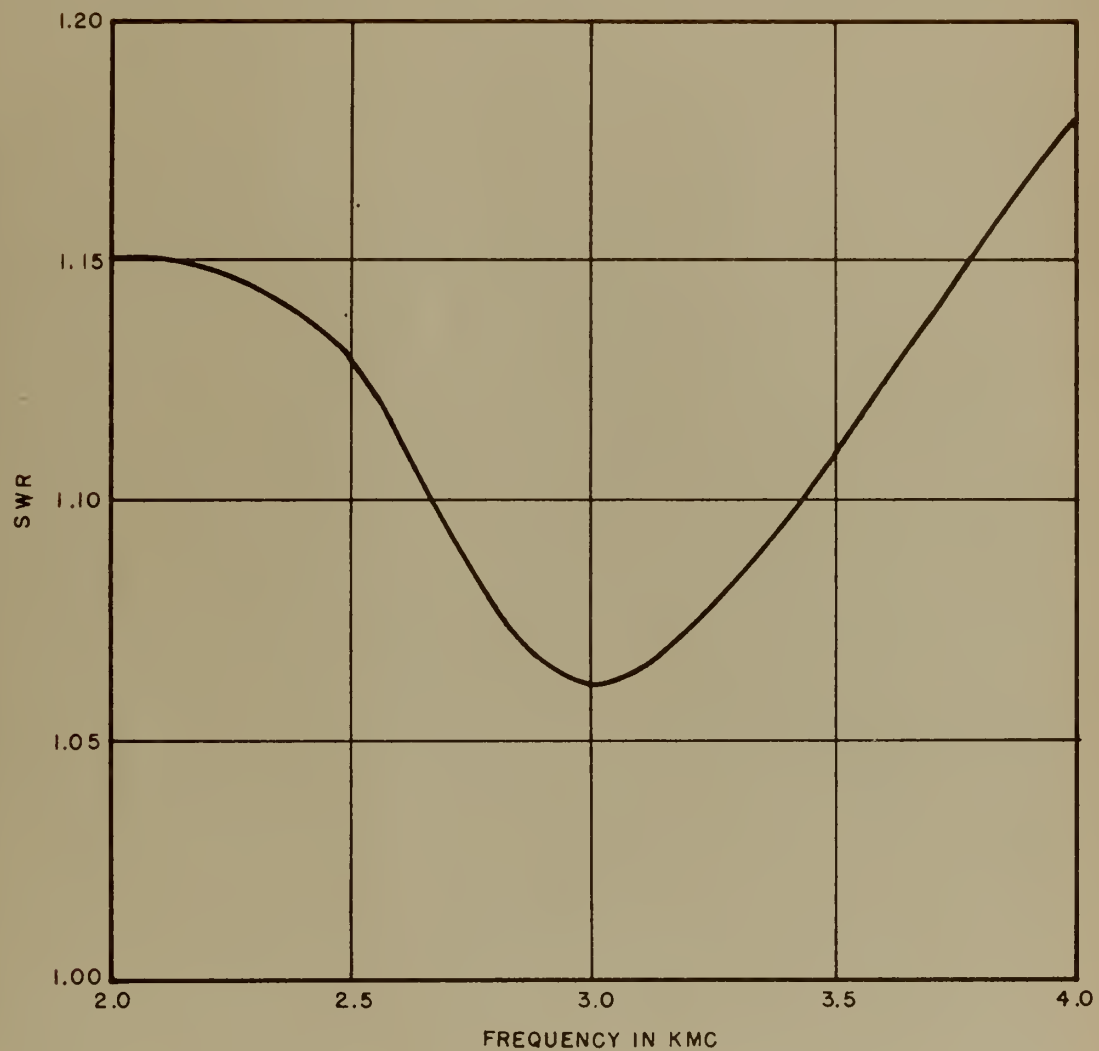


Figure 19. SWR of Coaxial to Strip Line Transition



1. Place the load or attenuator in the region of greatest field strength.
2. Construct the load or attenuator from a material that induces high loss to the incident energy.
3. Shape the load or attenuator so that it will gradually attenuate the incident wave and thus minimize reflection.

One of the many possible types of loads that may be constructed is shown in Figure 20. It will be noted that the load was designed in accordance with the basic concepts of load design. The main portion of the load is concentrated between the strip and the ground planes, the region of greatest field strength. The material used for the load is polyiron, which has excellent loss characteristics at microwave frequencies. The long narrow taper of the load, pointed in the direction of the oncoming wave, provides a means of gradual attenuation. The large block at the end, filling the space between the ground planes, provides mechanical strength as well as loss. Three of these loads are shown in Figure 55 as they were used in connection with a hybrid junction measurement.

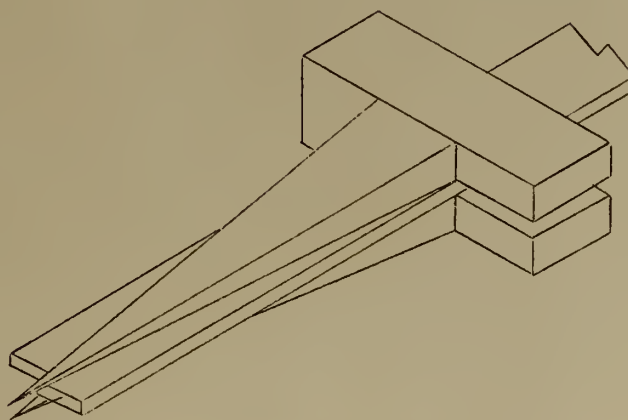


Figure 20. A Polyiron Load with a VSWR of 1.02

The load could also have been constructed with the point of the taper



centered between the ground plane and the strip, forming long narrow pyramids above and below the strip. This form should exhibit a lower reflection due to its more gradual taper.

A fixed attenuator, to dissipate part of the incident power and transmit the remainder, is designed in the same manner as a load, but in this case, the lossy material should not fill the space between the ground planes and the strip. A fixed attenuator is shown as part of the system of Figure 53. The flat diamond shaped piece of lossy material that is bolted to the opened ground plane is the lower half of the attenuator.

A variable attenuator, to attenuate a controllable amount of power, is constructed in accordance with the basic attenuator design requirements with a mechanical means of adjusting the amount of lossy material that is inserted in the region of strong electric field. Figure 53 shows three identical, rotary variable attenuators that result in a low SWR due to the gradual manner in which the lossy material is inserted over the strip.

The polyiron material, mentioned in the preceding portions of this section, is made from a mixture of powdered iron and aralydite. The attenuation and machinability of this material relies upon the compounding and curing of the ingredients. A detailed discussion of the loss characteristics and method for preparing polyiron that was developed at A. I. L. is provided in Appendix B.

Although polyiron may be used for satisfactory loads and attenuators in most applications, there are other materials that may be more convenient. I. R. C. resistance cards may be used singly or stacked to approximate the load shapes that have been previously discussed

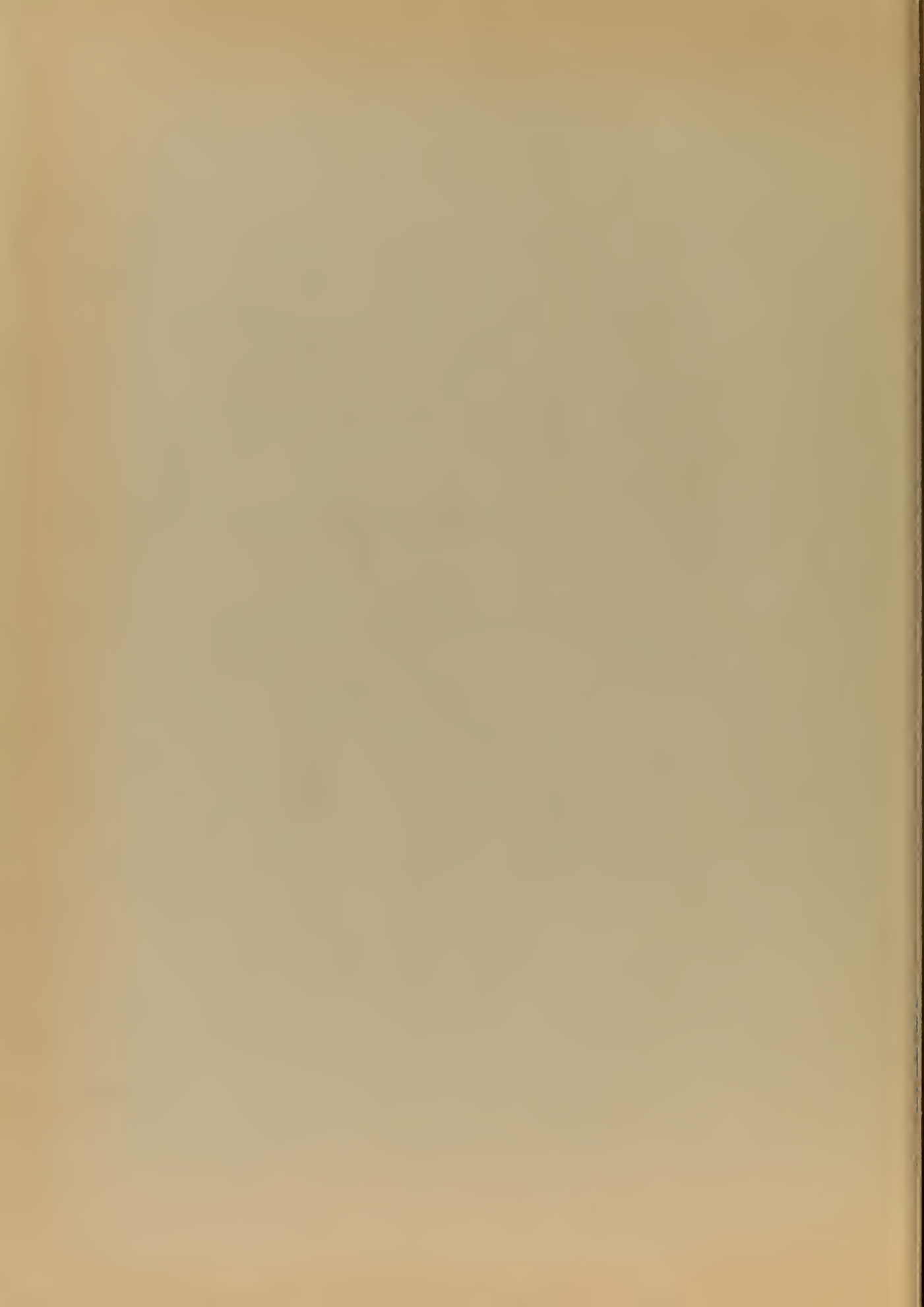


in this section. Since the loss is not as high as that of polyiron, loads made from resistance cards tend to become quite large. A load with a VSWR of 1.02 at 3,000 MC had a length of approximately six inches, which is twice the length of a comparable polyiron load. Resistance paper or cloth may be used for temporary loads by cutting out a trapezoidal section and winding it around the center conductor so that it forms a flattened cone. The paper or cloth should be wound until there is a gradual taper from the center conductor to the ground planes. A load was rapidly constructed from the black paper that accompanies photographic film and exhibited a resistance of 5000 ohms per square area. It had a VSWR of 1.3 at 5000 MC and certainly could have been improved if more care had been taken in its construction or if material with a higher loss had been used.

The loads and attenuators that have therefore been discussed consisted of lossy material in the region around the strip. This type is most commonly encountered, however the use of a high resistance center conductor should not be overlooked. For instance, the center conductor of a system may be extended by a length of nicrome of the same cross section to provide a matched load, or a fixed amount of attenuation may be attained by replacing a section of the center conductor with nicrome [40].

3. Bends in the Center Conductor

In a strip transmission line network, it is usually necessary to have center conductors which turn corners to properly connect the components of the network. It has been found that a square or uncompensated right angle bend introduces a theoretical and measurable VSWR of approxima-

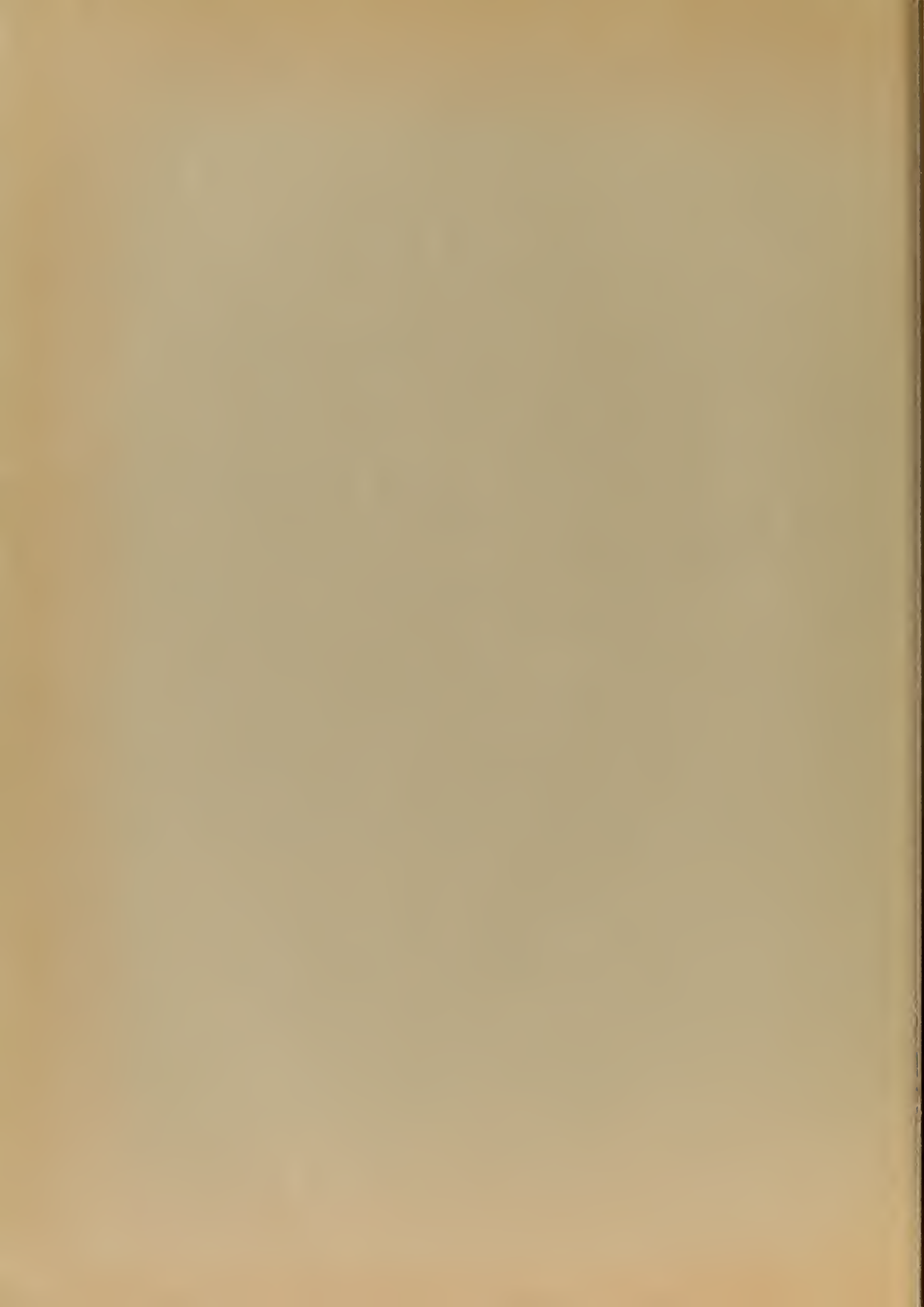


tely two, due to the added capacitance at the corner [34]. It would appear that if the sharp corner was replaced by a gradually rounded turn, the harmful effect of the corner would be removed. A rounded corner does reduce the reflection to a negligible value, but only when the radius of the turn is greater than five times the width of the strip. A much simpler and more effective means of reducing the discontinuity at a bend is to truncate the corner. Several apparently independent investigations [1] [29] [34] have shown that essentially reflectionless bends, i.e. VSWR's of 1.04 can be made in all four types of strip transmission lines for right angle bends with properly truncated corners.

The proper cut for minimum reflection for any angled bend up to 90° is determined by drawing lines from the inside corner to the outer edge. These lines should meet the outer edge of the strip at right angles. Then draw another line across the corner connecting the points where the first two lines intersected the outer edge of the strip. Cut off the corner along this line, and a virtually reflectionless bend is completed. Following this procedure, a right angled bend would have the corner cut off at a 45° angle. Should an angle of greater than 90° be required, two of the aforementioned bends can be used and placed in close proximity.

4. Tees and Power Dividers

With strip transmission line, power may be readily divided from one main arm to two or more side arms. In designing a tee or power divider, the pertinent considerations are the input impedance, the proper division of power, and the compensation of the discontinuity at the junction.



An impedance match at the input of a tee or power divider is obtained by having the sum of the characteristic conductances of the side arms equal to the characteristic conductance of the input arm. It must be realized, however, that with a simple tee, it is impossible to have an impedance match at all the arms [31]. The hybrid junction can be used in situations where this is required. In fact, the hybrid junction may have received the name "magic tee" from the fact that it is a tee matched at all arms.

The power delivered to each arm relative to the power in the input arm is given by the ratio of the input characteristic conductance to the characteristic conductance of each arm.

The problem of the discontinuity at the junction of a tee has been studied to a limited extent. Experimentally it has been found that a matched tee junction introduces a discontinuity and thus sets up a standing wave in the input arm. The discontinuity is due to additional capacitance caused by the large center conductor area at the junction. It may be removed by cutting a notch in the center conductor at the intersection of the two arms as shown in Figure 21.

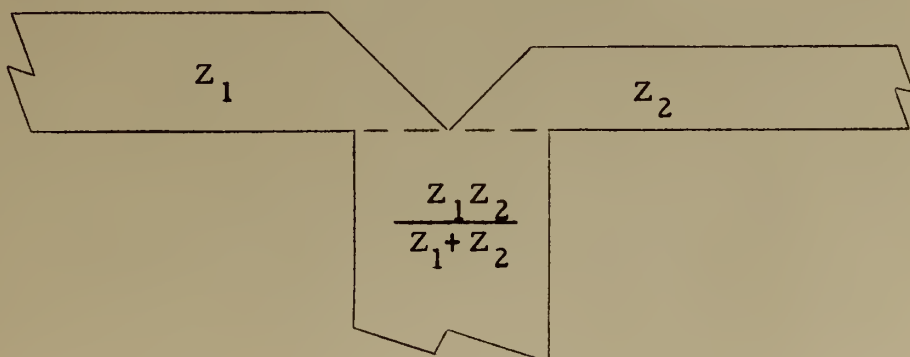
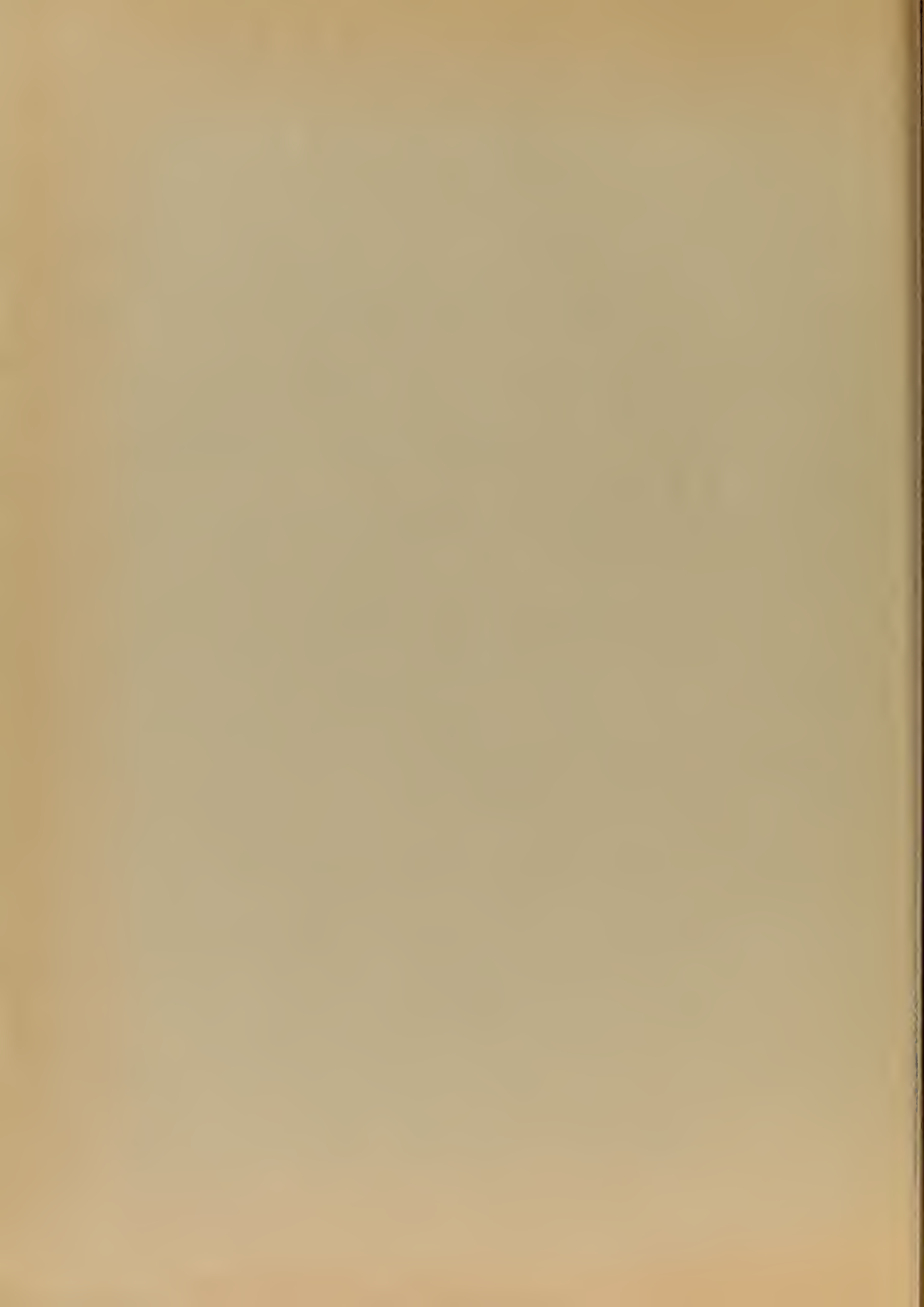


Figure 21. A Compensated Tee Junction



The proper size for the notch may be determined experimentally. Work at A. I. L. has shown that a 90° notch across the width of the side arms provides a reasonable input impedance match. If the reader desires to pursue this problem further in an analytical manner, an equivalent circuit has been derived and is available in reference [34].

A study of tee junctions is in progress at Stanford Research Institute and should be completed and available in the near future [15].

5. Line Impedance Transformers.

The familiar quarter-wave transformer provides a convenient means of transforming the impedance of one transmission line to match the impedance of another line or component. A single quarter-wave transformer furnishes a perfect impedance match at a single frequency, if its impedance is chosen as the geometric mean of the input and output line impedances, and the effect of the discontinuity is properly compensated. To provide an impedance match over a wide band of frequencies, a series of quarter-wave transformers or a tapered section may be employed. The impedance of each section of the series of quarter-wave transformers must be properly chosen to obtain the minimum variation of impedance over a wide range of frequencies. The selection of the natural logarithm of the ratios of adjacent impedance, in accordance with the terms of binomial expansion, has long been considered the proper method of design for a series of quarter-wave transformers [25]. An improved type of design that utilizes the terms of the Tchebyscheff polynomial [13] will be discussed here, since it can be shown analytically that the Tchebyscheff design will, for a given SWR, provide maximum bandwidth or for a given bandwidth, provide minimum SWR.



Figure 22 is a full size sketch of a Tchebyscheff design of a series of transformers. The complete design of this example and complete design information for a series of transformers in accordance with the terms of the Tchebyscheff Polynomial will be found in Appendix C .

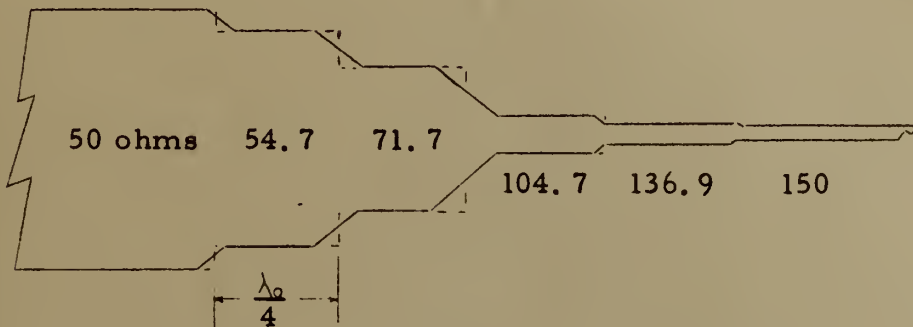


Figure 22. Tchebyscheff Design of a Series of
Quarter-wave Transformers

The effect of the discontinuity at the steps may be reduced if the corners are removed. Limited experimental investigations have indicated that a corner cut off at a 45° angle, as shown in Figure 13, reduces the effect of the discontinuity to a negligible value.

A direct comparison of computed and measured behavior of the Tchebyscheff design with strip transmission line is not available at this time. However, a comparison has been made with the coaxial line and the results given below are considered to be directly applicable to strip transmission line.

A three section, four step, coaxial line impedance transformer operating in the frequency range of 1,000 to 2,000 MC with

$$Z_{n+1} = 112.2 \text{ ohms and } Z_1 = 46.3 \text{ ohms}$$

The maximum VSWR computed was 1.034



The maximum VSWR measured was 1.045

The maximum VSWR was also computed for the binomial distribution and was 1.11.

The tapered section does not provide as good an impedance match as a series of transformers over a band of frequencies. However, it is mentioned here because it is simple to construct. All that is required is a linear taper from one strip width to the other. With a taper, minimum reflection occurs when the length of the taper is a multiple of a half-wavelength. An example of the results attained from a taper, returning again to coaxial line data, is:

Frequency range two to one

Taper length of 1.5 wavelengths (Equivalent of six quarter-wave sections)

Input and output impedance ratio of 1.63

Maximum SWR of 1.13

6. Stub and Capacitive Tuners.

A strip transmission line may often be used in conjunction with components, such as crystal detectors, that have input resistances and reactances which are different from the characteristic impedance of the line. An abrupt change of impedance must be corrected in any microwave system, and with strip transmission lines, there are several methods, either fixed or adjustable, that are available to compensate for the effects of impedance discontinuities. The methods are, in general; single or multiple stubs, capacitive screws or eccentrics, and gaps or holes in the center conductor. These are discussed individually

2
1

as follows:

Single or multiple stubs The tuning or matching stubs which are used with strip transmission line are like those used with coaxial line. Shunt stubs are most common because all that is required is a simple coplanar perpendicular extension of the center conductor. Fixed stubs are generally terminated in an open circuit since a stub with an open circuit termination may be simply etched or otherwise cut out when the center conductor is formed. The length, characteristic impedance, and position of single or multiple stubs may be determined by standard transmission chart techniques.

A stub of fixed length and impedance but adjustable in position may be made from a small block of metal with a slot cut in one end. This will allow the block to be slipped over the edge of the center conductor. The thickness of the block must be considered in determining the characteristic impedance of the strip.

Capacitive screws and eccentrics The impedance of a strip transmission line may be varied by changing the capacitance between the center conductor and the ground planes. In strip transmission lines, impedance changes of this type are usually used when it is desirable to do the tuning or matching after the system is completed. This is done by placing machine screws through the ground planes over the center of the strip; thus allowing the depth of penetration of the screw to be adjusted from the top of the ground plane. Or it may be accomplished by having eccentric discs of dielectric or metal that may be rotated from above the ground planes so that the area of the disc over the strip is smoothly variable.



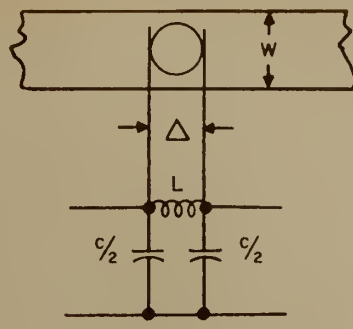
The eccentric may be somewhat more difficult and costly to manufacture, but due to its symmetry above and below the center conductor, it does not interrupt the balance of the line [8] [32]. Figure 12 of reference [8] is a sketch of capacitive tuning screws and a graph of the variation of response of a resonant element with tuning. Figures 9 and 10 of reference [32] illustrate the configuration and use of eccentric dielectric tuning elements.

Gaps or holes in the center conductor Tuning or matching of a fixed nature may be accomplished by cutting a hole or placing a gap in the center conductor. The effect of holes and gaps has been computed by Oliner and verified by measurements made at A. I. L. [29] [34]. The references give both the design considerations of Oliner and the unique measurement procedure used at A. I. L. Figures 23 and 24 provide the values of the reactances of a pi representation of a round hole in a balanced strip transmission line.

7. Slotted Sections.

Slotted sections are the most versatile measuring devices available to the microwave engineer. They are simple to construct in balanced strip transmission line and may be used in either the development of strip components or with conventional microwave components, when standard slotted sections with the desired characteristic impedance or frequency range are not available. Conversion from the strip slotted section to conventional components may be made with any of the transitions discussed in section 1. There are two types of strip slotted sections, the end probe shown in Figure 25 and the slotted ground plane





EQUIVALENT CIRCUIT

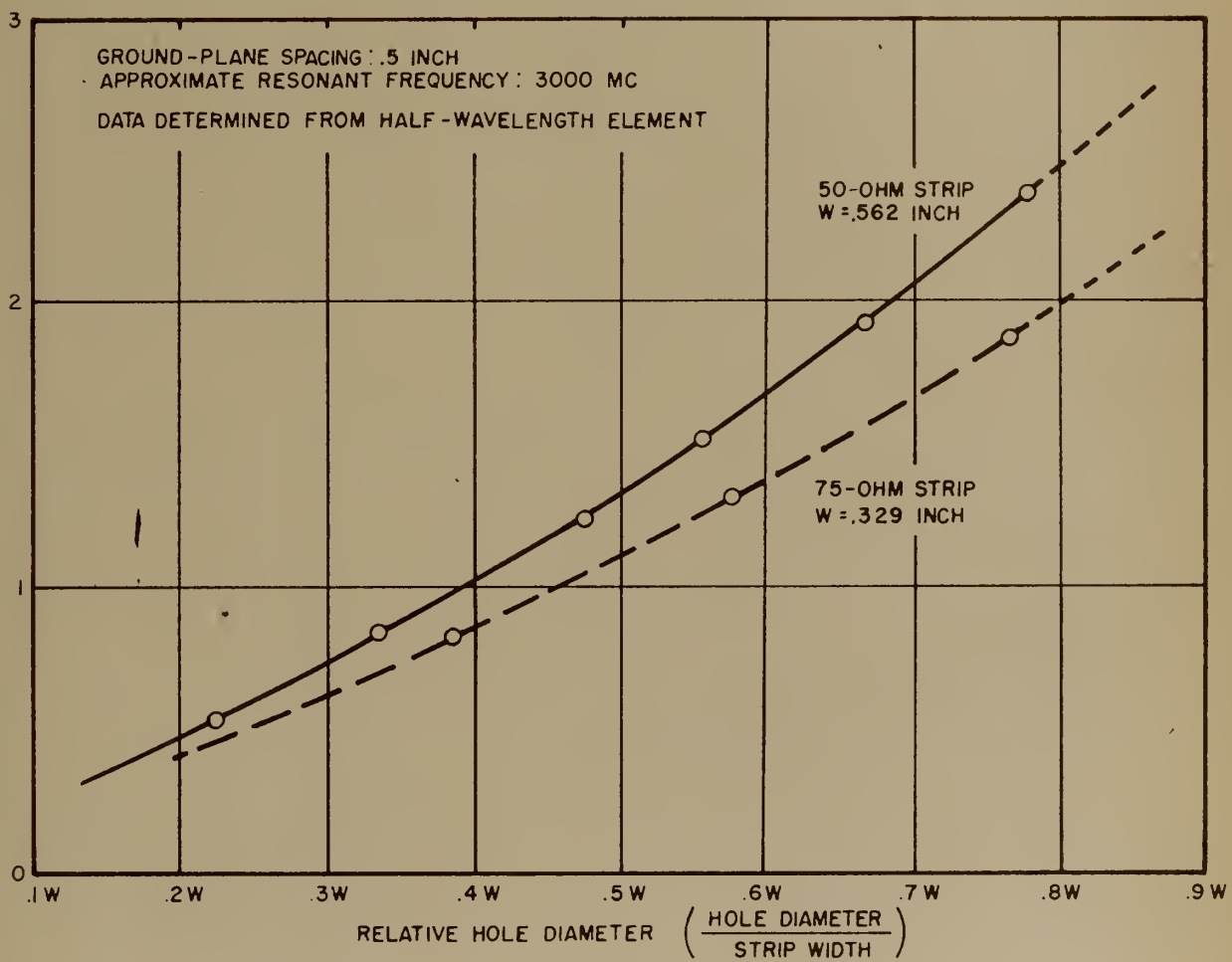


Figure 23. Series Inductance of Round Hole in the
Center Conductor



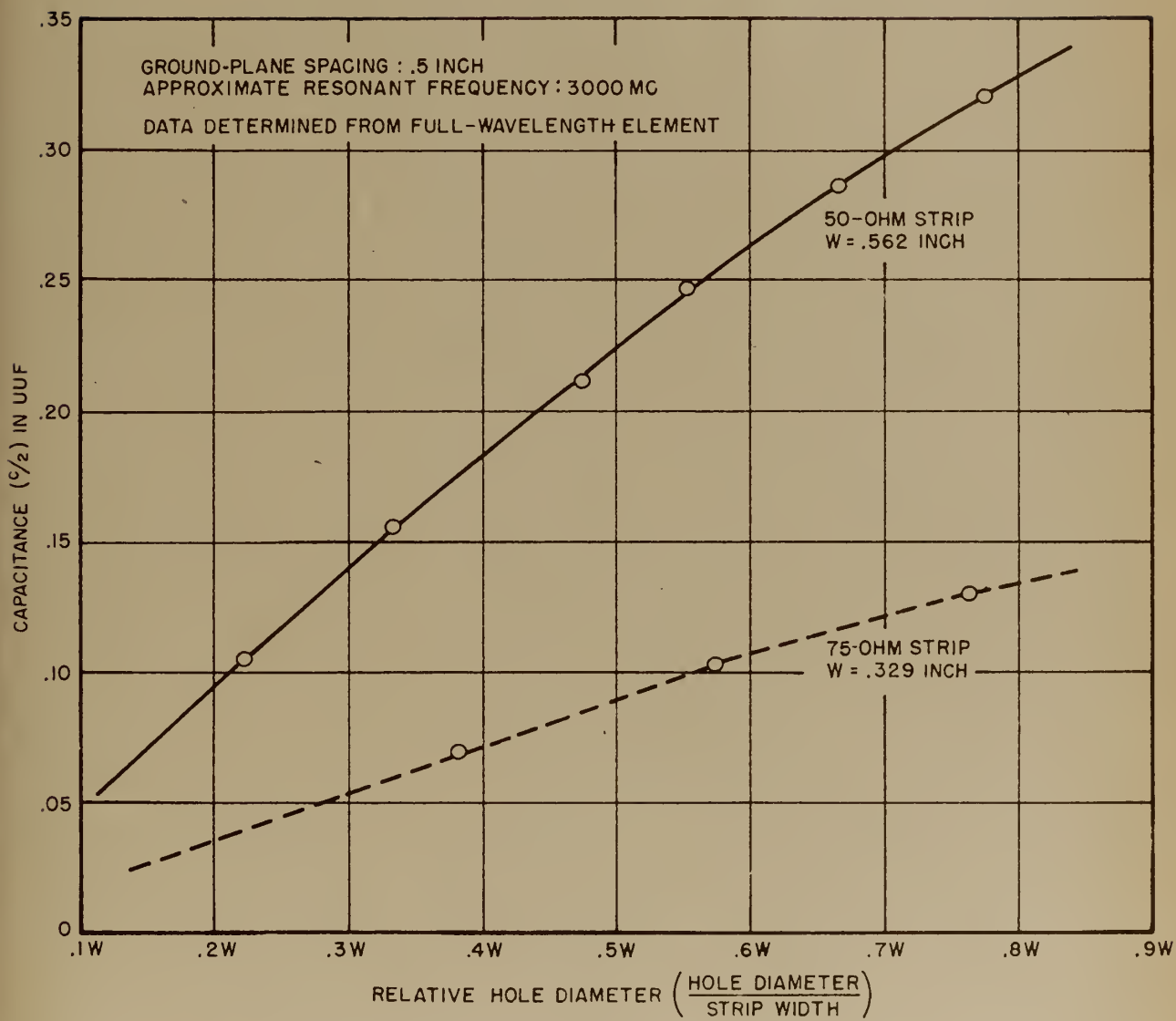
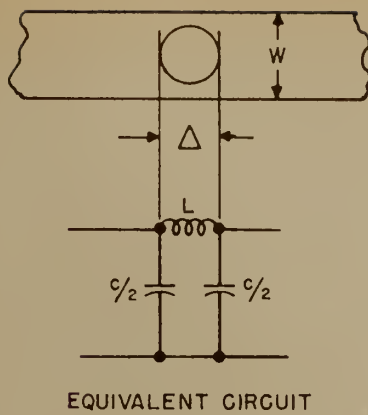


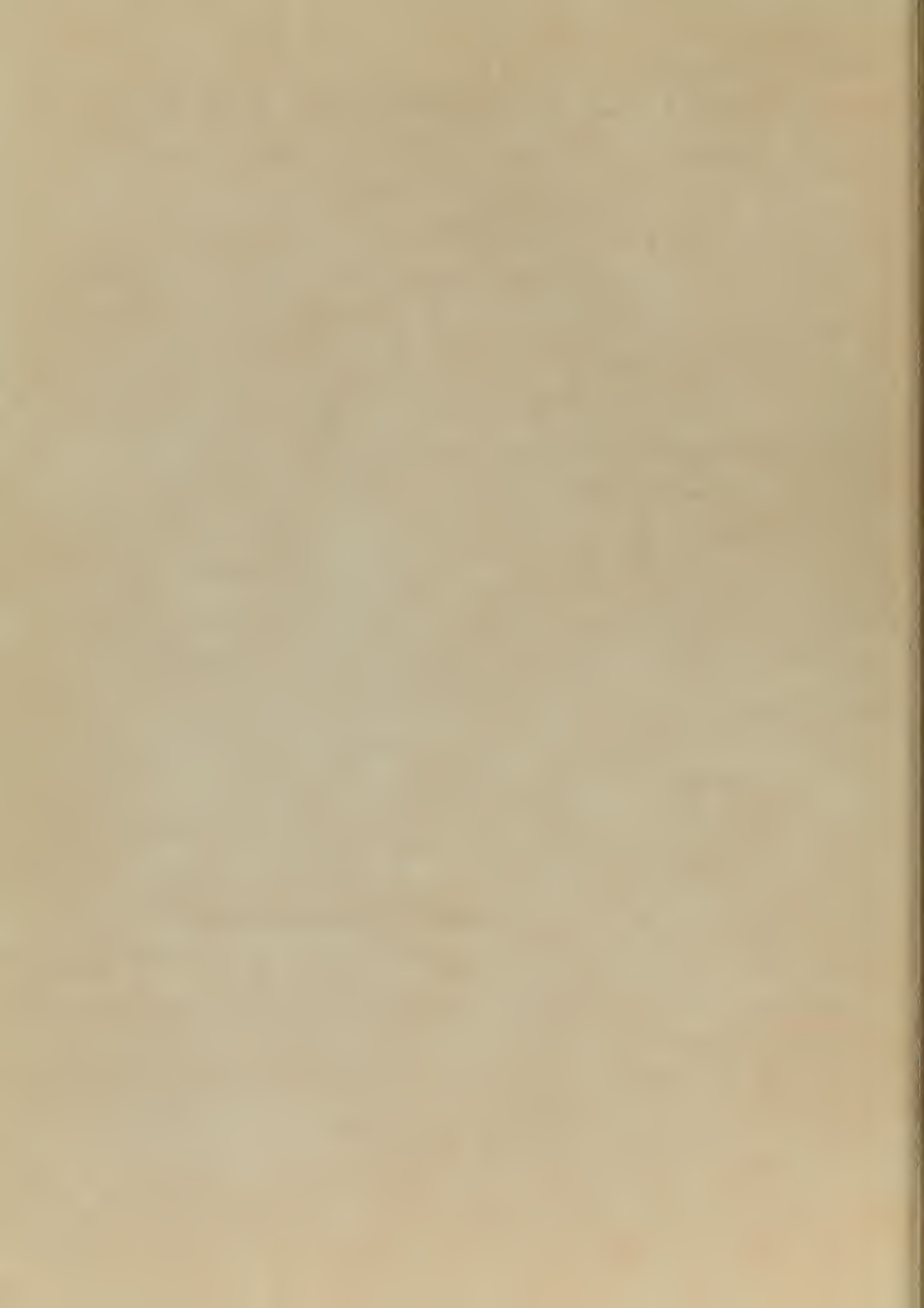
Figure 24. Shunt Capacitance of Round Hole in Center Conductor



shown in Figure 26.

The end probe section closely resembles the well known Hewlett Packard slab line [42]. Its advantage over the slotted ground plane section is that the fields in the vicinity of the strip are not disturbed by a slot. The slight error that this section might cause in the measurement would be due to the energy that is necessarily drawn by the probe and the disruption of the fields by the probe. This device serves best when measuring a straight length of strip. With a complex system that extends in both directions from the line to be measured, there may be difficulty in getting the probe into the desired position. Also special consideration must be given to allow for variation in ground plane spacing. The end probe slotted section of Figure 25 has a unique solution to this problem. The carriage from a conventional slotted section is fitted to the flanges of the channel beams that form the ground planes. A series of three step notches and mounting holes are provided to allow the ground plane spacing to be adjusted to $1/4"$, $3/8"$, or $1/2"$. A standard tuned probe assembly is used with the probe length, increased so that it is able to extract power from a strip that is placed well within the ground planes. Using the standard carriage provides an inexpensive, mechanically movable carriage for accurate positioning of the probe.

The slotted section with the slot in the ground plane is more versatile, simpler to construct generally, and is completely independent of ground plane spacing. It is versatile because the slot may be placed wherever desired in any system no matter how complex. It is simple to construct since all that is required is a standard machine cut slot in one of the ground planes and a probe to fit in the slot. However, there



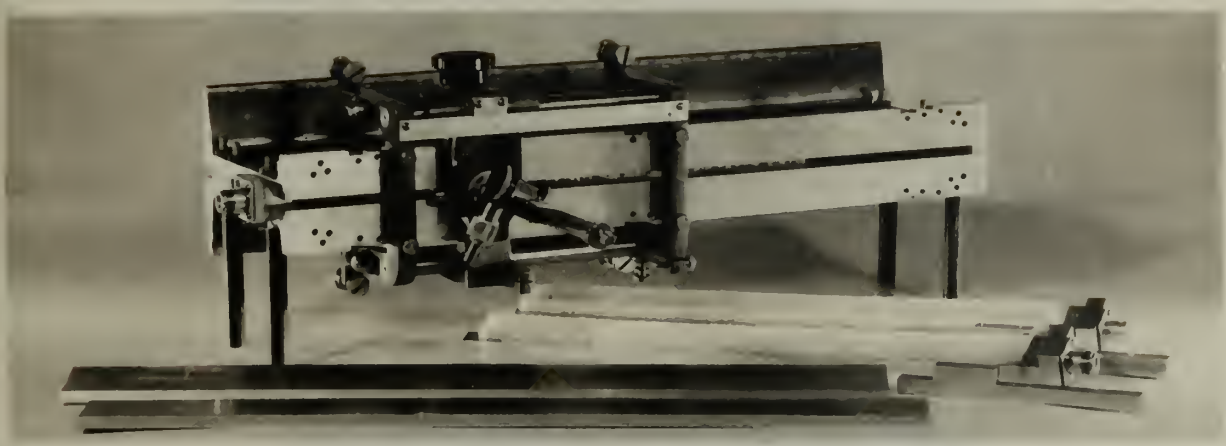
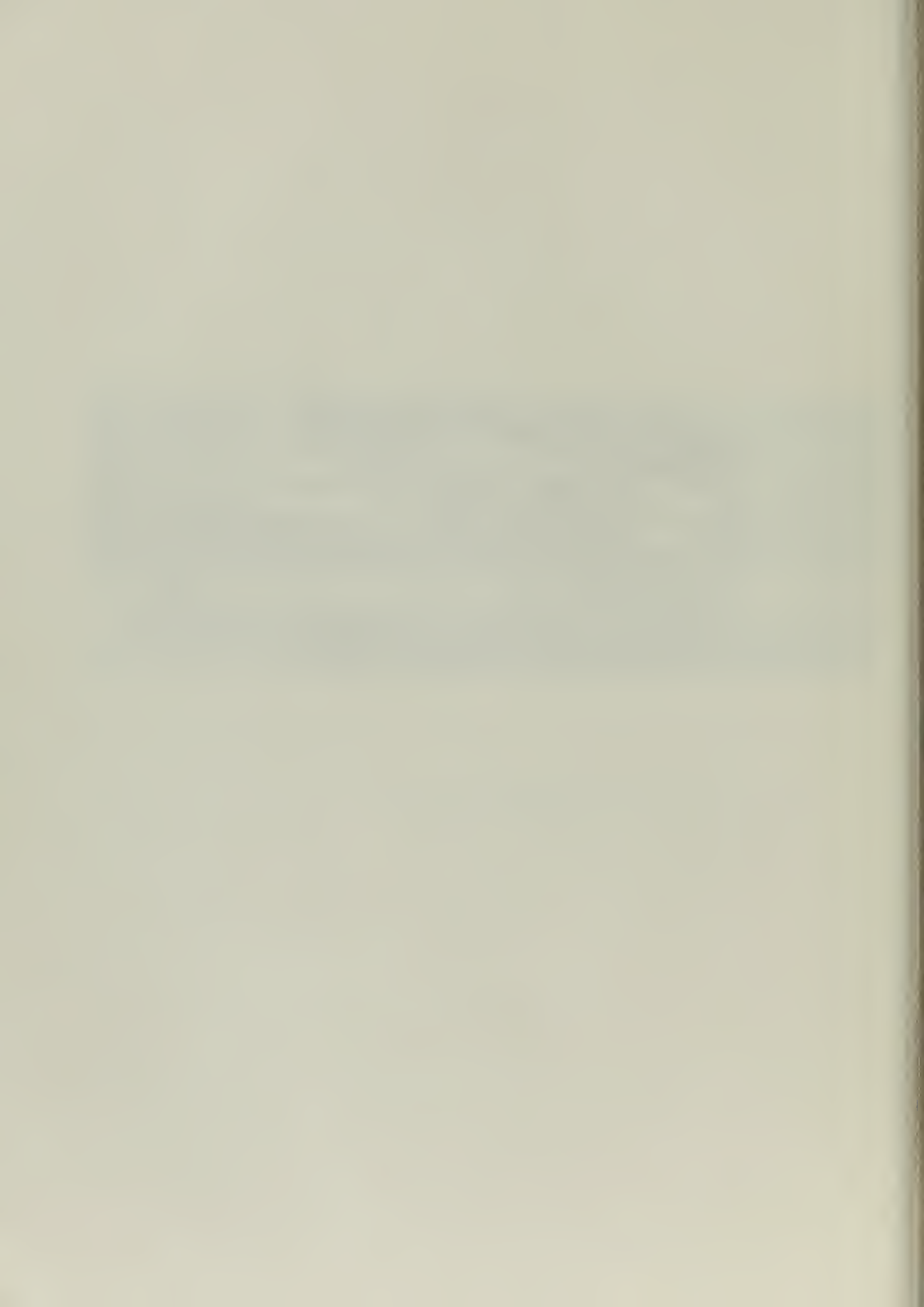


Figure 25. End Probe Slotted Section



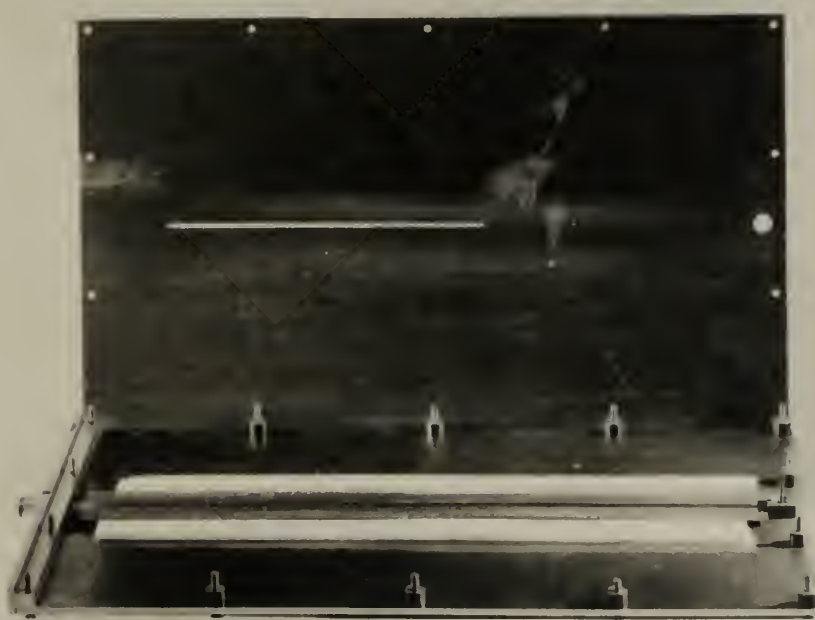
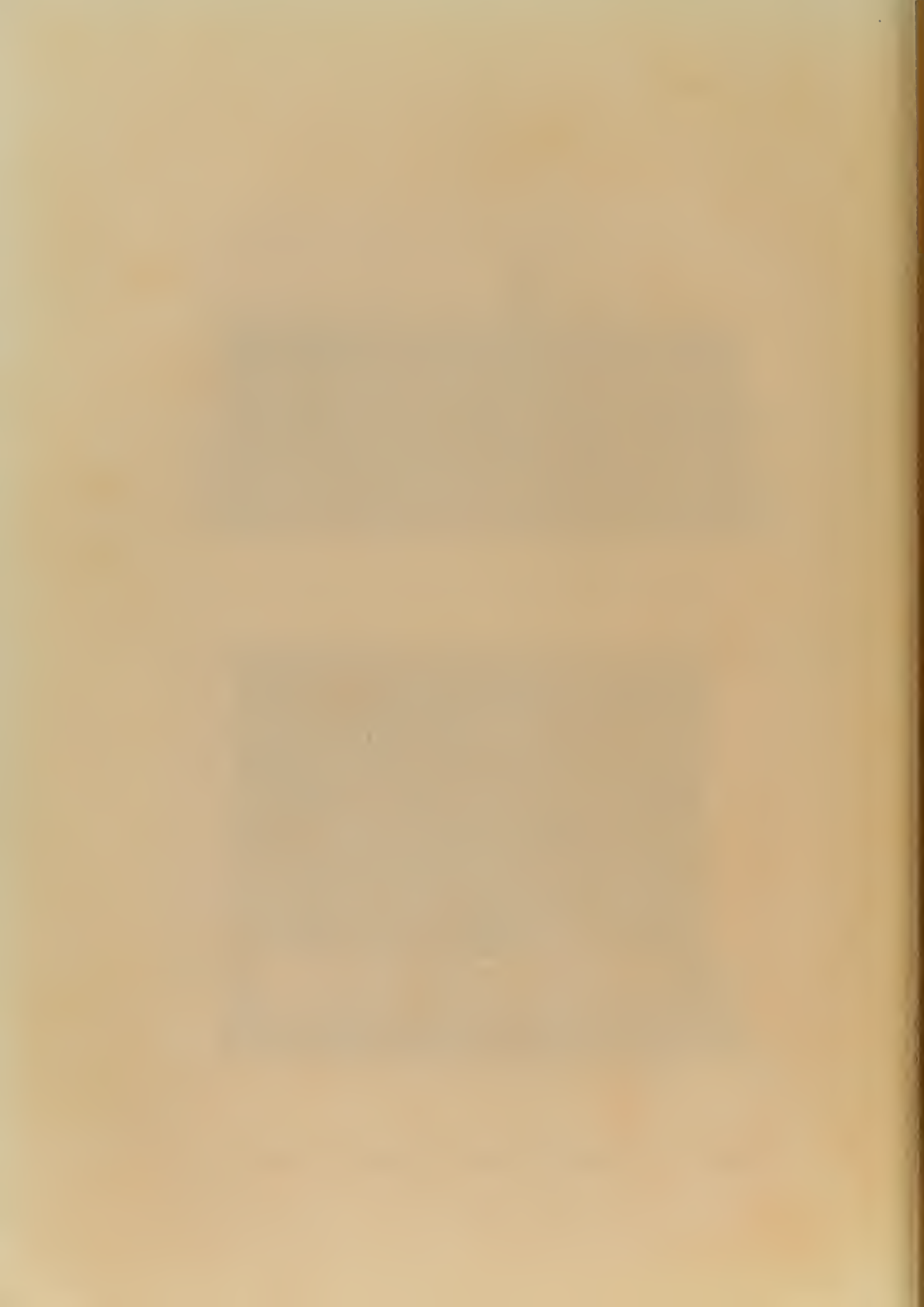


Figure 26. Slotted Ground Plane Slotted Section



are several refinements that may be taken from standard slotted section design that can increase the measurement accuracy. For instance, taper the ends of the slot to reduce the discontinuity at the beginning and end of the slot. If tapering is too costly a machine operation, small sections of lossy material may be placed at the ends to reduce the affect of the discontinuity. The slot should be as short and narrow as possible to limit radiation. Two wavelengths of probe travel is generally ample. To provide an accurate position marker, the probe must not rotate. This can be accomplished in either of two ways. First, with a ridge in the block that supports the probe, allowing the probe to travel along the slot but not turn. If the ridge is made to fit into the slot accurately and is flush with the underside of the top ground plane, there will be some reduction of the slot interference in the vicinity of the probe. The second method, as illustrated in Figure 26 has a guide on the outer surface of the slotted ground plane to provide accurate positioning of the probe. A standard steel scale may be used for distance measurements; however, graph paper could be used as a temporary measure. The vernier indicator was made and scribed by hand. In the slotted line pictured, no precaution was taken at the ends of the slot, and it could have been thinner and shorter, but good results were obtained with measurements of well-matched loads that were made in the center of the slot showing a VSWR of 1.05.

8. Low and High Pass Filters.

Low and high pass filters have long been standard features of microwave networks. With balanced strip transmission line, these filters may be rapidly constructed at low cost to be used as part of con-



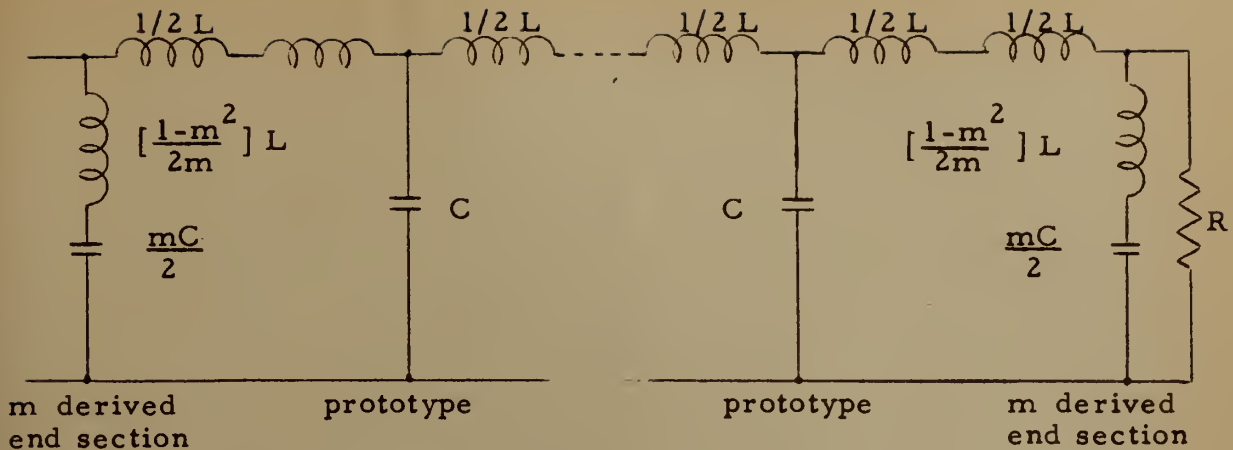
ventional microwave networks or ideally as part of a strip transmission line system. Strip transmission line filters are now commercially available with adaptors to connect to coaxial cable.

The theory and design of coaxial line filters based on the effect of the changes in the line impedance may be found throughout the literature. A particularly complete coverage of the principles and design of transmission line filters, including specific design details, may be found in Chapters 26 and 27 of Very High Frequency Techniques [36]. A slightly different approach to the problem, believed to originate with H. Keene at A. I. L. is based on the consideration of the protrusions from the sides of the center conductor of a strip transmission line as shunt stubs, not as a change in line impedance. This approach leads to a rather straightforward analysis of the problem. However, both methods of attack result in essentially identical designs. The consideration of the side elements of the filter as shunt stubs will be discussed here briefly, due to its simplicity and because it is not generally available in the literature.

The design of a low or high pass filter in general consists of replacing the elements of the well-known lumped constant equivalent circuit with series and parallel sections of transmission line of appropriate length and characteristic impedance.

The following is the lumped constant or equivalent circuit of a low pass filter with "m" derived end matching sections [18].





Where:

$$C = \frac{1}{\pi f_c R} \quad \text{By definition} \quad (1)$$

$$L = \frac{R}{\pi f_c} \quad \text{By definition} \quad (2)$$

Therefore:

$$X_C = \frac{1}{2\pi f_c C} = R/2 \quad (3)$$

$$X_L = 2\pi f_c L = 2R \quad (4)$$

From relations (3) and (4) we may draw a new equivalent circuit for the prototype.

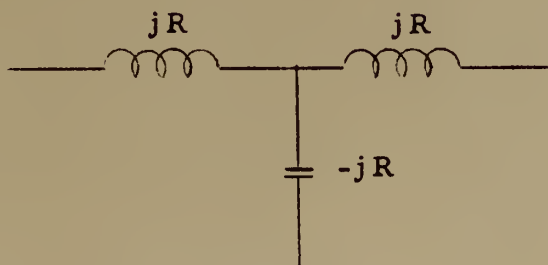


Figure 27 shows the center conductor configuration that will provide the electrical characteristics required by the equivalent circuit.



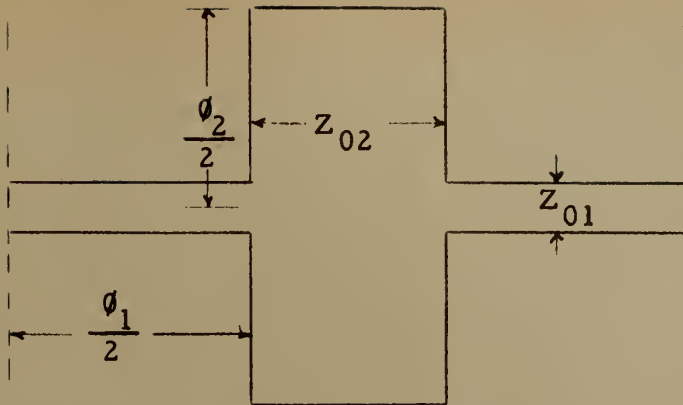


Figure 27. Prototype Section for Strip

Transmission Line Low Pass Filter

The design of a low pass filter proceeds as follows:

1. Select Z_{01} . This value should be as high as possible commensurate with ground plane spacing and minimum width allowable for mechanical consideration.
2. Determine ϕ_1 . The section of line terminated by the transverse element is represented by the induction cross arm of the equivalent circuit and is determined from the familiar transmission line relationship:

$$Z_{sc} = j Z_0 \tan \phi_1 \quad (5)$$

This equation may be used since it has been shown experimentally that there is a voltage mode or equivalent short circuit at the ends of the prototype section. Therefore:

$$jR = j Z_{01} \tan \phi_1 / 2$$

$$R/Z_{01} = \tan \phi_1 / 2$$

$$\phi_1 / 2 = \arctan R/Z_{01}$$



3. Determine ϕ_2 . The length of the transverse elements are determined from the consideration of the minimum high frequency that the filter may be allowed to pass energy again. The lowest frequency above f_c that will not interfere with the operation of the filter is selected. The geometric mean of this frequency and f_c is determined. Then $\phi_2/2$ is computed to be a quarter wavelength at this mean frequency. $\phi_2/2$ should actually be made somewhat shorter than the computed value, since the fringing capacitance at the end of the elements lengthens them slightly [28] [29] [34].

4. Determine Z_{02} . The transverse element is actually two open circuited elements in parallel. Therefore, from the relation:

$$Z_{oc} = -j Z_0 \cot \phi$$

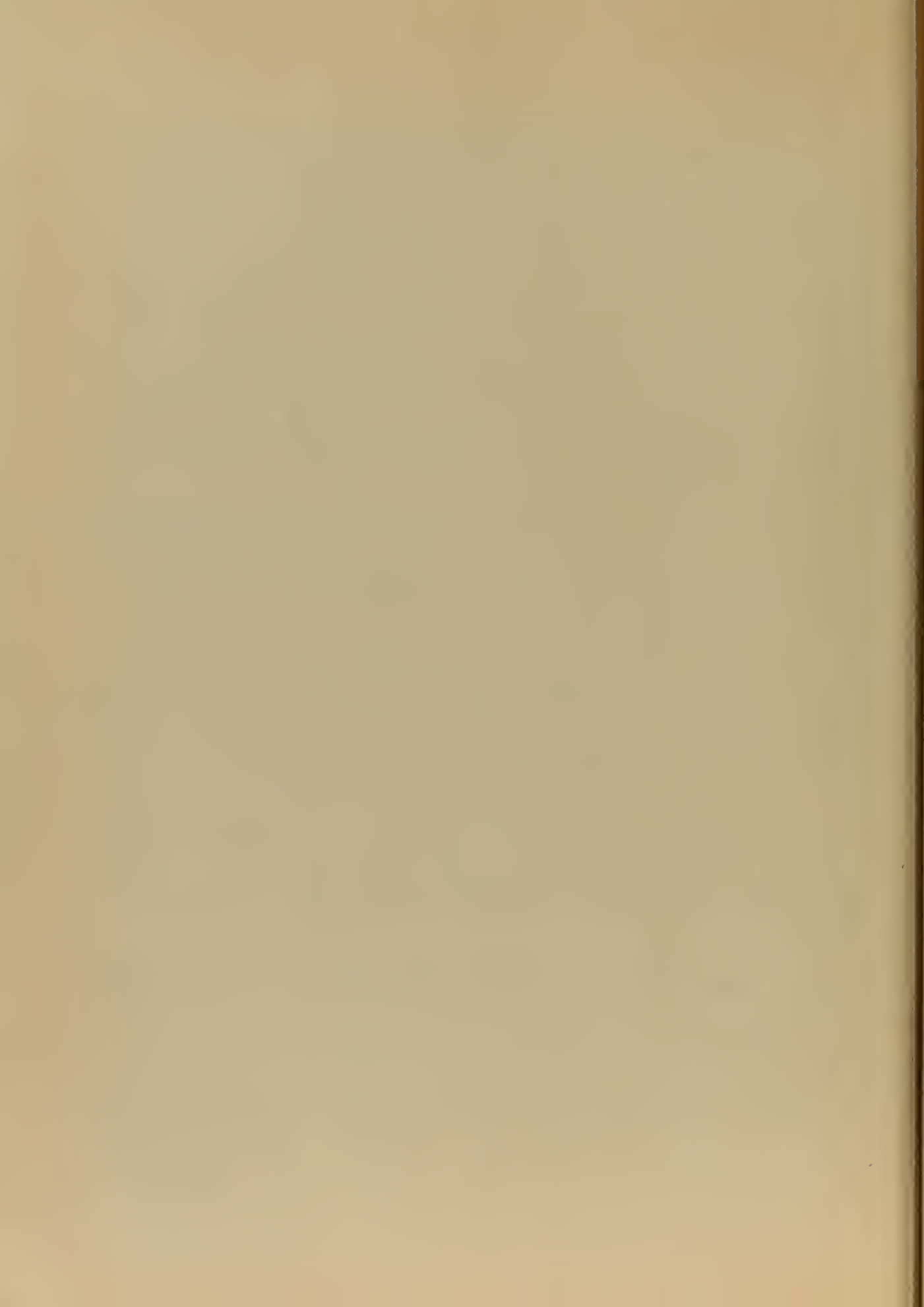
$$2[-jR/2] = -j Z_{02} \cot \phi/2$$

$$Z_{02} = -j R \tan \phi/2$$

5. The values for the "m" derived matching sections are obtained in the same manner using the appropriate values from the equivalent circuit.

6. The number of prototype sections employed is determined by the sharpness of cut-off desired. The attenuation at cut-off increases about six DB per octave for each additional section.

Figure 28 is the actual size center conductor for a stripline low pass



filter with $f_c = 1500$ MC, input and output impedance = 50 ohms,
ground plane spacing = 1/4 inch.

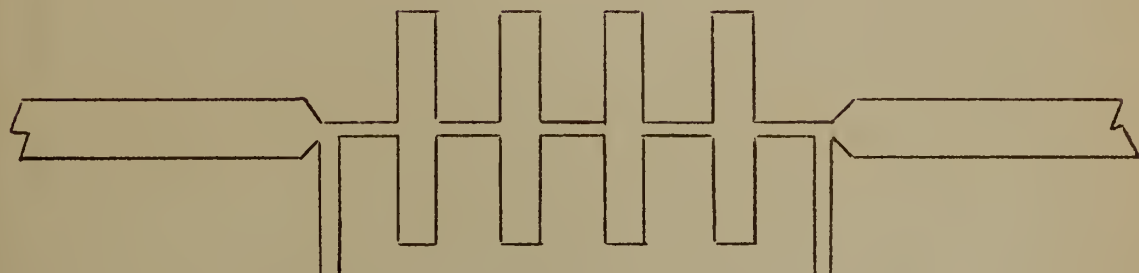


Figure 28. The Center Conductor of a Low Pass Filter

The normalized input resistance and reactance of a twelve section low pass S band filter without the "m" derived impedance matching end sections is shown in Figure 29. Note how the input resistance falls off to zero in the rejection band i.e. frequencies above f_c . This follows from theoretical expectation because where there is no input resistance the network cannot dissipate power.

Figure 30 shows the response of a twelve section, low pass, S band filter with "m" derived impedance matching in sections ($m = .6$).

A comparison of the response of a five section filter designed by the method discussed in this section and a varying impedance filter designed in accordance with reference [36] is shown in Figure 31. Both of these filters had matching end sections.

High pass filters may be designed in the same manner as the low pass filter. The equivalent circuit of the high pass filter requires lengths of transmission line approximately one quarter wavelength longer than is required for the low pass filter.

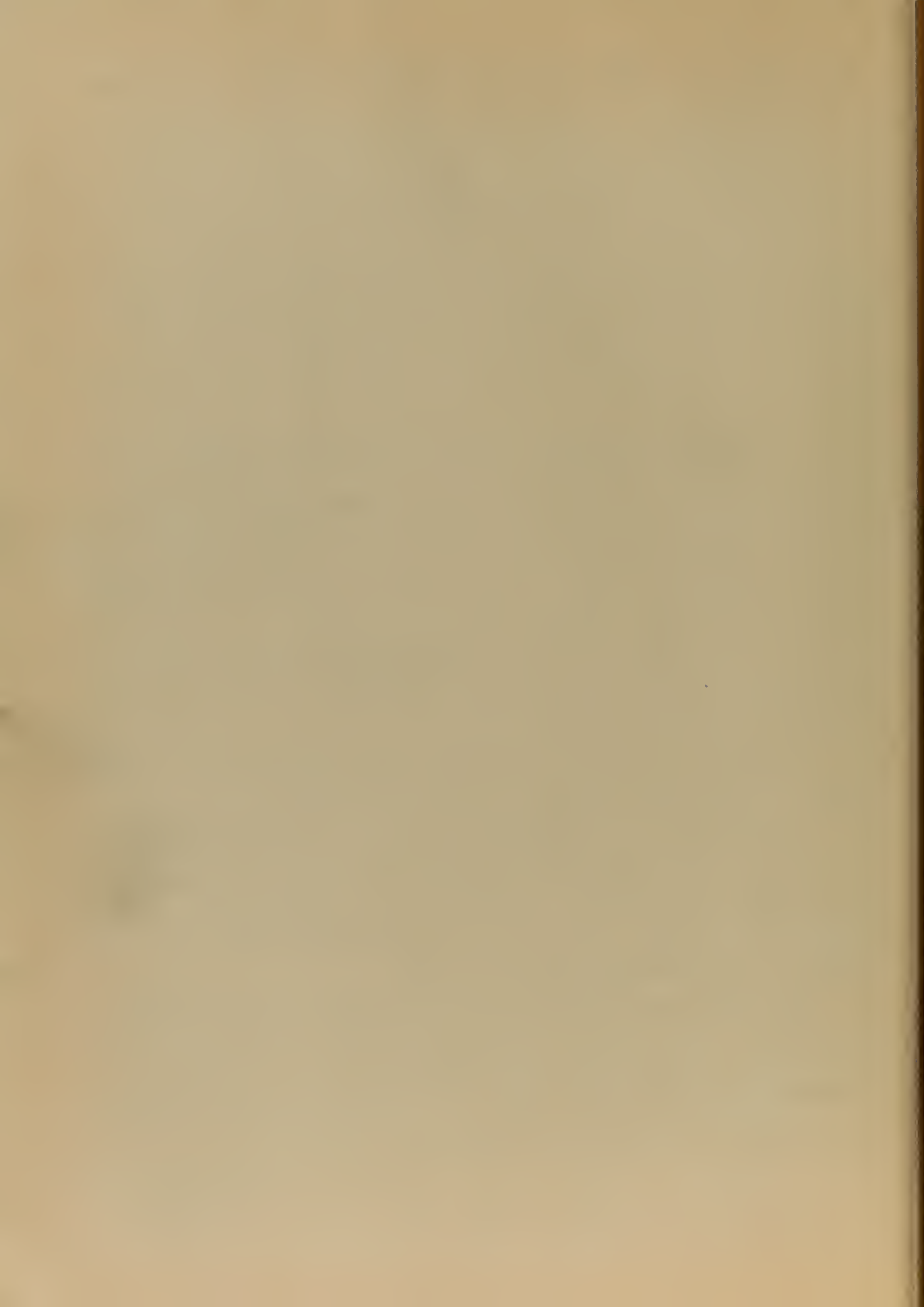


Figure 29. The Input Impedance and
Reactance (Normalized) of a Low
Pass C Band Filter

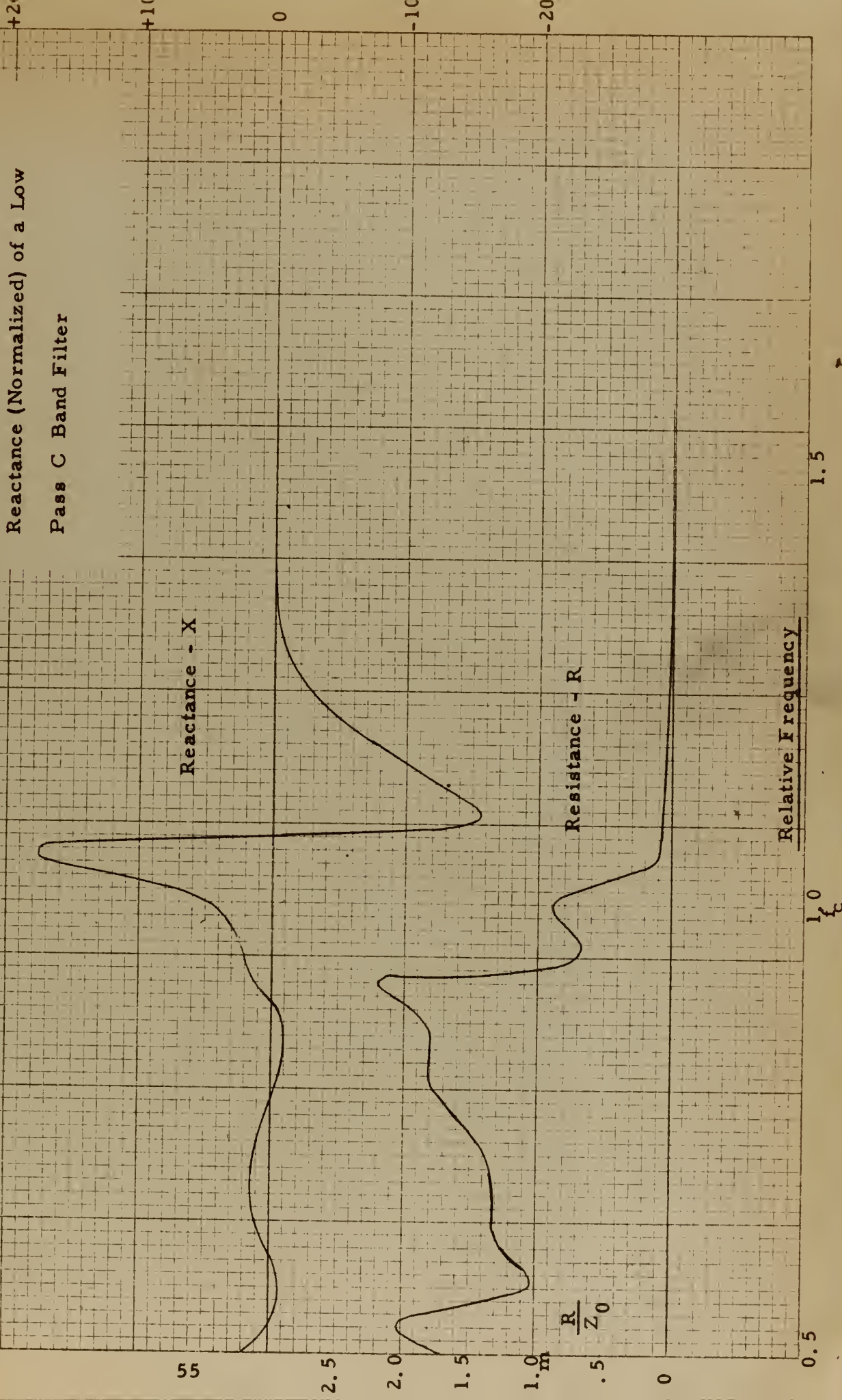
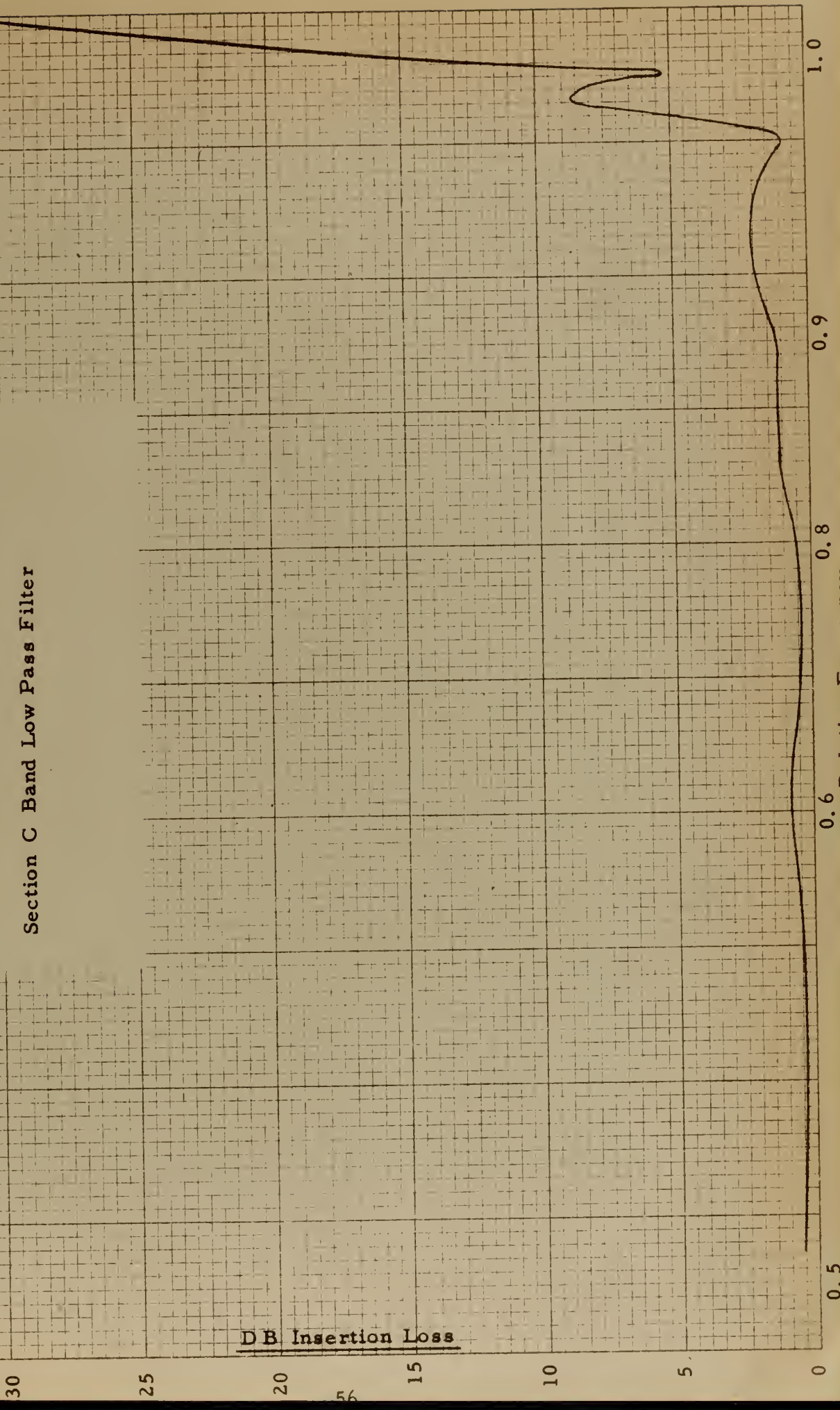




Figure 30. The Response of a Twelve

Section C Band Low Pass Filter





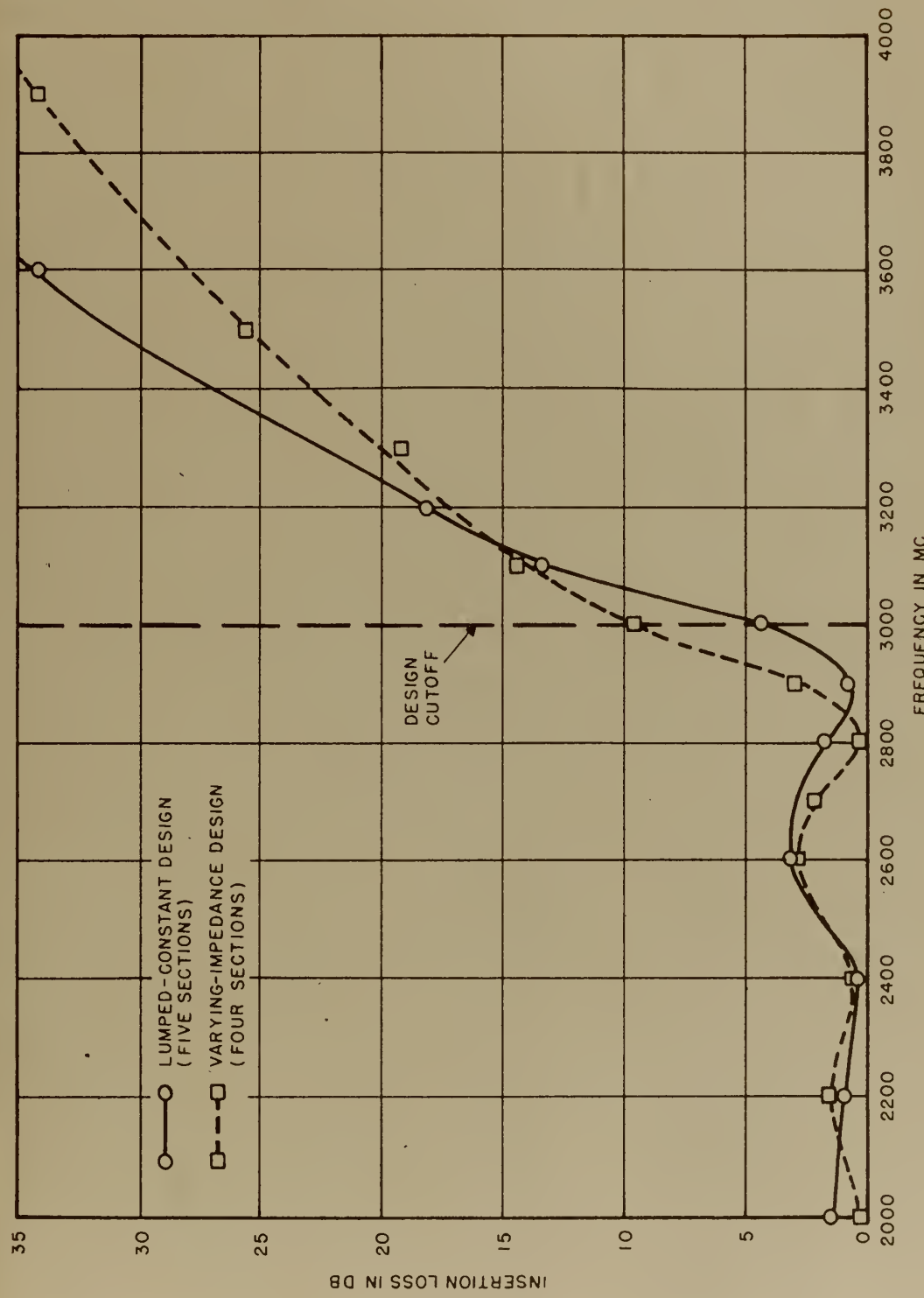


Figure 31. Tests of Preliminary Low Pass Filter Designs

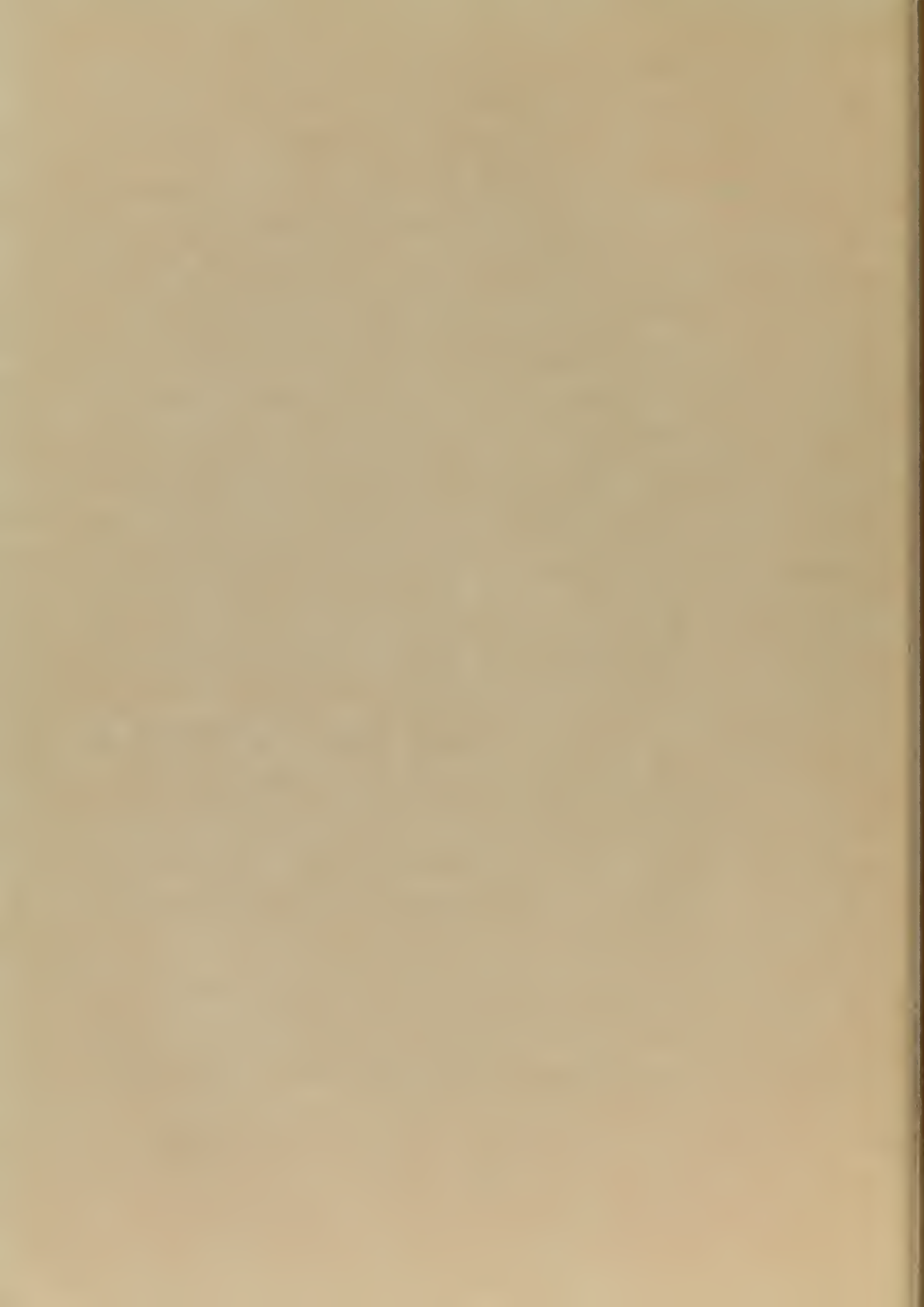


Both low and high pass filters are easily constructed using the strip-line technique, with fixed capacitance in place of the effective capacitance of the short lengths of line. Figures 32 and 33 illustrate a high pass filter of this type, and Figure 34 shows its response versus frequency. The cut off frequency of the filter is 600 MC and the resonant frequency of the impedance matching end sections is 462 MC. The series capacitance in the main line is achieved by placing gaps in the top and bottom strips, staggered so that one overlaps the other forming a series of small two-plate capacitors with Teflon glass dielectric. The values of capacitance required, about two to six micro micro farads, are easily obtained by adjusting size of the overlap. Initial experiments indicated that there was radiation between the plates due to an unbalance in the potential on each side of the center conductor, however this was eliminated by connecting the top and bottom strips at the critical points of unbalance with small pins. The shunt inductive elements are lengths of line of the proper length, terminated by a shorting block.

Low pass filters may be constructed as shown in Figures 35 and 36. Two-plate capacitors are formed by etching small identical areas of metal on opposite sides of the dielectric. One side is grounded and the opposite side is connected to the length of line that serves as the series inductance. The inductive lengths of line are curved merely to reduce the overall size of the filter.

9. Resonant Elements and Narrow Band Pass Filters.

The performance of the resonant cavities used with coaxial line and waveguide may be adequately and simply attained with resonant lengths



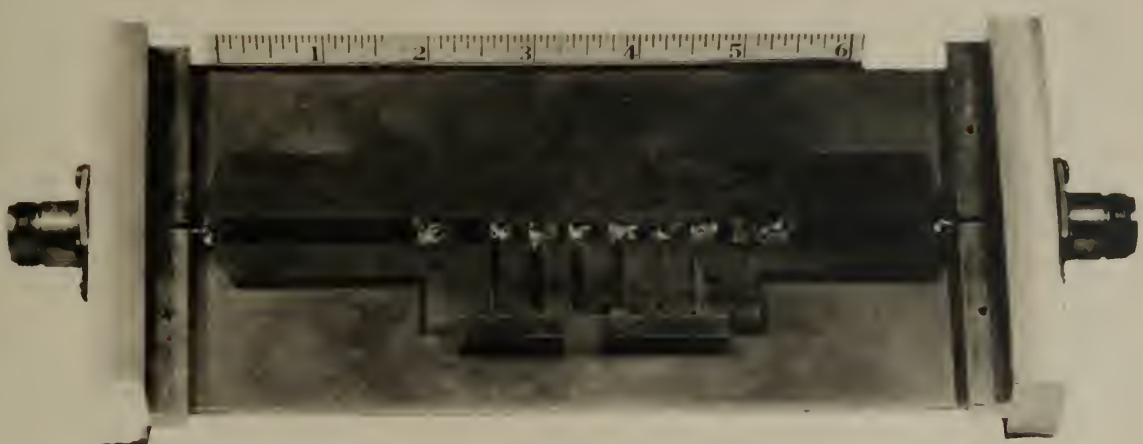


Figure 32. Stripline High Pass Filter with
Fixed Capacitive Elements



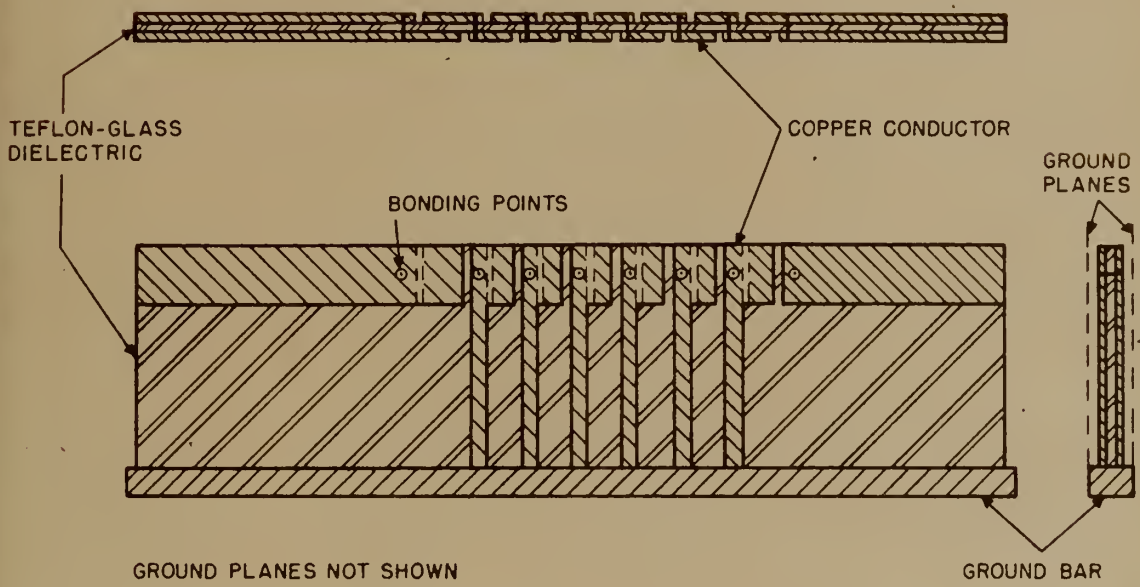
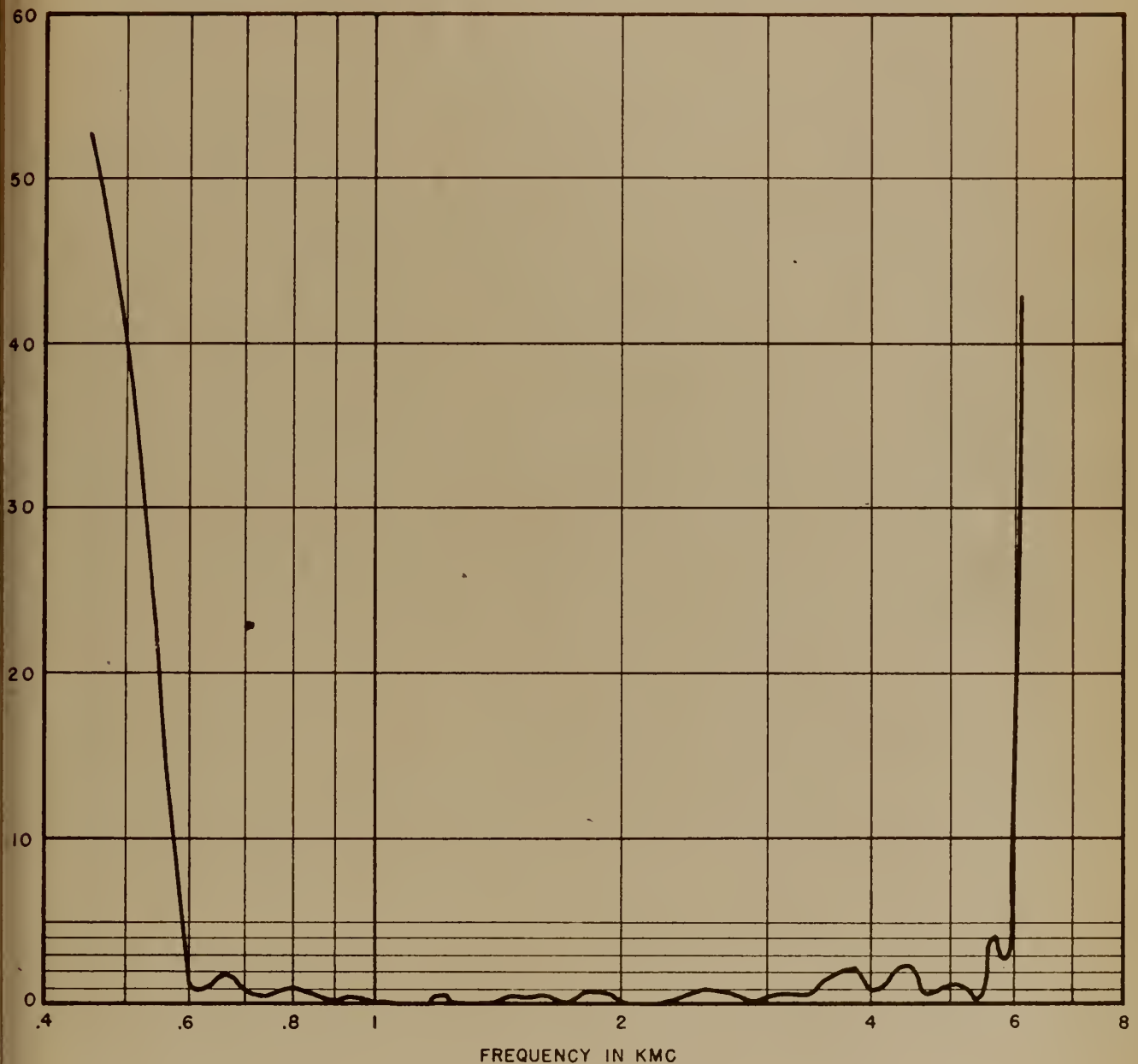


Figure 33. Stripline High Pass Filter with
Fixed Capacitive Elements





**Figure 34. Response of Stripline High Pass Filter
with Fixed Capacitive Elements**



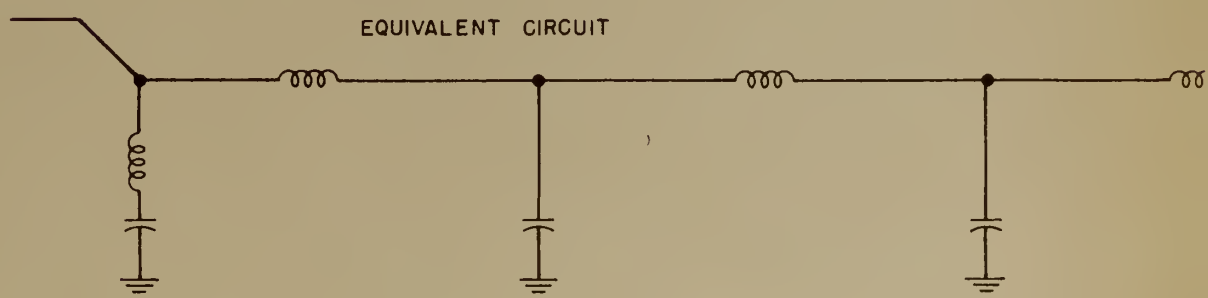
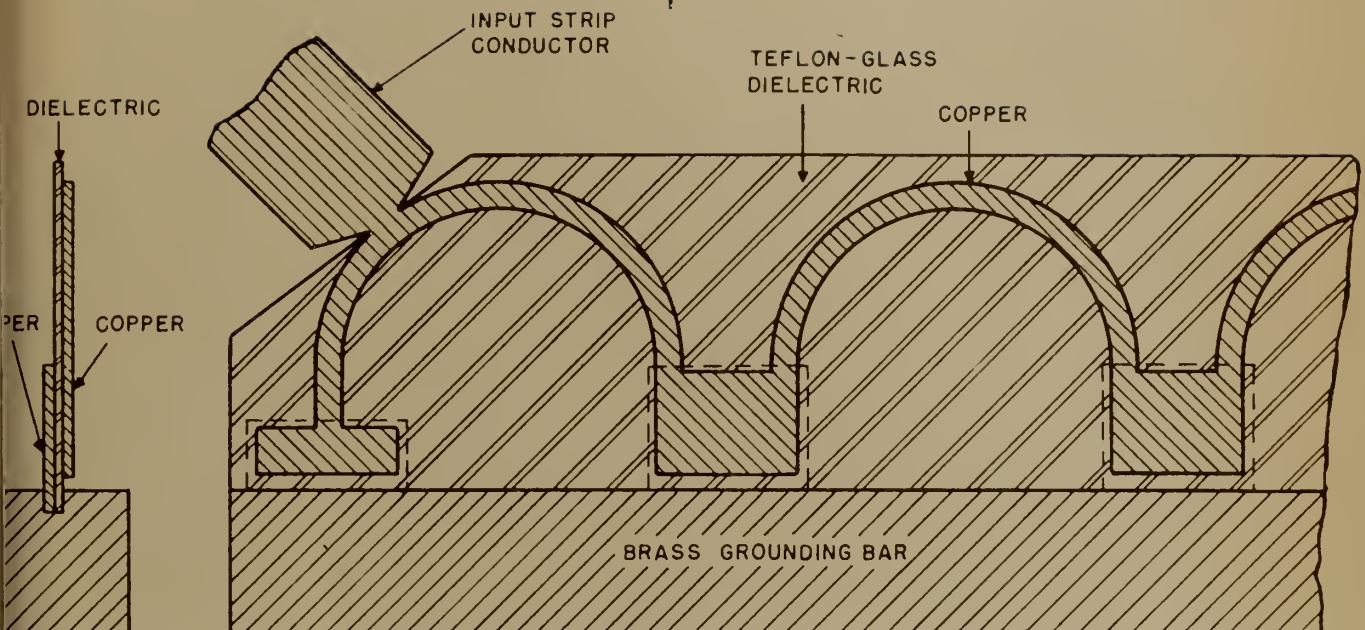
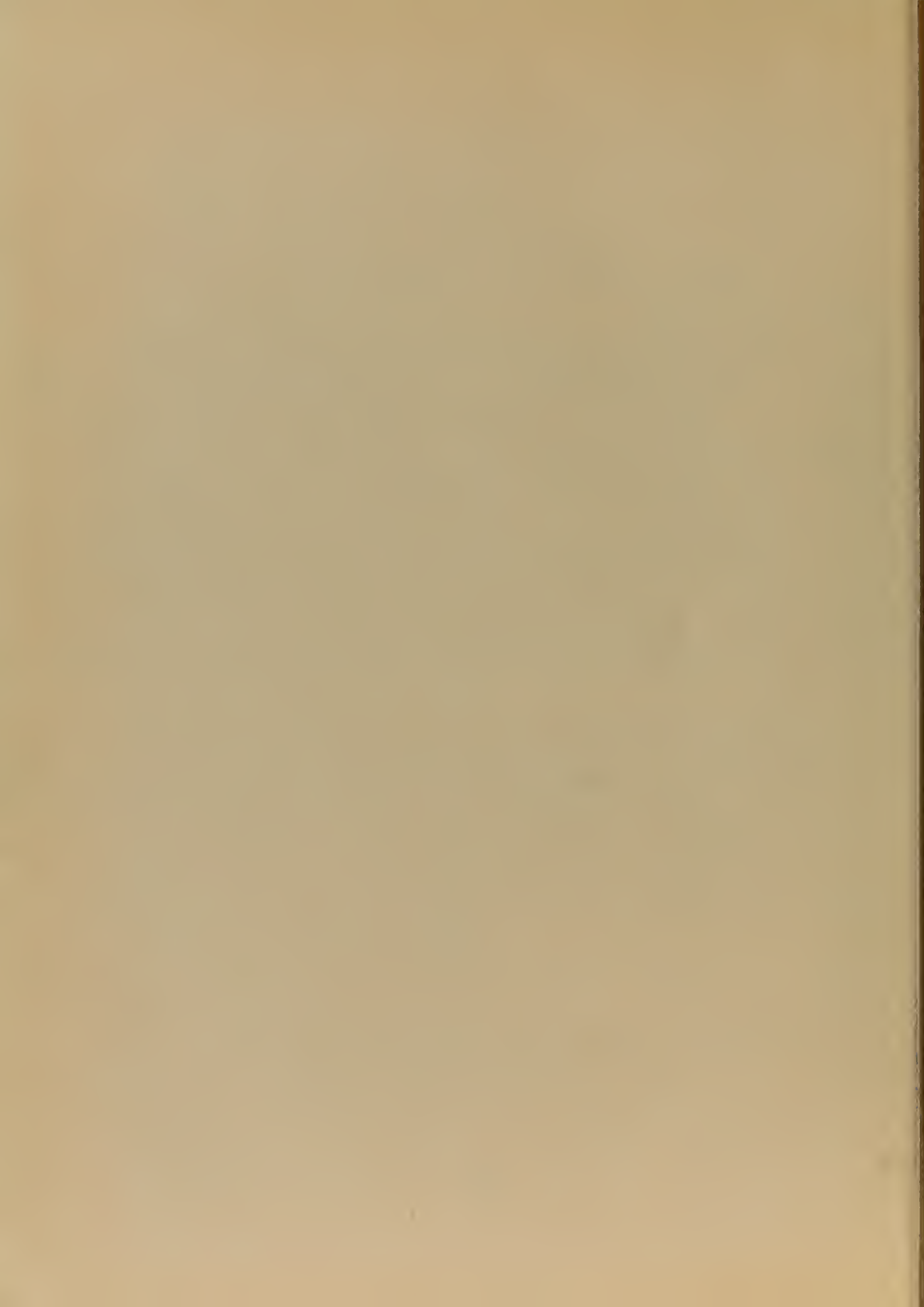


Figure 35. Construction of Compact Stripline Low Pass Filter with Fixed Capacitive Elements



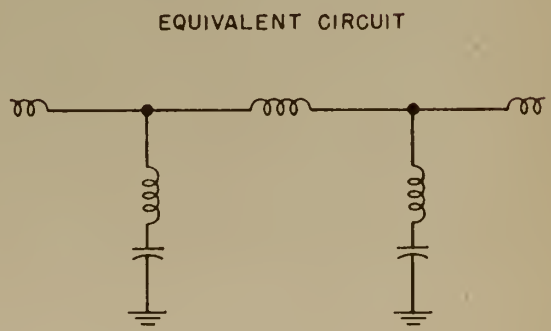
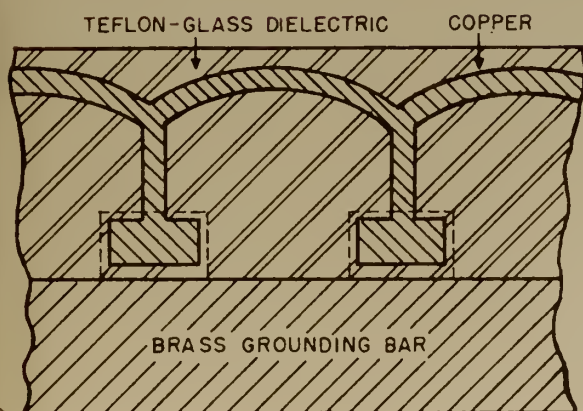
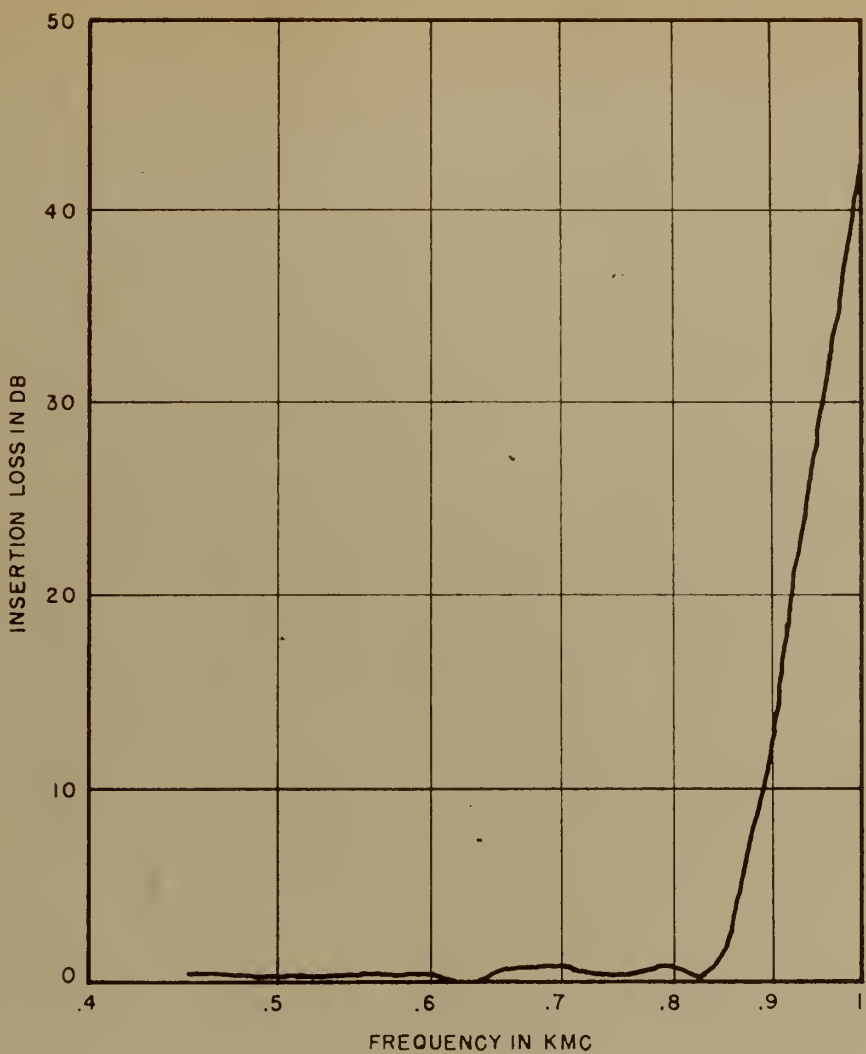


Figure 36. Response of Compact Stripline Low Pass Filter



of balanced strip transmission line. With the resonant element technique, stable transmission and rejection filters with extremely narrow frequency bands can be placed between the ground planes of a strip transmission system simply by altering the configuration of the center conductor [8] [20] [32].

Figure 37 shows a strip transmission line resonant element filter. Actual prism resonant cavities could be built between the ground planes, but the excellent results obtained from resonant elements has made research in this direction unnecessary.

The basic concept of strip transmission line resonant elements is a relatively simple one. Cut two gaps on the center conductor leaving a fixed length of resonant element in series with the line. The frequencies that cause the length of the element to be an integral number of half wavelength will be passed while all other frequencies will be severely attenuated. The actual design of a practical filter is complicated by the attenuation along the line, the loading effects of the gap capacitance, and the effect of voltage distribution when multiple elements are used.

The series and fringing capacitance at the gap has been determined experimentally [8] [29]. The results of the measurement at A. I. L. are shown in Figures 38 and 39. This data conforms with calculations that were made from an analytically determined equivalent circuit of the gap [34]. The voltage distribution, which alters the effect of the capacitance at the gaps, is shown in Figures 40 and 41. These factors will be discussed further during the development of resonant element filter design.

The unloaded Q of the circuit is of primary importance in the design

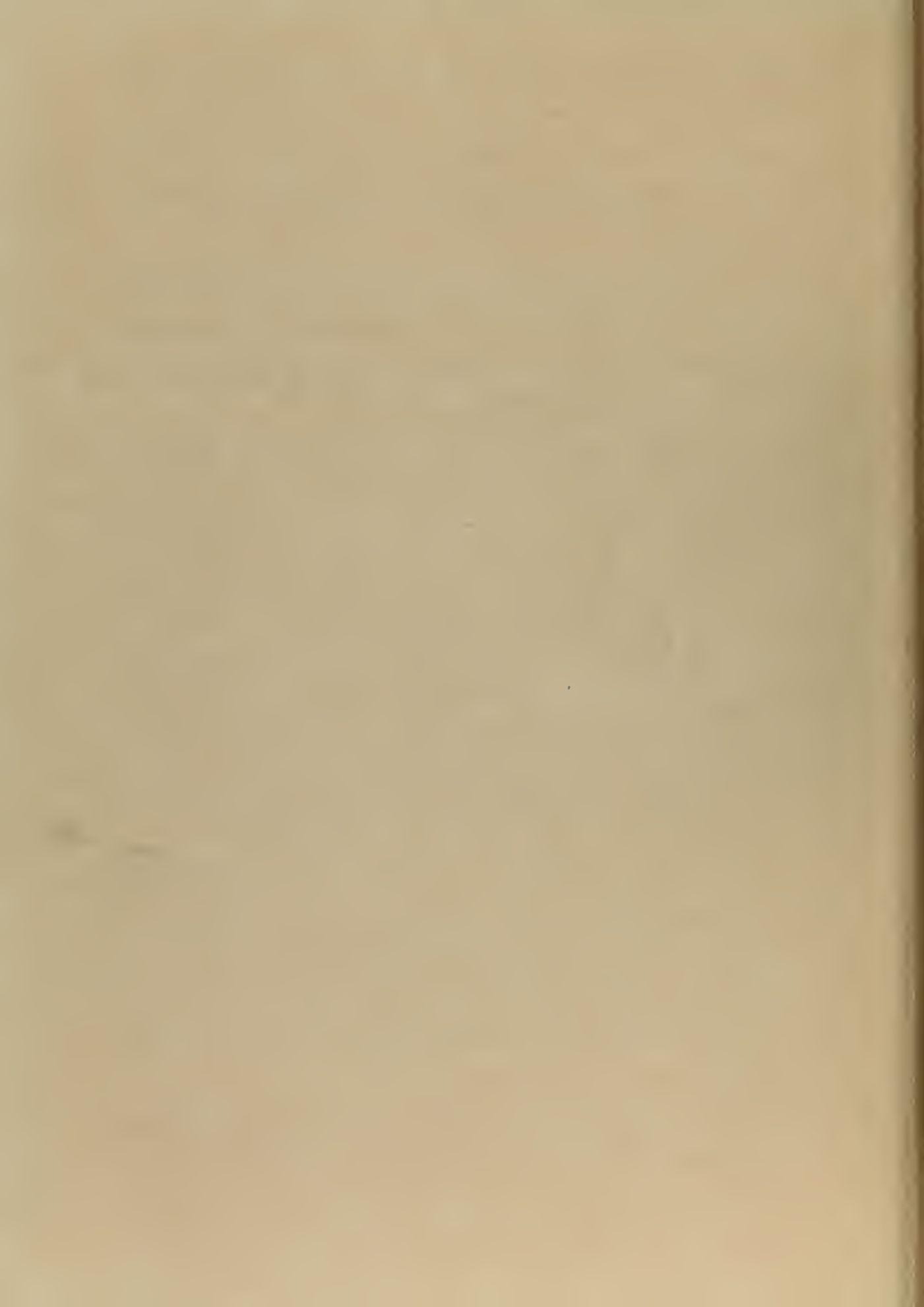
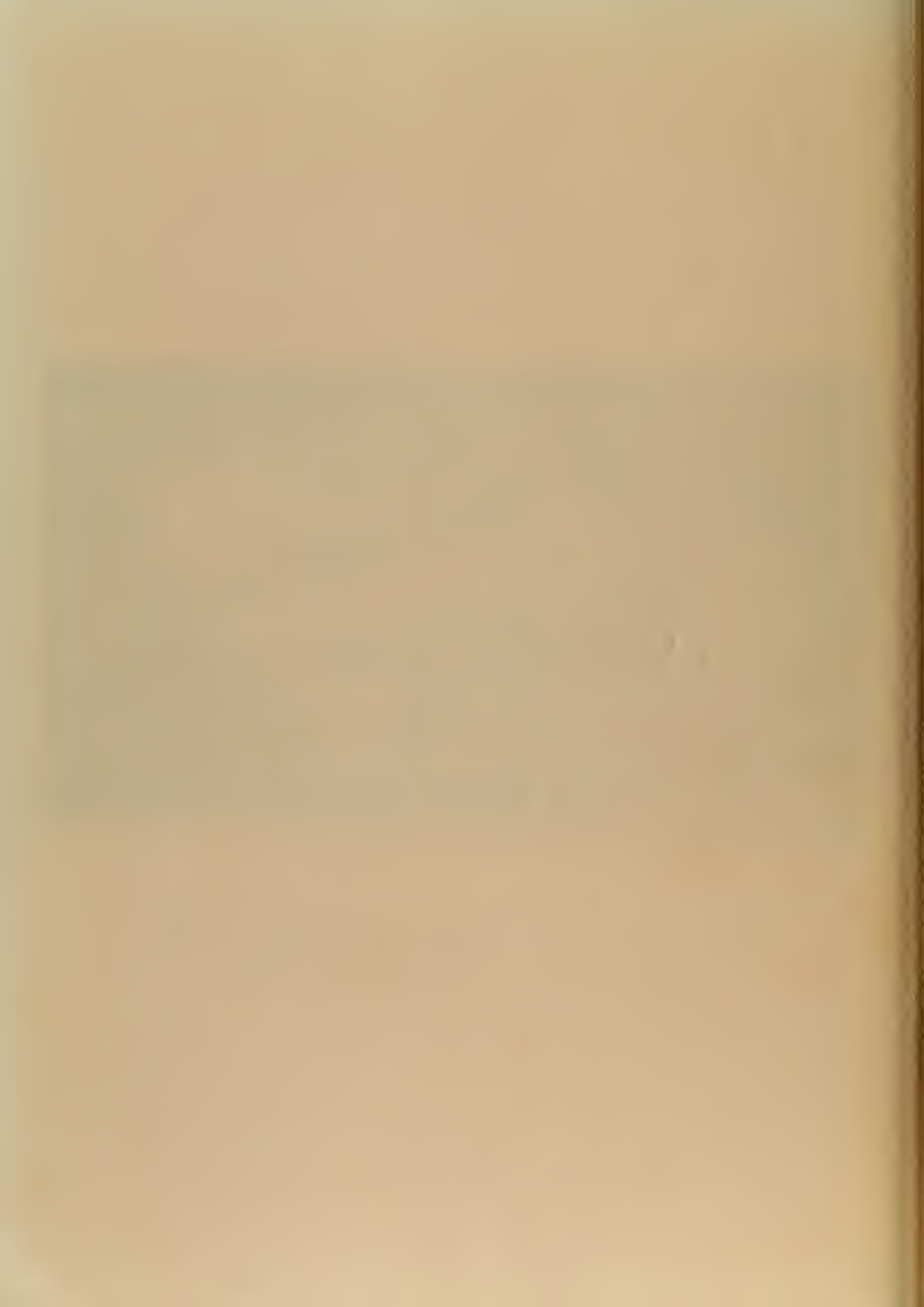




Figure 37. A Full Wave Resonant Element Narrow Band
Pass Filter for KU Band Frequencies



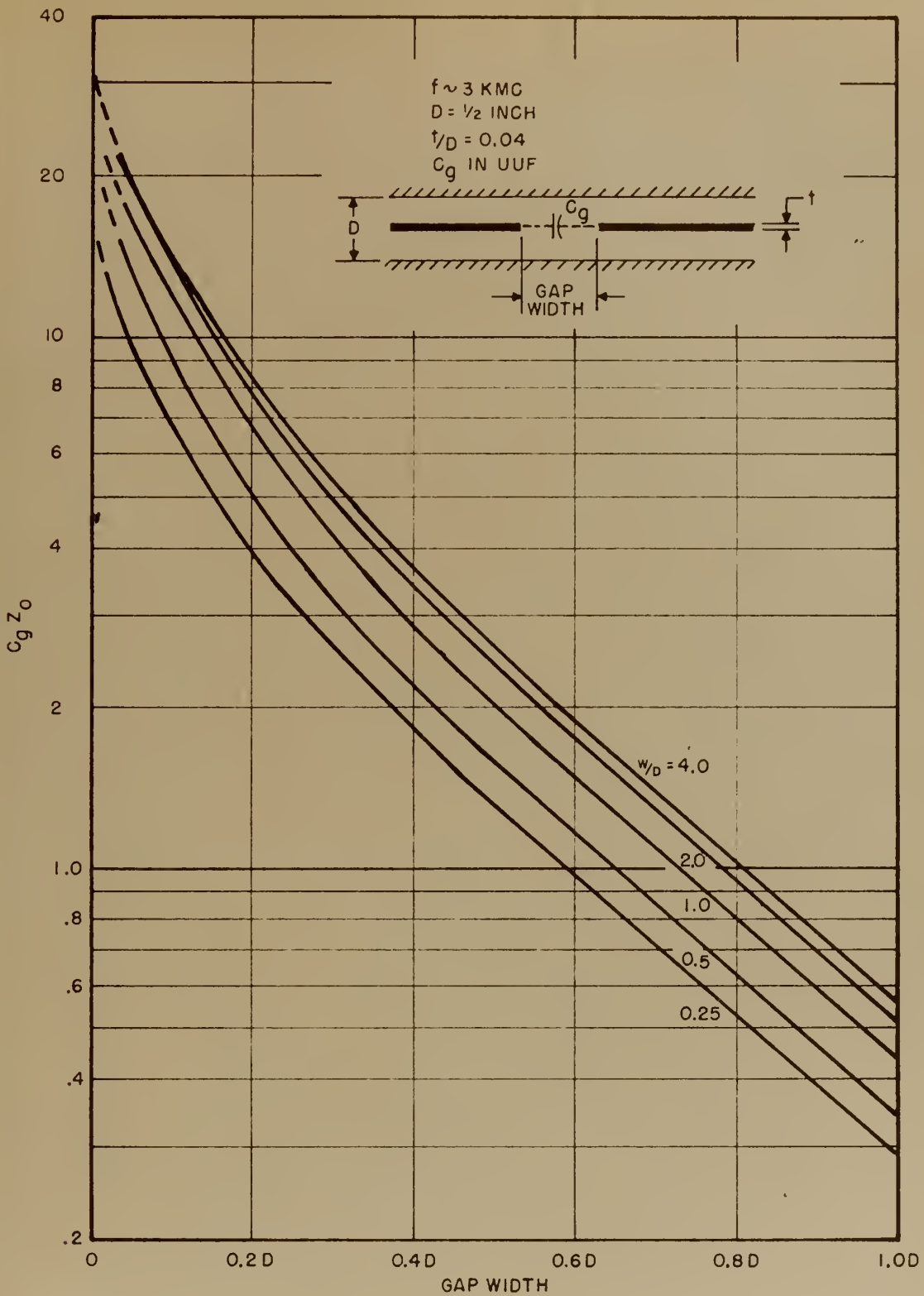


Figure 38. Gap Capacitance as a Function of Gap Width



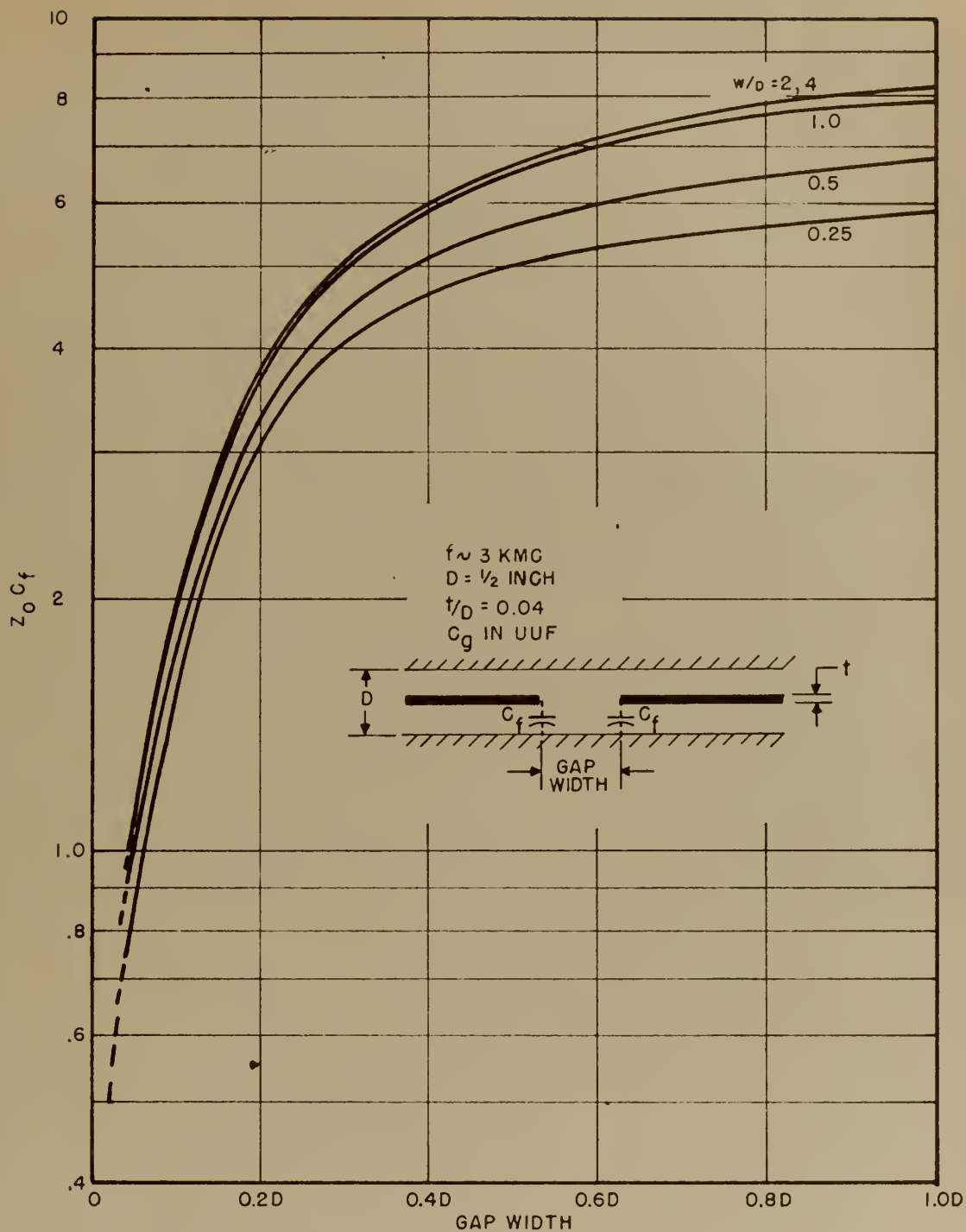
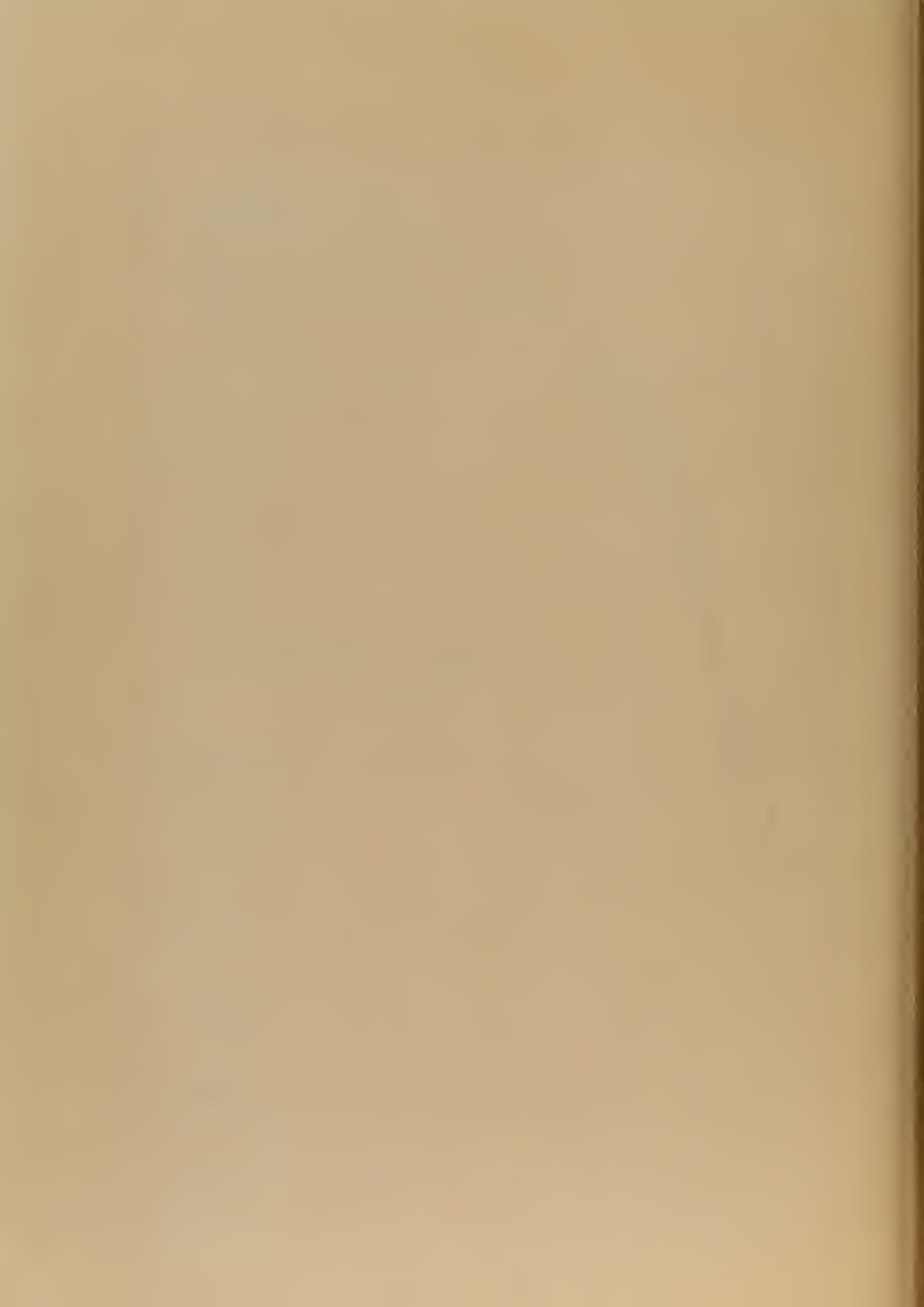
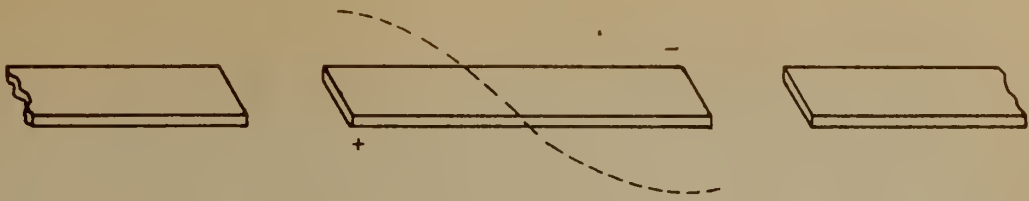
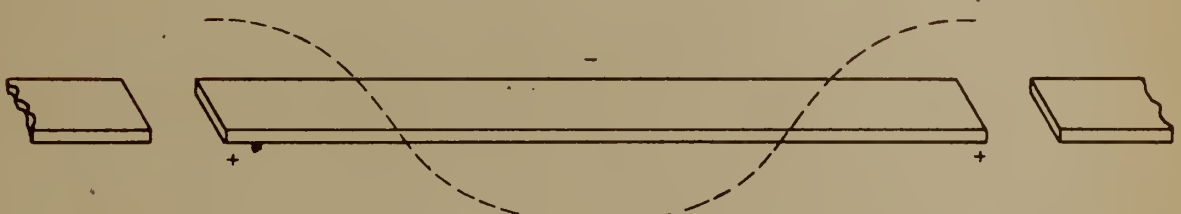


Figure 39. Fringing Capacitance as a Function of Gap Width





VOLTAGE DISTRIBUTION ON HALF-WAVELENGTH RESONANT ELEMENT
(GROUND PLANES OMITTED FOR CLARITY)



VOLTAGE DISTRIBUTION ON FULL-WAVELENGTH RESONANT ELEMENT

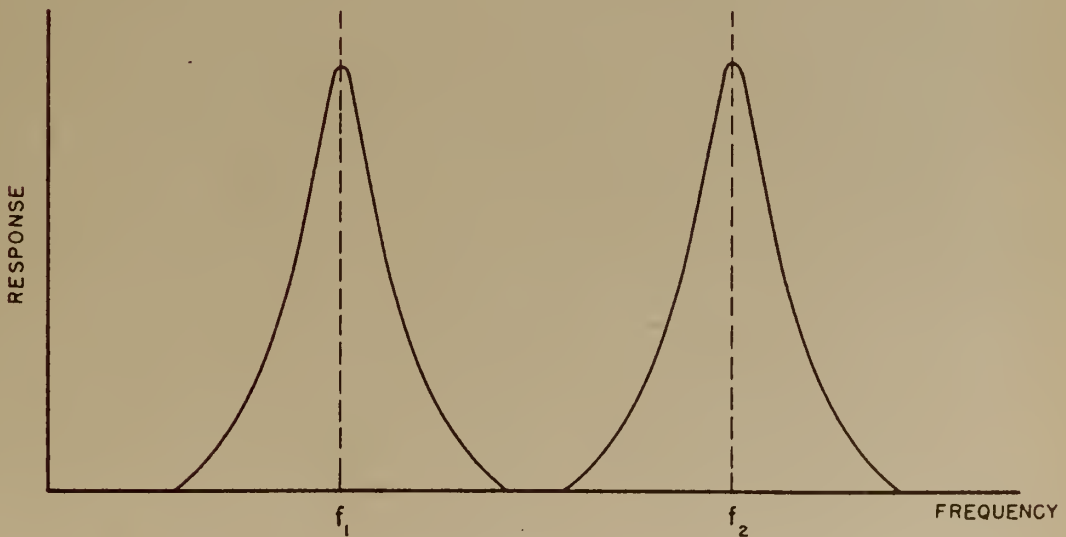


Figure 40.



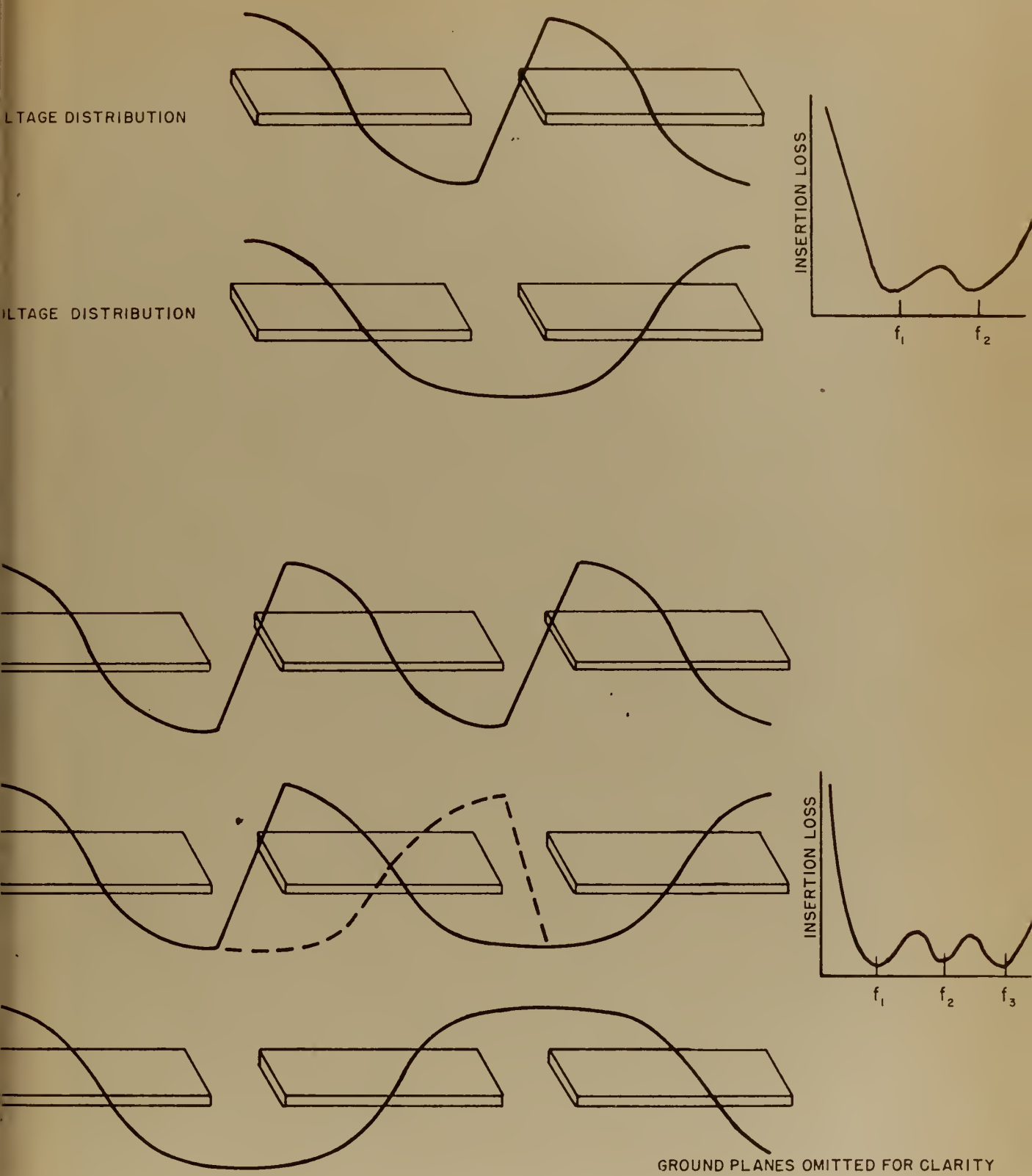
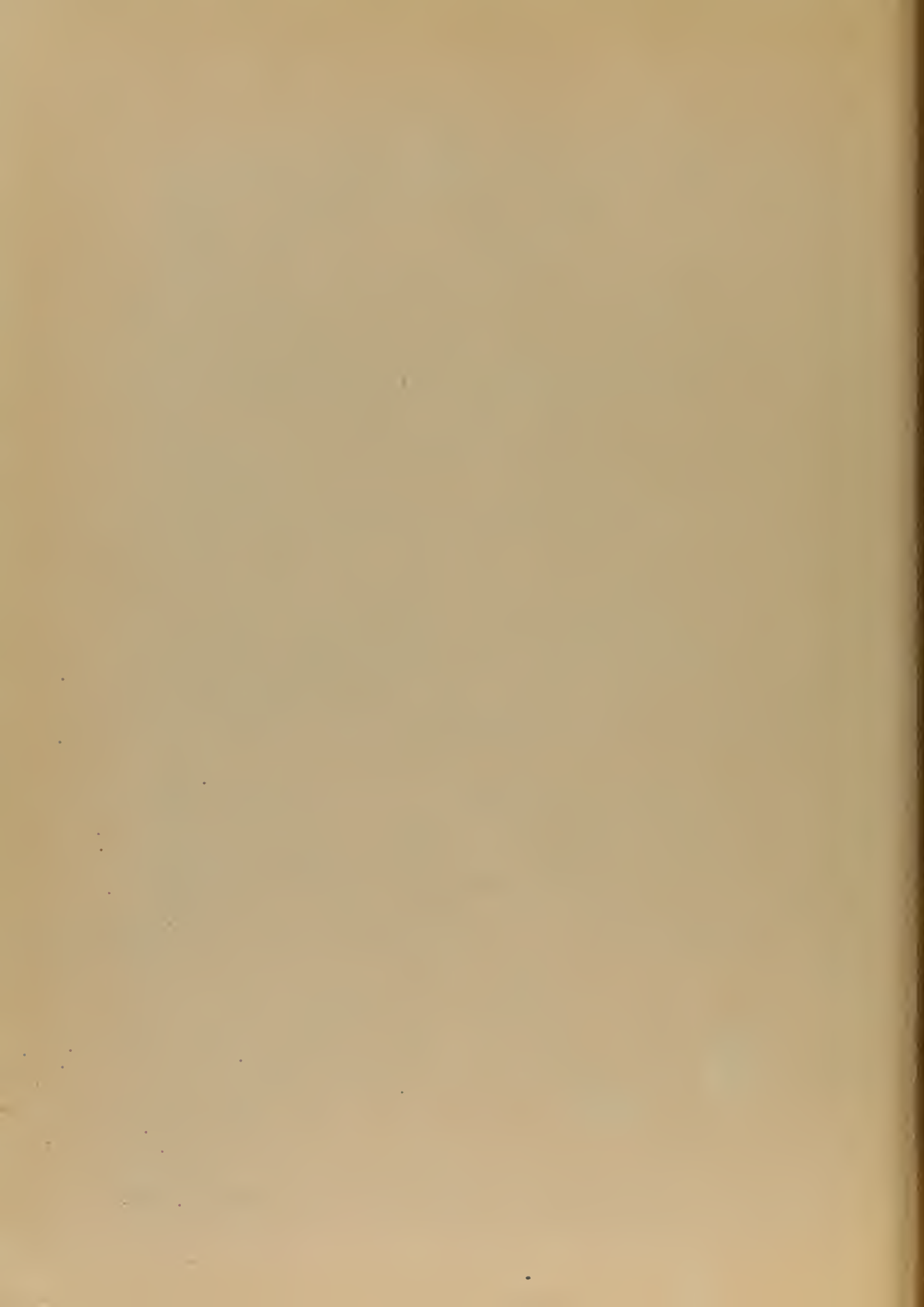


Figure 41. Voltage Distribution in Two and Three Element Filters



of a narrow band filter. It is directly related to the attenuation, previously discussed, by the standard relation valid for any TEM transmission line:

$$Q_u = \frac{\beta}{2\alpha_{\text{nepers}}} = \frac{27}{\alpha_{\text{DB}/\lambda}}$$

The unloaded Q of a resonant element may be easily measured. The following procedure is applicable with equal coupling and matched input and output impedances.

1. Measure loaded Q. It is the ratio of the resonant frequency to the difference in frequency of the points where the output is down three DB from its value at resonance.
2. Measure insertion loss. This is readily accomplished by substituting a lossless connector for the filter at the resonant frequency, and measuring output power in both cases.
3. Calculate the transmission factor

$$T = \frac{\text{output circuit power}}{\text{available power to a matched load}} = \frac{\text{output power with filter}}{\text{output power with connector}}$$

4. Calculate the unloaded Q. This relationship is easily derived or is available in the hand books [19]

$$Q_u = \frac{Q_1}{1 - \gamma T}$$

The agreement between the computed unloaded Q determined from the theoretical attenuation and the measured Q is shown in Figure 42. The measurements were made with silver plated center conductors and ground planes with a characteristic impedance of 50 ohms, and a ratio of thickness of center conductor to ground plane spacing of 0.04.

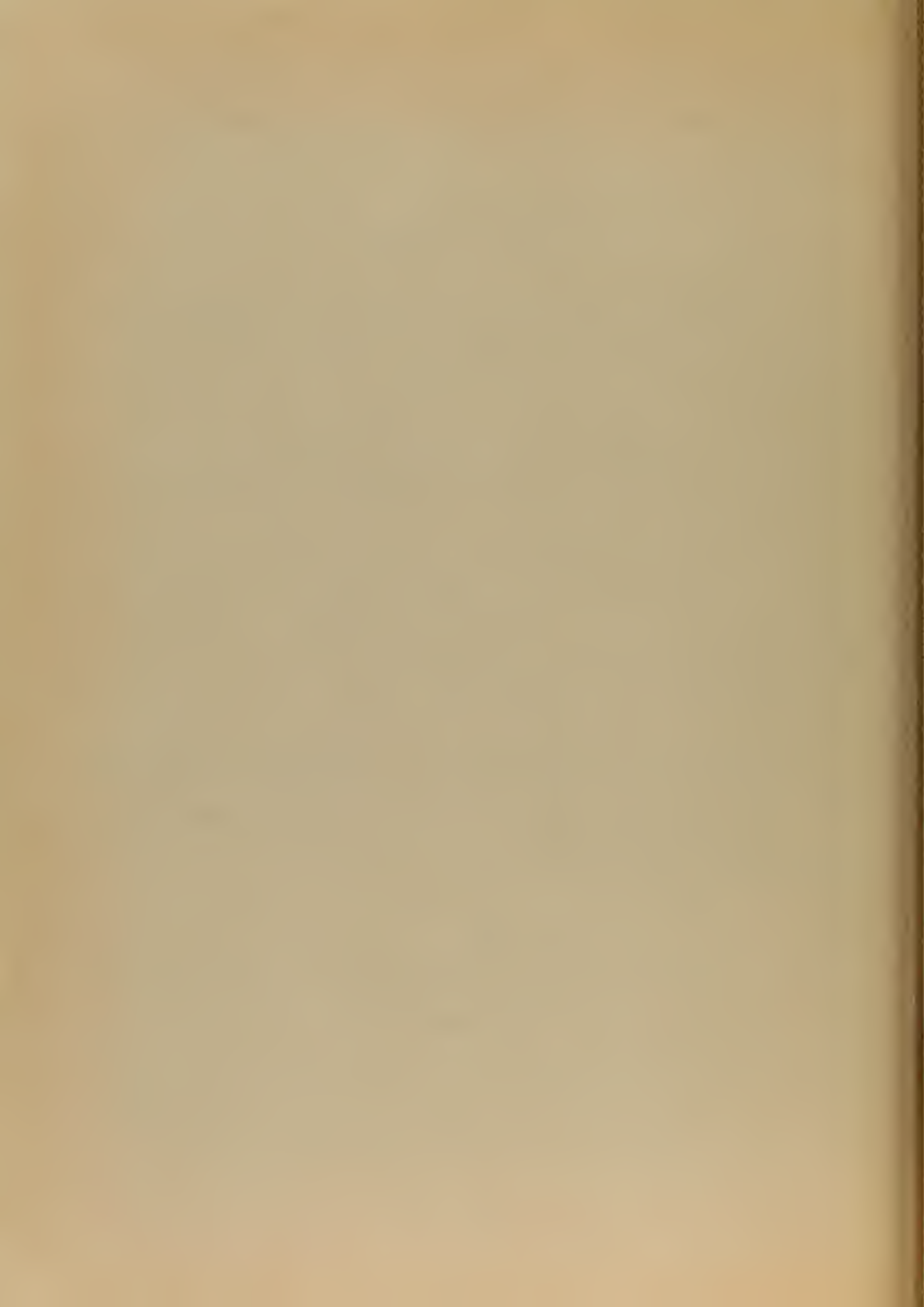
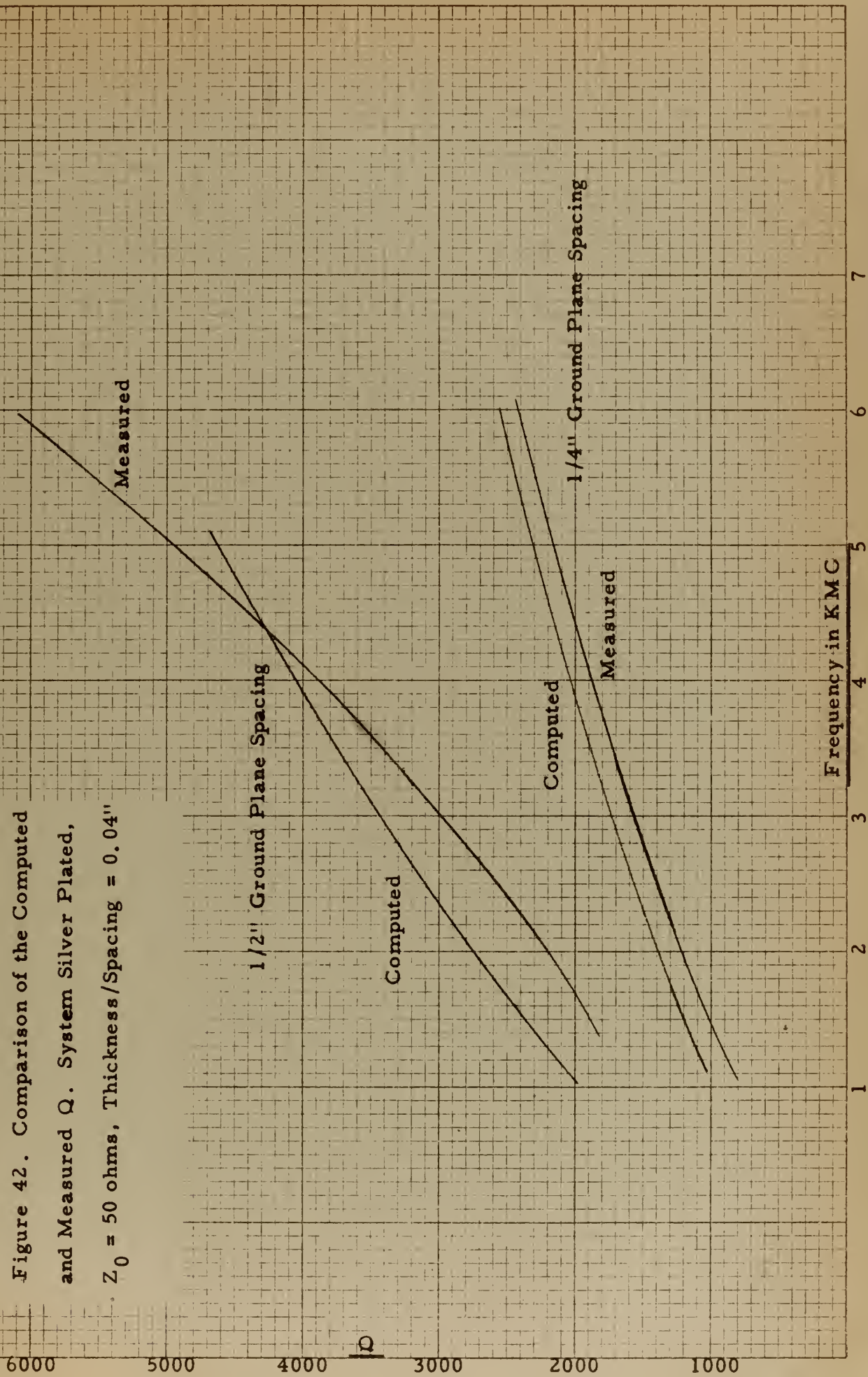
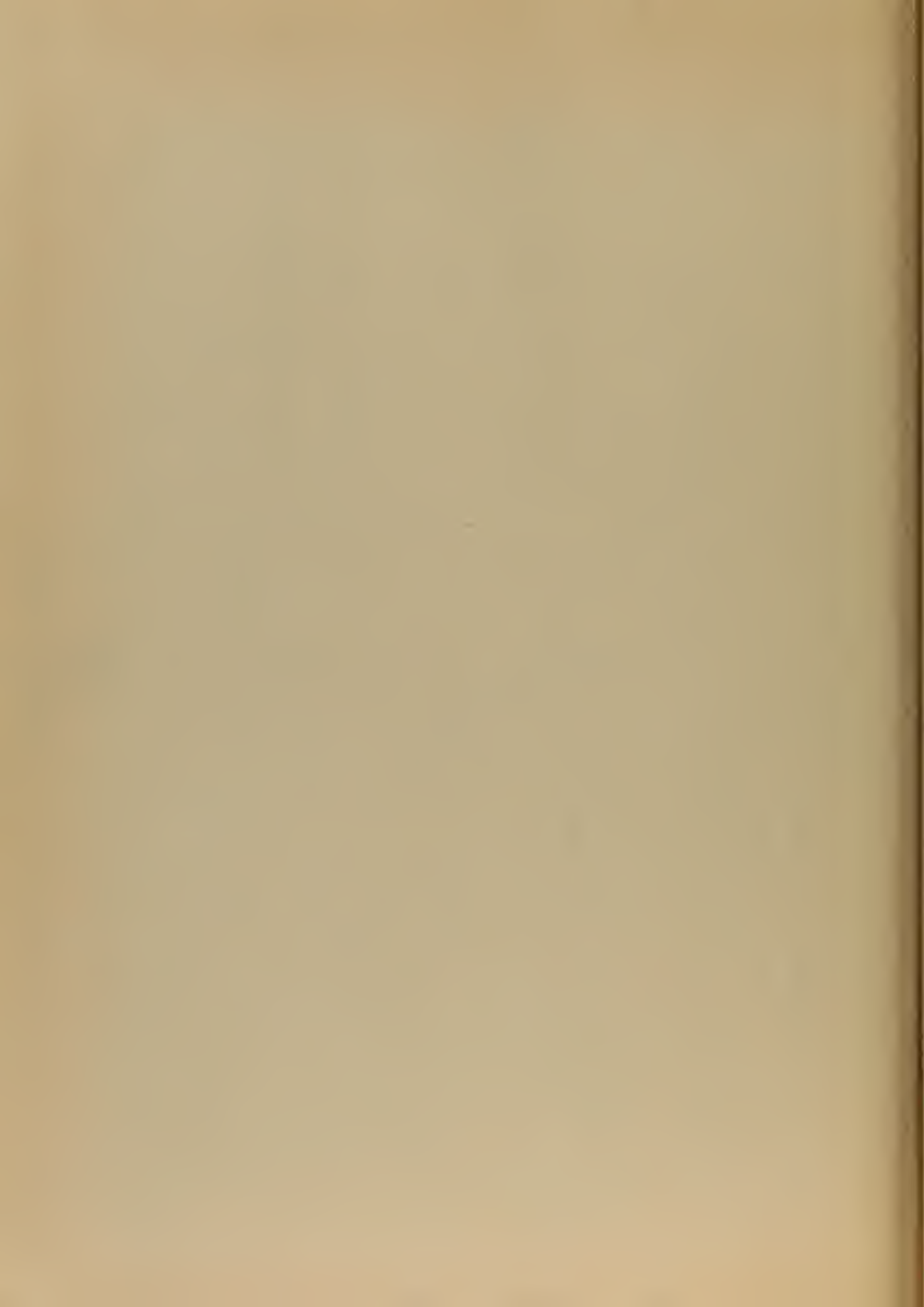


Figure 42. Comparison of the Computed
and Measured Q. System Silver Plated,
. $Z_0 = 50$ ohms, Thickness/Spacing = 0.04"





The gap capacitance effectively lengthens a resonant element as a top loading capacitor lengthens a short antenna. A convenient method for representing the effective gap capacitance is shown in Figure 45. The physical resonant length of a loaded element is determined by subtracting the effective line length that is added by the gap capacitance. The length of a halfwave element may then be expressed by:

$$L = \frac{1}{2\pi} [\pi - \arctan \frac{X_{c1} X_{f1}}{Z_0 [X_{c1} + X_{f1}]} - \arctan \frac{X_{c2} X_{f2}}{Z_0 [X_{c2} + X_{f2}]}]$$

since the loading capacitance is determined from:

$$X = -j Z_0 \cot [90^\circ - \theta] = -j Z_0 \tan \theta$$

with X_c and X_f the capacitance as shown in Figure 43. The capacitors are considered in parallel, assuming that the impedance of the input and output lines are small compared to X_c and may be neglected.

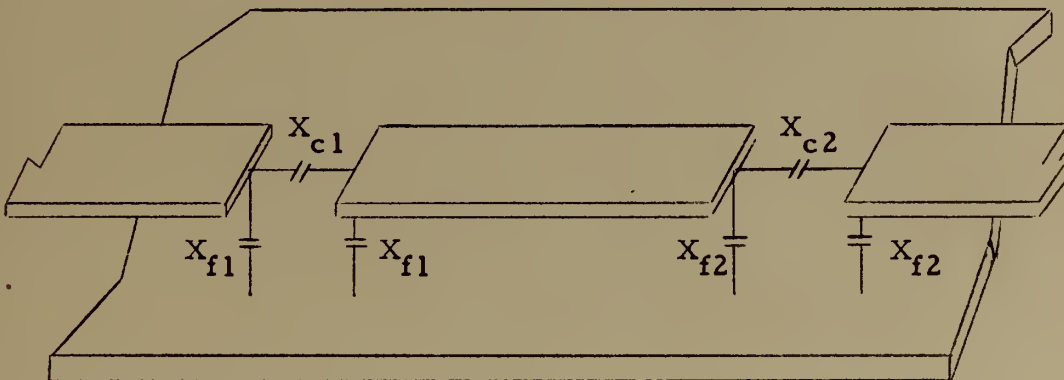
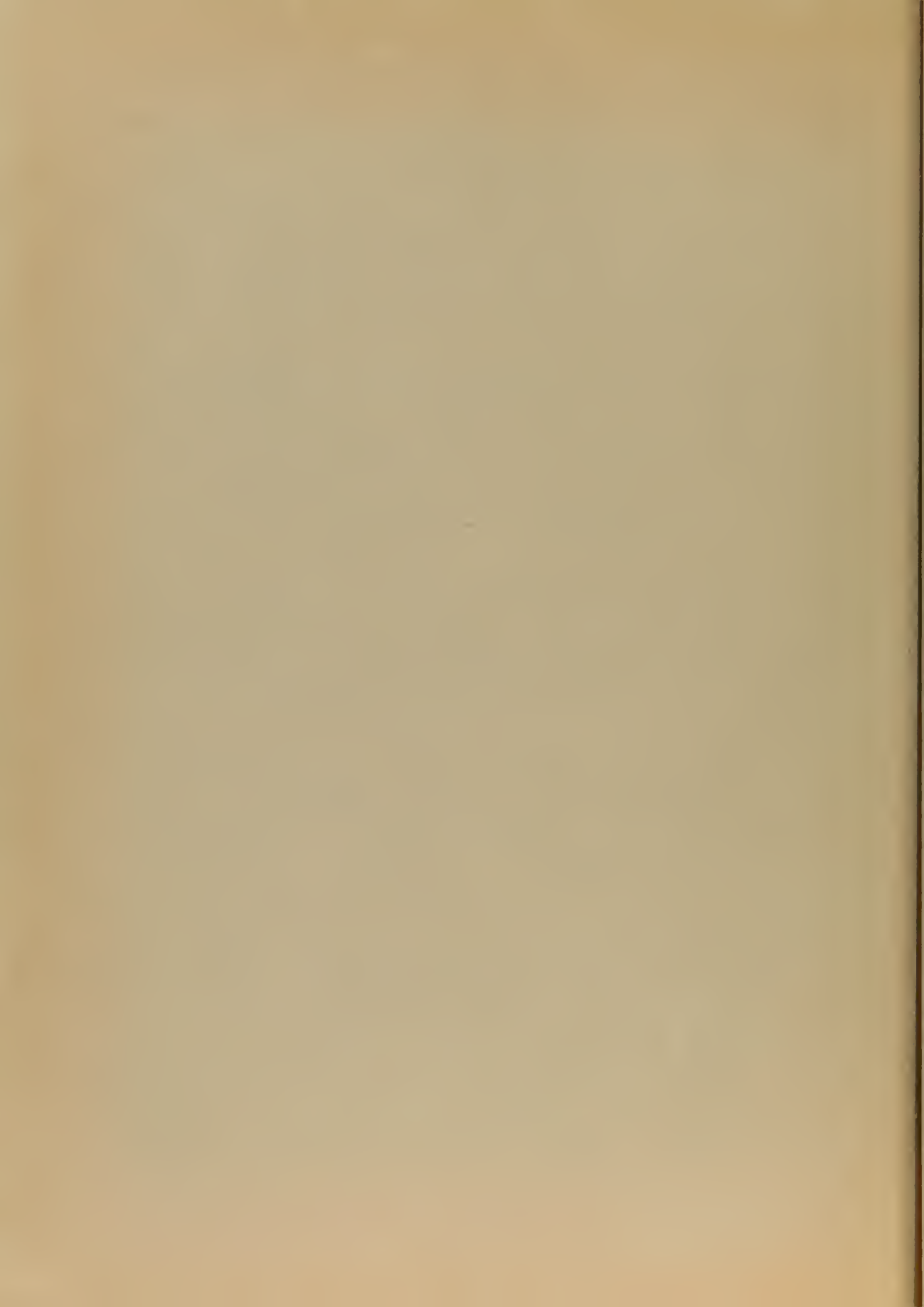


Figure 43. A Single Resonant Element Filter With Top Ground Plane Removed Showing Gap Reactance X_c and Fringing Reactance to Both Ground Planes X_f .

To determine the band pass characteristics of the filter, the loaded Q must be computed. The following procedure has been used at the



Airborne Instruments Laboratories to determine the loaded Q. Assume a fictitious loaded Q based on infinite unloaded Q [29].

$$Q_L' = X_c^2 - 1 \quad \text{with } Q_U = \infty$$

then

$$\frac{1}{Q_L} = \frac{1}{Q_L'} - \frac{1}{Q_U}$$

With the complete design requirements of a single element filter available, additional elements may be added. The voltage distribution of multiple elements within the pass band of the filter precludes the use of a synchronously tuned multiple element filter. However, by judicious selection of the gap spacing and the resonant lengths of the individual elements, the frequencies of the individual resonances may be obtained in accordance with the Butterworth or Tchebyscheff distribution to optimize the skirt selectivity and the flatness of the pass band[27]. The manner in which the voltage distribution along the filter effects the frequencies of resonance is shown in Figure 41. Considering the two element filter of the illustration, it can be seen that the fixed length elements provide two resonant frequencies. This effect results from the change in the effect of the capacitance due to the change in the voltage at the gap. At f_1 there is a voltage null or an effective ground point between the elements. therefore, the capacitance at the end of each of the elements is effectively the sum of C_f plus C_y in parallel. At f_2 there is no voltage difference across the gap, therefore C_y has no effect and the terminating capacitance is merely C_f . This effect is



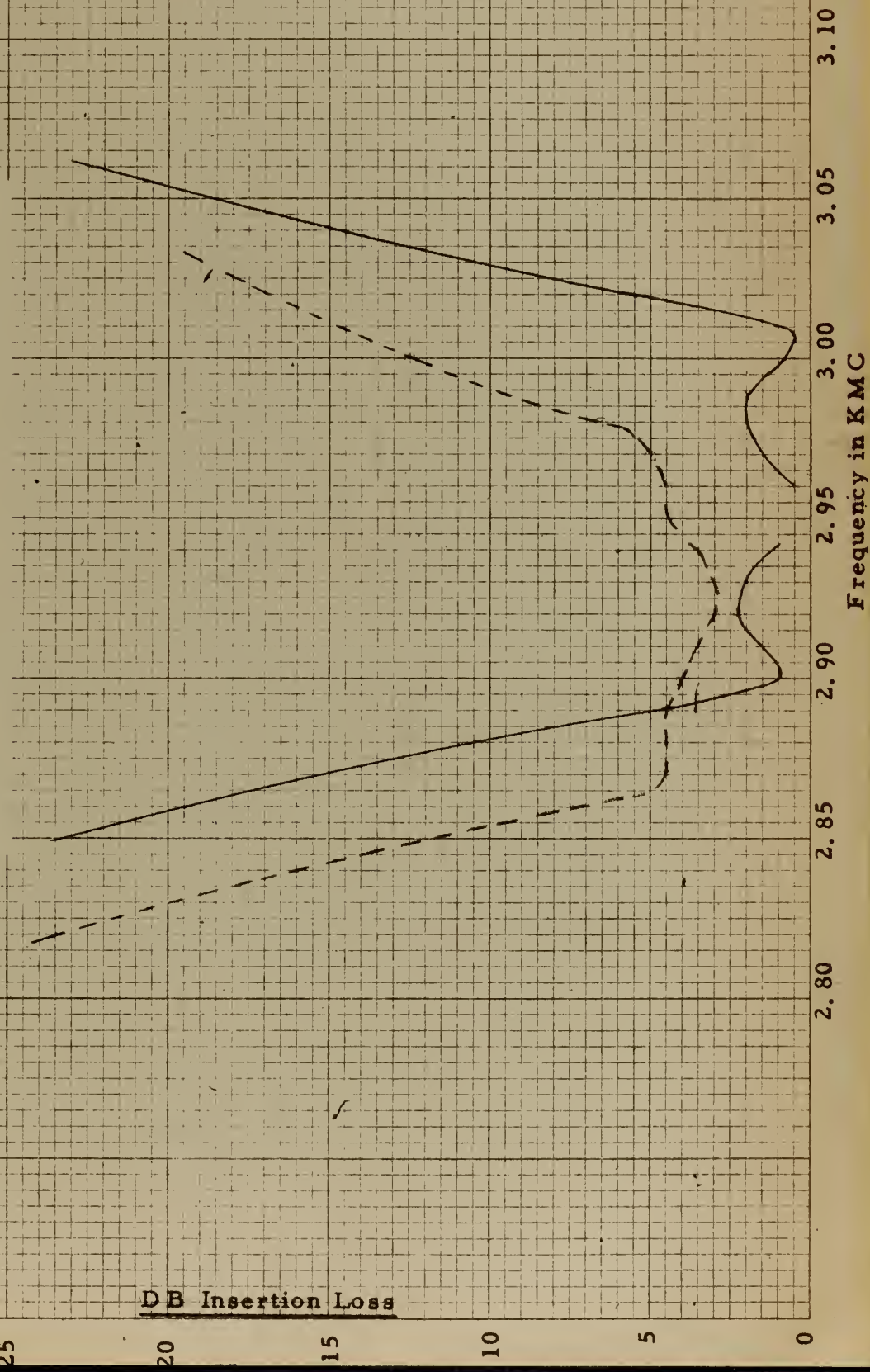
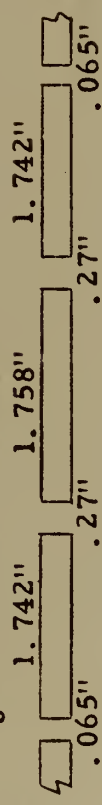
shown schematically in Figure 45.

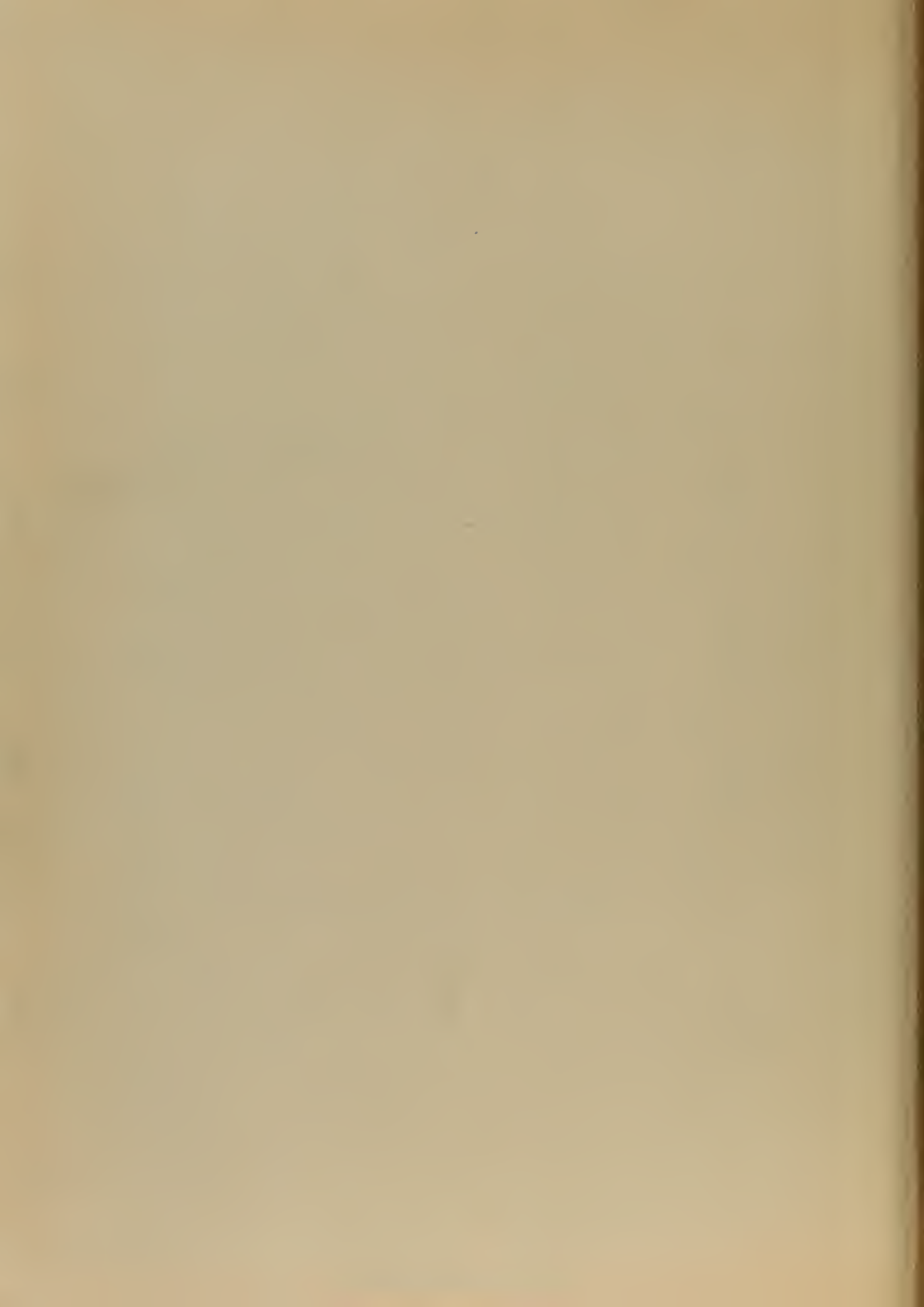
Figure 44 shows the response of a three element filter with the zero DB reference that of a straight through coupler. The three distinct humps in the response curve are due to the different voltage distributions along the filter. It is also interesting to note the detrimental effect of the polyfoam in this application where a high Q is required.



Figure 44. The Response of a Three Element Narrow Band Filter

$$Z_0 = 50 \text{ ohms, Spacing} = 1/2"$$





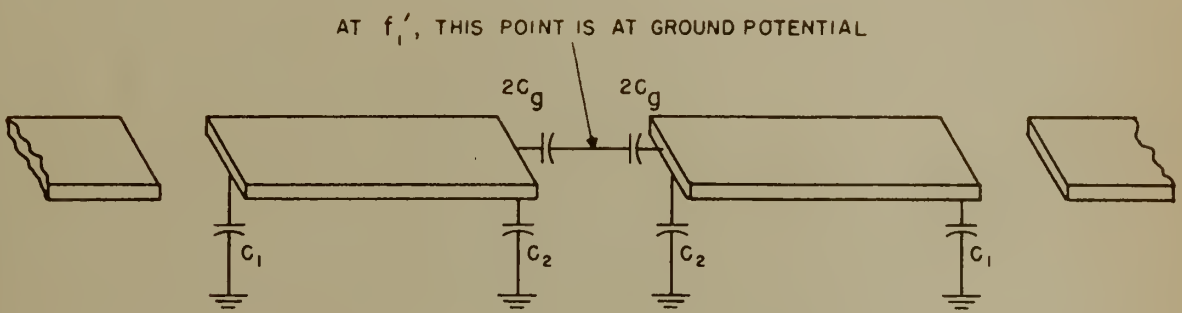


FIGURE 7. EFFECTIVE CAPACITANCES DETERMINING f'_1

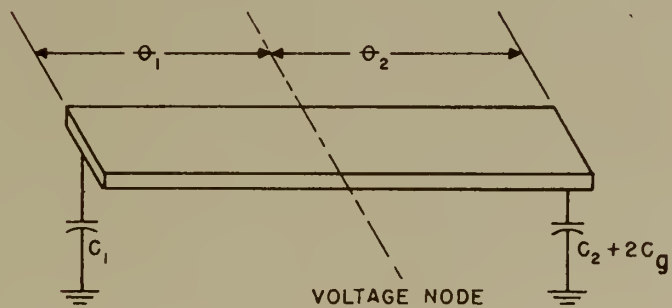
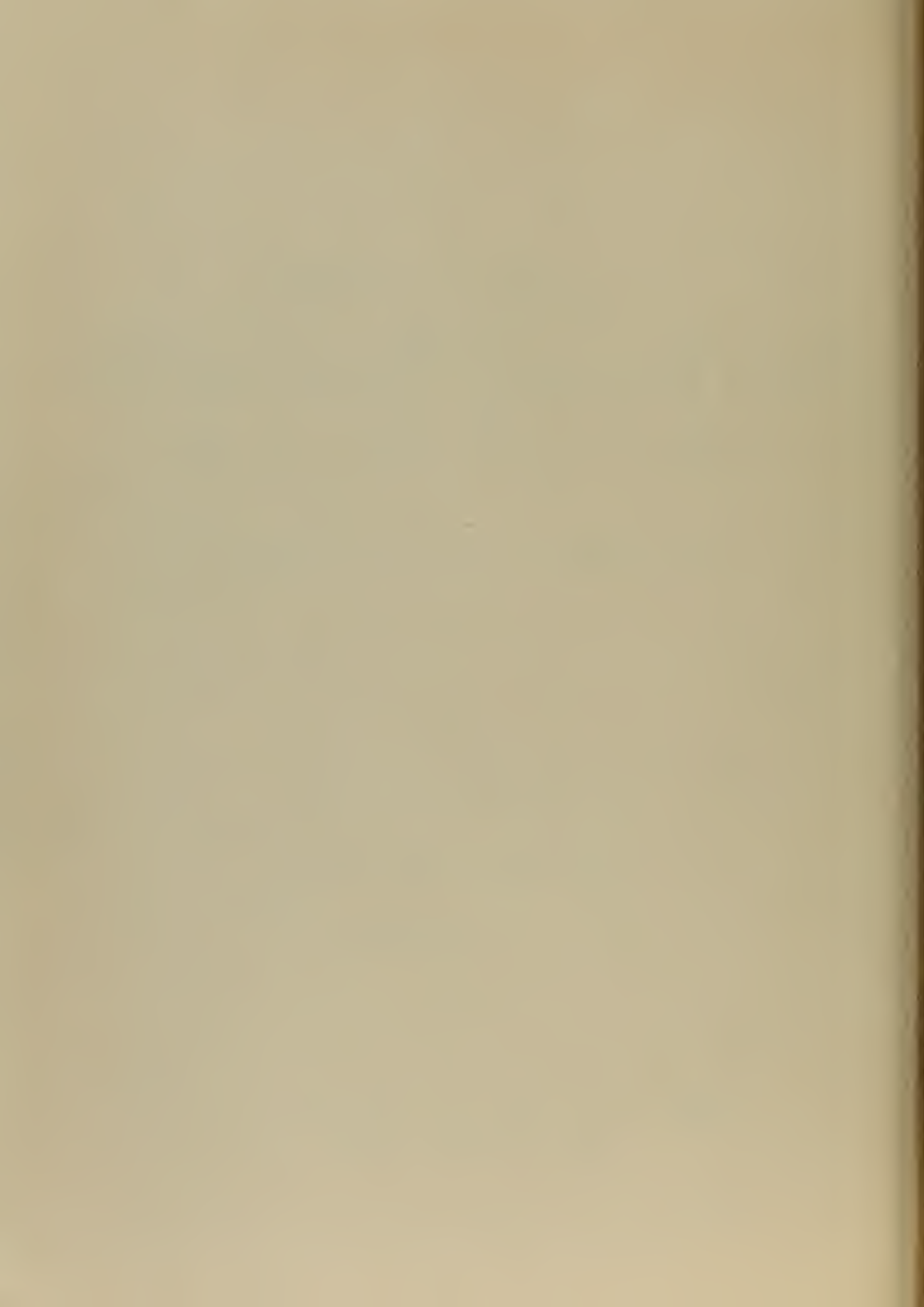


Figure 45. Schematic Representation of a
Resonant Element Filter



CHAPTER IV

THE SHUNT HYBRID JUNCTION

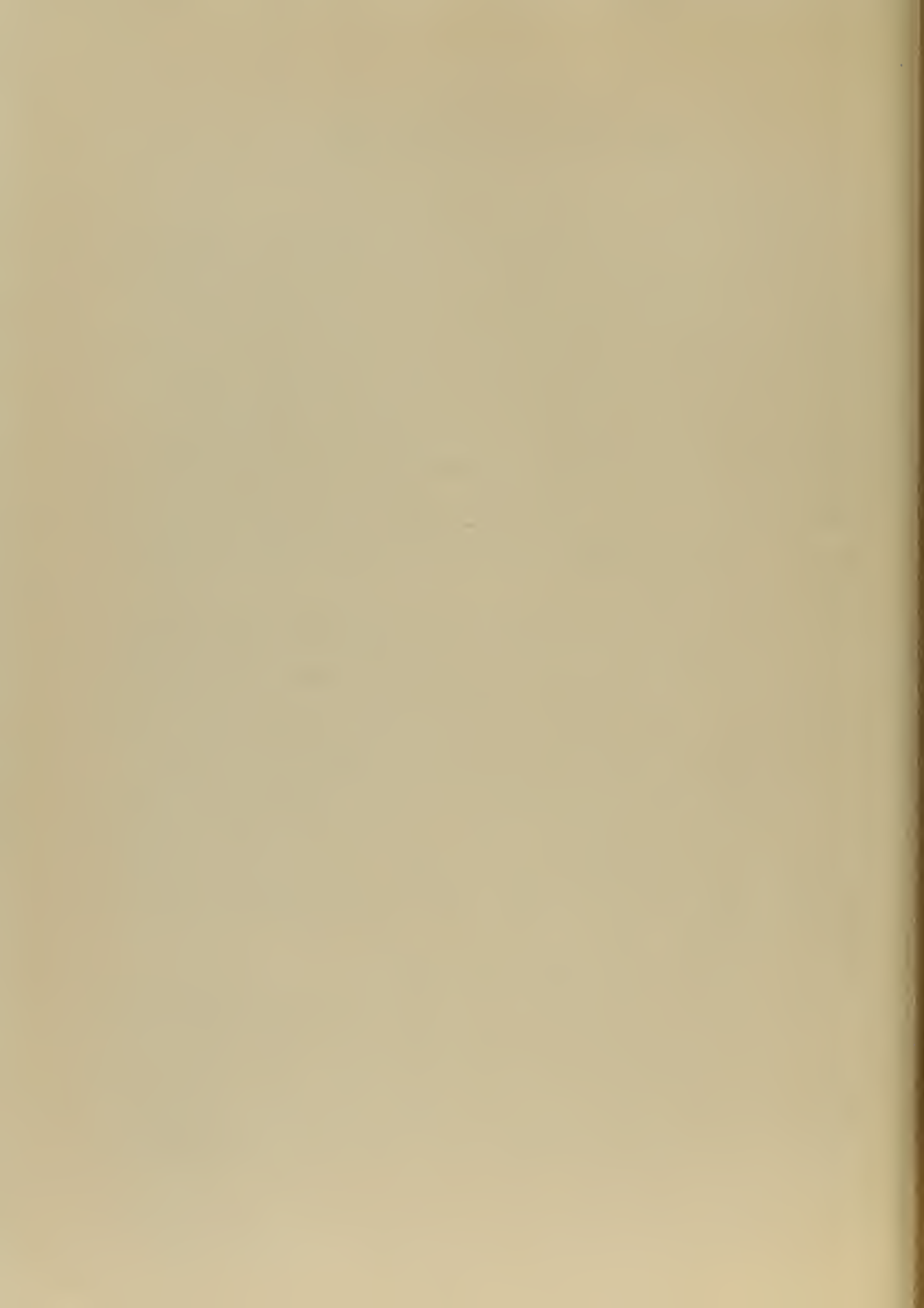
1. Introduction

The hybrid junction has long held an important place in coaxial and waveguide transmission systems, but it has not been used to its full advantage because of constructional difficulties and high cost. However, now with the strip transmission line technique, the hybrid junction may easily be constructed inexpensively and interest in exploiting all its possibilities has been renewed. Several of the more common uses are: balanced mixers, baluns, directional couplers, tees with all three arms matched, and means for providing isolation for two systems feeding power to a single line.

The strip transmission line hybrid junctions, like those of coaxial line and H plane waveguide, is a shunt hybrid junction, because the load impedances are effectively connected to the junction in parallel. All of the shunt hybrid junctions, whether strip transmission line, coaxial line, or H plane waveguide, will have the same response to changes in frequency, load impedance etc. Therefore, the general remarks and analysis of this chapter and Appendix D are directly applicable to all forms of the shunt hybrid junction.

2. Characteristic of the shunt hybrid junction

The hybrid junction is a versatile device that may be constructed in several forms with many interesting applications. The reader is probably familiar with many of these, so rather than dwell on this point, the junction will be analyzed mathematically. Then, after the characteris-



tics of the junctions analyzed become apparent several of the more common practical applications will be discussed.

To develop the characteristics of the shunt hybrid junction, a general equivalent circuit will be drawn and the analysis will be made on the basis of that circuit. This form of analysis follows from the work of Budenbaum [9]. Figure 46 represents the center conductor of an arbitrary four arm strip transmission line junction, with arm characteristic admittances Y_{on} , connecting line characteristic admittances Y_n , and connecting line mean lengths L_n .

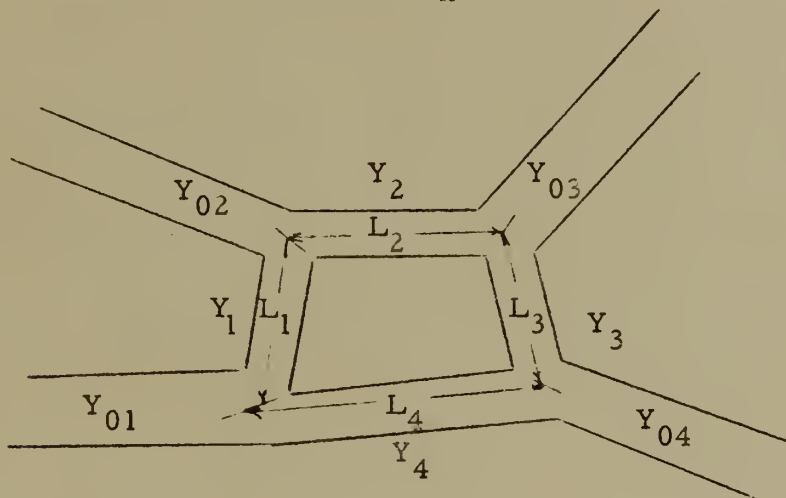
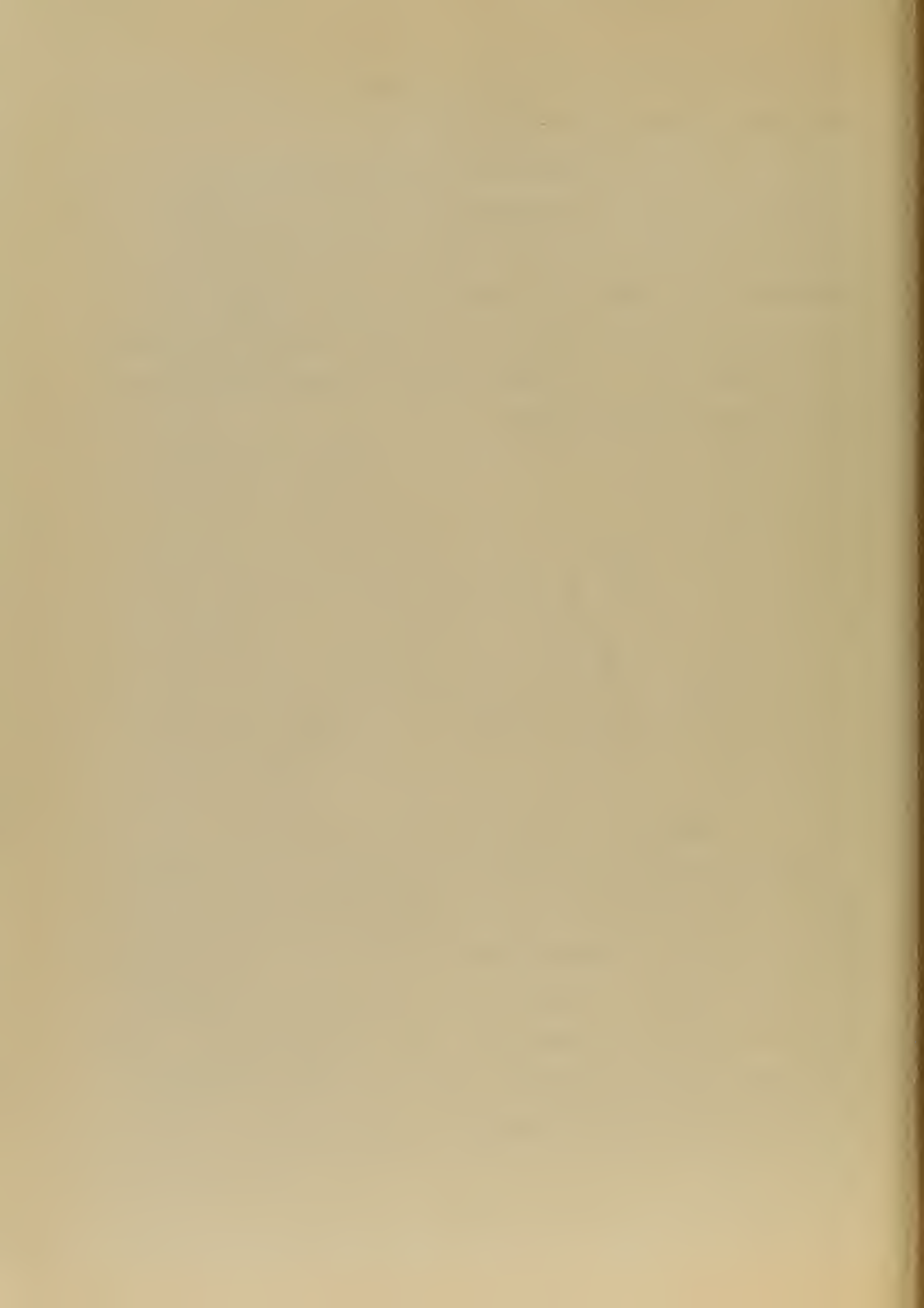


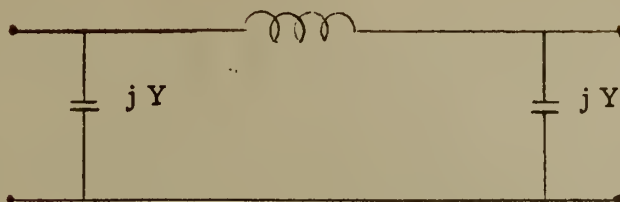
Figure 46. An Arbitrary Four Arm Junction.

As the first step in determining the equivalent circuit of the junction, a pi equivalent of the lengths of transmission line that connect the arms will be drawn, assuming lossless lines. Only lines of one quarter and three quarter wavelength will be considered; since these are the only connecting line lengths used, at the design frequency. Lines of arbitrary lengths representing frequencies off the design frequency are reserved for the general discussion of Appendix D.



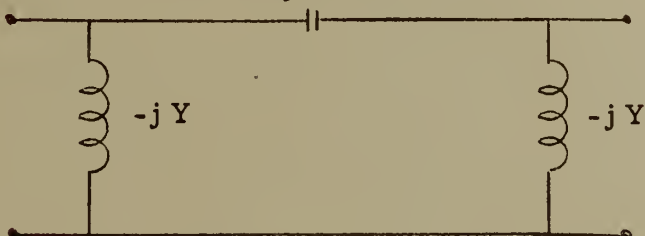
for $L = \lambda/4$ the pi equivalent circuit is:

-j Y



for $L = 3\lambda/4$ the pi equivalent circuit is:

jY



Now armed with the equivalent circuits for the lines around the ring of the junction, we are prepared to attack specific cases.

Case 1.

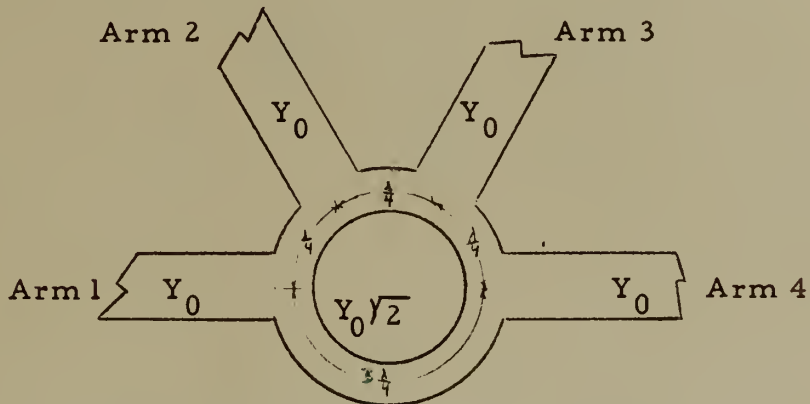
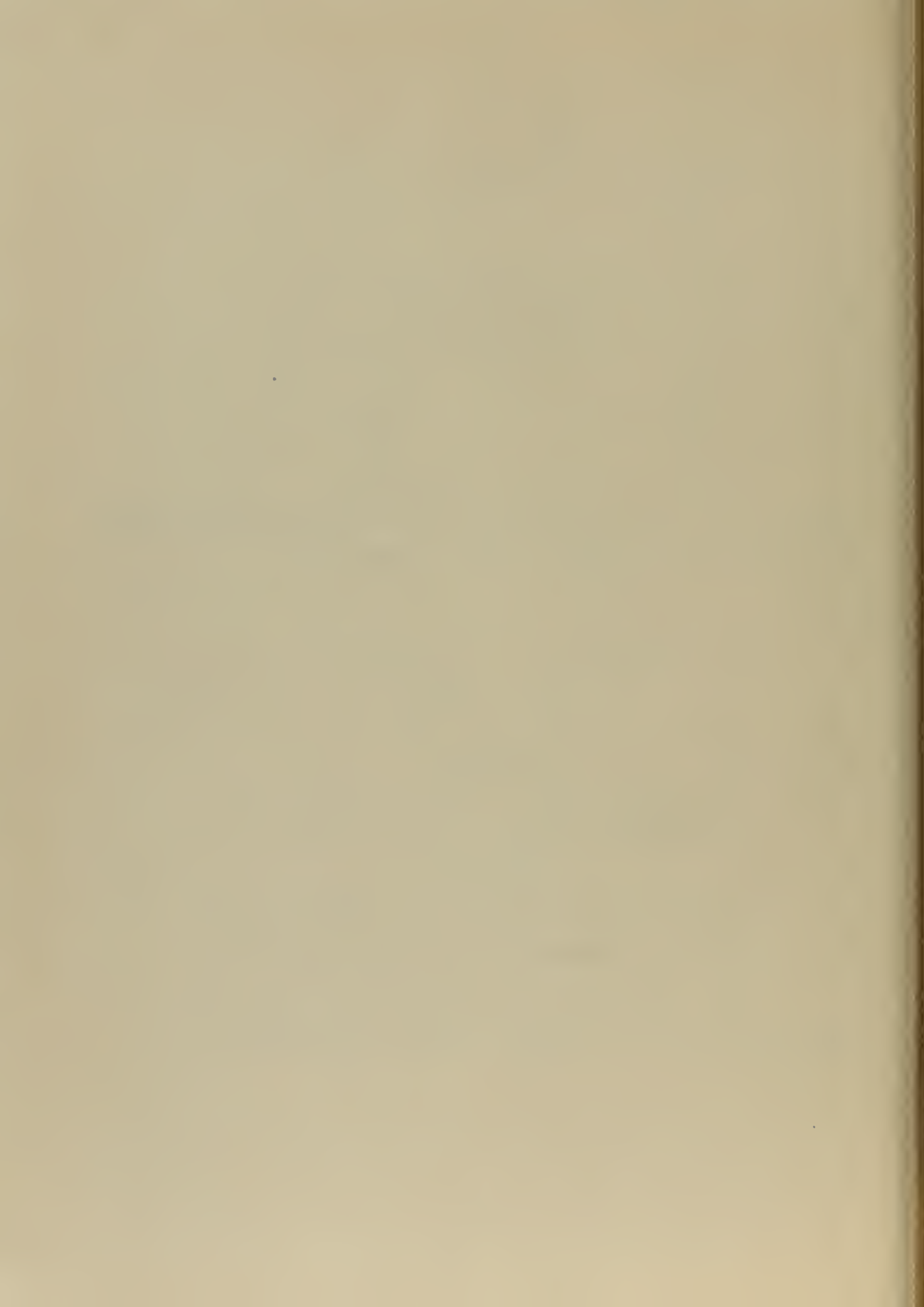


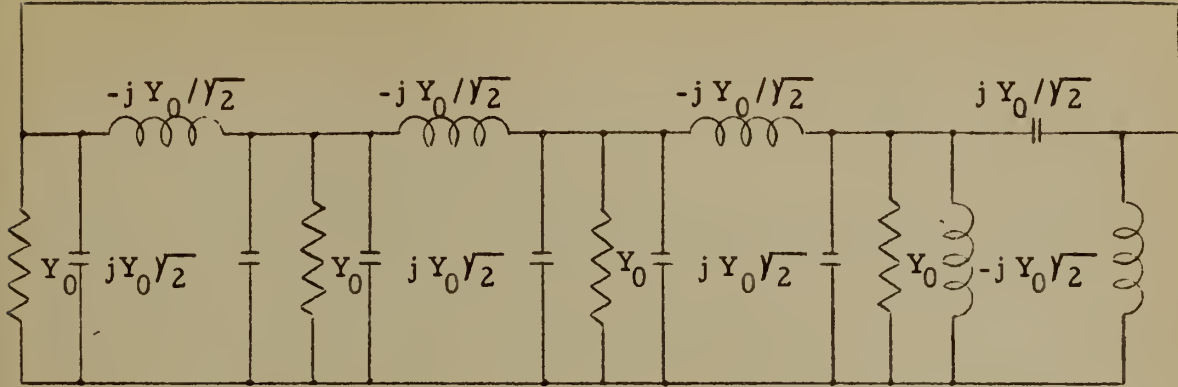
Figure 47. An Actual Size Center Conductor for a C

Band Strip Transmission Line Hybrid Junction With

$$Y_0 = \frac{1}{70} \text{ mhos, and a ground plane spacing} = 3/8"$$

The equivalent circuit of the hybrid junction shown in Figure 47 is:





From this equivalent circuit we may write the admittance determinant using nodal analysis:

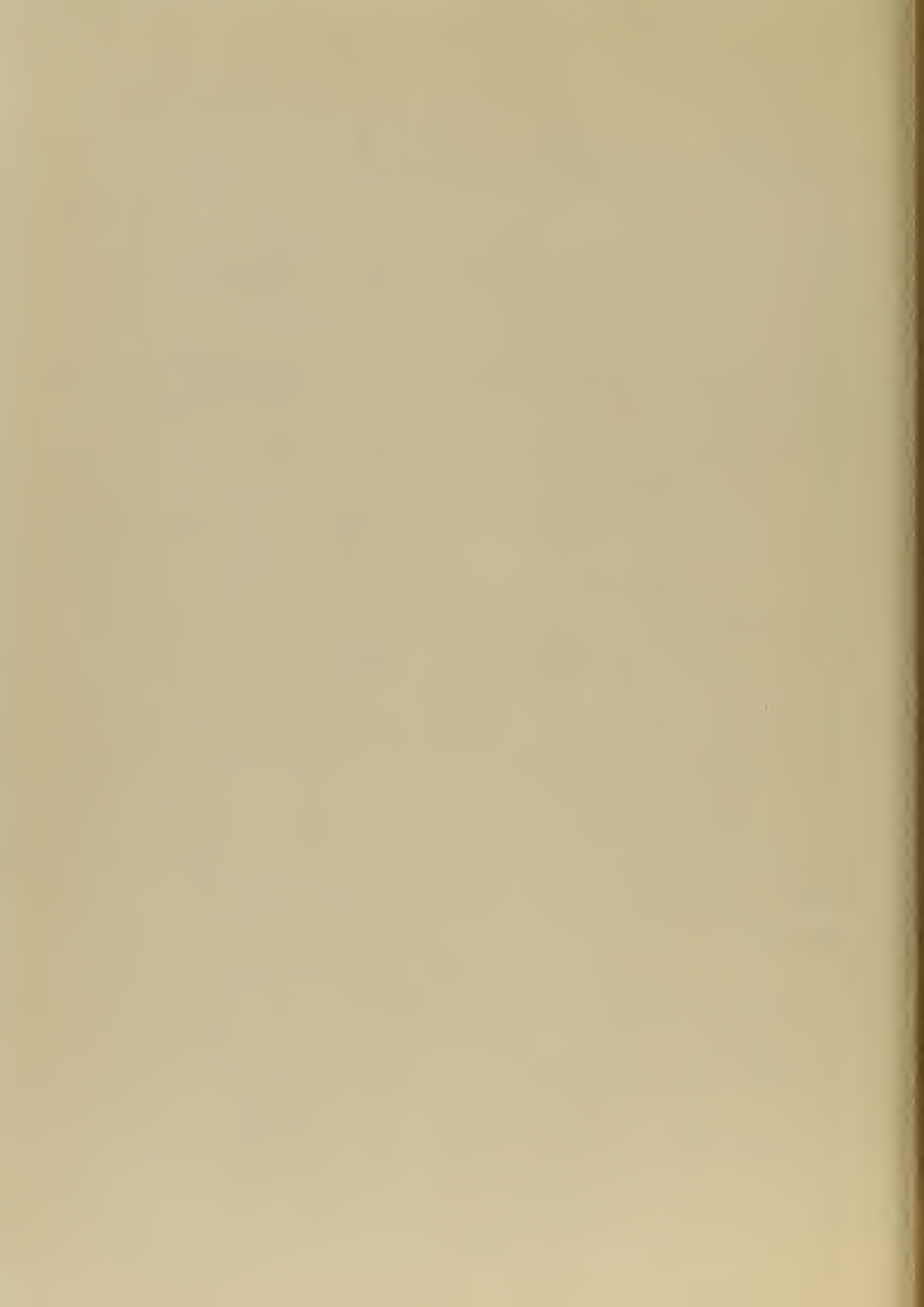
$$\Delta = \begin{vmatrix} Y_0 & j\frac{Y_0}{Y_2} & 0 & -j\frac{Y_0}{Y_2} \\ j\frac{Y_0}{Y_2} & Y_0 & j\frac{Y_0}{Y_2} & 0 \\ 0 & j\frac{Y_0}{Y_2} & Y_0 & j\frac{Y_0}{Y_2} \\ -j\frac{Y_0}{Y_2} & 0 & j\frac{Y_0}{Y_2} & Y_0 \end{vmatrix}$$

From the determinant, the cofactors Δ_{mn} , and the total value Δ are obtained. The symmetry of the determinant greatly simplifies the computation.

$$\Delta_{11} = \Delta_{22} = \Delta_{33} = \Delta_{44} = 2 Y_0^3$$

$$\Delta_{12} = \Delta_{21} = \Delta_{34} = \Delta_{43} = \Delta_{23} = \Delta_{32} = -j\sqrt{Y_2} Y_0^3$$

$$\Delta_{14} = \Delta_{41} = +j\sqrt{Y_2} Y_0^3$$



$$\Delta_{13} = \Delta_{31} = \Delta_{24} = \Delta_{42} = 0$$

$$\Delta = 4 Y_0^4$$

From elementary theory [7] :

The input admittance Y_{nn} of arm n is defined as:

$$Y_{nn} = \frac{I_n}{E_n} = \frac{\Delta}{\Delta_{nn}}$$

The transfer admittance from arm m to n is defined as:

$$Y_{mn} = \frac{I_m}{E_n} = \frac{\Delta}{\Delta_{mn}}$$

Therefore, the input admittance of all four arms

$$Y_{11} = Y_{22} = Y_{33} = Y_{44} = 2 Y_0 = Y_{\text{line}} + Y_{\text{junction}}$$

From this we can see that all four arms are matched. The input admittance, as calculated, includes the admittance looking into the junction and the admittance of the load.

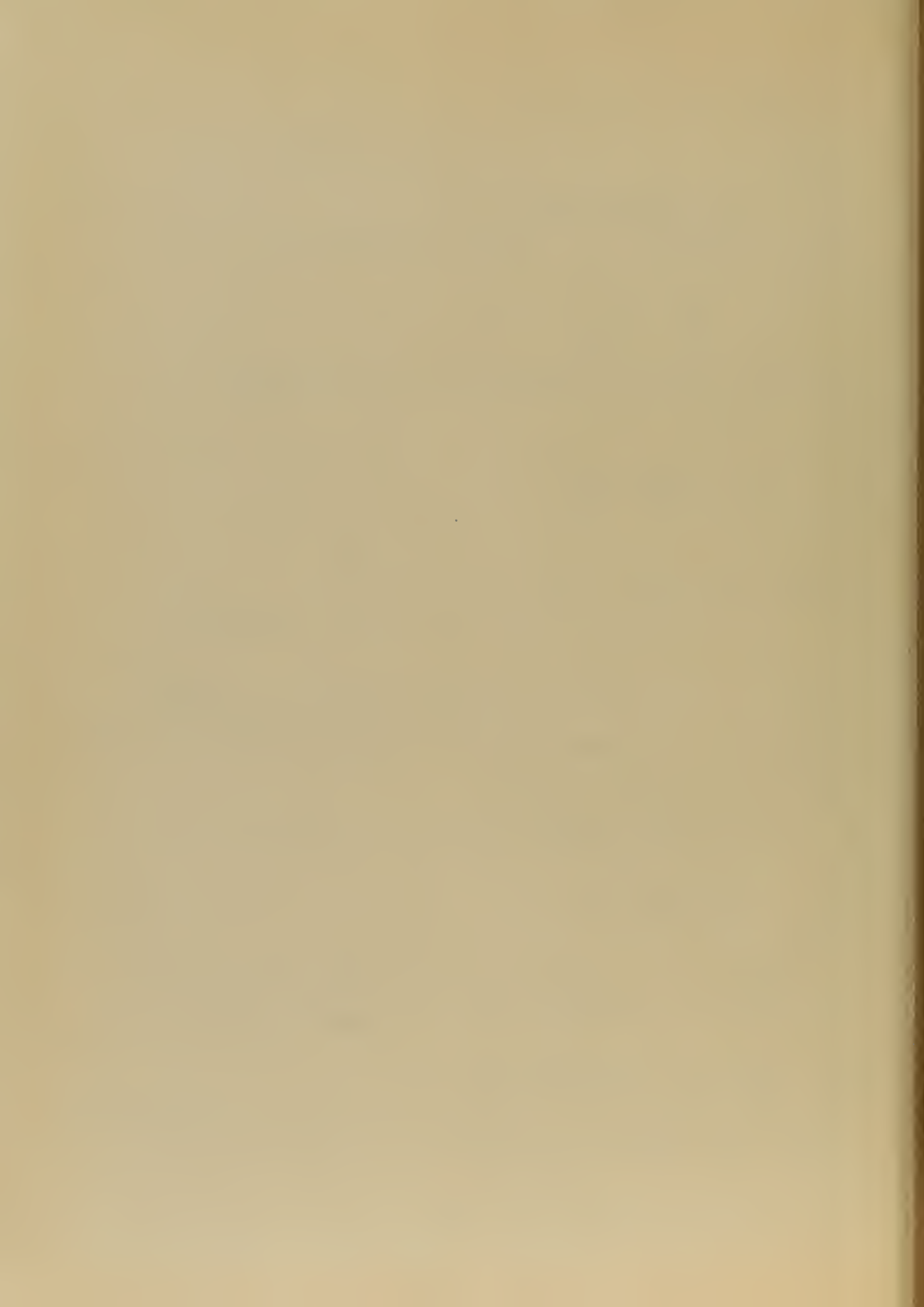
There is perfect isolation between arms one and three

$$Y_{13} = Y_{31} = \infty$$

$$\frac{I_1}{E_3} = \infty \quad \text{Therefore: } E_3 = 0 \quad \text{with a finite current applied at arm 1.}$$

$$\text{and } \frac{I_3}{E_1} = \infty \quad \text{Therefore: } E_1 = 0$$

With a current applied at terminal one, the voltage at terminals two and



and four are 180° out of phase.

$$\frac{\Delta_{12}}{\Delta_{14}} = \frac{-j\gamma_2 Y_0^3}{+j\gamma_2 Y_0^3} = -1 = 180^\circ$$

The voltage at terminal two and four are in phase when a current is applied at terminal three

$$\frac{\Delta_{32}}{\Delta_{34}} = \frac{-j\gamma_2 Y_0^3}{-j\gamma_2 Y_0^3} = +1 = 0^\circ$$

The power applied to terminal one or three is divided equally between arms two and four.

$$P_n = |E_n|^2 Y_{nn} \text{ By definition:}$$

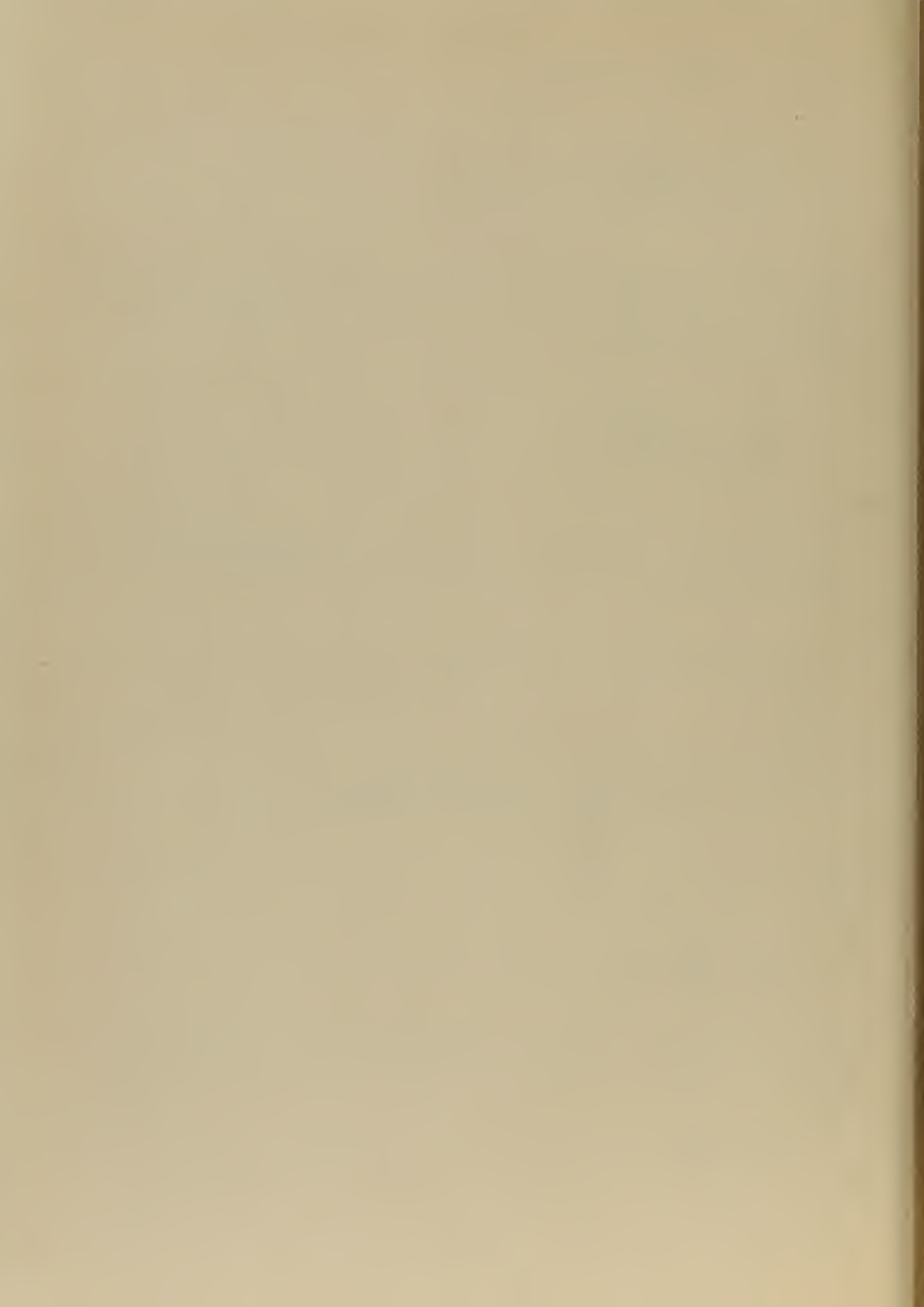
$$\frac{P_1}{P_2} = \frac{|I_1 Y_{11}|^2 Y_{11}}{|I_1 Y_{12}|^2 Y_{22}} = \frac{|I_1|^2 Y_0|^2 2 Y_0^2}{|I_1|^2 Y_2 Y_0|^2 2 Y_0^2} = 1/2$$

Similarly:

$$\frac{P_1}{P_4} = \frac{P_3}{P_2} = \frac{P_3}{P_4} = 1/2$$

Current from arms two and four add at arm three and subtract at arm one.

$$Y_{21} = -Y_{41}$$



$$Y_{23} = Y_{43}$$

Case II

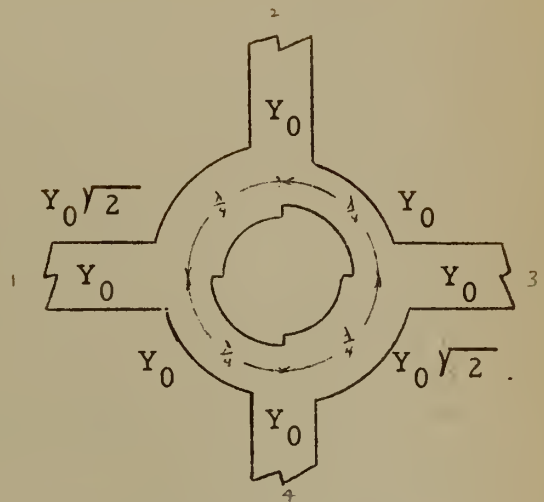
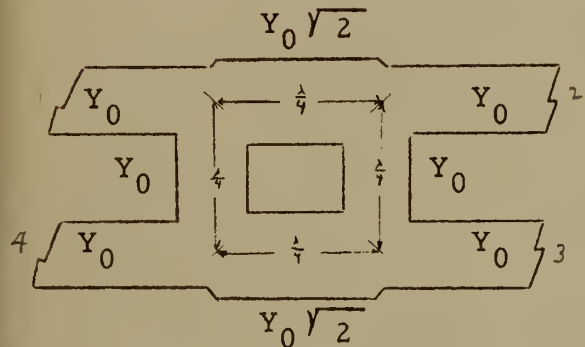
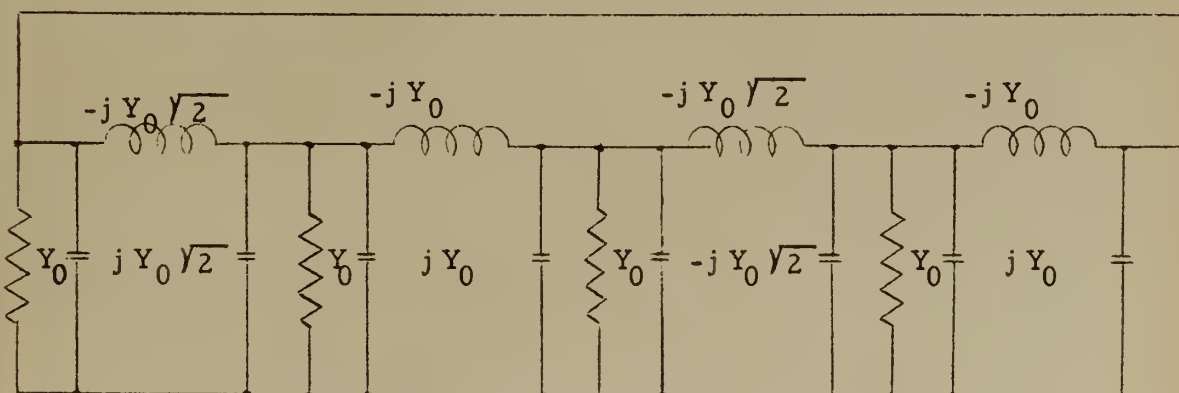
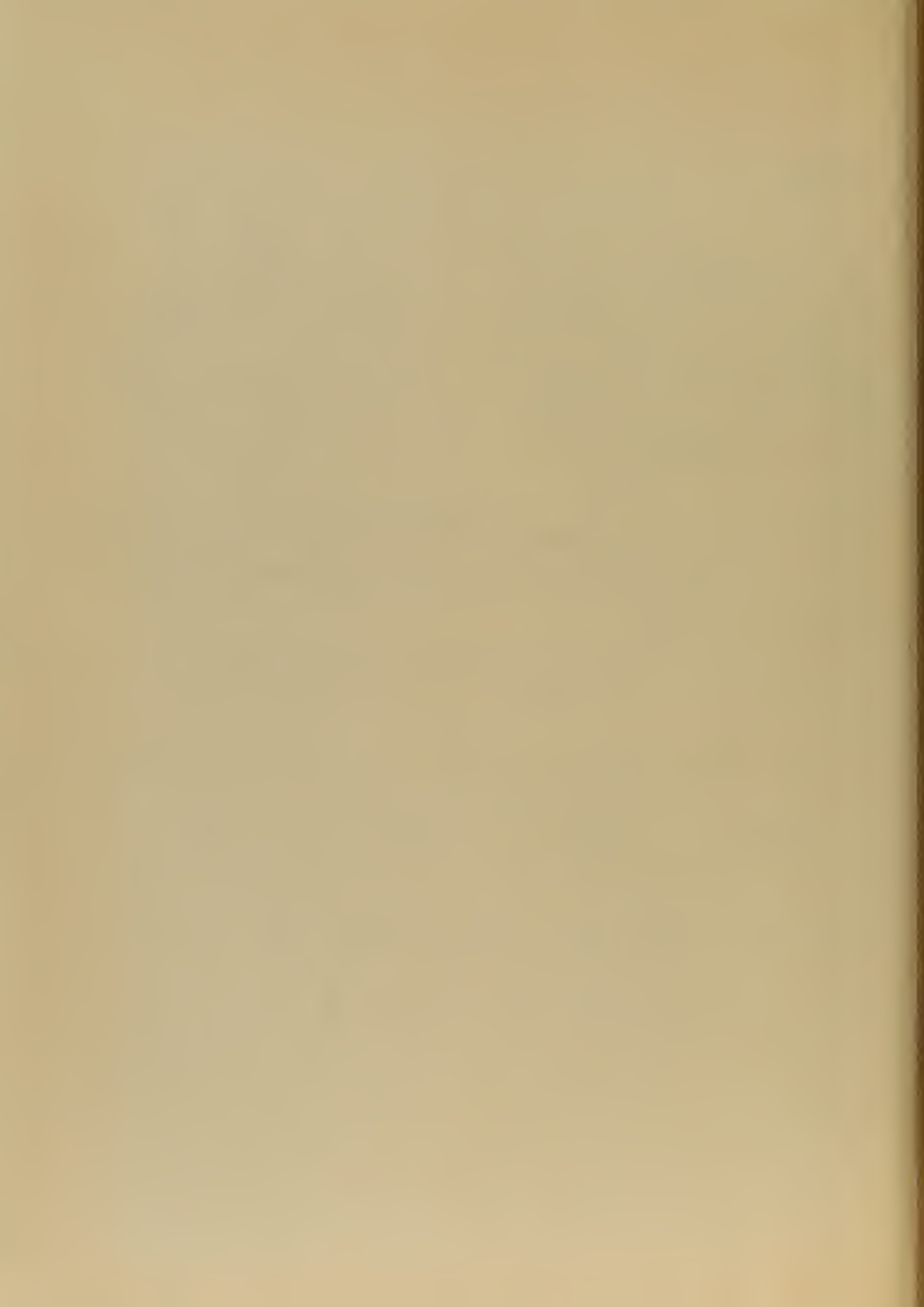


Figure 48. Two Hybrid Junctions with Identical Electrical Characteristics.

Shown actual size with Z_0 of 50 ohm ground plane spacing of 1/4", frequency at 5000 MC.

The equivalent circuit of the junction shown in Figure 48 is:





From this we obtain the determinant:

$$\Delta = \begin{vmatrix} Y_0 & jY_0\sqrt{2} & 0 & jY_0 \\ jY_0\sqrt{2} & Y_0 & jY_0 & 0 \\ 0 & jY_0 & Y_0 & jY_0\sqrt{2} \\ jY_0 & 0 & jY_0\sqrt{2} & Y_0 \end{vmatrix}$$

The cofactors and value of the determinant are:

$$\Delta_{11} = \Delta_{22} = \Delta_{33} = \Delta_{44} = 4Y_0^3$$

$$\Delta_{12} = \Delta_{21} = -j2\sqrt{2}Y_0^3$$

$$\Delta_{31} = \Delta_{13} = \Delta_{24} = \Delta_{42} = -2\sqrt{2}Y_0^3$$

$$\Delta_{34} = \Delta_{43} = j2\sqrt{2}Y_0^3$$

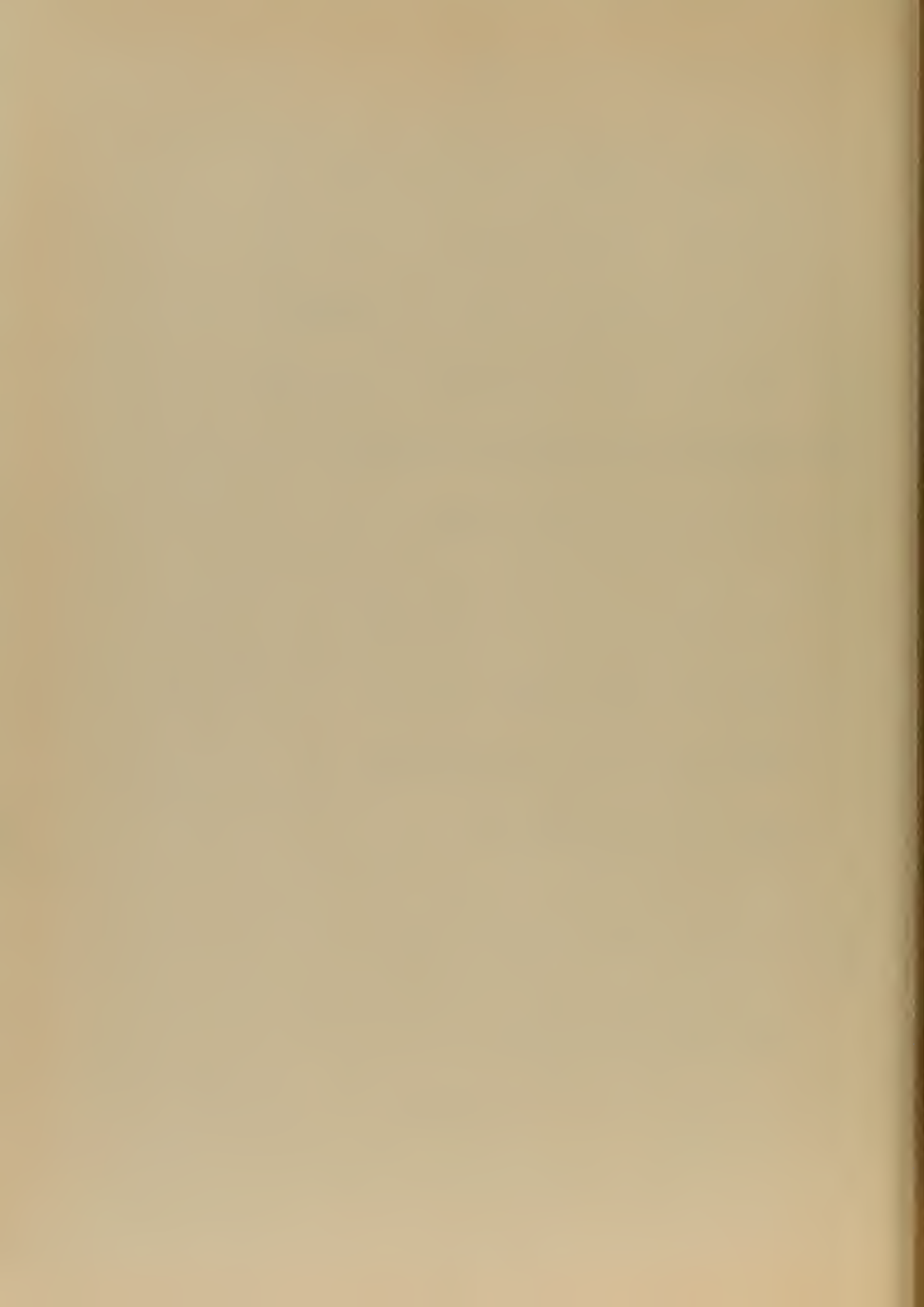
$$\Delta_{14} = \Delta_{41} = \Delta_{23} = \Delta_{32} = 0$$

$$\Delta = 8Y_0^4$$

and the input and transfer admittances are:

$$Y_{11} = Y_{22} = Y_{33} = Y_{44} = 2Y_0$$

$$Y_{12} = Y_{21} = j2\sqrt{2}Y_0$$



$$Y_{13} = Y_{31} = Y_{24} = Y_{42} = -2\sqrt{2} Y_0$$

$$Y_{34} = Y_{43} = j2\sqrt{2} Y_0$$

$$Y_{14} = Y_{41} = Y_{23} = Y_{32} = \infty$$

Following the procedure used in Case I, it is apparent that: the input to all four arms is matched, there is perfect isolation between arms one and four, with a signal applied to either arm one or four the output from arm two or three are 90° out of phase, power input to arms one and four divides evenly between arms two and three, and the voltage produced at arms one and four by the currents at arms two and three add in quadrature.

Case III

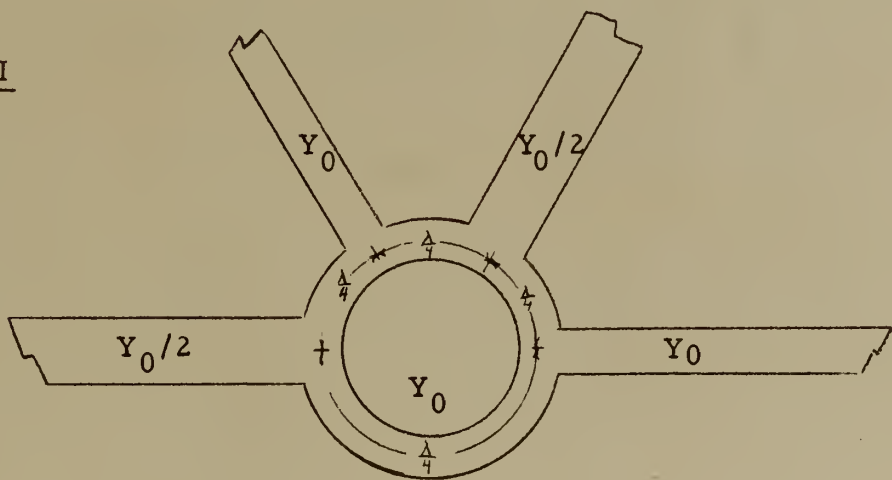
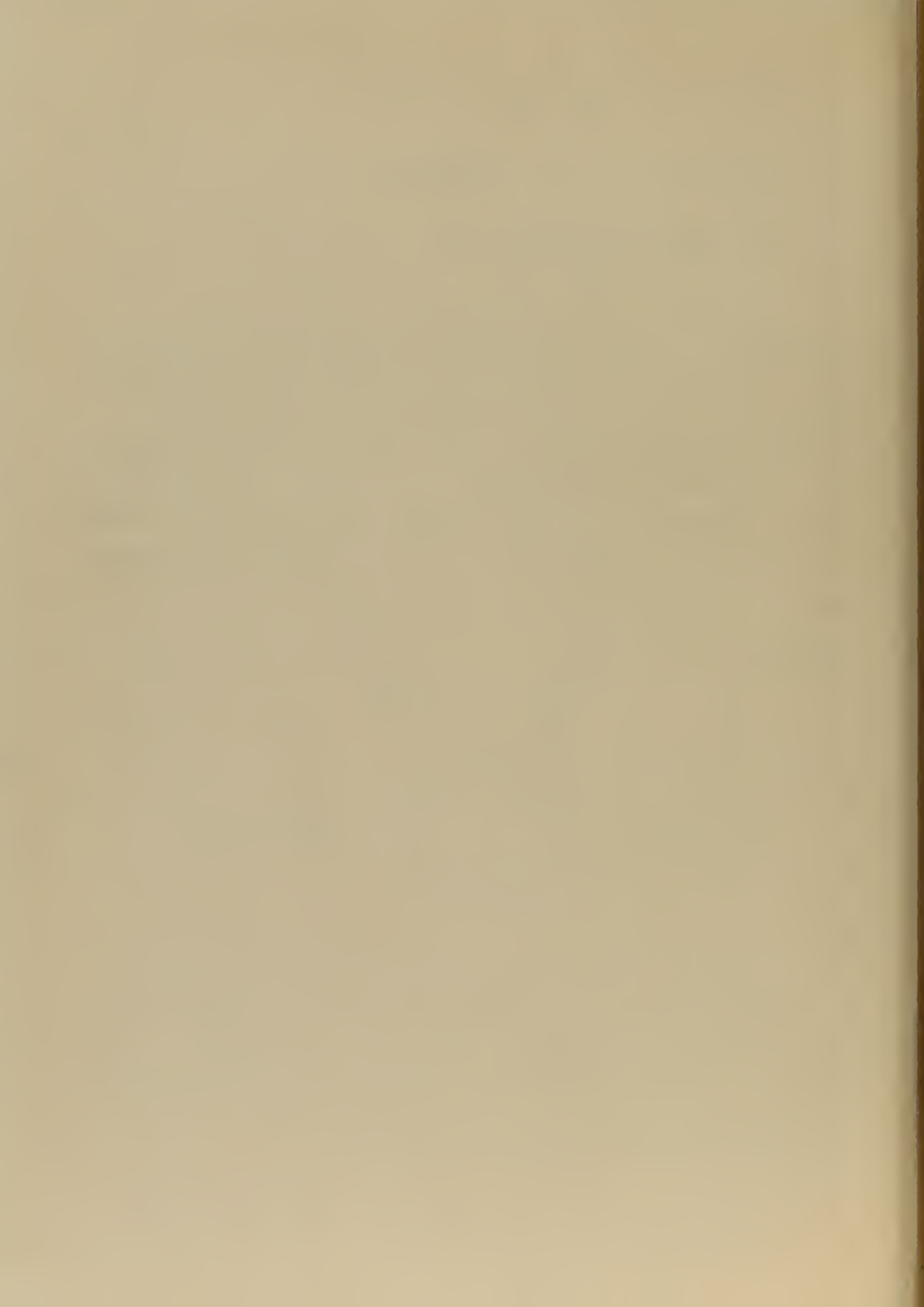


Figure 49. Hybrid Junction with Different Arm Admittances

The procedure for the analysis of this junction is similar to that of Cases I and II, and the details are left to the interested reader. This junction has the same characteristics as that of Case I except that the admittance of arms one and three are different.



3. Practical Applications for the Hybrid Junction

From the characteristics of the hybrid junction deduced from the preceding section, numerous practical applications may be determined, and many of these will be enumerated here. These applications by no means exhaust all the possibilities, and the reader should be able to provide countless other uses, as well as many ramifications to those considered.

Tee Junction with Three Arms Matched -- The impedance of all of the arms of the hybrid junction analyzed are matched to the respective lines at the design frequency. Therefore, the junction may serve as tees with all of the arms matched.

Directional Coupler with Three DB Coupling -- The junction may serve as directional couplers with three DB coupling, since the analyses show that one-half the input power is coupled to each of two output arms.

Hybrid Transformer -- The hybrid junction may serve as a hybrid transformer; i. e., a transformer with two independent inputs that are isolated from each other, yet both provide power to a common output. A consideration of the analysis shows that the junction has complete isolation between two arms and the inputs from both these arms are evenly divided between the other two arms. The following schematic of a hybrid junction, Figure 50, illustrates how this property may be applied to a radar system. The object here is to have the transmitter power coupled to the antenna, and the returned echo coupled to the receiver with no coupling of the power transmitted to the receiver.



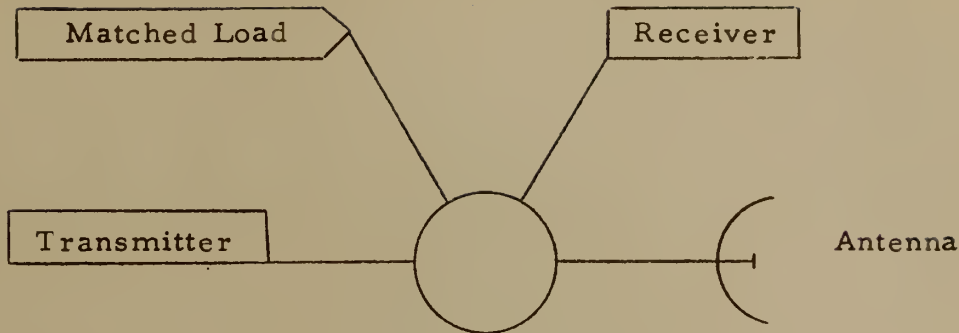


Figure 50. Hybrid Transformer Radar Antenna Coupling Unit

From this is can be seen that the receiver and transmitter can utilize the same antenna without TR and ATR tubes. There is a six DB loss in this system, due to the transmitted power that is dissipated in the load and the signal power that is returned to the transmitter.

Balun -- The hybrid junction of Cases I and III serve as ideal baluns. The signal input to one arm (arm one) is evenly divided and applied to two other arms (arms two and four) 180° out of phase.

Balanced Mixer -- The hybrid junction of Cases I and III through a remarkable combination of the majority of its properties serves as an excellent balanced mixer. One form of a hybrid junction balanced mixer is shown schematically in Figure 51.

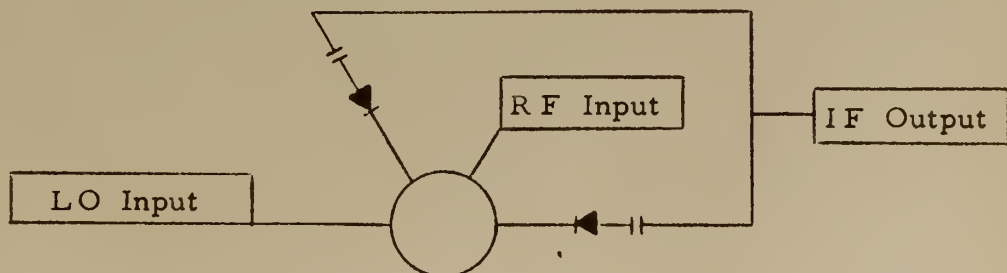
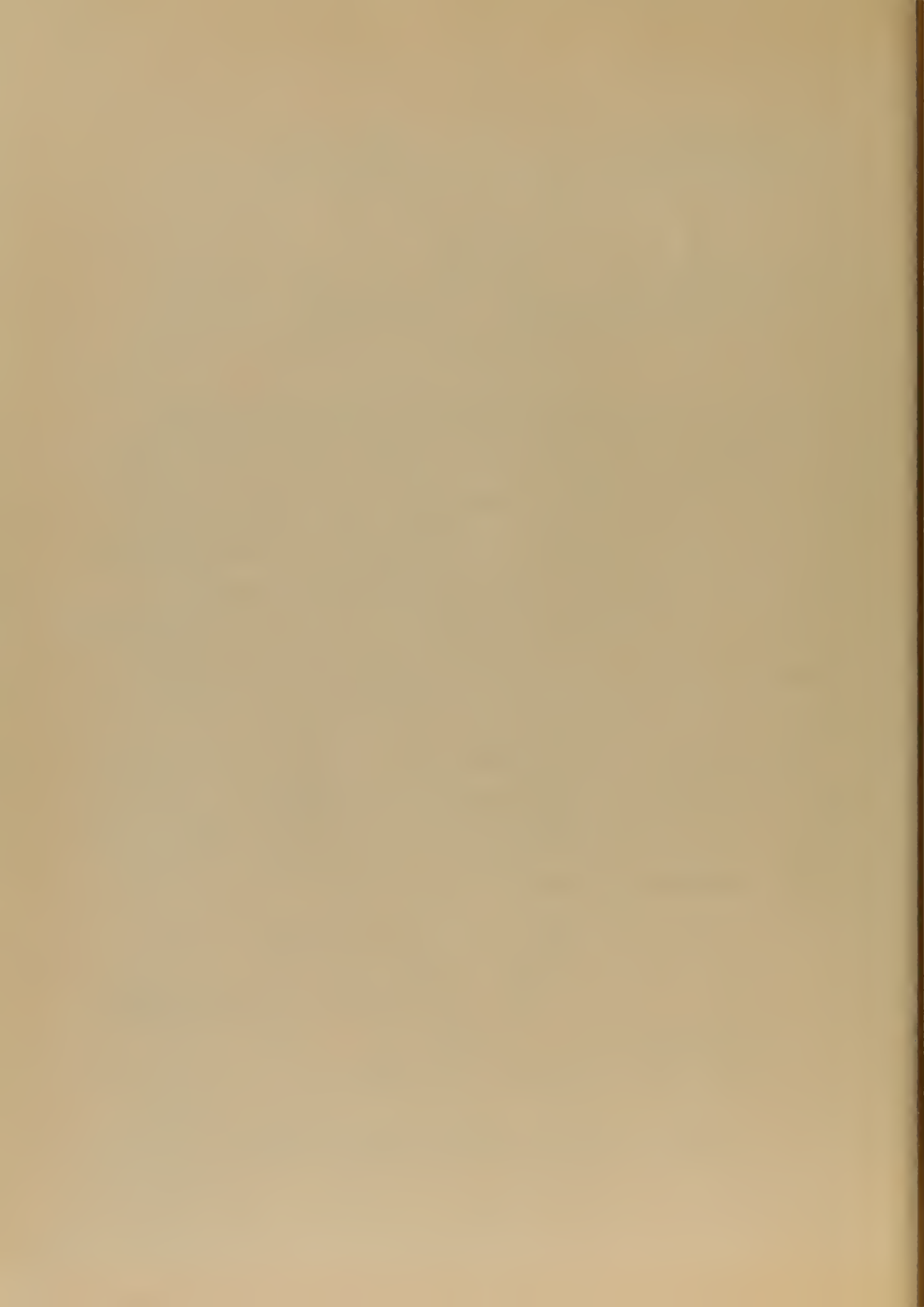
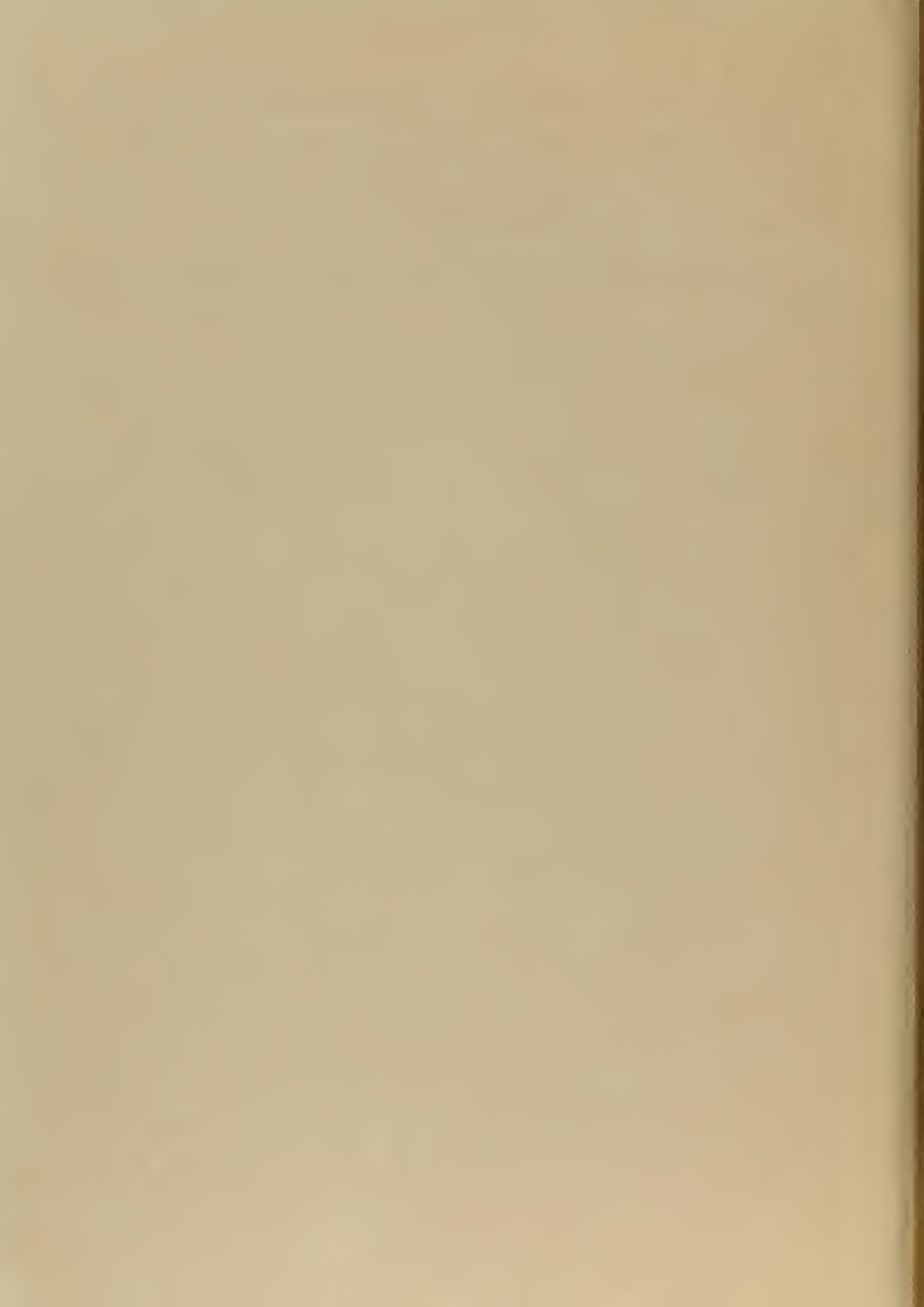


Figure 51. Hybrid Junction Balanced Mixer



The balanced mixer utilizes the following Case I and III hybrid junction properties that were developed in the analyses: there is no coupling between arms one and three; the input from arm one is 180° out of phase and balanced at arms two and four; the input from arm three is in phase and balanced at arms two and four; there is no coupling between two and four.



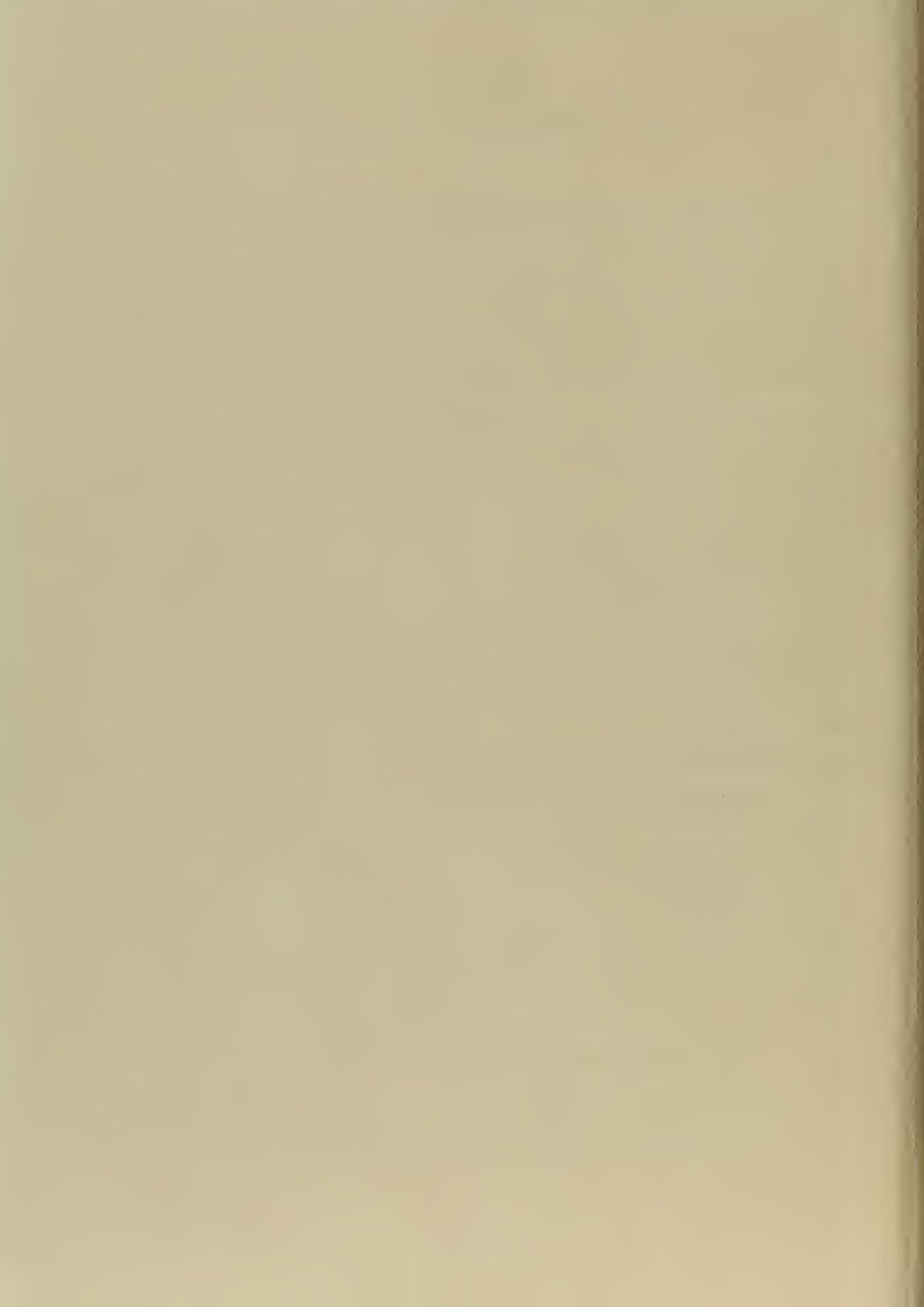
CHAPTER V

STRIP TRANSMISSION LINE SYSTEMS

As a fitting completion to this phase of the treatise, complete strip transmission line systems will now be discussed. A few specific systems will be covered to show how the individual components are employed to provide useful, practical devices. These examples show what has been done with this new concept and provide an insight into the type of development that may be expected in the near future.

A system that utilizes many of the components that have been considered in this paper is shown in Figures 51 and 53. It is a prototype strip line receiver front end, for use at the "C" band frequencies. The system was developed by the Airborne Instruments Laboratories for the Raytheon Manufacturing Company under contract from the Bureau of Ships of the U. S. Navy [20]. The strip line portion of the system is approximately 15" x 6 1/2" x 1". Comparing this system with the waveguide system shown in Figure 54 the neat compact form of the strip line system will be immediately appreciated. Noting the type of construction employed in the strip line system, the relative ease with which it may be manufactured should be apparent. The ease of manufacturing has been verified by the relatively low initial production cost estimates. Over and above the cost of producing these systems, the fact that in an emergency a device of this sort could readily be produced in large quantity could significantly assist in planning for wartime production.

The following brief discussion of the operation of the system will show how the many individual strip line components are used to provide



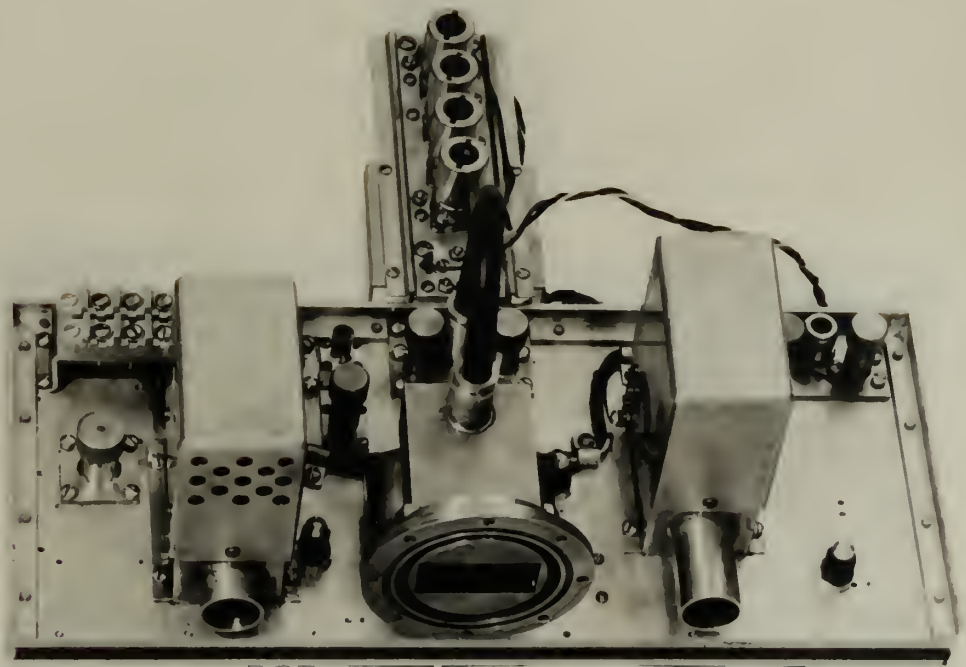


Figure 52. Prototype C Band Receiver Front End

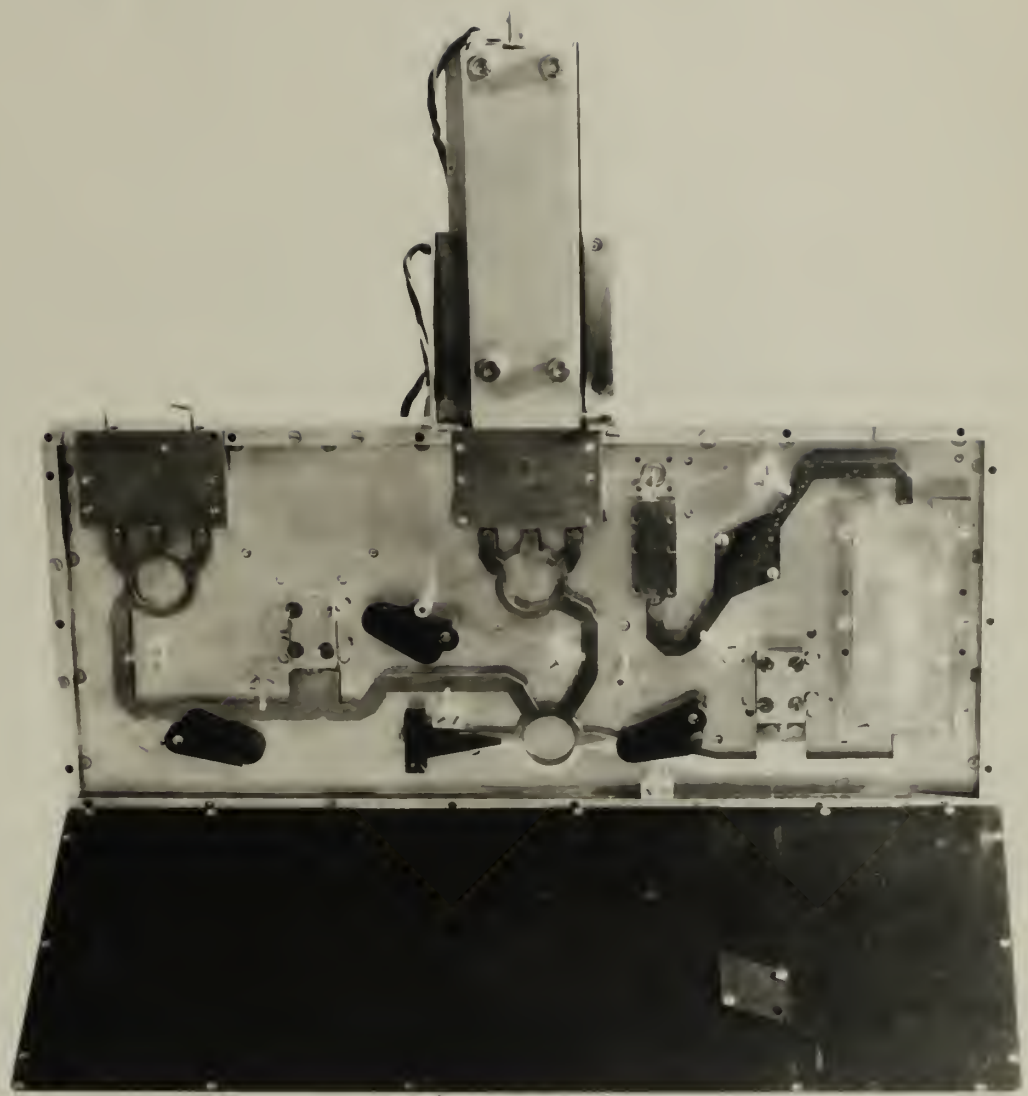
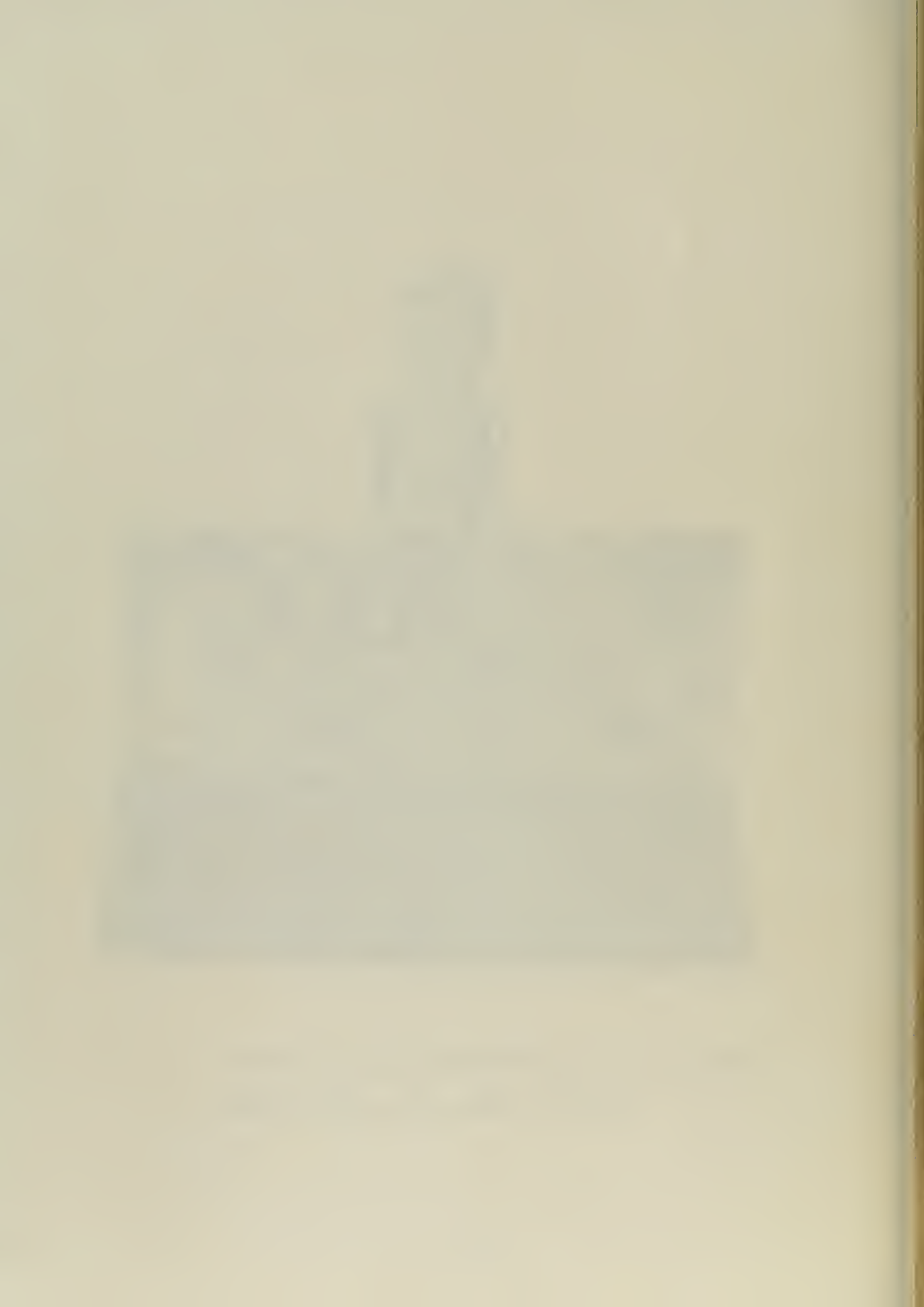


Figure 53. Prototype C Band Receiver Front End,
Opened to Expose Strip Line Circuitry



the complete device. Starting from the waveguide to coaxial line transition where the input signal is introduced into the system. The RF signal is brought through the coaxial line to arm three of central hybrid junction. This hybrid junction serves as a balanced mixer with the IF output taken from arms two and four. The IF output is detected and passed to the conventional IF amplifier that extends from the back of the system. The crystal detectors are shown adjacent to RF coaxial input to the mixer. There are two local oscillator inputs to the balanced mixer. They are introduced into the network at the two tees that are shown. The inputs are fed to the mixer through the lower hybrid junction which is serving as a directional coupler. A 3 DB power loss must be accepted here because half the power from either local oscillator is dissipated in the matched load on arm four of the junction. The amount of power from either local oscillator to the mixer is controlled by the variable attenuators, shown on the input strip lines. The signal from the left local oscillator also goes through another variable attenuator to an AFC balanced mixer. While the signal from the right local oscillator also goes through a high-Q strip line transmission resonator, that is sealed against the effects of humidity, to a fixed attenuator and then to a detector and output terminal.

This prototype system met the Bureau of Ships environmental specifications for electronic equipment. The noise figure, about 11 DB including a broadband TR RF loss and a 2 DB 30 MC IF amplifier, is the same as could be expected from a comparable receiver made with waveguide.

A second system performing essentially the same function as the

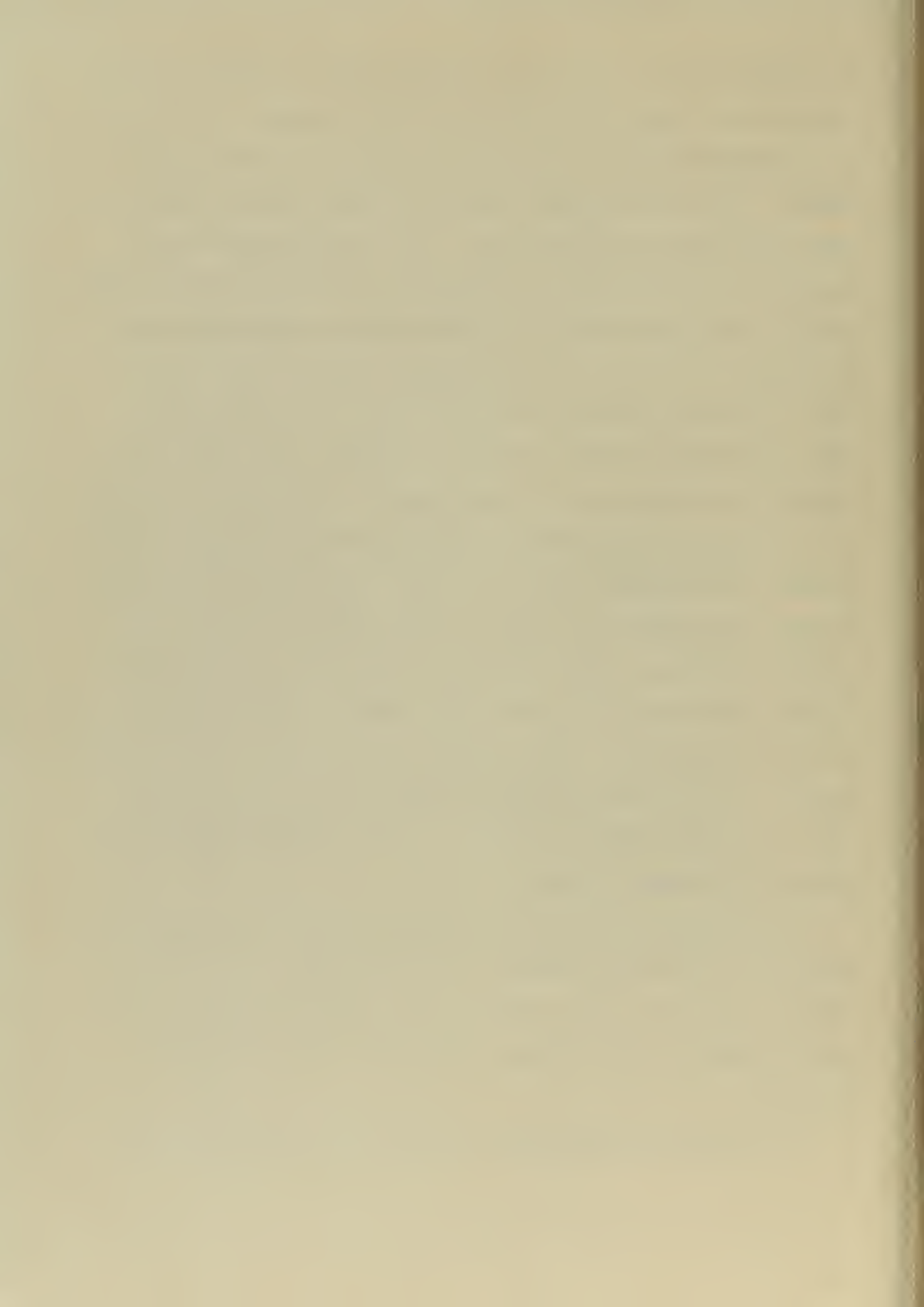
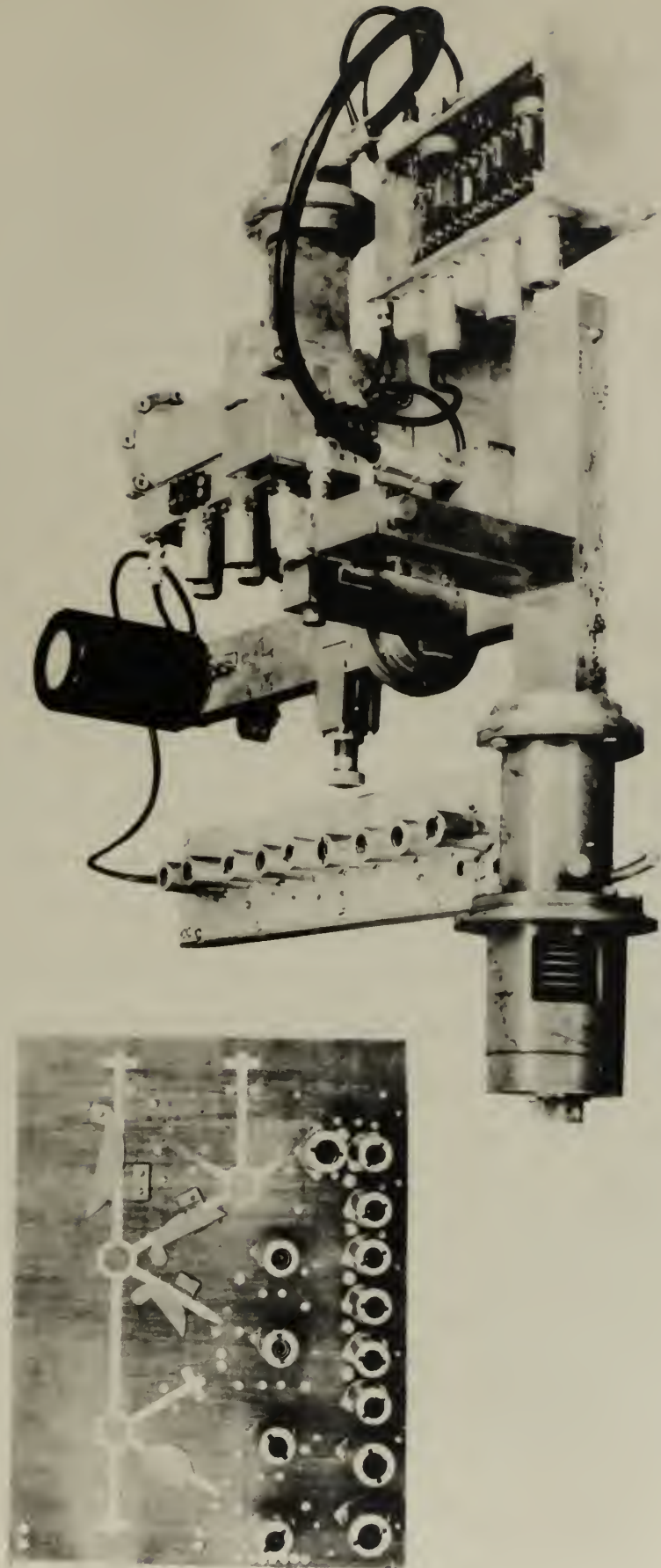
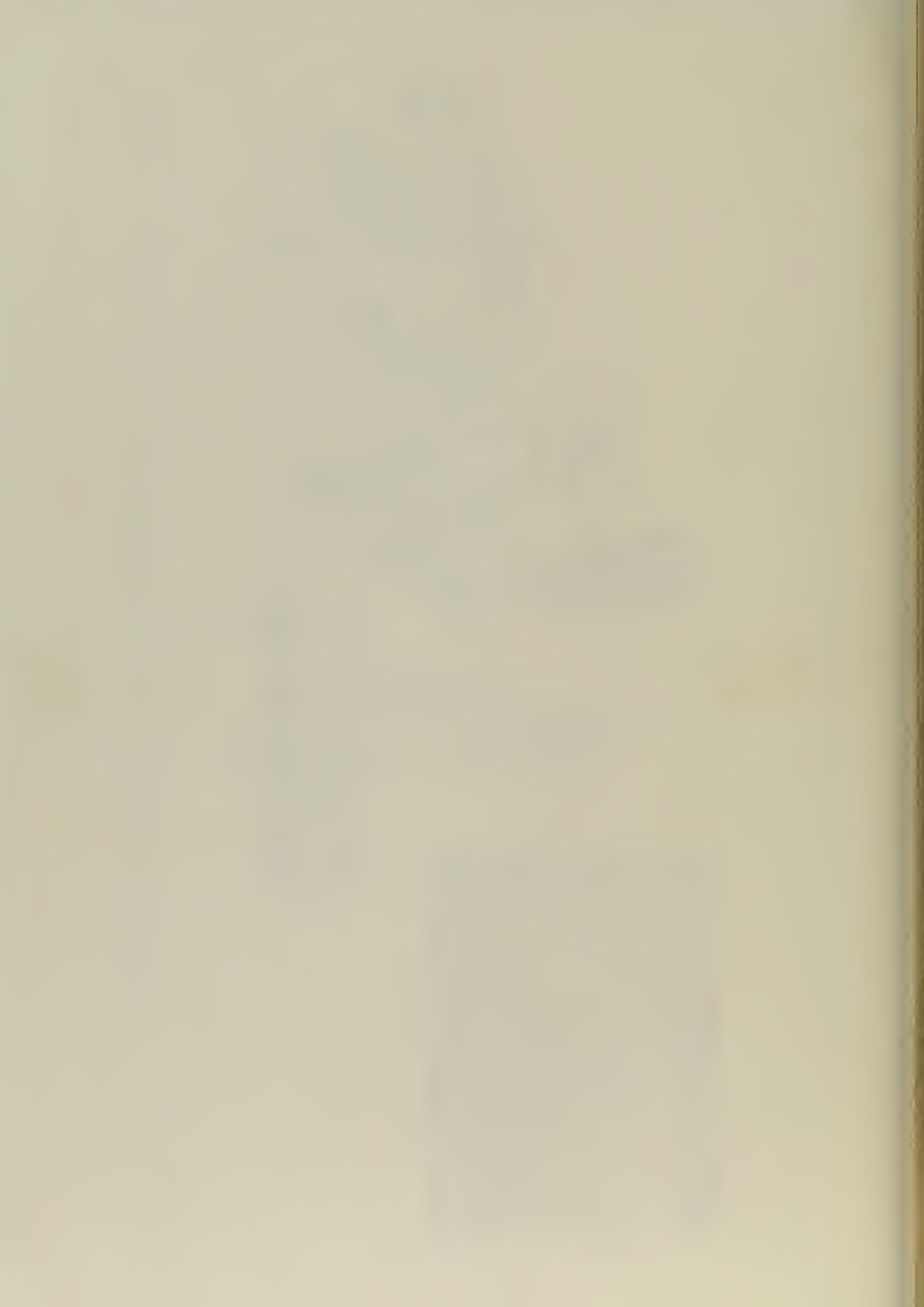


Figure 54. Conventional Waveguide and Microstrip C Band Receivers

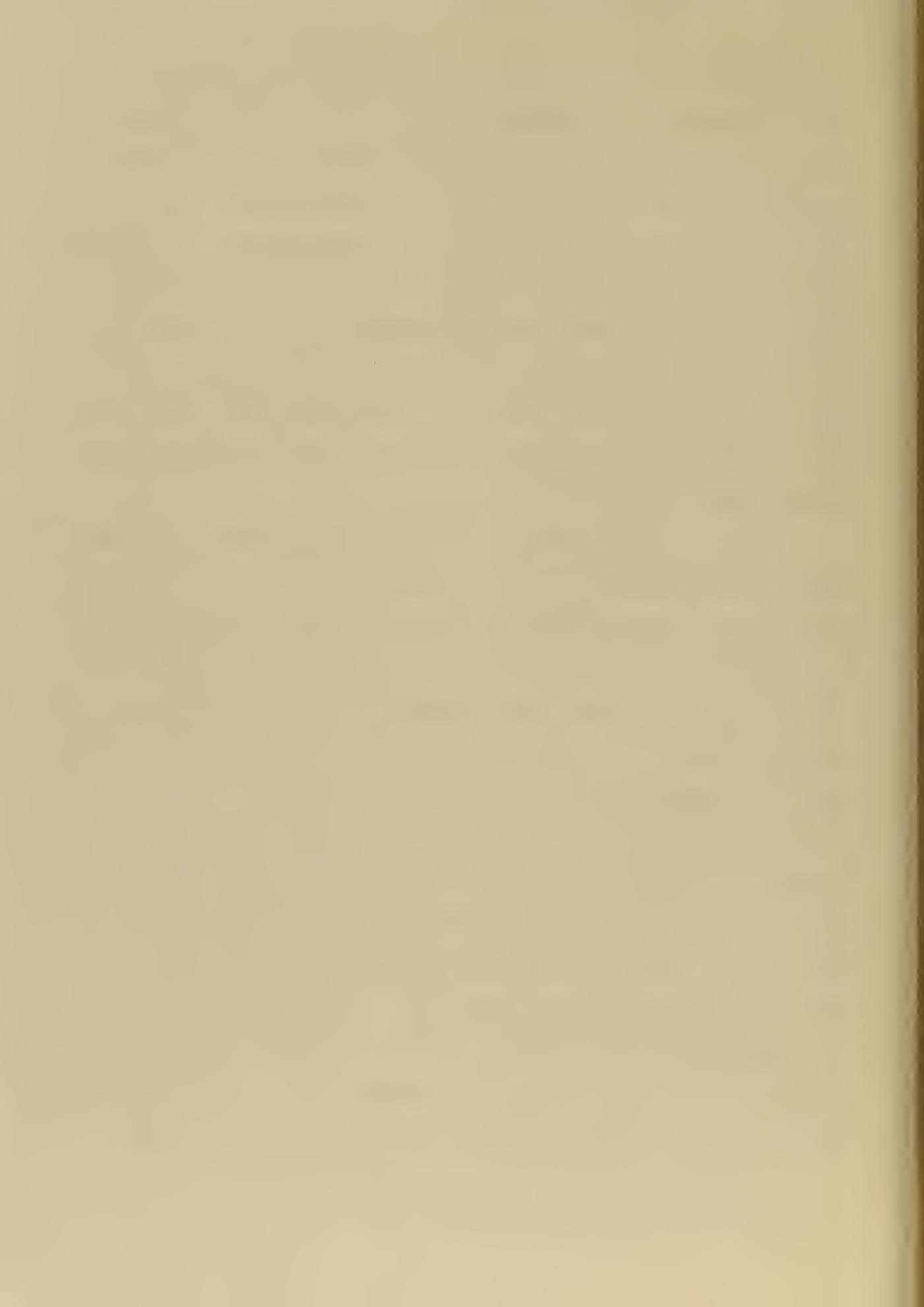




preceding system, but constructed using the microstrip technique, is shown in Figure 54. This system, developed by the Federal Telecommunication Laboratories, is smaller, lighter and less expensive than the strip line system. However, it also has disadvantages. There is more loss in the system due to the dielectric and radiation. The system must be shielded to contain the radiation from the strip. An external resonator must be employed since microstrip is not a high Q device.

The technique of printing the low frequency circuitry on the dielectric as shown in the figures results in great savings in cost, weight, and time of production. This technique may also be used with stripline and sandwich line.

The last system to be discussed is one that is presently under development at the Airborne Instruments Laboratory for the Sperry Gyroscope Company under contract from the Army Signal Corps. It is a stripline system with seven RF inputs, seven balanced IF outputs, a single local oscillator input. The ground plane dimensions are limited to approximately 36" x 12" x 1". The system, as initially proposed, was to have seven hybrid junctions to serve as the balanced mixers. The local oscillator signal was to be fed to the mixers through a series of tees so arranged that each pair of mixers was connected to a tee and two pairs were grouped and connected to another tee and so on down to the main local oscillator input line where a hybrid junction was employed as the final tee to reduce somewhat the input SWR. A matched load was inserted to represent an eighth mixer to provide the necessary symmetry. A proposed modification to the system involved feeding the local oscillator signal to the mixer through a series of power dividers to allow space

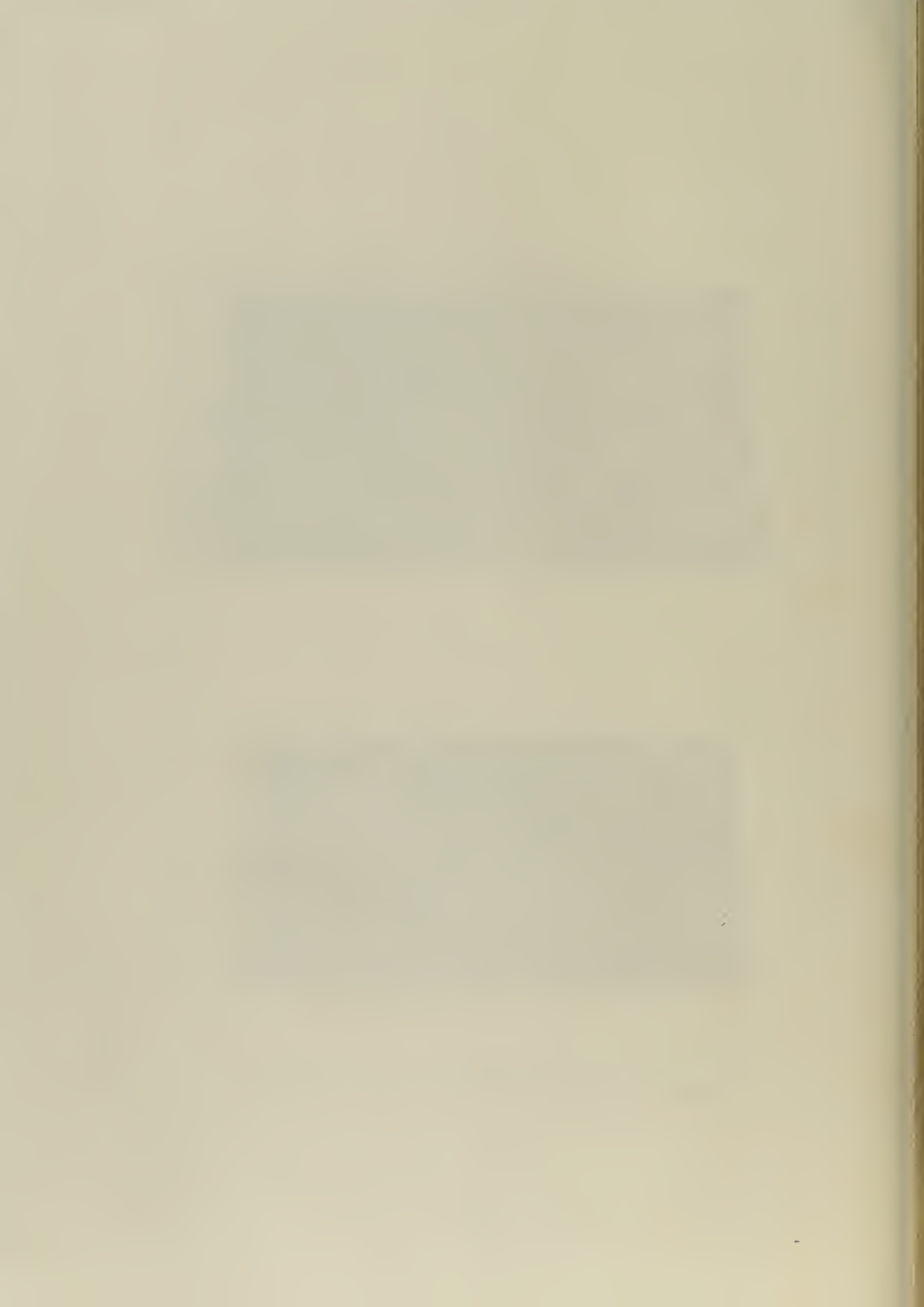


within the ground planes to etch the IF circuitry on the unused portion of the dielectric sheet.

This brief discussion should be sufficient to permit the reader to visualize the stripline mixer system and appreciate its advantages over the waveguide system that would have to be built to provide the same function. Figure 55 shows the arrangement that was used to test an individual hybrid junction that was to be incorporated in the final system. Figure 26 shows the test setup for an individual crystal detector.



Figure 55. Hybrid Junction Test Arrangement



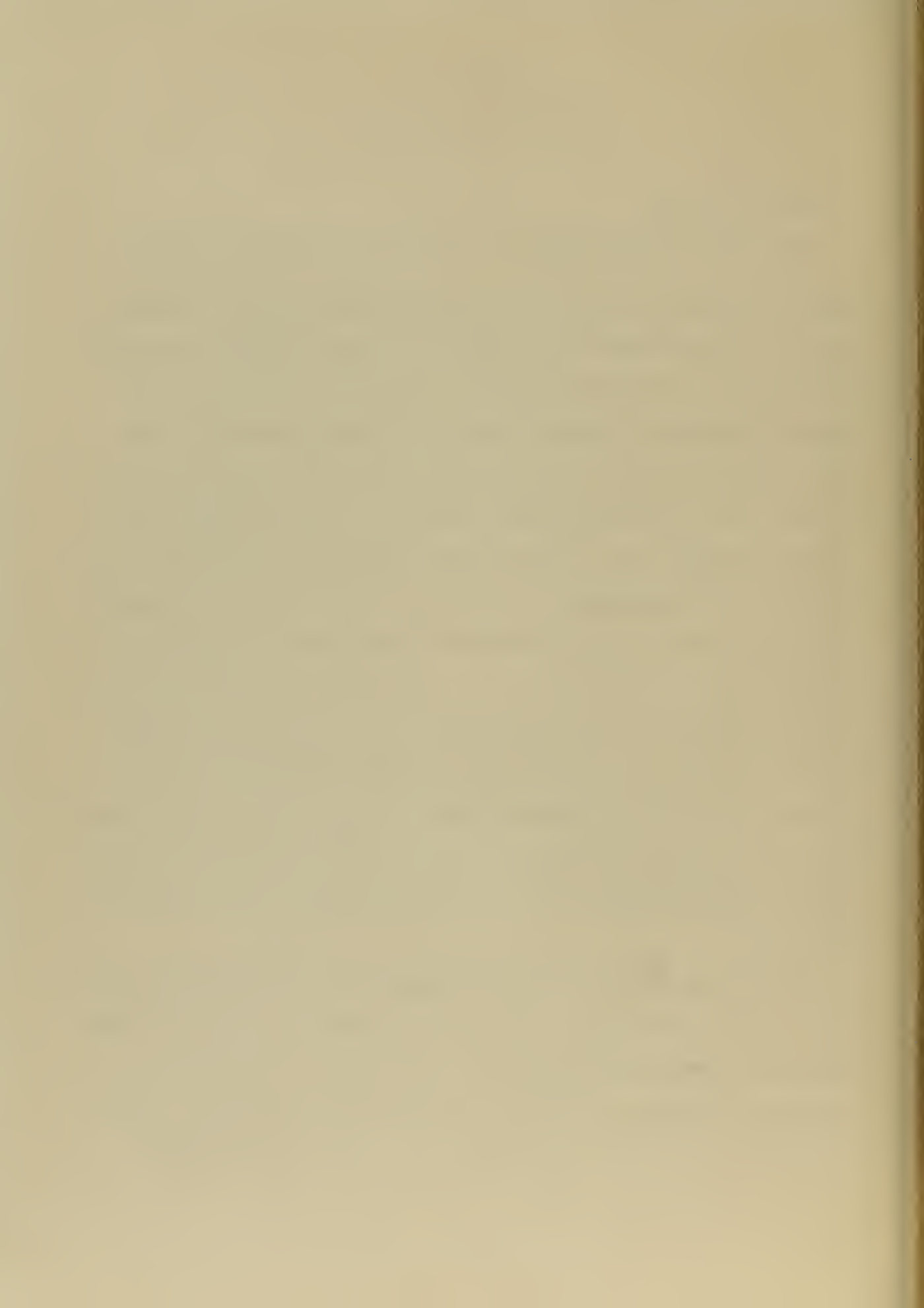
CHAPTER VI

PRINTED ANTENNAS

1. Basic concepts

Microwave antennas may be constructed employing the methods and materials that are used with strip transmission lines, if the basic principles of practical antenna theory are applied to attain useful radiation patterns. The strip transmission line technique provides a new means of constructing antennas, particularly arrays of dipoles, that have long been considered impractical with usual antenna construction, because of the complex and precise construction that is required at the microwave frequencies. The flexibility of this new technique seems destined to open a completely new field of microwave antenna development, and also to induce engineers interested in microwave antennas to dust off their early editions of the I. R. E. to find low frequency antenna systems that now may be readily adapted for use in the microwave region. The Chereix-Mesny array is a good example of the revival of an early antenna [11]. It was developed in 1929 as a large, low frequency array supported by tall towers, and now it may be used at microwave frequencies by printing the entire circuit on a flat dielectric sheet less than two feet square.

Printed antennas offer other advantages in addition to opening a new field of practical antennas. The low cost and ease of construction make printed antennas an ideal medium for experimental development both for antennas destined for use at microwave frequencies and for models of antennas to be used at lower frequencies. Universities offering

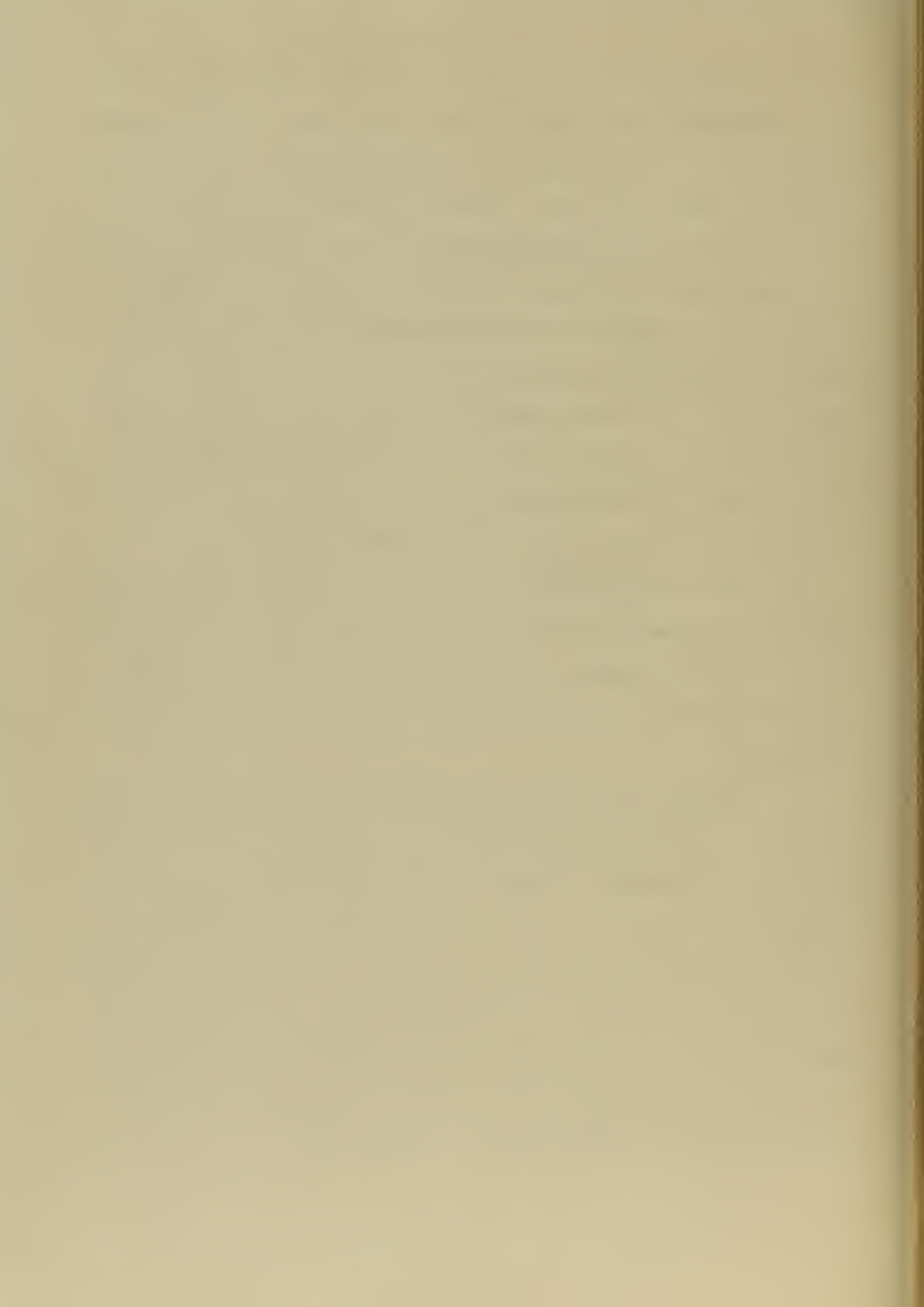


courses in practical antenna design may eliminate many of the "canned" type of laboratory experiments that have been required due to the prohibitive length of time necessary for students to construct complex antenna arrays of their own design. The use of the printed antenna technique in the laboratory would permit students to design and construct antennas to the limit of their knowledge and imagination within the laboratory time allotted. The yagi antenna discussed later in this section is an example of what could be done in one or two laboratory periods. The author designed, built and completely tested the array in a single day. It must be noted, however, that an automatic antenna pattern plotter was available for obtaining the radiation patterns.

2. Characteristics and Design of Printed Antennas

The initial considerations for the design of an antenna array are the proper length of individual elements to obtain the desired current distribution, the input impedance, and the methods of obtaining the proper phase relationship between the elements to provide the desired radiation pattern.

The elements in a printed antenna will be slightly shorter than their cylindrical counterparts in a normal antenna array. The difference in length is caused by the rectangular cross-section of the printed antenna elements and the presence of the dielectric sheet supporting the array. Data for determining the equivalent circular cross section of a rectangular element are available in the literature [30]. The amount that the elements must be shortened due to the effect of the dielectric sheet is determined experimentally through the use of a slotted line, or by an examination of the radiation pattern of the antenna.



The input impedance of several types of printed antennas has been measured and found to agree favorably with theory. The input impedance of a single vertical quarter-wave element above a ground plane was two percent greater than the theoretical value and the input impedance of the colinear array shown in Figure 56 was nine percent greater than computed.

The radiation patterns of a half-wave folded dipole centered one wavelength above a six wavelength square ground plane is shown in Figure 57. From this we can see the pattern compares well with the calculated pattern. There is a slight reduction in the length of the upper pair of lobes and it is considered due to the limited size of the ground plane.

The half-wave elements of a colinear array may all be fed in phase by joining the adjacent stubs as shown in Figure 56. The simple stubs provide the required 180° phase shift, however, it was found that the stubs caused cross-polarized radiation. The undesired radiation was removed by adding a second stub in parallel with the original one as shown in Figure 58. The radiation pattern of a five element colinear array is shown in Figure 59. It is interesting to note that the balanced feed for this antenna was obtained by placing double shorted stub in the stripline feed.

A twelve-element yagi array as shown in Figure 60 was constructed and its radiation pattern is shown in Figures 61 and 62. The patterns show that the simple construction provided satisfactory results with a well defined major lobe and a front to back power ratio of 2.8 .

The broadside array is the most promising type of printed antenna.



Figure 56. Input Impedance Test Arrangement



Figures 63 and 64 show a forty element coplanar broadside array a quarter-wavelength above the ground plane. The facility with which a complex array may be constructed is easily seen from an examination of these photographs. The array and its associated feed is shown schematically in Figure 65. The radiation patterns in Figures 66 and 67 show the excellent directional characteristics and low side lobe level of the array. The YZ plane beam width of 13° and YX plane beam width of 21° were identical with that calculated. A final model of a forty element coplanar array, similar to one shown in Figure 14, has recently been completed. This array is novel in that the metal antenna configuration is etched on one side of FF 91 fiberglass. The fiberglass is a particularly weather-proof material and with the array etched on the inside surface, it provides a compact and inexpensive radome. The antenna was developed for the Army Signal Corps and appears destined to find wide application in portable field equipment.

A thirty element coplanar broadside array a quarter-wavelength above a ground plane with its associated hybrid junction balun feed is shown schematically in Figure 68. Its power radiation pattern is shown in Figures 69 and 70.

The schematic diagrams and photographs of the arrays illustrate many of the interesting design and construction features of printed antennas. Two forms of feed are shown, a power divider and parallel line; and two methods of obtaining a balanced drive, the hybrid ring balun, and the quarter-wave stub in one of a pair of feed lines. The photographs also show the free use of polyfoam to support the arrays and feeds.



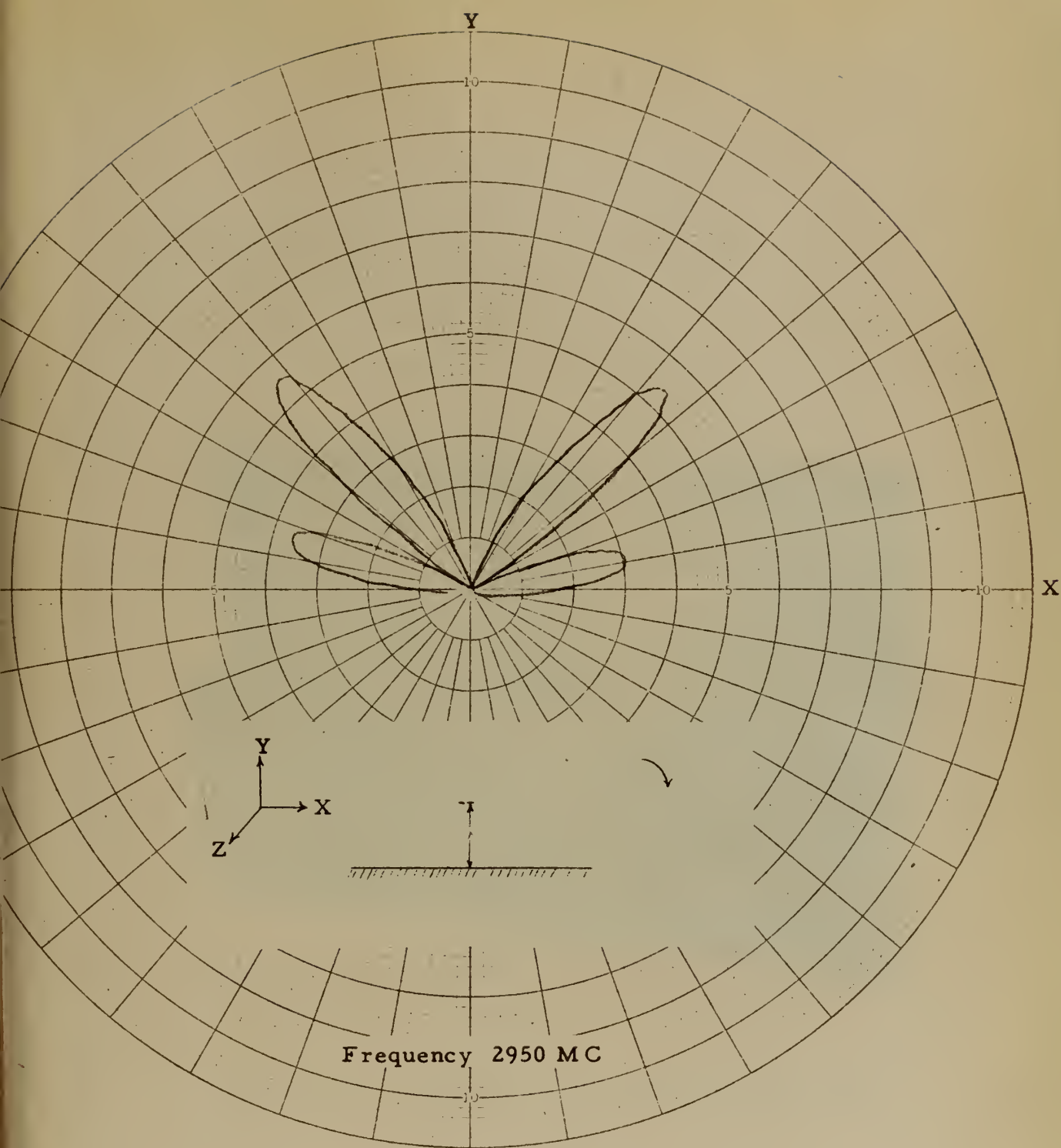
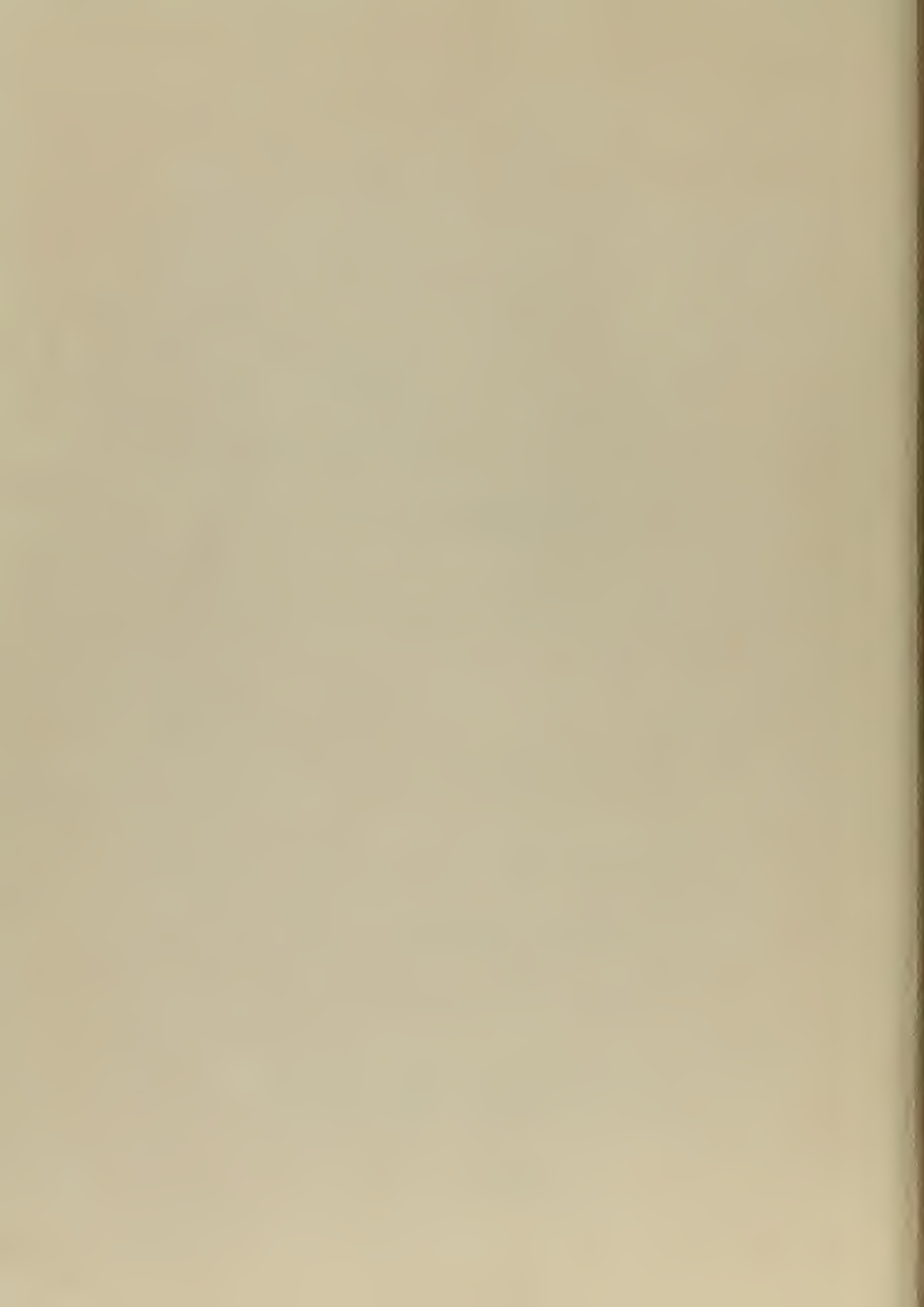


Figure 57. Radiation Intensity Pattern in XY Plane
For Folded Half-wave Dipole Antenna



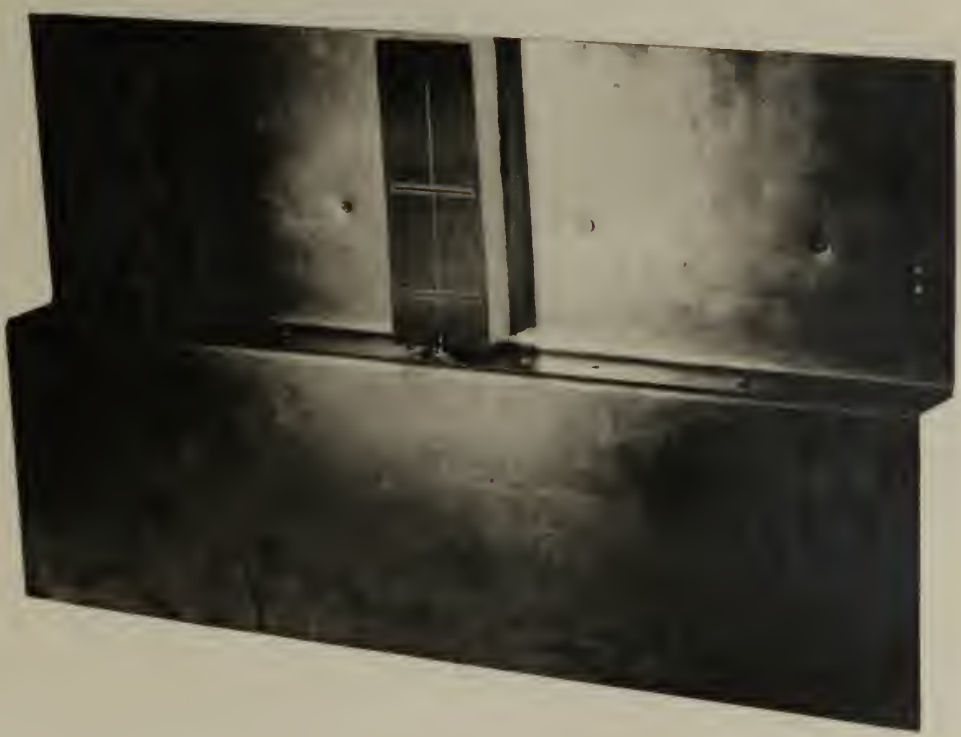


Figure 58. Collinear Array with Unbalanced Feed



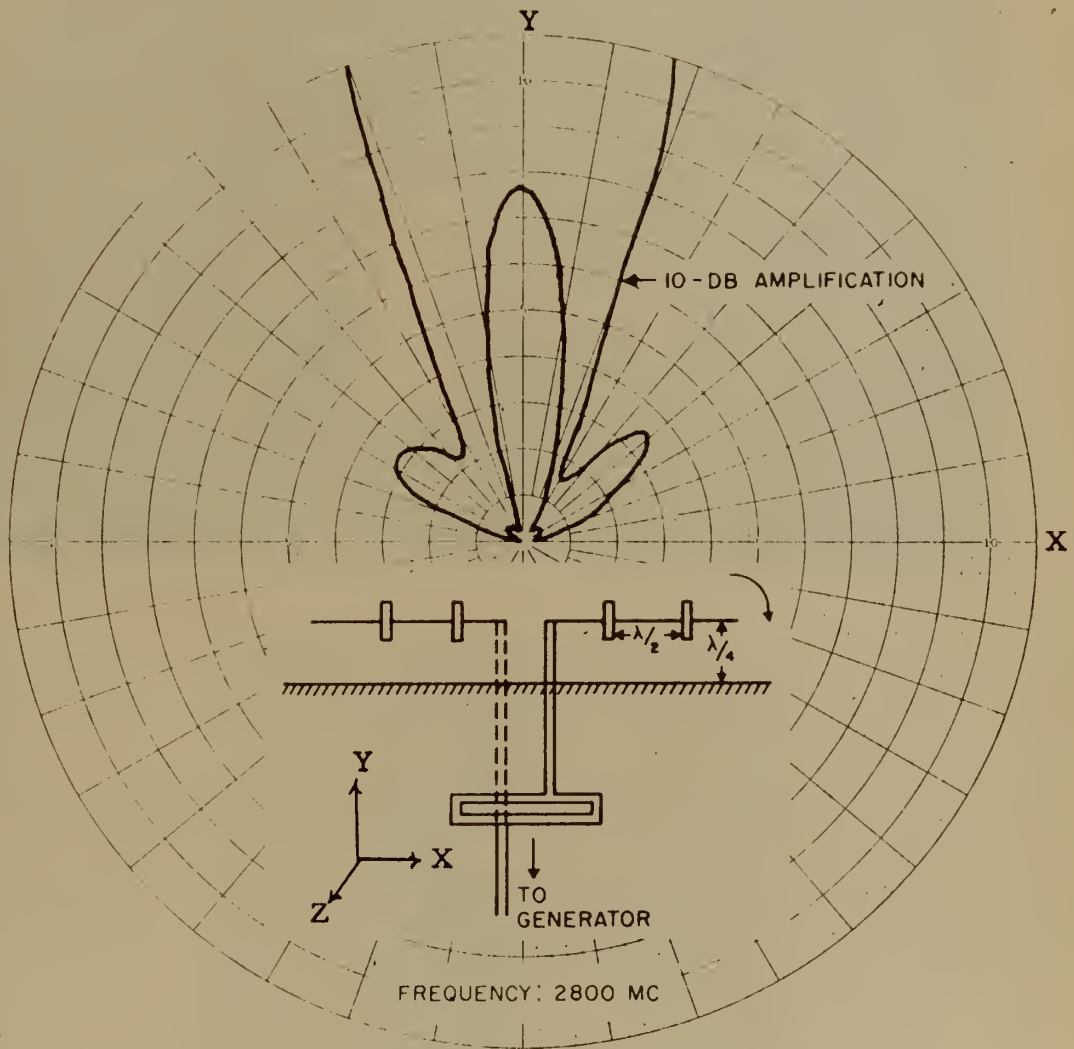


Figure 59. Radiation Intensity Pattern in XY Plane
for Five Element Collinear Array

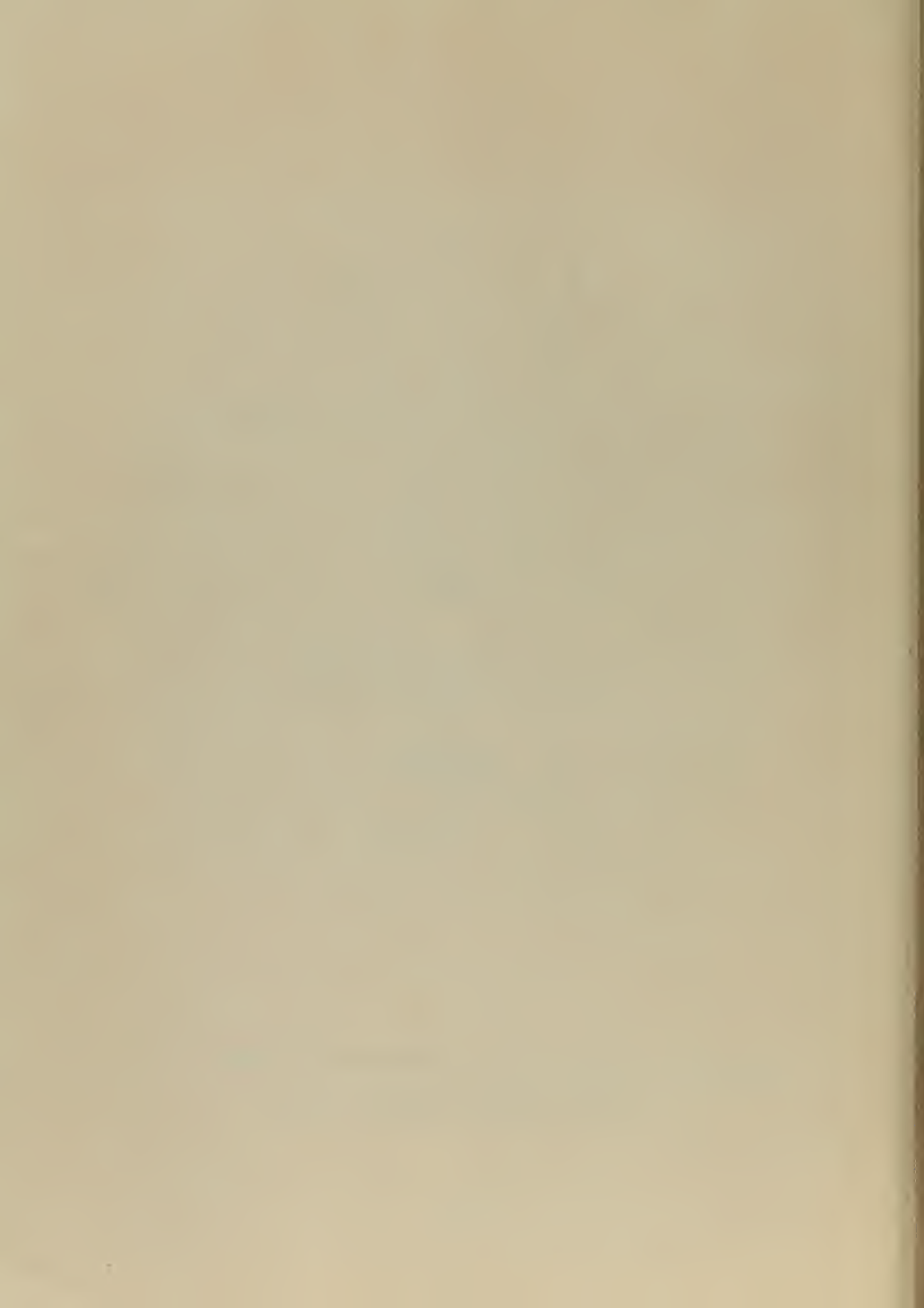
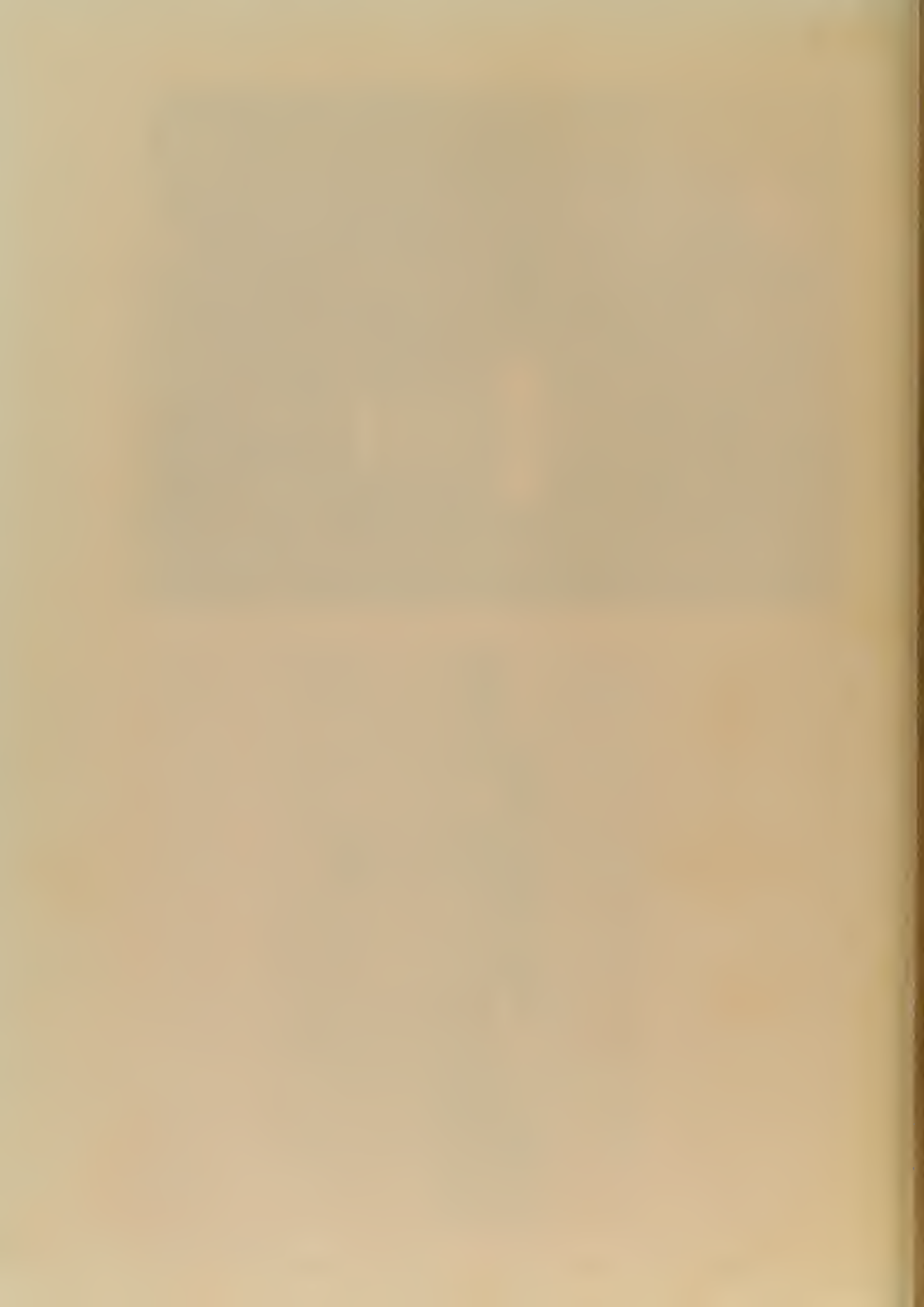




Figure 61. Twelve Element 3000 MC Yagi Array



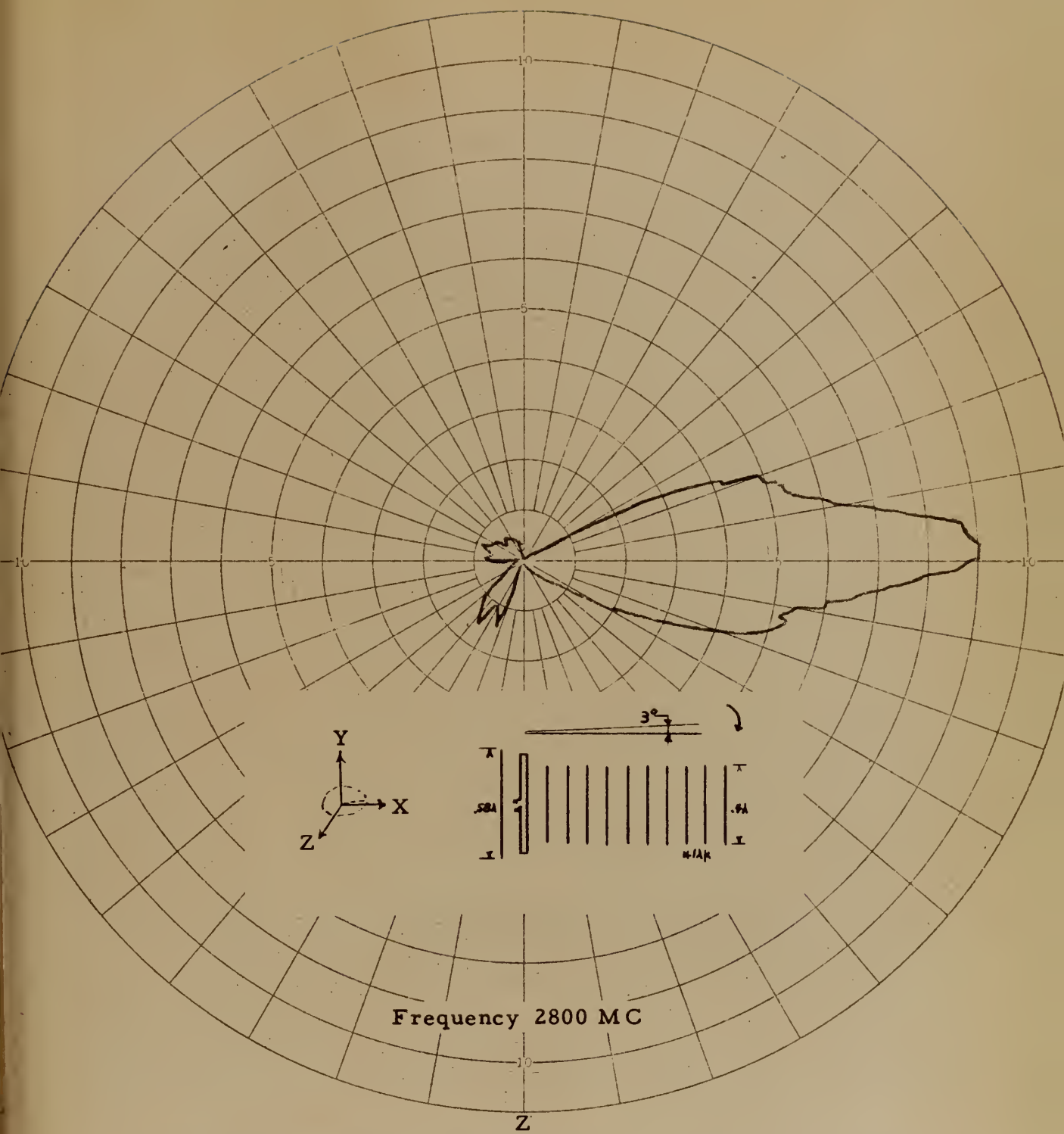
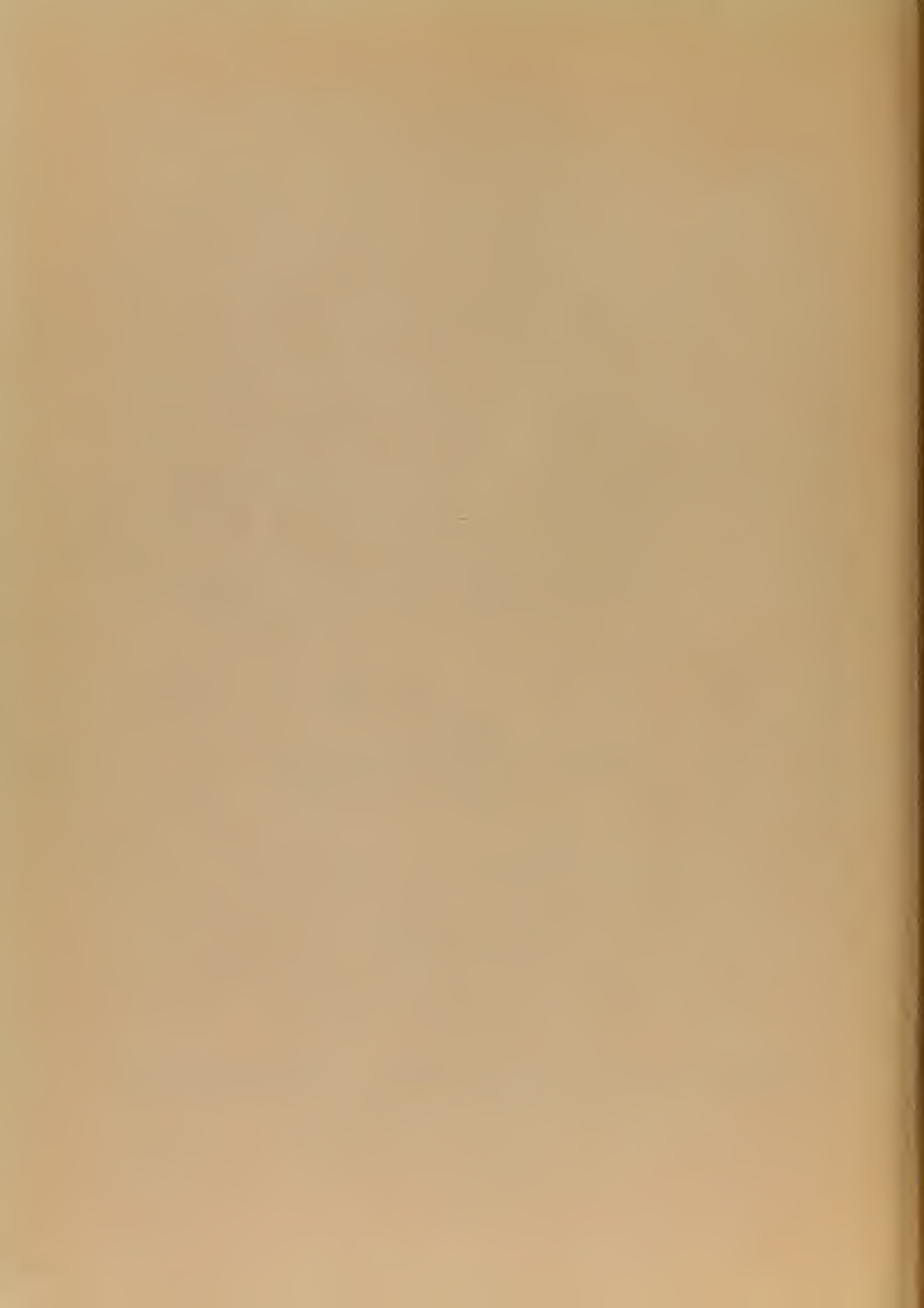


Figure 61. Radiation Intensity Pattern 3° Above the XZ Plane
for Twelve Element Yagi Array



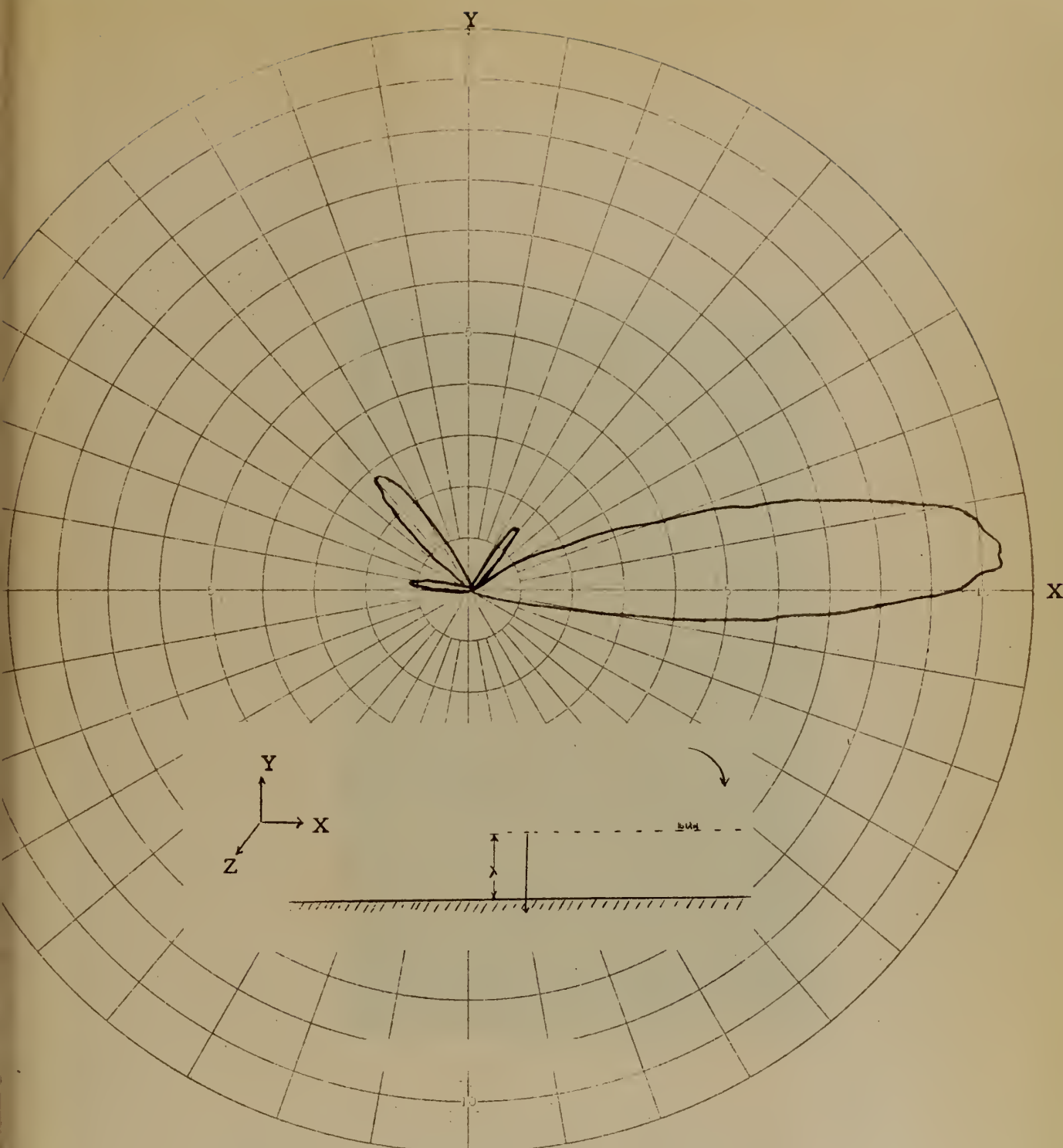


Figure 62. Radiation Intensity Pattern in XY Plane
for Twelve Element Yagi Array

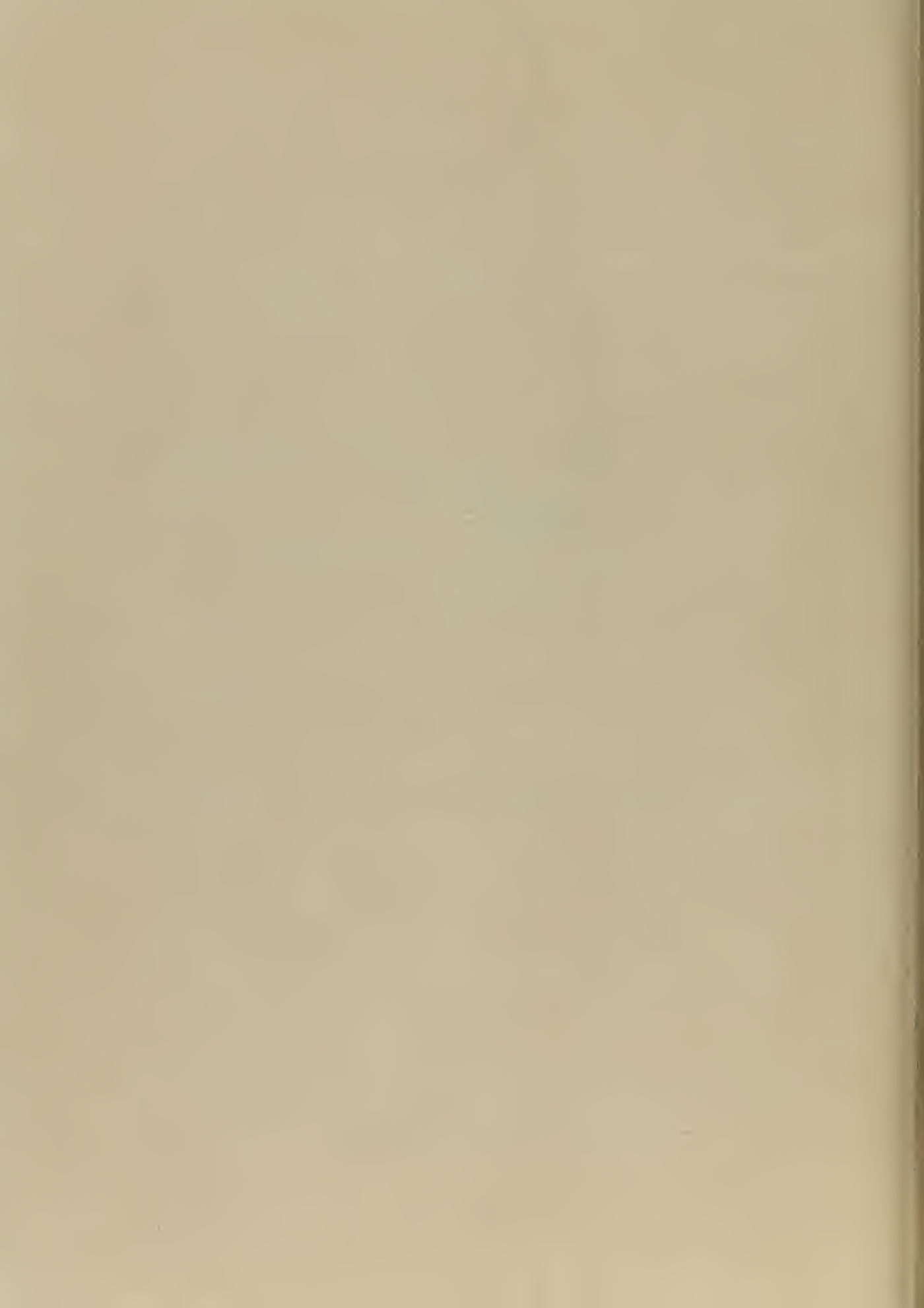




Figure 63. Forty Element Coplanar Array



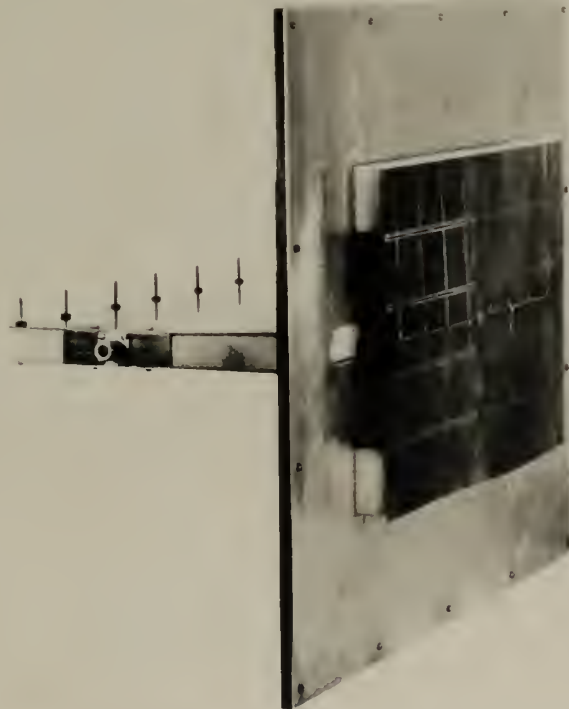
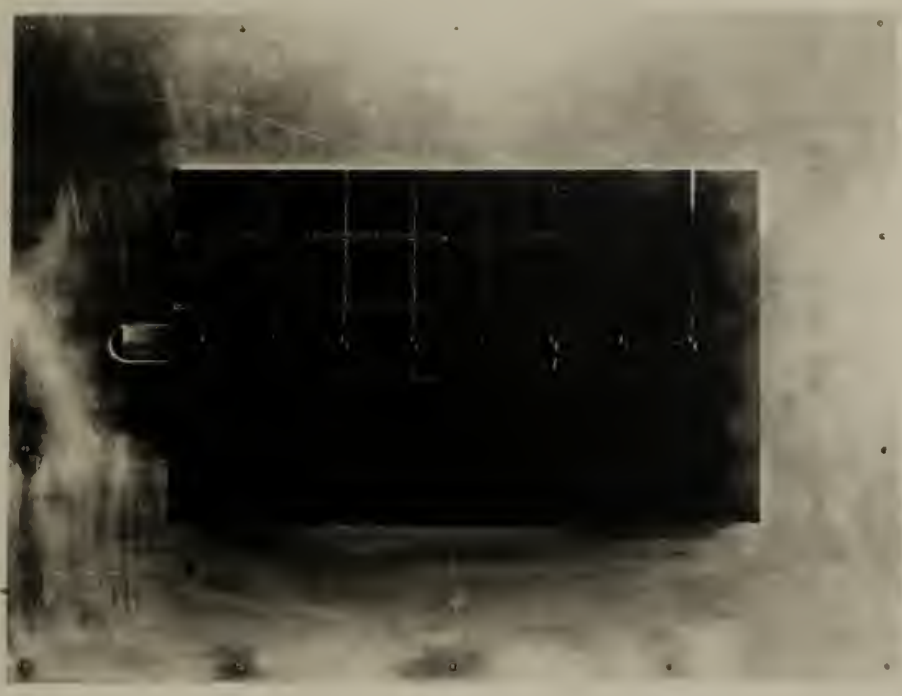
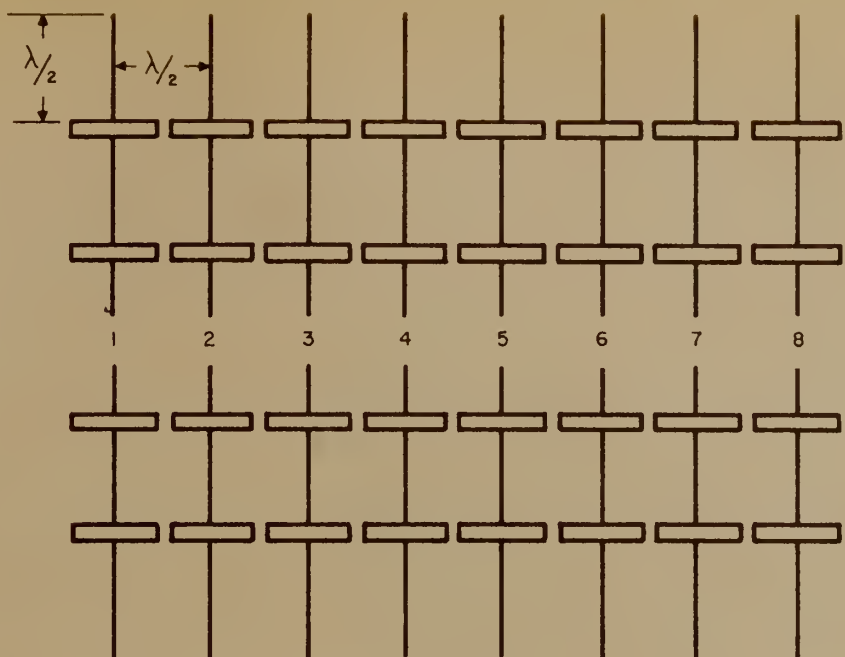
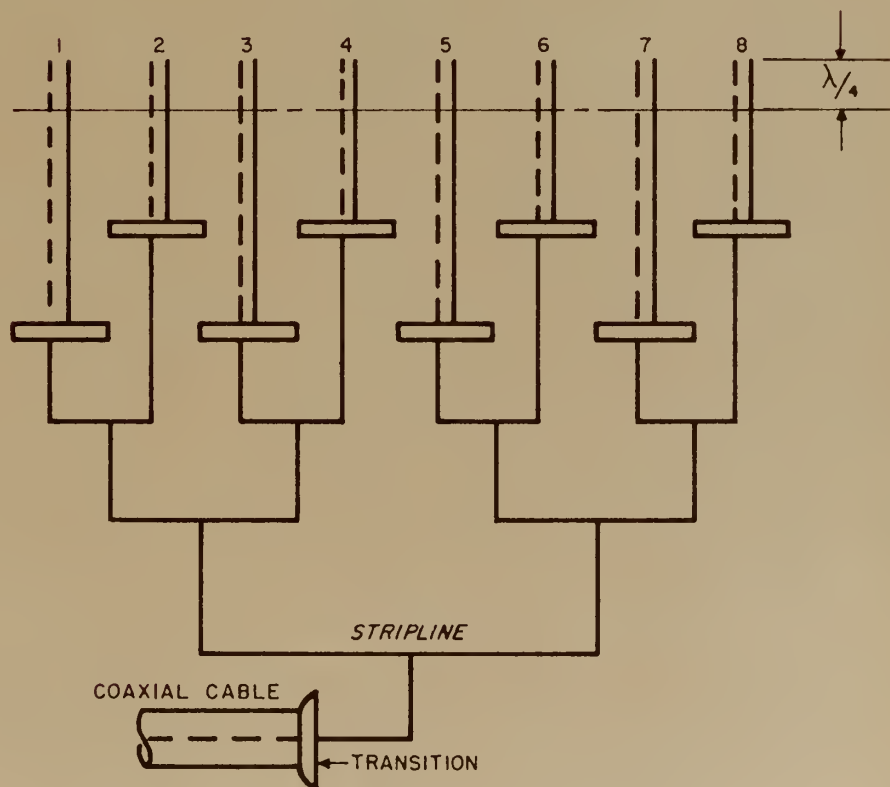


Figure 64. Forty Element Coplanar Array





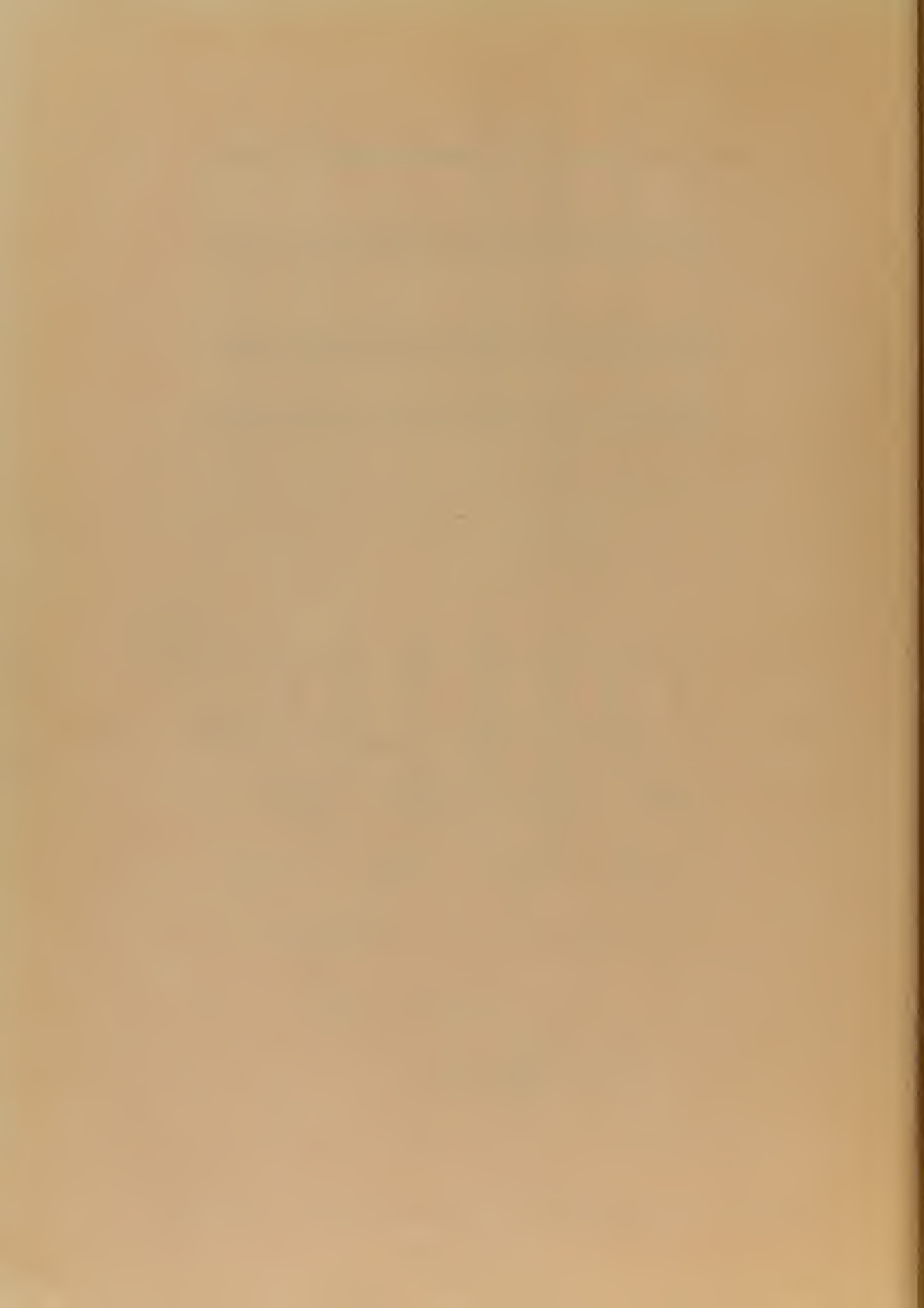
A. ARRAY



B. FEED

Figure 65. Forty Element Coplanar Array with Double Stub

Balun Feed



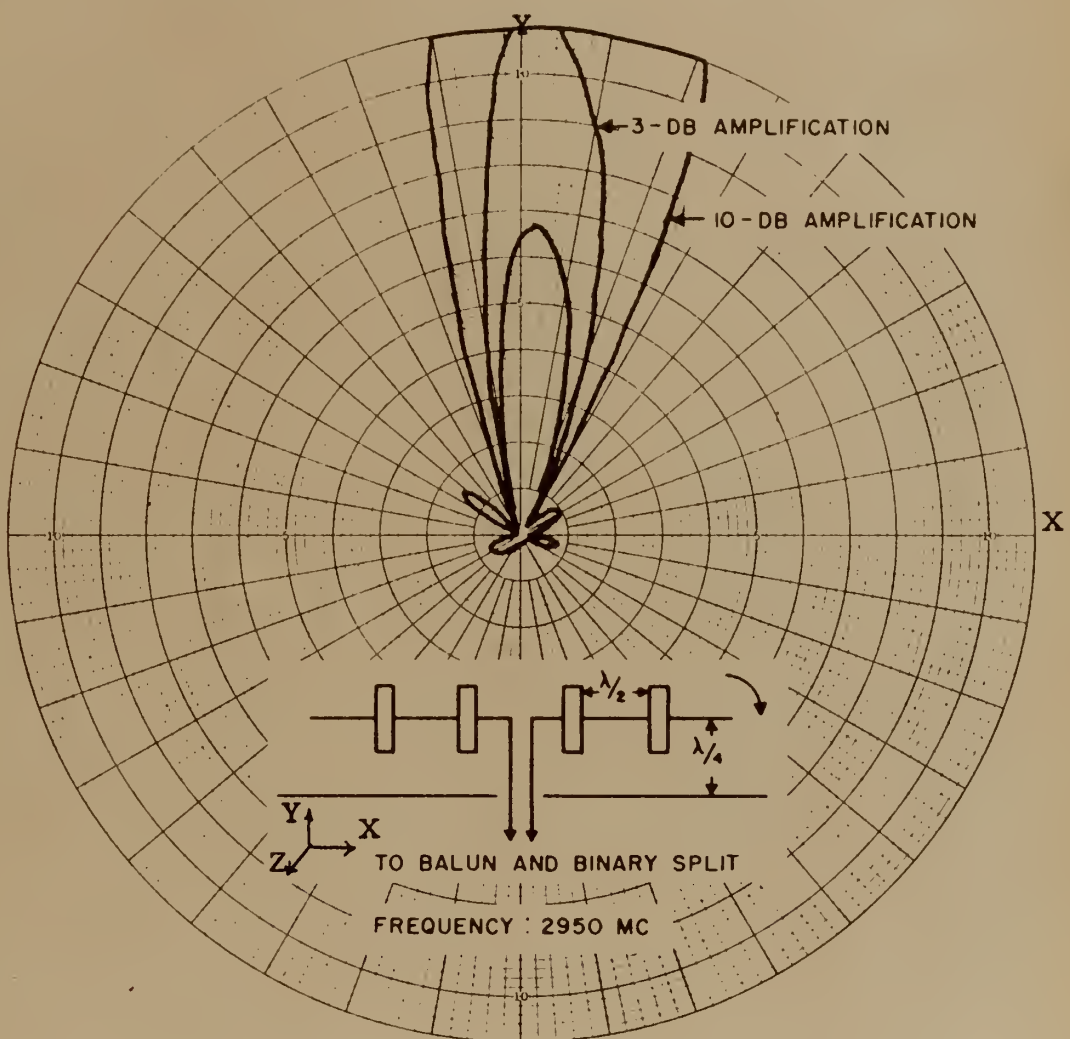


Figure 66. Radiation Intensity Pattern in XY Plane
for Forty Element Coplanar Array



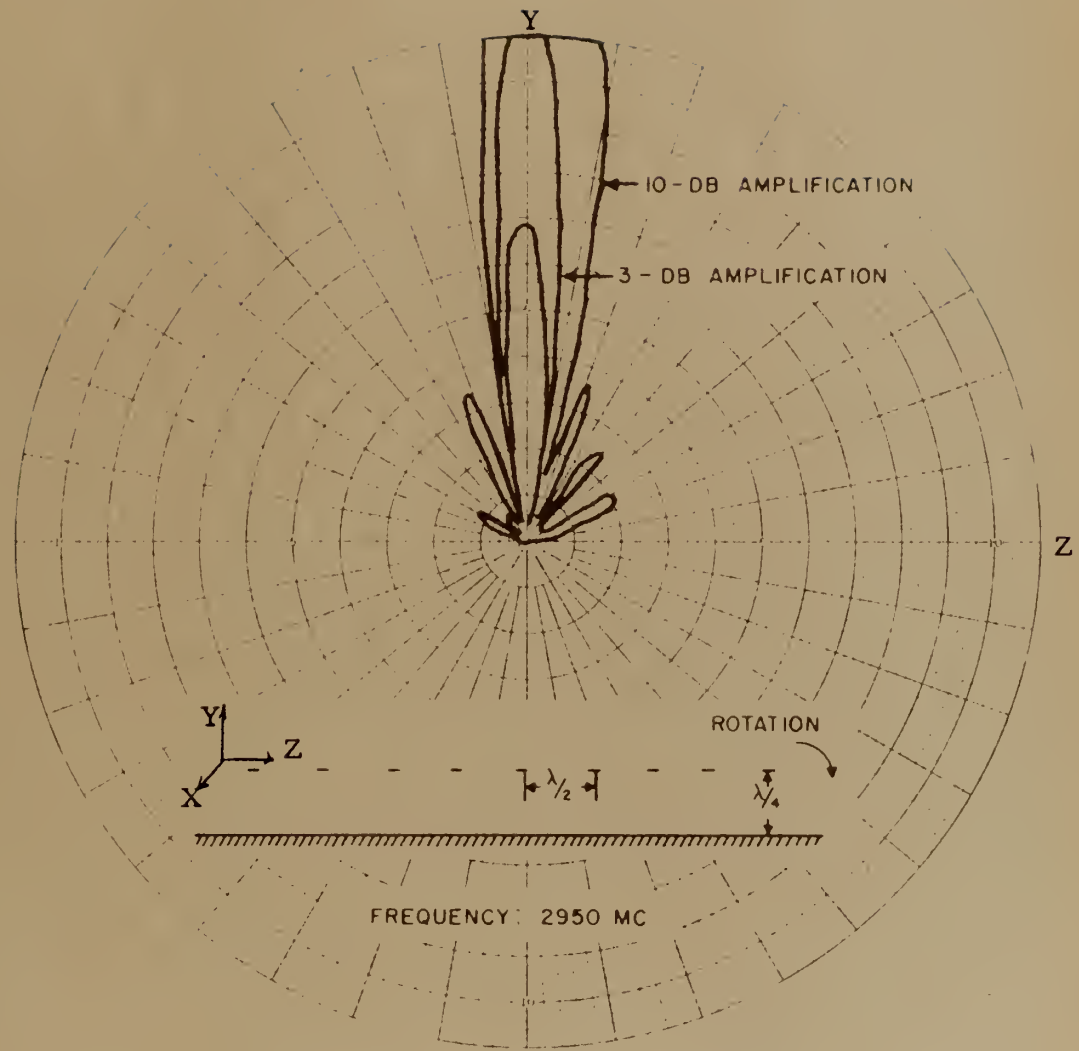
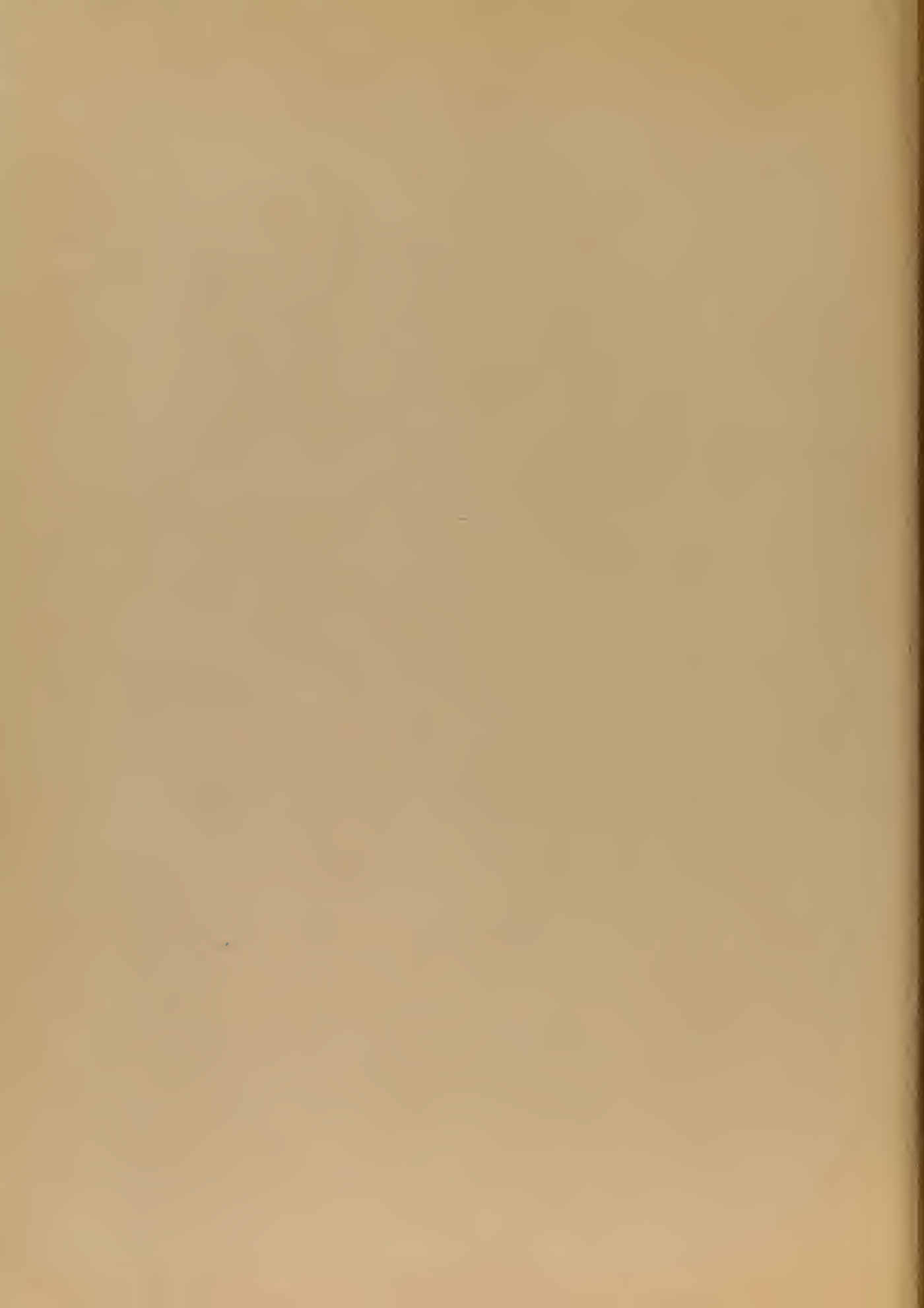


Figure 67. Radiation Intensity Pattern in YZ Plane
for Forty Element Coplanar Array



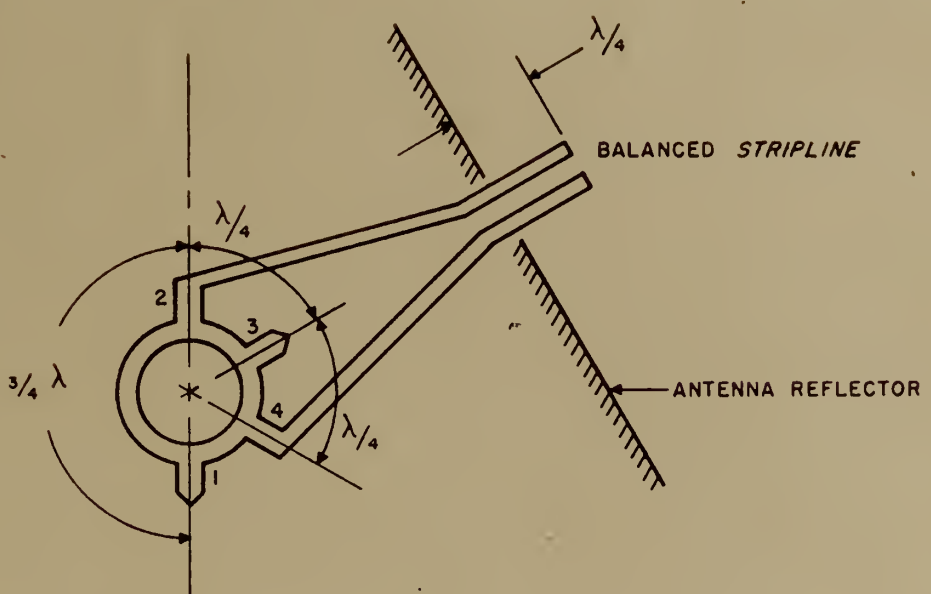
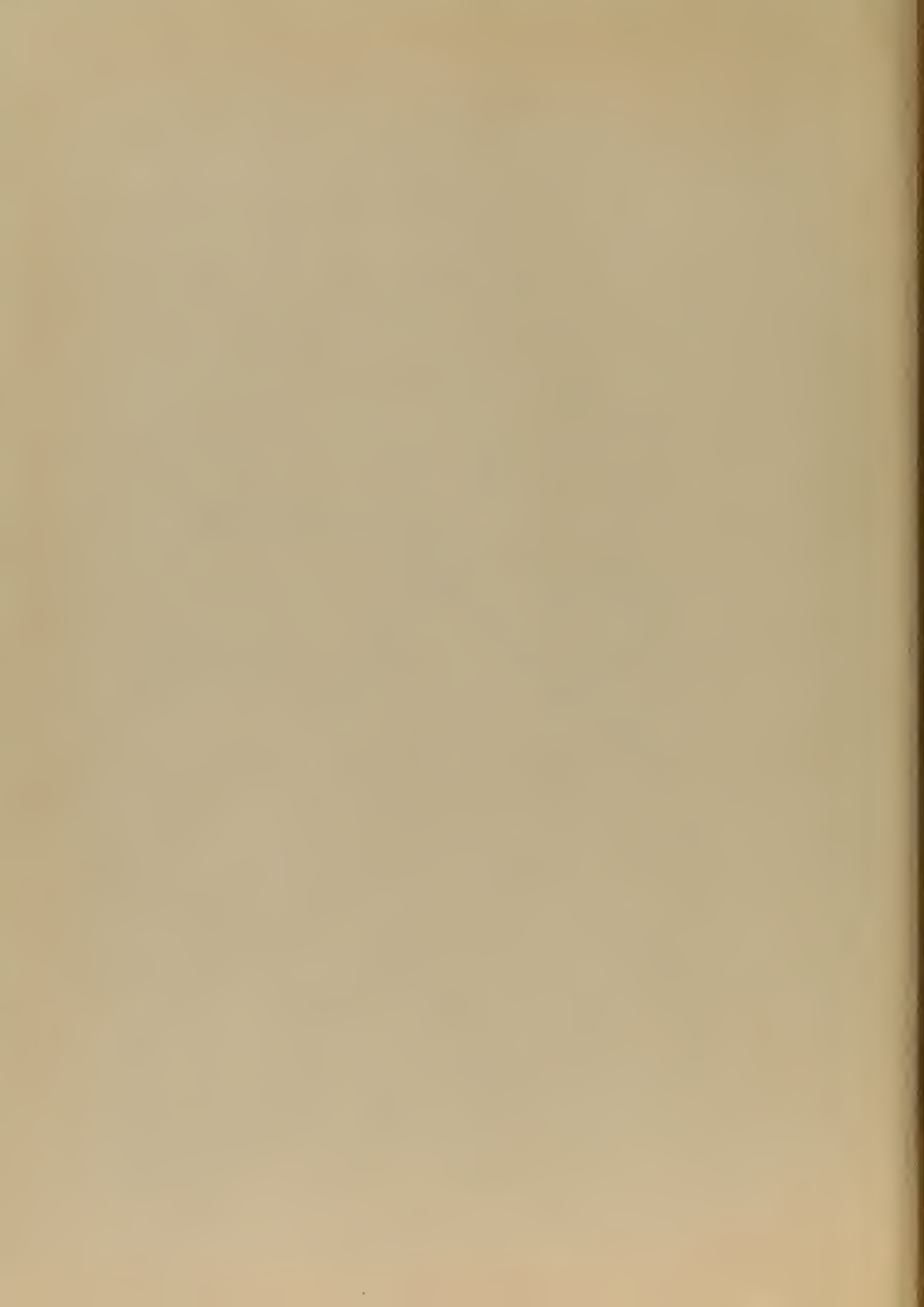


Figure 68a. Hybrid Junction Balun

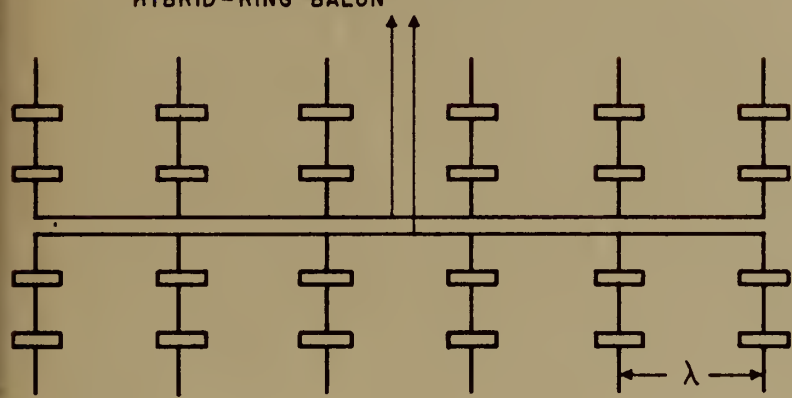


The printed Chereix-Mesny array is shown in Figure 70. This array, without the top and bottom rows of parasitic elements, exhibited half power beam widths of 14° , measured parallel to the width of the array. The measured beam widths were essentially the same as the computed values, and the side lobe level was down approximately 10 DB.

Printed antennas may also be constructed as arrays of slot antennas. These are well adapted to the printing technique, however, their use is not considered general enough to warrant discussion here. Several interesting papers which discuss printed slot antennas in detail have been published and are included in the Bibliography [5] [38].



BALANCED TRANSMISSION LINE TO
HYBRID-RING BALUN



TO ARMS 2 AND 4 OF
HYBRID-RING BALUN

(See Figure
68a Page 113)

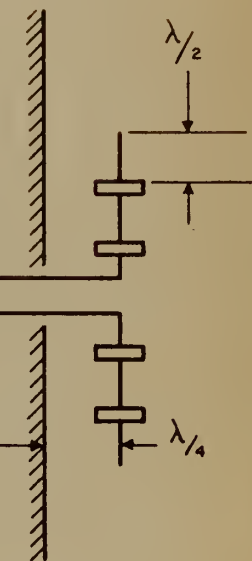
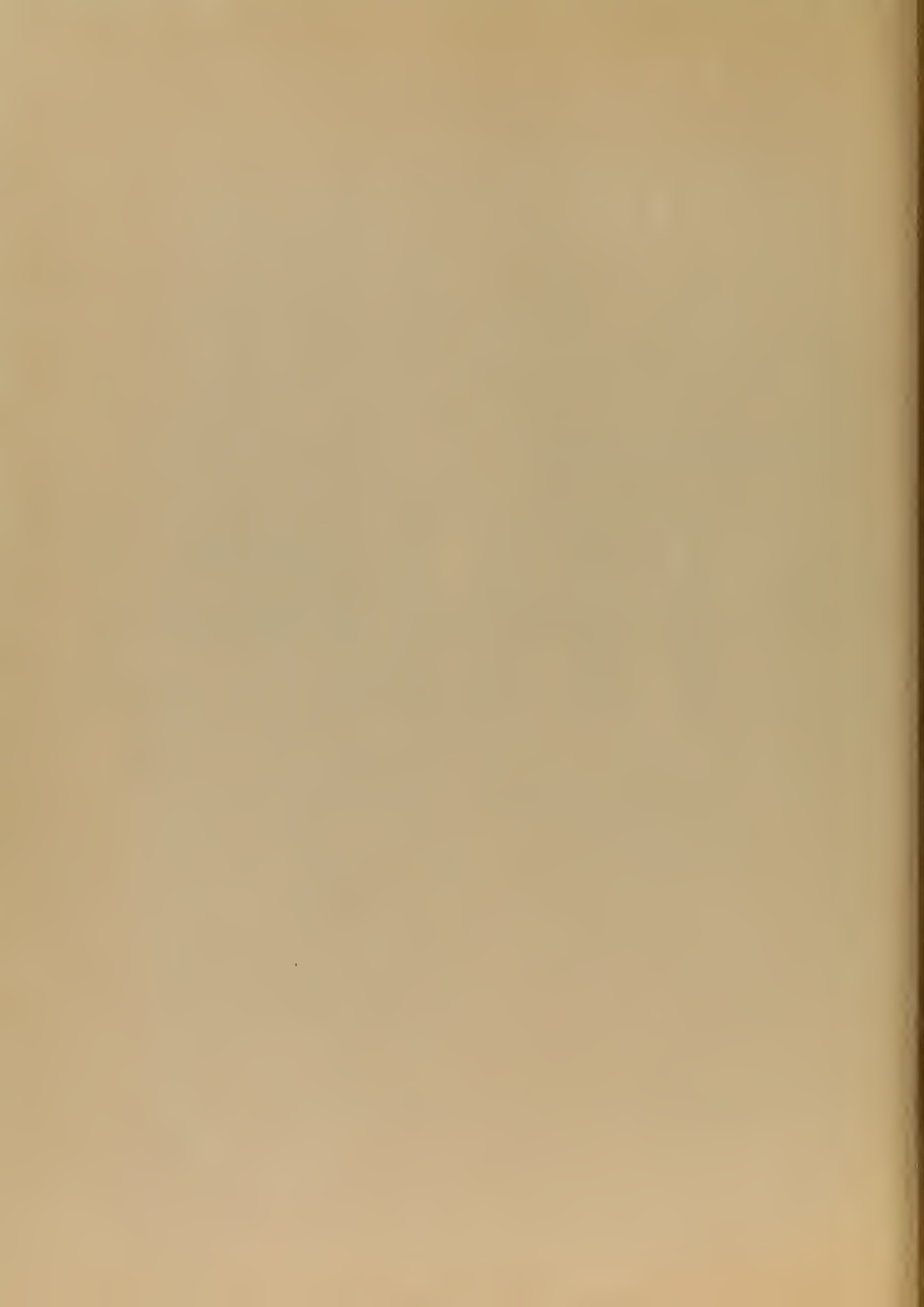


Figure 68. Thirty Element Coplanar Array



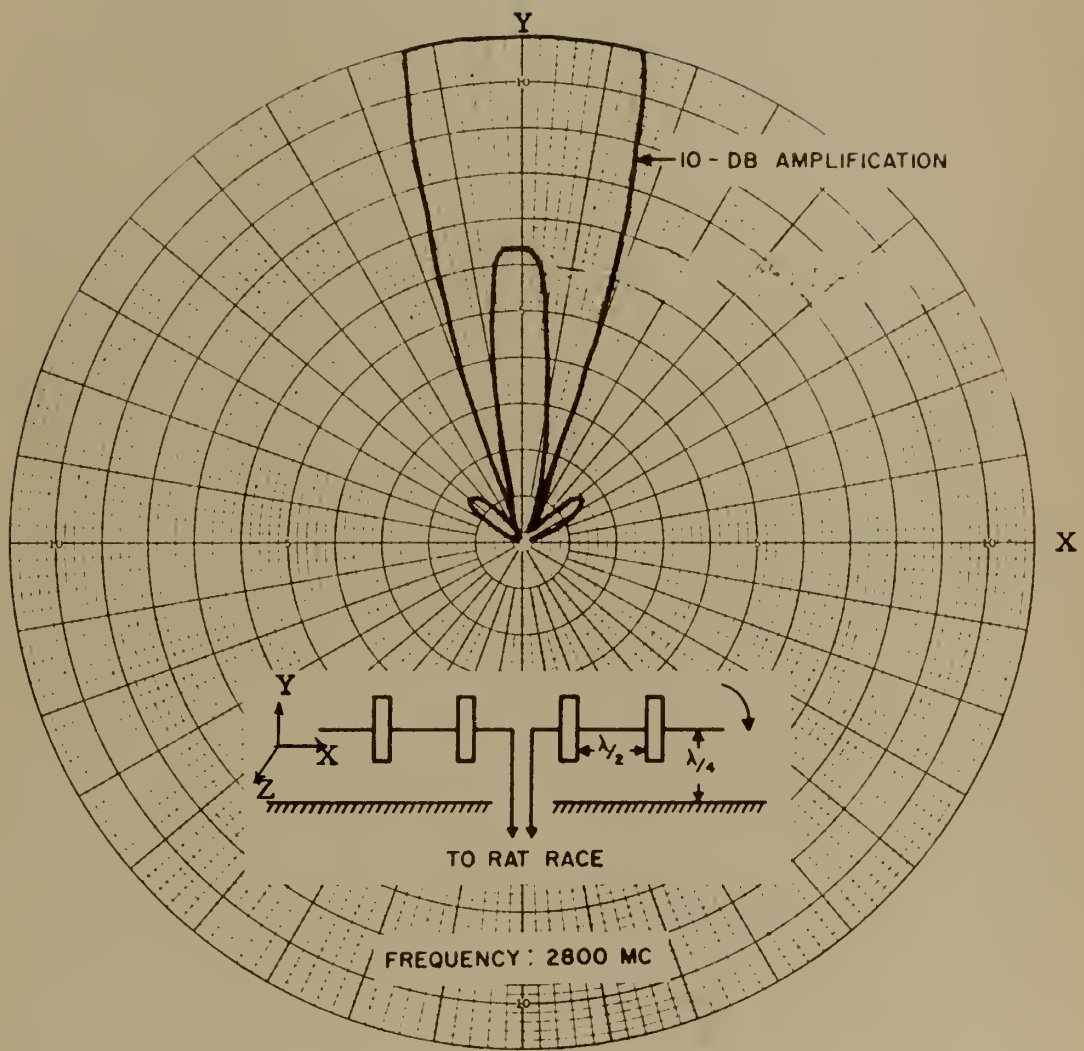


Figure 69. Radiation Intensity Pattern in XY Plane
for Thirty Element Coplanar Array



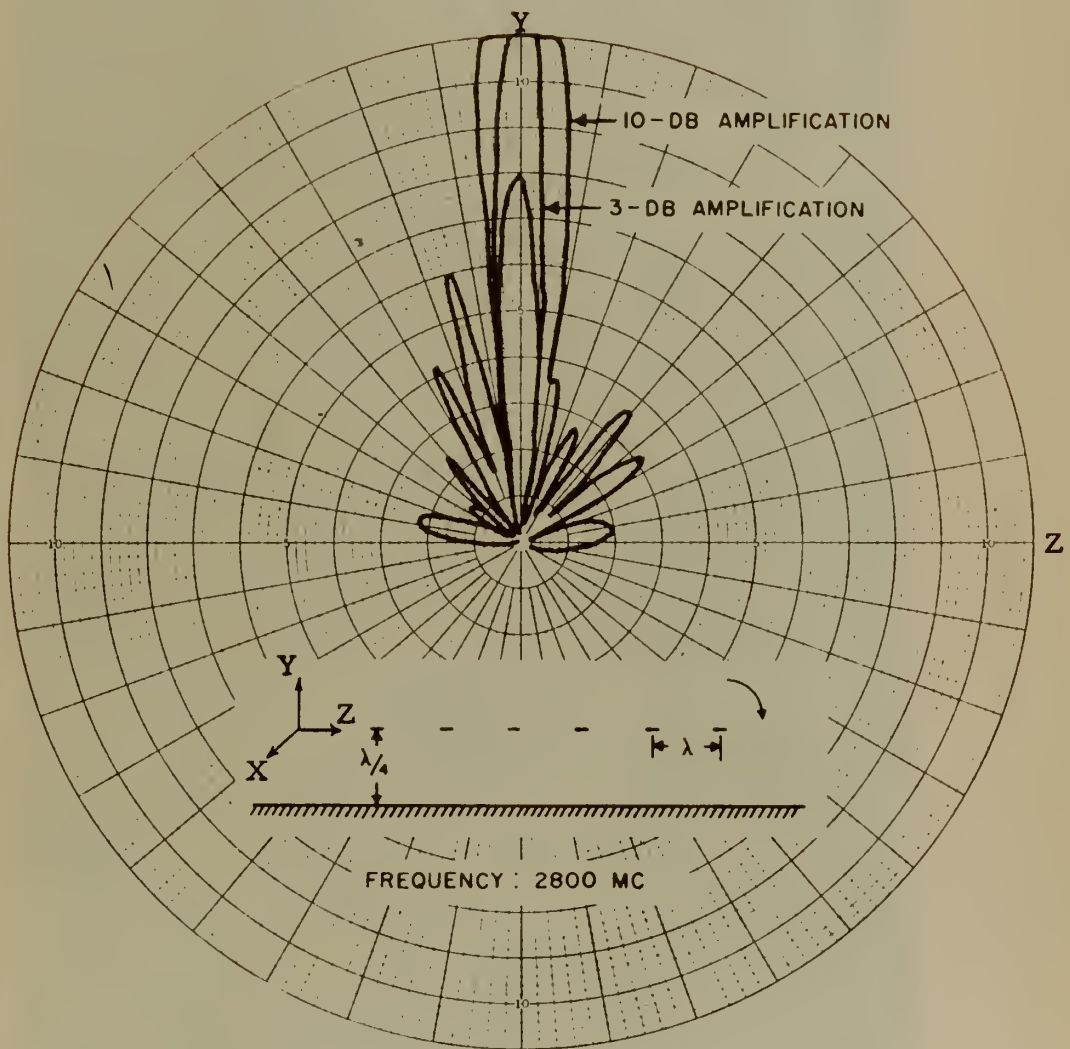


Figure 70 . Radiation Intensity Pattern in YZ Plane
for Thirty Element

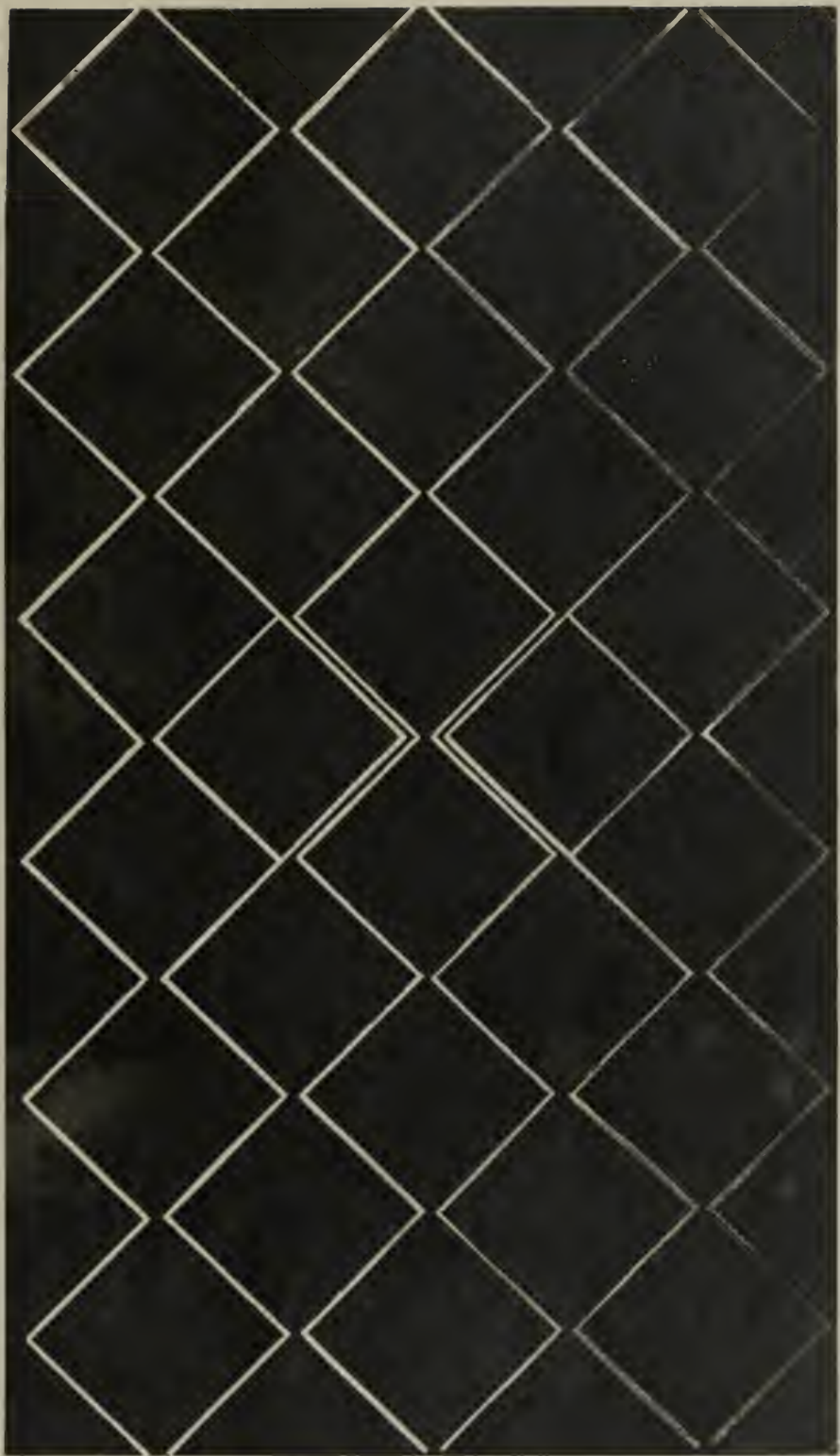
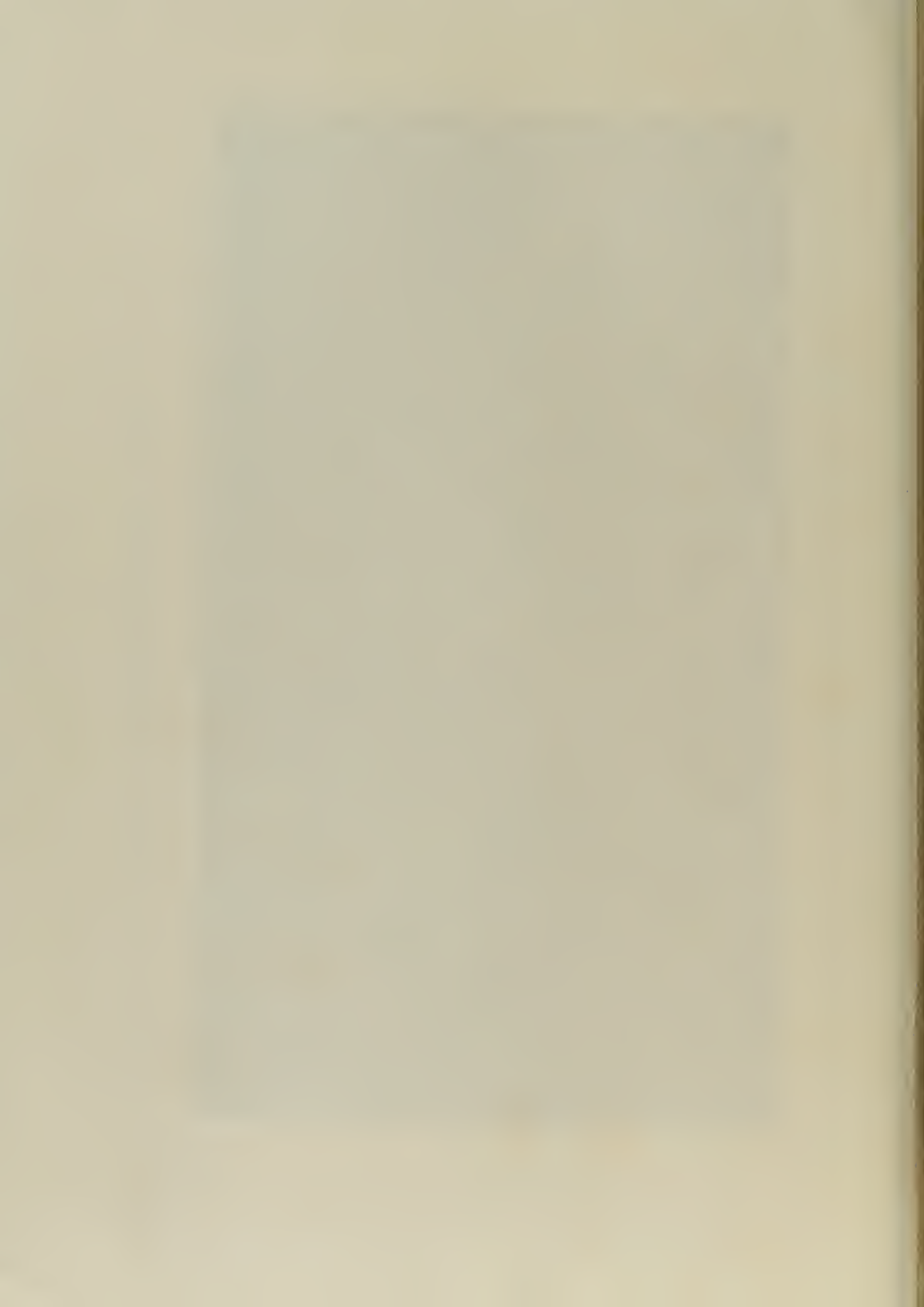
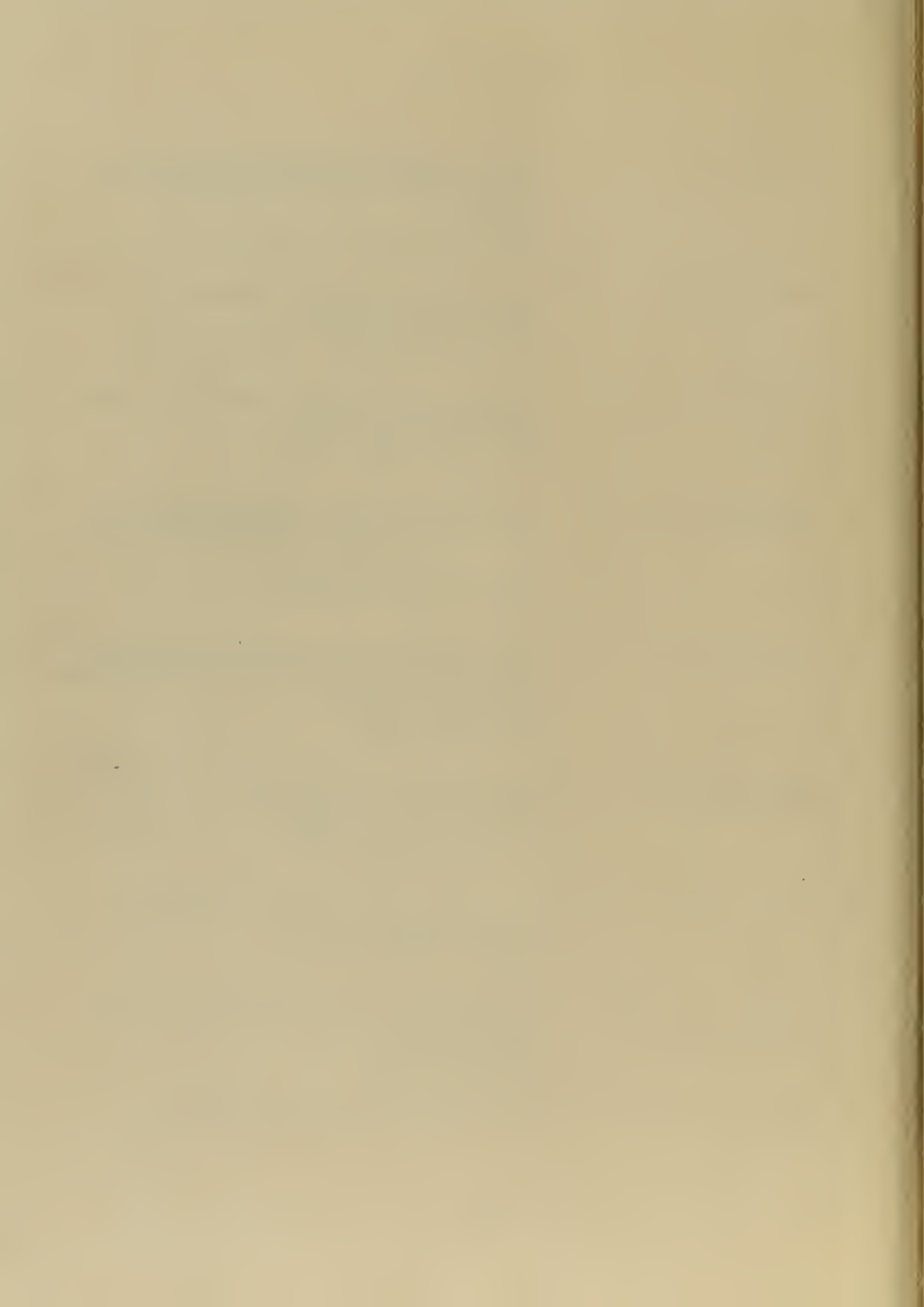


Figure 71. Printed Chereix-Messny Array



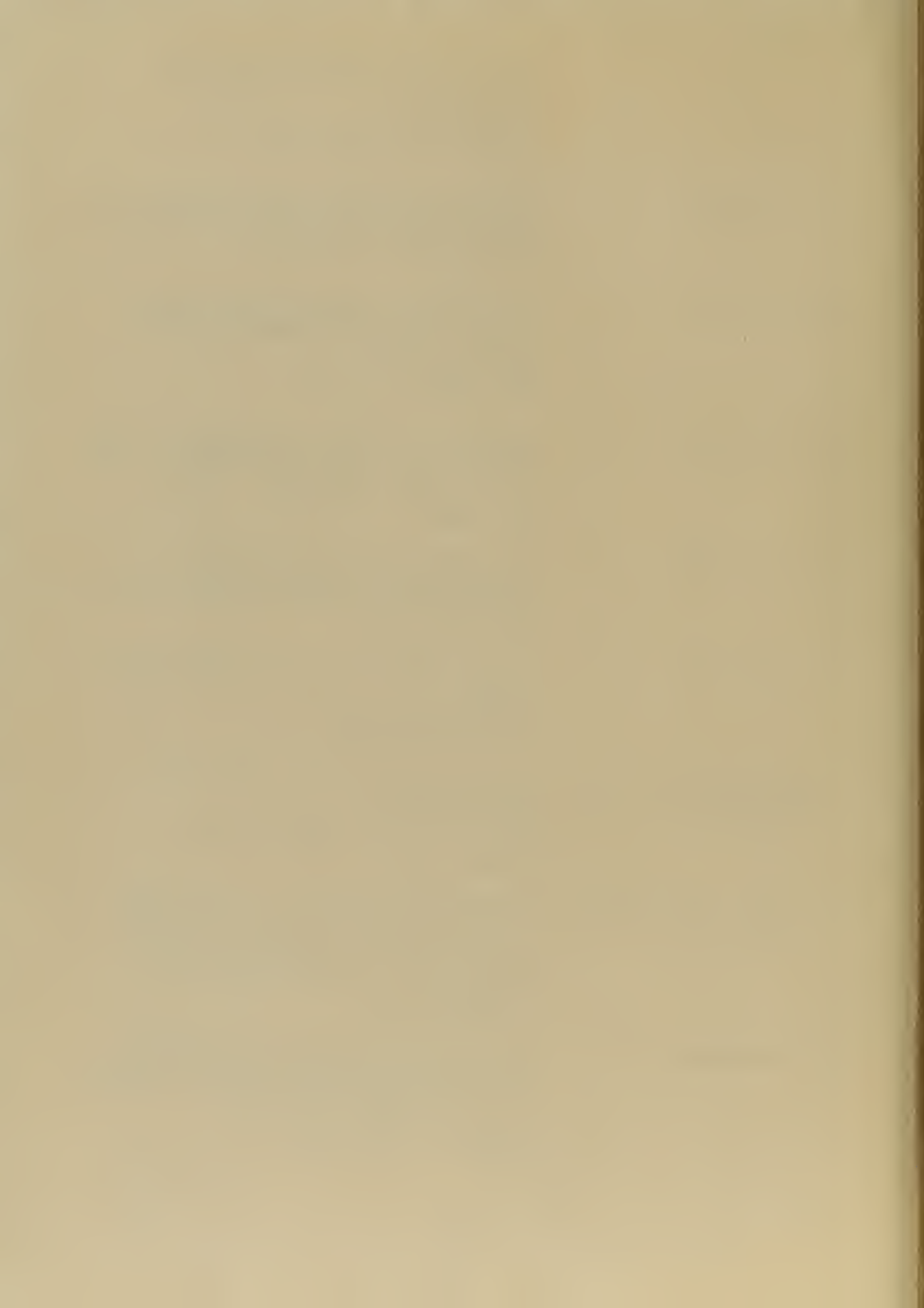
BIBLIOGRAPHY

1. Arditi, M. CHARACTERISTICS AND APPLICATIONS OF MICROSTRIP FOR MICROWAVE WIRING Federal Telecommunication Laboratories September 1954
2. Barrett, R. M. MICROWAVE PRINTED CIRCUITS - A HISTORICAL SURVEY Air Force Cambridge Research Center 20 September 1954
3. Begovich, N. A. CHARACTERISTIC IMPEDANCE OF STRIP TRANSMISSION LINES Hughes Aircraft Company 11 October 1954
4. Begovich, N. A. and Morgolin, A. R. THEORETICAL AND EXPERIMENTAL STUDY OF A STRIP TRANSMISSION LINE Technical Memo No. 234 Hughes Aircraft Company Research and Development Laboratory 12 May 1950
5. Bittner, B. J. PHOTOETCHING TECHNIQUES FOR THE PRECISION FABRICATION OF WAVEGUIDE ANTENNA ARRAYS Sandia Corporation 11 October 1954
6. Black, K. G. and Higgins, T. J. RIGOROUS DETERMINATION OF THE PARAMETERS OF MICROSTRIP TRANSMISSION LINES University of Wisconsin 11 October 1954
7. Bode, H. W. NETWORK ANALYSIS AND FEEDBACK AMPLIFIER D. Van Nostrand Company 1945
8. Bradley, E. H. and White, D. R. J. BANDPASS FILTERS USING STRIP LINE TECHNIQUES Melpar Incorporated 11 October 1954
9. Budenbom, H. T. ANALYSIS AND PERFORMANCE OF

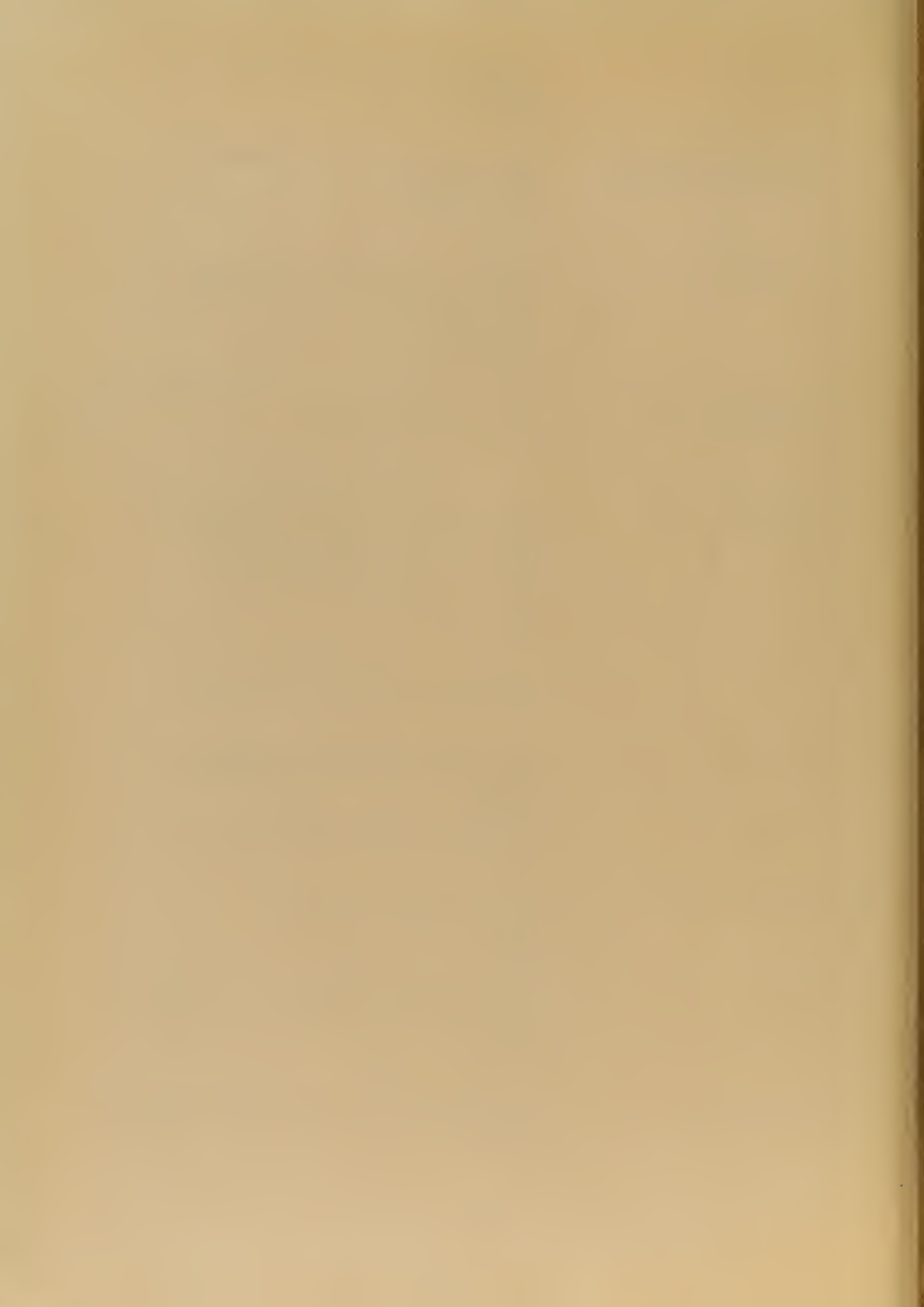


WAVE GUIDE HYBRID RINGS FOR
MICROWAVES
Bell System Technical Journal
Volume XXVII, Page 473
1947

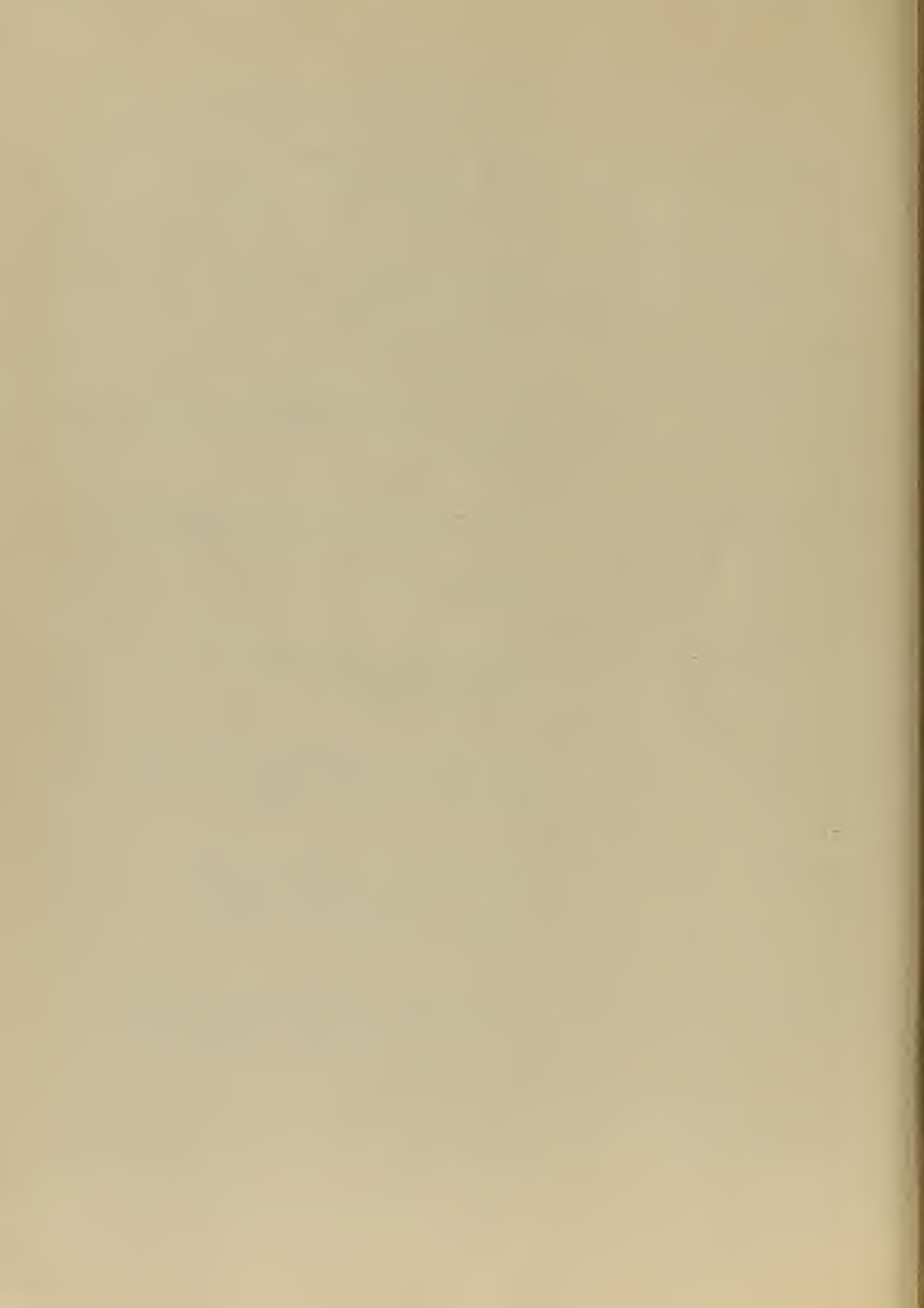
10. Carlson, E. A BROAD-BAND MICROSTRIP CRYSTAL
MIXER WITH INTEGRAL DC RETURN
Sylvania Electric Products
12 October
11. Chireix, H. FRENCH SYSTEM OF DIRECTIONAL-
AERIALS FOR TRANSMISSION ON
SHORT WAVES
The Wireless Engineer
May 1929
12. Cohn, S. B. CHARACTERISTIC IMPEDANCE OF THE
SHIELDED - STRIP TRANSMISSION LINE
Transactions of the IRE
Volume MTT-2, Number 2, Page 52
July 1954
13. Cohn, S. B. OPTIMUM DESIGN OF STEPPED
TRANSMISSION LINE TRANSFORMERS
Stanford Research Laboratories
11 October 1954
14. Cohn, S. B. PROBLEMS IN STRIP TRANSMISSION
LINES
Stanford Research Institute
23 September 1954
15. Cohn, S. B. and STRIP TRANSMISSION LINES AND
Robinson, L. A. and COMPONENTS
Shimizo, J. First Quarterly Report
Stanford Research Laboratories
October 1954
16. Cooper, H. W. and MEASUREMENTS OF ATTENUATION
Ringebach, M. E. AND PHASE VELOCITY OF VARIOUS
LAMINATE MATERIALS AT L-BAND
Maryland Electronic Manufacturing
Corporation
11 October 1954
17. Deschamps, G. A. DETERMINATION OF REFLECTION
COEFFICIENT AND INSERTION LOSS OF
A WAVEGUIDE JUNCTION
Journal of Applied Physics
Volume 24, Page 1046
1953



18. Everett, W. L. COMMUNICATION ENGINEERING
Mc-Graw - Hill
1937
19. Federal Telephone
and Radio Company REFERENCE DATA FOR RADIO
ENGINEERS
Third Edition
1953
20. Fromm, W. E. CHARACTERISTICS AND SOME
APPLICATIONS OF STRIPLINE
COMPONENTS
Airborne Instruments Laboratory
11 October 1954
21. Frost, A. D. and
Mingins, C. R. MICROWAVE STRIP CIRCUIT RESEARCH
AT TUFTS COLLEGE
Tufts College
11 October 1954
22. Fubini, E. and
Fromm W. and
Keen, H. NEW TECHNIQUES FOR HIGH-Q STRIP
MICROWAVE COMPONENTS AND
MICROWAVE APPLICATIONS OF
HIGH-Q STRIP COMPONENTS
Convention Record of the I R E
Part 8, Page 91
March 1954
23. Fubini, E. G. STRIPLINE RADIATORS
Airborne Instruments Laboratory
11 October 1954
24. Goubau, G SURFACE WAVES AND THEIR
APPLICATION TO TRANSMISSION
LINES
Journal of Applied Physics
Volume 21, Number 11, Page 1119
November 1950
25. Hansen, W. W. "NOTES ON LECTURES"
Stanford University
Chapter 6
26. Hoyt, W. H. Jr. THE MUTUAL AND INPUT IMPEDANCE
OF STRIPS BETWEEN PARALLEL
PLANES
Purdue University
11 October 1954
27. Huggins, W. H. THE NATURAL BEHAVIOR OF BROAD-
BAND CIRCUITS

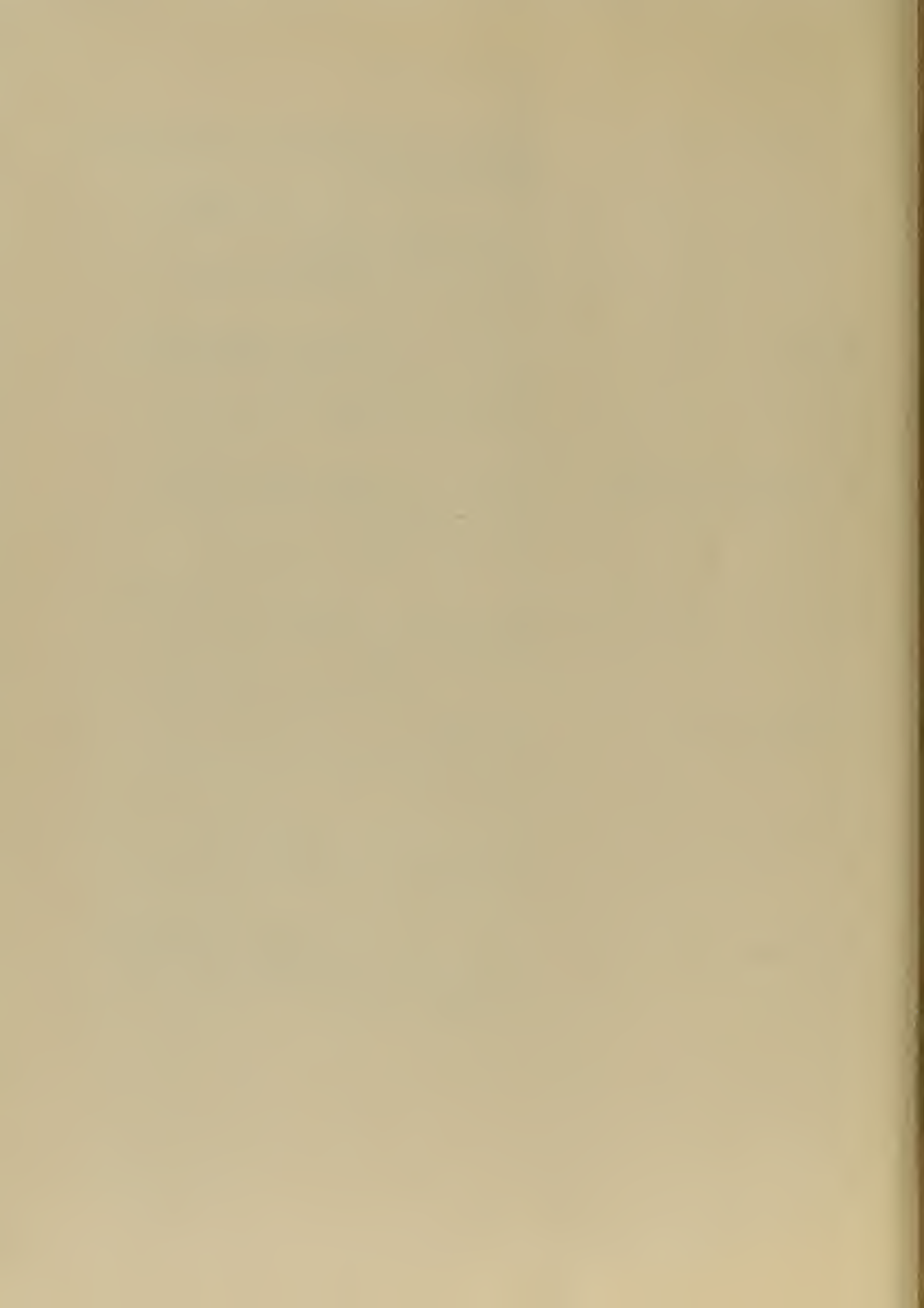


- Report E5013A
Electronic Research Laboratory
November 1948
28. Jasick, H. CUTOFF WAVELENGTH OF FIRST
WAVEGUIDE MODE
Memorandum to E. G. Fubini
30 July 1953
29. Keen, H. S. STRIP TRANSMISSION LINE
INVESTIGATION
Progress Reports
Airborne Instruments Laboratory
September 1953
30. Marcuvitz, N. WAVEGUIDE HANDBOOK
M. I. T. Radiation Laboratory Series
Volume 10
McGraw - Hill
1951
31. Montgomery, C. G. PRINCIPLES OF MICROWAVE CIRCUITS
Dicke, R. H.
Purcell, E. M.
M. I. T. Radiation Laboratory Series
Volume 8
McGraw - Hill
1948
32. Moore J. F. and RESONATOR AND PRESELECTOR IN
Michelson, M. BALANCED STRIP LINE
Raytheon Company
11 October 1954
33. Morano, T. MICROWAVE TRANSMISSION DESIGN
Data Publication Number 23-80
Sperry Gyroscope Company
May 1944
34. Oliner, A. A. EQUIVALENT CIRCUITS FOR
DISCONTINUITIES IN BALANCED
STRIP TRANSMISSION LINE
Polytechnic Institute of Brooklyn
11 October 1954
35. Pease, R. L. and A UNIVERSAL APPROXIMATE FORMULA
Mingins, C. R. FOR CHARACTERISTIC IMPEDANCE OF
STRIP TRANSMISSION LINES WITH
RECTANGULAR INNER CONDUCTORS
Tufts College
11 October 1954
36. Reich, H. J. VERY HIGH - FREQUENCY TECHNIQUES



McGraw - Hill
1947

37. Rumsey, V. H. REPORT PUBLISHED BY THE COMBINED RESEARCH GROUP N. R. L. DURING THE WAR YEARS
38. Sommers, D. J. SLOT ARRAY EMPLOYING PHOTO-ETCHED TRI-PLATE TRANSMISSION LINES
Sanders Associates Incorporated
11 October 1954
39. Storer, J. E. A SIMPLE GRAPHICAL ANALYSIS OF A TWO-PART WAVEGUIDE JUNCTION
Proceedings of the IRE
Volume 48, Number 3, Page 1004
August 1953
40. Torgow, E. N. and Griemann, J. W. E. MINIATURE STRIP TRANSMISSION LINE FOR MICROWAVE APPLICATIONS
Polytechnic Institute of Brooklyn
11 October 1954
41. Tyrrell, W. A. HYBRID CIRCUITS FOR MICROWAVE
Proceedings of the IRE
Volume 35, Number 11, Page 1294
November 1947
42. Wholey, W. B. and Elpred, W. N. A NEW TYPE OF SLOTTED LINE SECTION
Proceedings of the IRE
Volume 38, Number 3, Page 244
March 1950
43. Wild, N. R. PHOTOETCHED MICROWAVE TRANSMISSION LINES
Sanders Associates Incorporated
11 October 1954
44. Zublin, K. E. STRIP TYPE COMPONENTS FOR 2000 MEGACYCLE RECEIVER HEAD-END
General Electric Company
11 October 1954



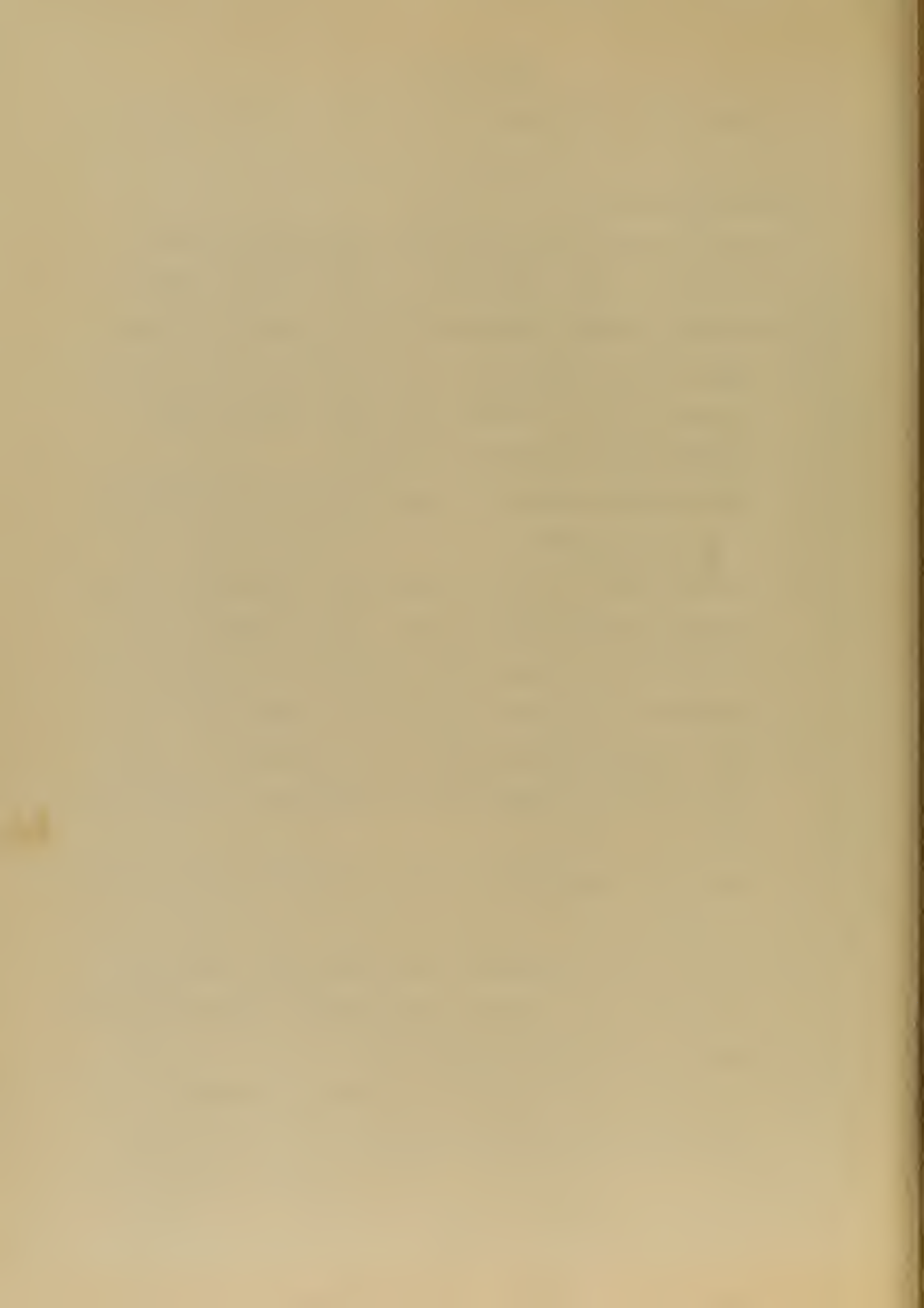
APPENDIX A

LAYOUT AND CONSTRUCTION OF CENTER CONDUCTORS

1. Photo etching process

The center conductor of a strip transmission line, made from either solid metal or metal clad dielectric sheets, may be formed by the photo etching process, following this brief outline of the process.

- a. Make a large scale black and white drawing of each side of the complete layout. The large size is used to insure sharp straight edges after photo reduction.
- b. Photograph the drawing and obtain a negative exactly the size of the actual layout.
- c. Coat both sides of a well-cleaned sheet of material with a light sensitive enamel, such as Empire cold-top enamel. Mechanically whirling the sheet while it dries is recommended, since the enamel coating must cover the sheet uniformly.
- d. Place the photographic negative and coated sheet in a contact printer with the negative over the coated sheet, emulsion side down.
- e. Expose the coated sheet with the proper light, 3200 A for cold top enamel.
- f. Repeat the process with the reverse negative for the opposite side of the sheet. Extreme caution must be exercised to insure perfect register of the two patterns.
- g. Develop the exposed sheet using a suitable developer, Mallemkodt for the cold top enamel.



- h. Carefully rinse the developed sheet with a gentle stream of water.
- i. Heat the developed sheet to harden the enamel pattern.
- j. Place the sheet in an aerated etching bath until all the unwanted material is removed. A solution of Ferric Chloride diluted to 38 - 40 Be may be used.
- k. Wash the etched pattern and clean off the enamel with a solvent or charcoal block, and the center conductor is completed.

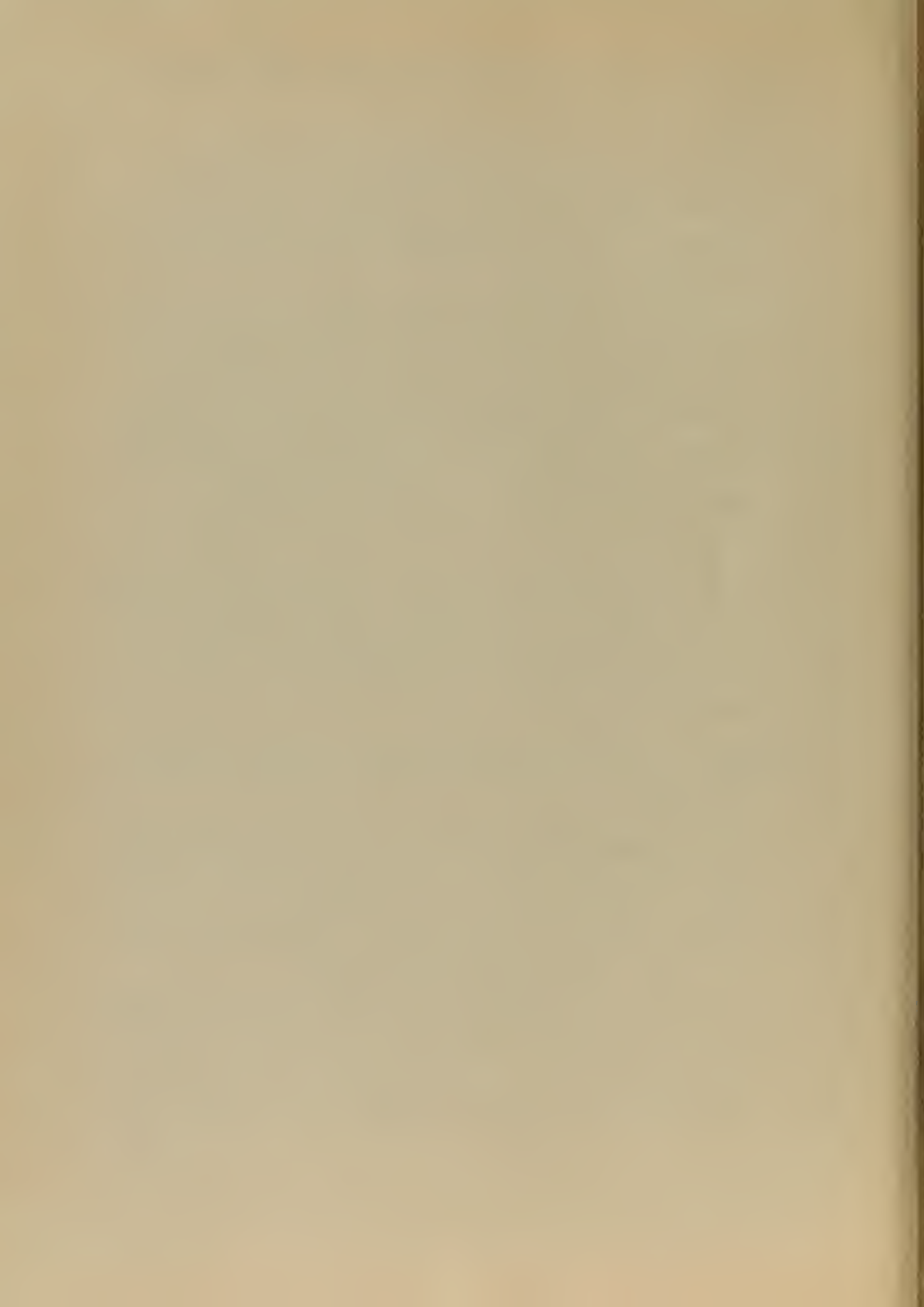
This process has been used with both copper clad dielectrics and solid conductors. Center conductors .020 inches thick of solid brass etched by this process have shown very slight undercutting.

2. The hand process

The key to successful hand cut center conductor pattern is the proper marking of the material. A height gauge has been found to be an ideal instrument for scribing the center conductor pattern with an accuracy of 0.0001 inches.

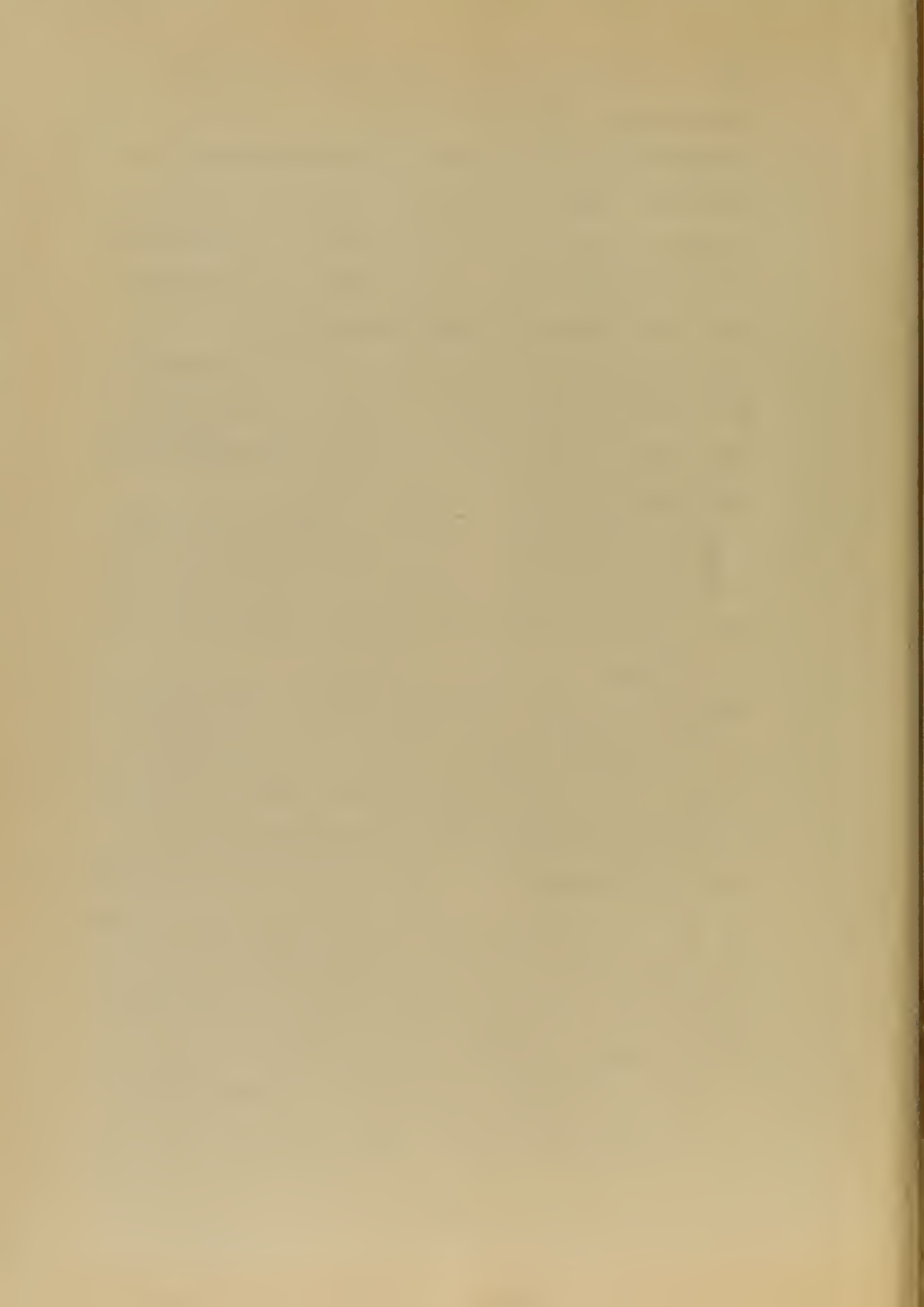
A method of cutting out the center conductor pattern utilizing a height gauge follows:

- a. Insure that there is at least one square corner with straight edges. A squaring shear is recommended for this operation.
- b. Paint the surface of the material with Dygum or other metal dye so that scribed lines will show clearly.
- c. List the dimensions of all the lines to be drawn with reference to the straight edges. The height gauge will only inscribe lines parallel to the edges. In some cases, the lines to be



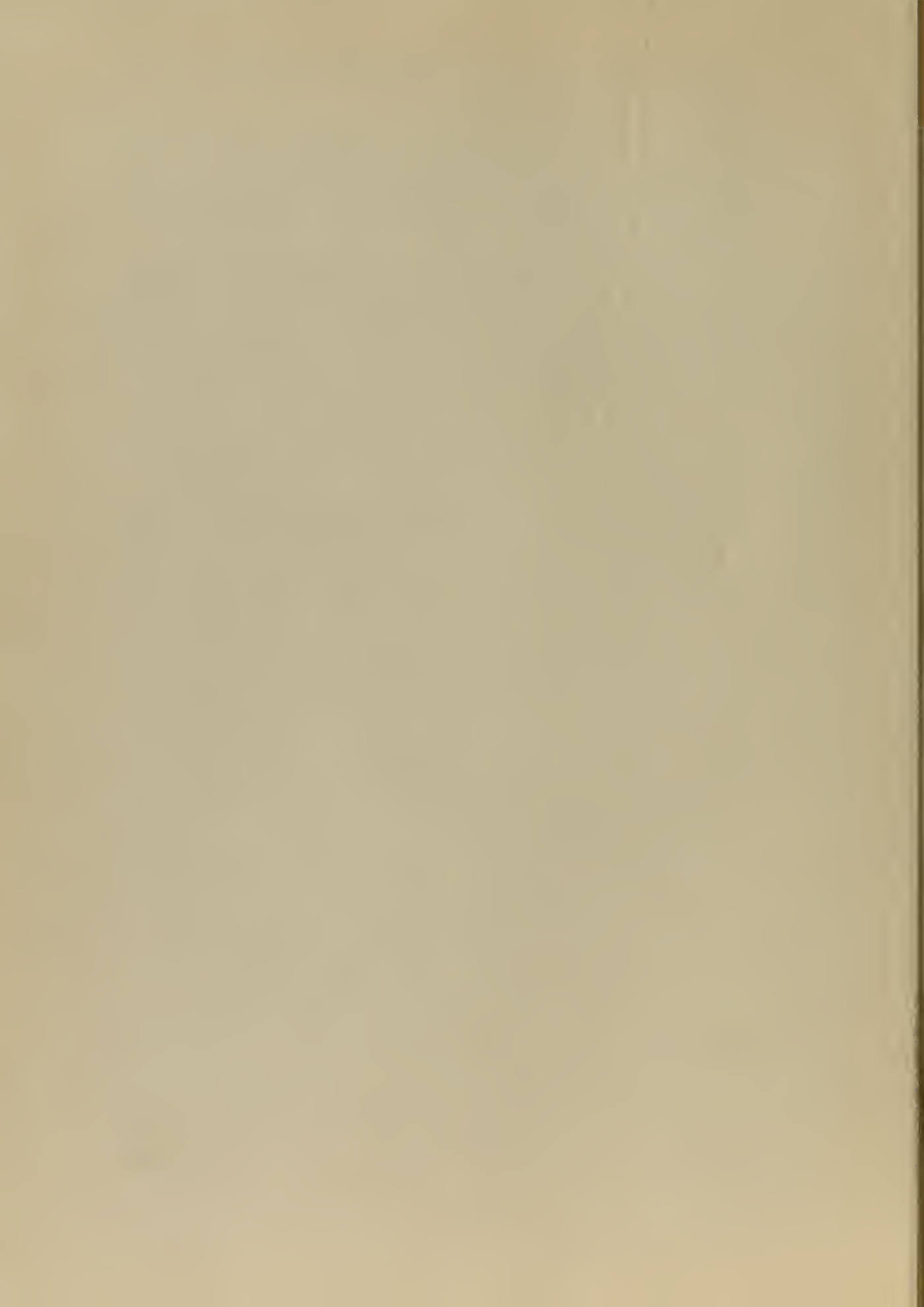
drawn are not parallel to the edges of the finished piece. In these instances, use a larger piece of material than is required so that the lines may be drawn parallel to the edges of the oversized piece. Then the desired size sheet may be cut out after the lines are drawn. The Cheriex-Mesny array shown in Figure 71 was scribed on an oversized sheet. The corners were then cut off to provide the finished product.

- d. Set the height gauge in accordance with the list of dimensions.
- e. Scribe a line for each setting of the height gauge. Reverse the sheet and scribe the opposite side before changing the setting of the gauge. This assures perfect register.
- f. Scribe each line firmly. Maintain constant pressure against a flat base plate to insure a uniformly straight line. Do not repeat on the same side since the scribe tends to creep when overscribing.
- g. With metal clad dielectric sheets, remove unwanted metal by carefully cutting along the guide lines, then peeling off the excess. A razor blade type hand cutter, which easily follows along the indented mark made by the scribe of the height gauge, is recommended for this operation. Exercise caution not to cut all the way through the metal, because the dielectric sheet would also be scored and much of the support strength would be lost. The proper depth of cut to remove the metal with a clean edge is easily determined with practice.
 1. After the scribed lines have been accentuated by the cutter, raise a corner of the metal in the region that



is to be removed and with small long-nosed pliers, peel away the unwanted material.

2. Check the accuracy of register by holding the finished sheet up to a bright light and looking for shadows that would indicate a non-perfect register.
- h. With the solid metal conductor, cut away the unwanted metal after the lines are scribed with either hand shears, a band saw, or other suitable machine tools.



APPENDIX B

POLYIRON ATTENUATION CHARACTERISTICS AND DETAILED MIXING AND CURING INSTRUCTIONS.

Mixture 1:

four parts by weight of GAF Carbonyl iron powder grade E,
one part by weight of Aralydite CN 502 epoxy resin,
six to ten percent (of the Aralydite) of Cathyist 951,
six percent is the lower limit for curing,
ten percent sets in about five minutes.

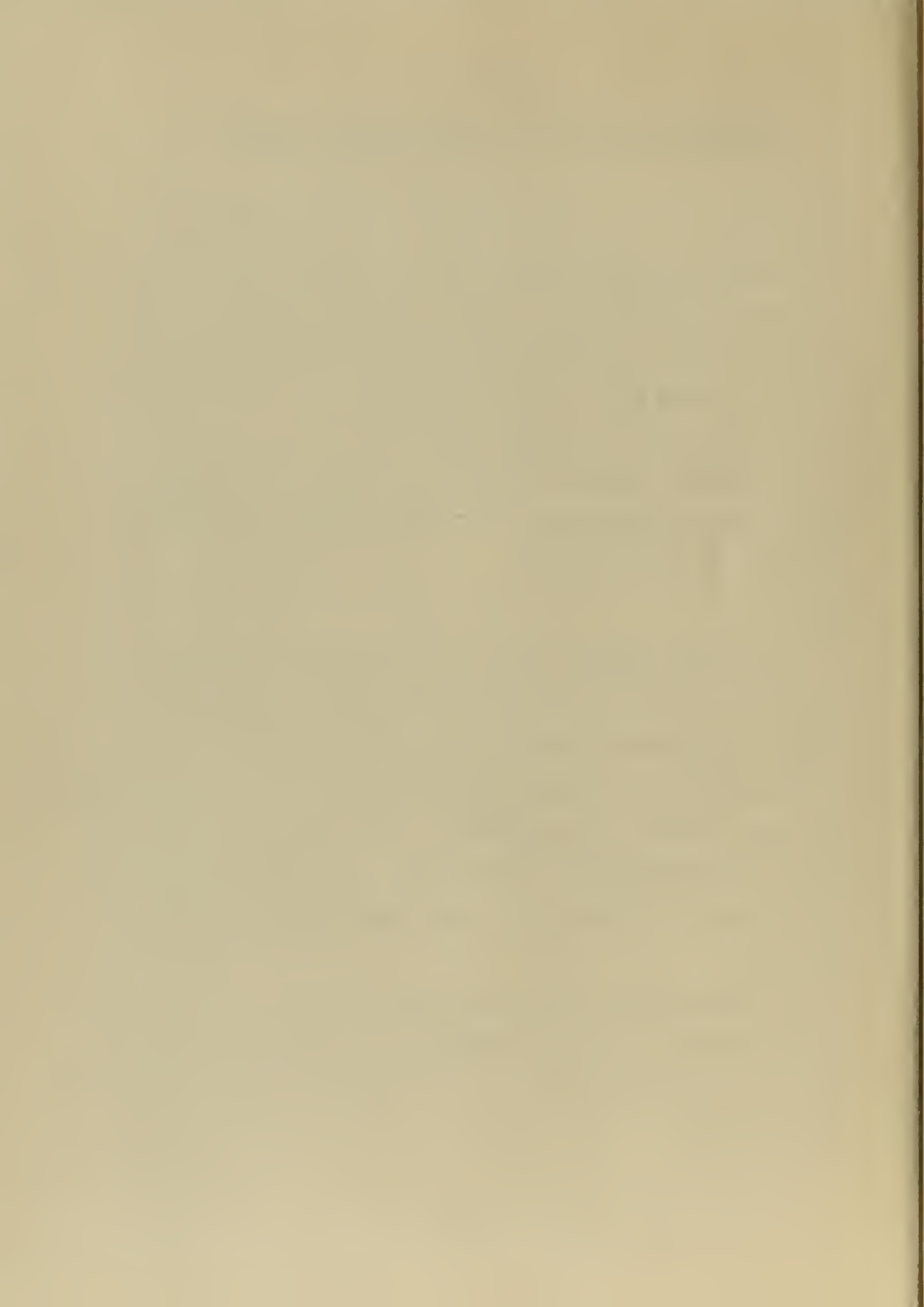
This mixture is easily machined and provides good attenuation characteristics, approximately four to eight DB per inch in the frequency range of two to six KMC.

Mixture 2 :

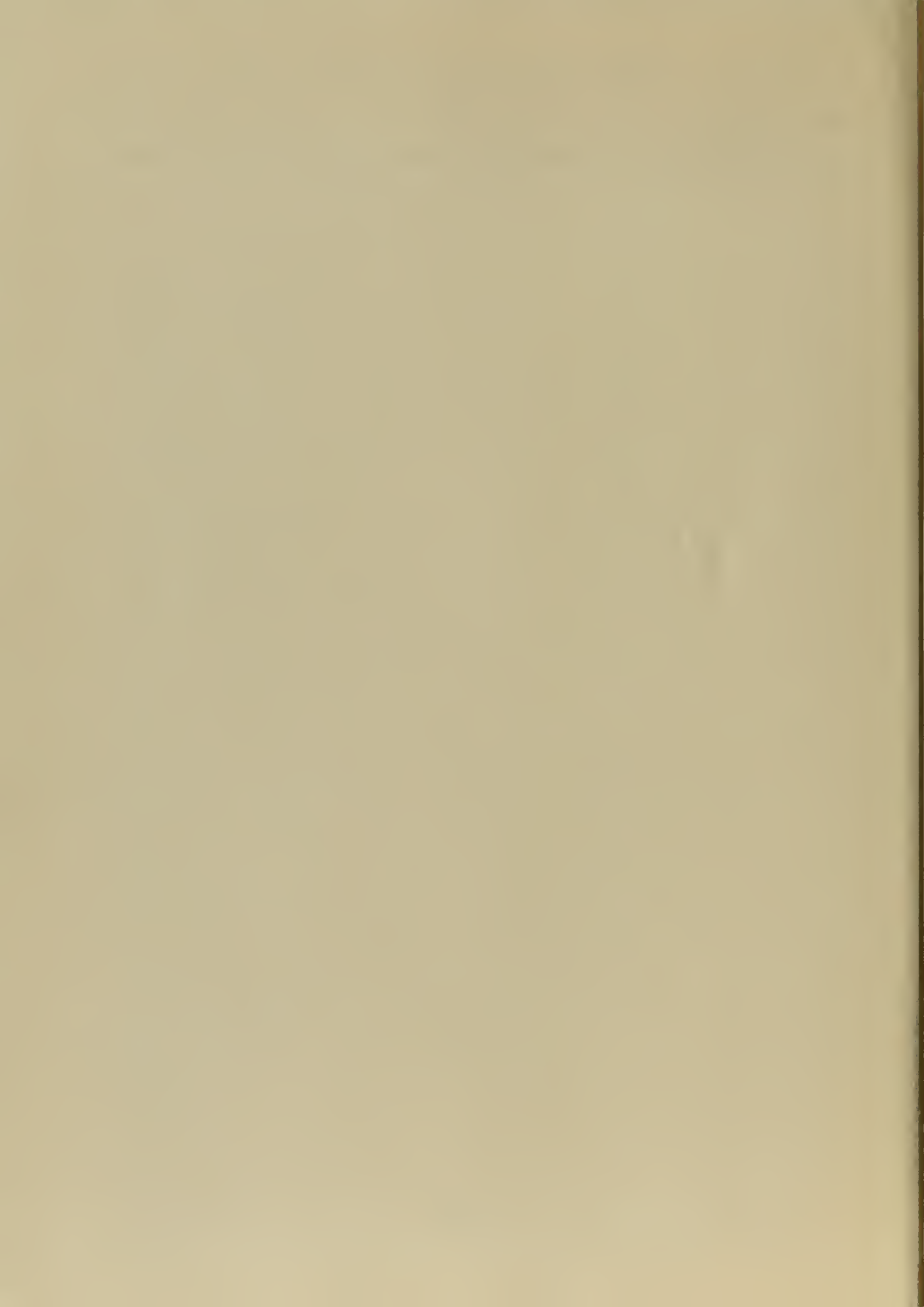
eight parts by weight of GAF Carbonyl iron powder grade E,
one part by weight of Aralydite CN 504 epoxy resin,
six to ten percent (of the Aralydite) of Catlyist 951.

This mixture is best for moulding; the Aralydite 504 is less viscous. The large percentage of iron makes the mixture brittle and difficult to machine, but the attenuation characteristic of this mixture is excellent, greater than nine to fifteen DB per inch in the frequency range of two to six KMC.

The mixtures are cured at room temperature or in an oven at 120° F for two to twenty-four hours, depending on the percentage of Catlyist. The curing time is not critical, but the temperature should remain essentially constant.



It is best to stir the mixture in a glass container with a wire bent into a gooseneck. To prevent the formation of air bubbles in the mixture, care should be used while stirring so that the surface is not disturbed.



APPENDIX C

TCHEBYSCHEFF DESIGN FOR SERIES OF QUARTER-WAVE TRANSFORMERS

The following discussion furnishes the basic information that is necessary for the Tchebyscheff design of a series of quarter-wave impedance matching transformers.

In the design band the maximum VSWR is:

$$S_{\max} = 1 + \frac{\ln [Z_{n+1}/Z_1]}{T_{n-1}[1/\cos\theta_1]} \quad (1)$$

or the VSWR at any particular frequency is:

$$S = 1 + \ln \frac{Z_{n+1}}{Z_1} \times \frac{T_{n-1}[\cos\theta/\cos\theta_1]}{T_{n-1}[1/\cos\theta_1]} \quad (2)$$

where:

Z_{n+1} is the higher terminating line impedance

Z_1 is the lower terminating line impedance

$\theta = 2\pi L/\lambda$ the electrical length of the element at the frequency of interest

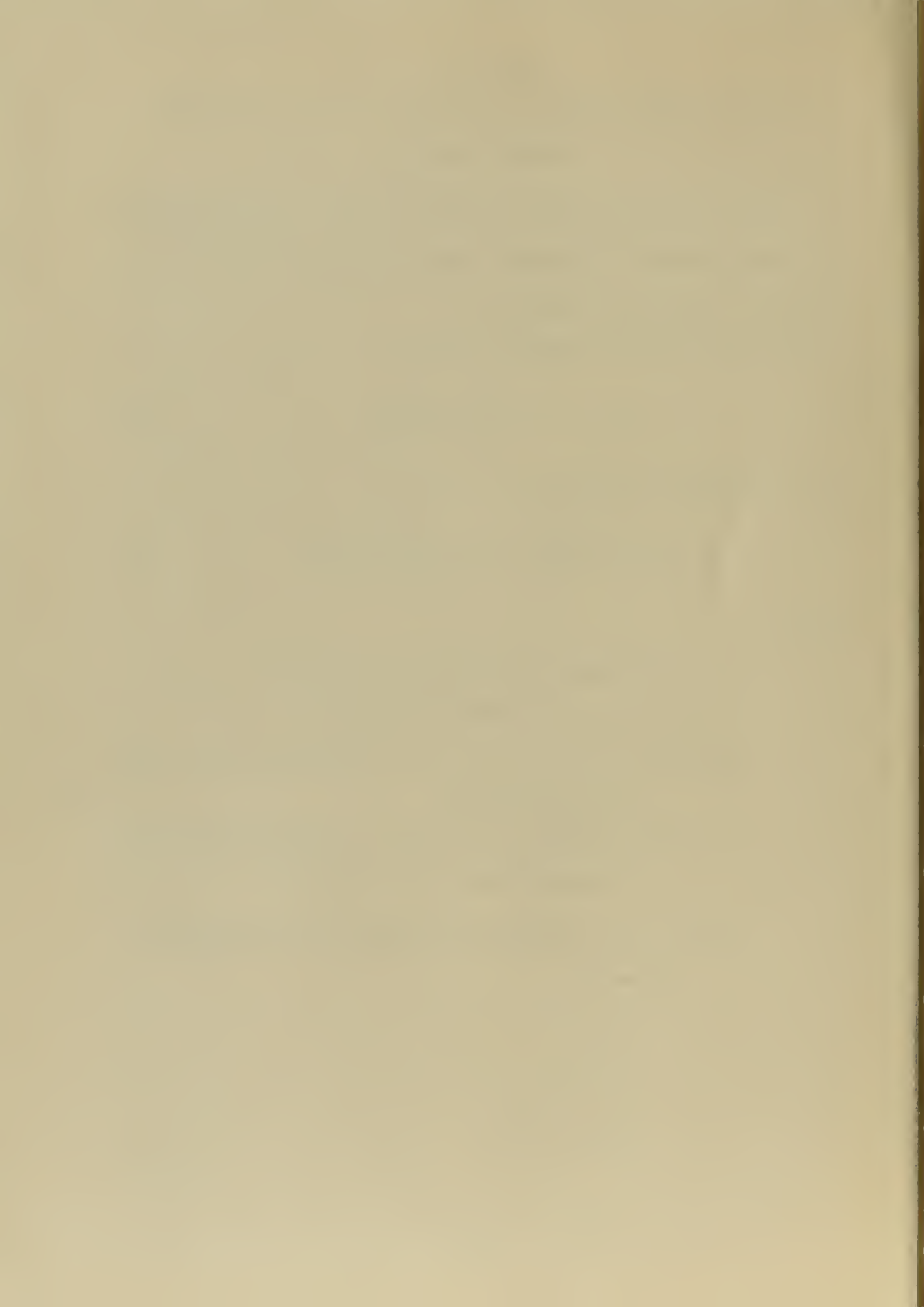
$\theta_1 = 2\pi L/\lambda_1$ the electrical length of the element at the low frequency end of the design band

$T_m(x)$ is the Tchebyscheff polynomial of the m^{th} degree defined by:

$$T_0(x) = 1$$

$$T_1(x) = x$$

$$T_2(x) = 2x^2 - 1$$



$$T_3(x) = 4x^3 - 3x$$

$$T_{m+1}(x) = 2x T_m(x) - T_{m-1}(x)$$

or $T_m(x)$ may be computed from the following equivalent expressions:

$$T_m(x) = \cos [m \cos^{-1} x] \quad x < 1$$

$$T_m(x) = \cosh [m \cosh^{-1} x] \quad 1 < x$$

The physical length of the quarter-wave elements is determined by:

$$L = \frac{\lambda_0}{4} = \frac{\lambda_1 - \lambda_2}{2[\lambda_1 + \lambda_2]} \quad (3)$$

where:

λ_0 is the wavelength at the design center of the frequency band

λ_1 is the wavelength at the low frequency end of the frequency band

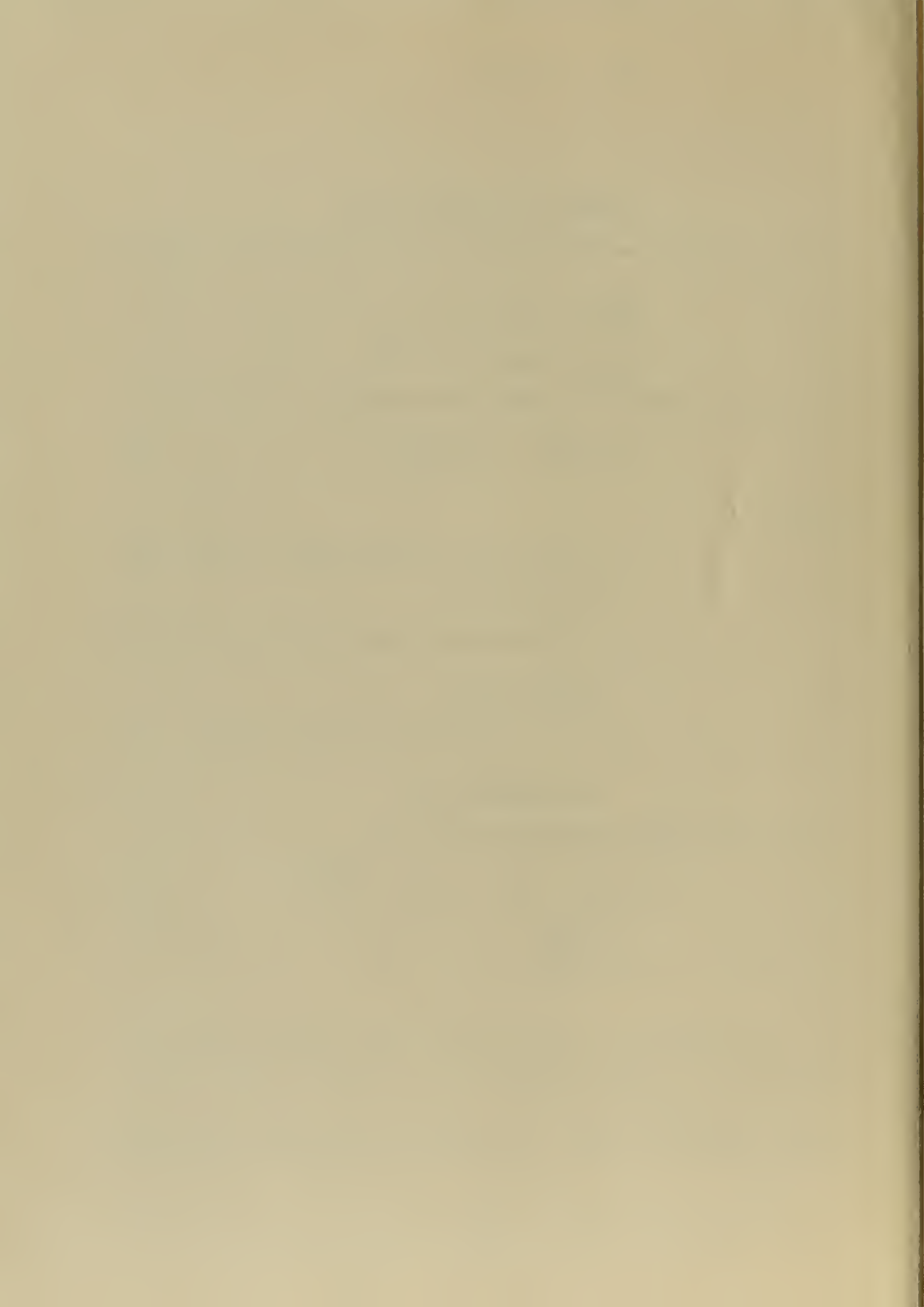
λ_2 is the wavelength at the high frequency end of the frequency band

Now for convenience define the quantity "p":

$$p = f_2/f_1 = \lambda_1/\lambda_2 = \phi_2/\phi_1 = \frac{180^\circ - \phi_1}{\phi_1} \quad (4)$$

therefore: $\phi_1 = \frac{180^\circ}{1+p}$

The following six rules provide a means of determining the coefficients a_m of the Tchebyscheff polynomial by means of an easily constructed table. The method was developed for an antenna



application by R. E. Graves, in a paper as yet unpublished.

1. In the first column first row place the number 2.

2. In the second column second row place x_0 , where:

$$x_0 = 1/\cos\theta_1$$

3. For additional entries in the first column multiply the number that is in the second column of the row above by $2x_0$ and subtract the number that is directly above in the first column.

4. In any other column add the elements to the left and right in the row above, multiply by x_0 , then subtract the number that is directly above in the same column.

5. Where there is no entry assume it to be zero.

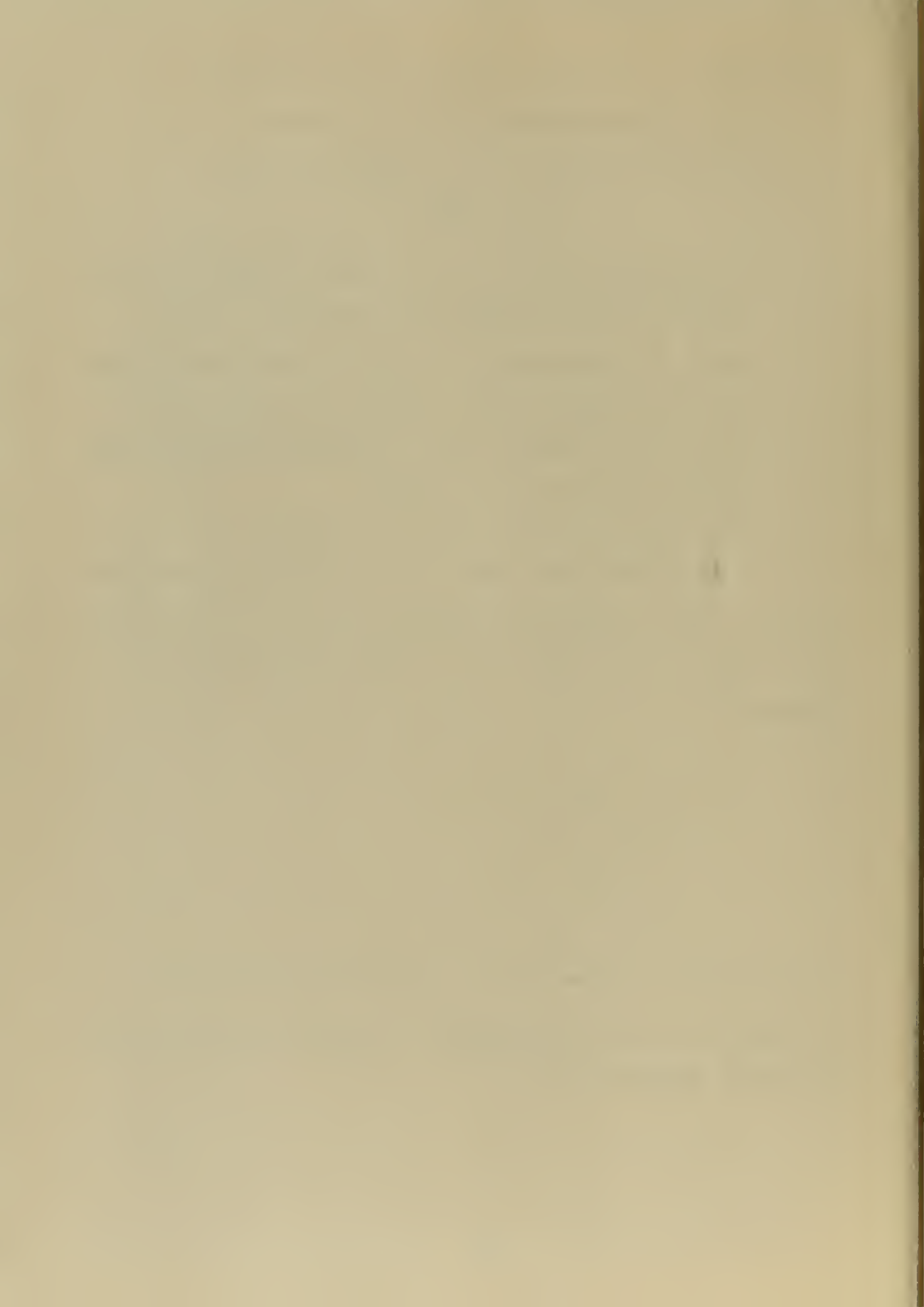
6. The elements in each row are in the ratio of the a_m constants.

Example: The following table is computed for a two-to-one frequency band. With $p = 2$, $\theta_1 = 60^\circ$, and $x_0 = 2$ from the above given relationships.

2		
2		
6	4	
18	8	
66	48	16

From the table, the values of the a_m constants are determined.

The number of steps in the transformer is equal to n , and the number of elements is equal to $n-1$.



$$a_m$$

$n = 1$	1
$n = 2$	1 1
$n = 3$	1 3/2 1
$n = 4$	1 9/4 9/4 1
$n = 5$	1 3 33/8 3 1

The values of the impedances are determined by:

$$\ln \frac{Z_{m+1}}{Z_m} = \frac{a_m \ln [Z_{n+1}/Z_1]}{a_1 + a_2 + a_3 + \dots + a_n} \quad (5)$$

Using formula (5), starting at either of the known end impedances, i.e., $Z_{m+1} = Z_{n+1}$ or $Z_m = Z_1$, the characteristic impedance of each section of the series may be progressively determined.

Example: A two step, single section quarter-wave transformer.

From the table of a_m constants for $n = 2$, $a_1 = 1$, $a_2 = 1$.

From equation (5):

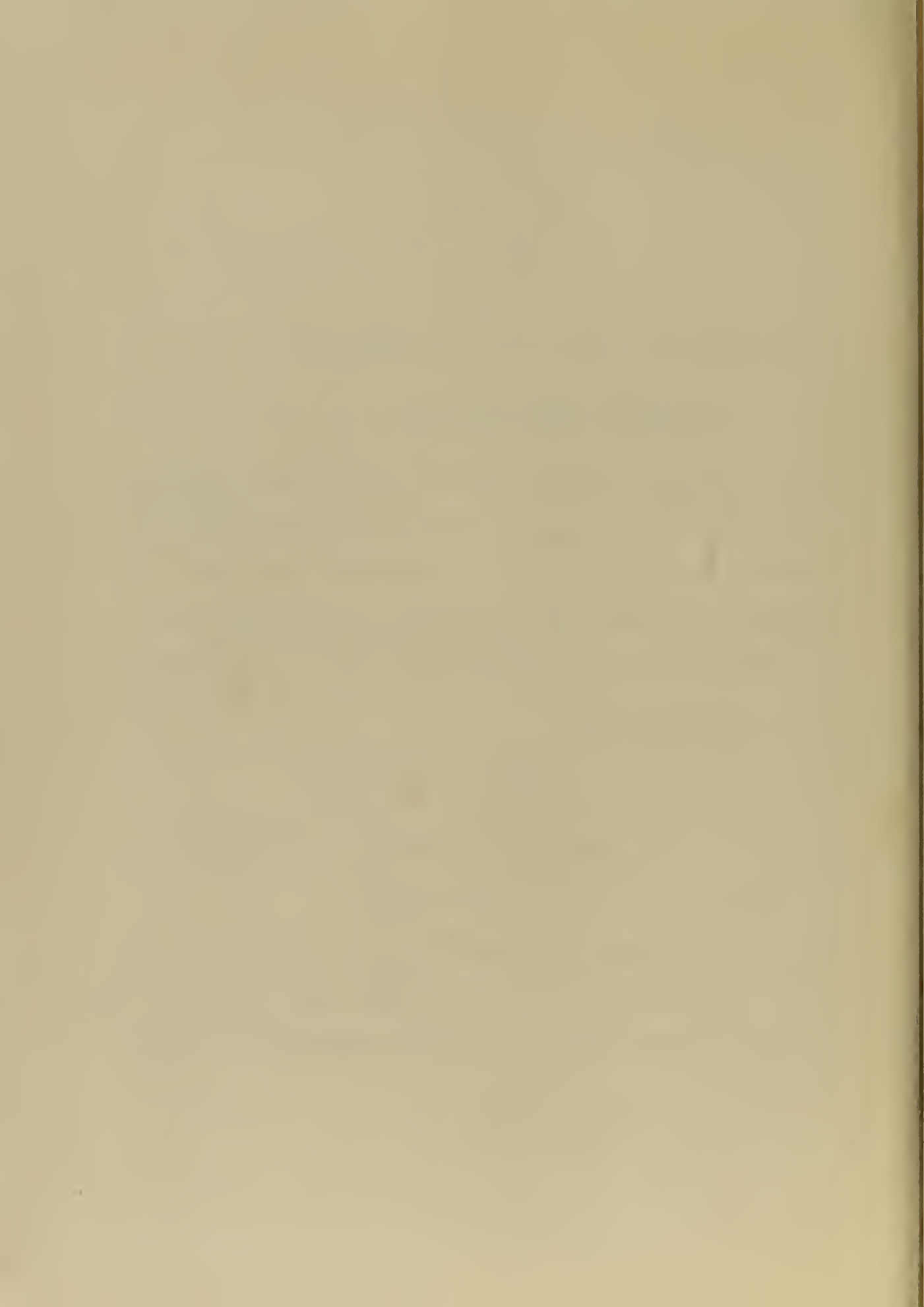
$$\ln \frac{Z_{m+1}}{Z_m} = \frac{1 \ln [Z_3/Z_1]}{2}$$

or: $\ln [Z_2/Z_1] = \ln [Z_3/Z_2] = \ln \sqrt{Z_3/Z_1}$

Therefore: $Z_2 = \sqrt{Z_1 Z_3}$

Example: A five step, four section impedance transformer to operate with minimum VSWR in the frequency band of from 3,000 to 6,000 MC, and with an input impedance of 150 ohms and the output impedance 50 ohms.

$$p = 2; \theta = 60^\circ; Z_{n+1} = 150; Z_1 = 50.$$



The required a_m constants may be determined from the $n = 5$ line of the previously calculated table.

Proceeding as in the previous example:

$$\ln [Z_2 / 50] = \frac{\ln [150 / 50]}{1+3+33/8+3+1} = 0.0906$$

Therefore: $Z_2 = 54.7$ ohms

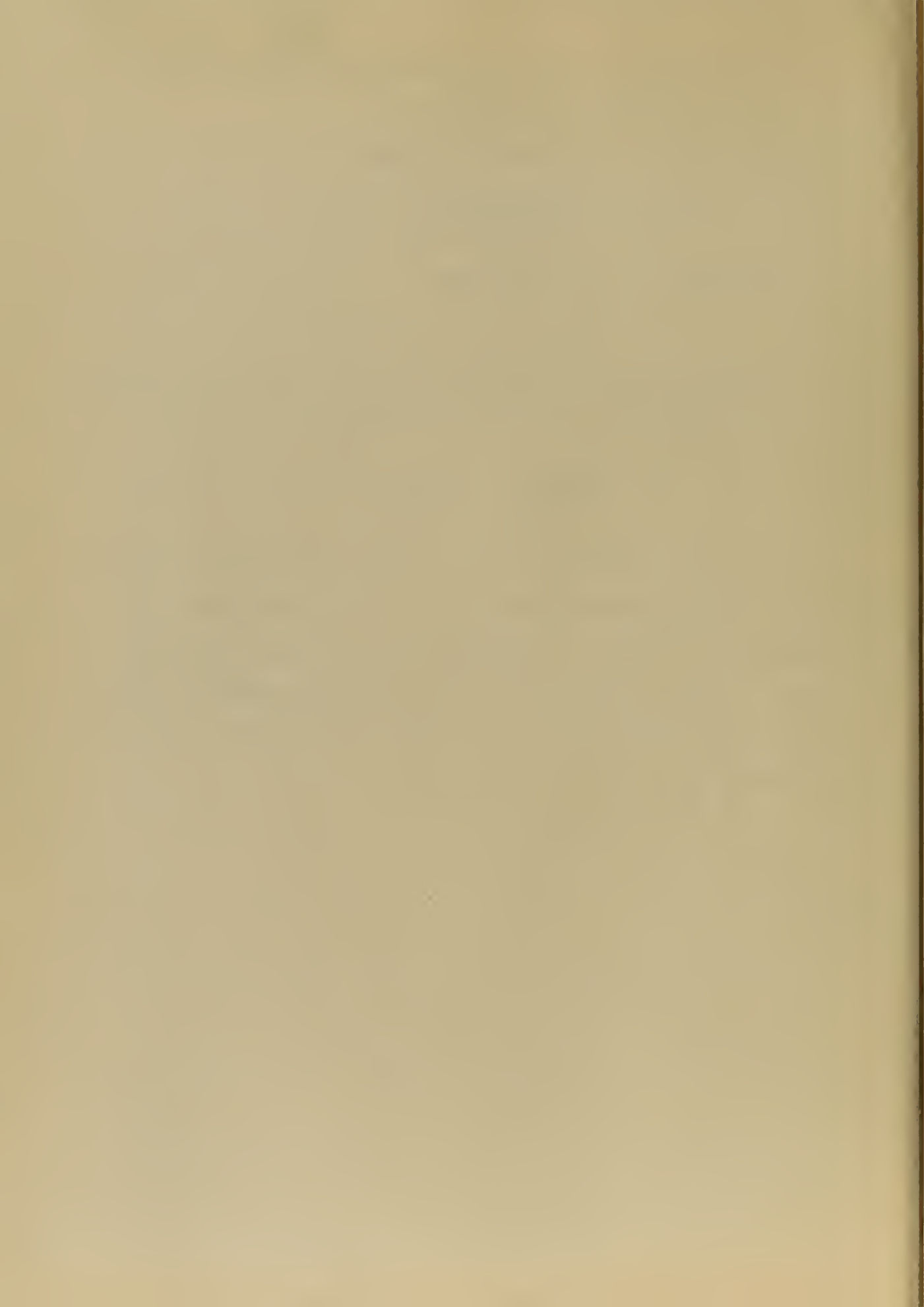
$$\ln [Z_3 / 54.7] = 3 \times 0.0906$$

Continue the routine until all the impedances have been determined.

The lengths of the sections are obtained from formula (3):

$$L = \frac{\lambda_1 \lambda_2}{2[\lambda_1 + \lambda_2]} = \frac{10 \times 5}{2[10 + 5]} = 1.67 \text{ cm.}$$

Reference to the characteristic impedance nomograph, Figure 8 will permit the determination of the width of the center conductor, commensurate with ground plane spacing and conductor thickness. Figure 22 shows the actual size of the series of transformers computed with a one inch ground plane spacing and 0.050 inch conductor thickness.



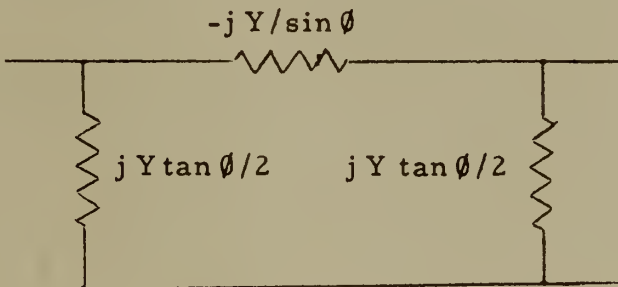
APPENDIX D

THE BEHAVIOR OF THE HYBRID JUNCTION OVER A WIDE FREQUENCY RANGE

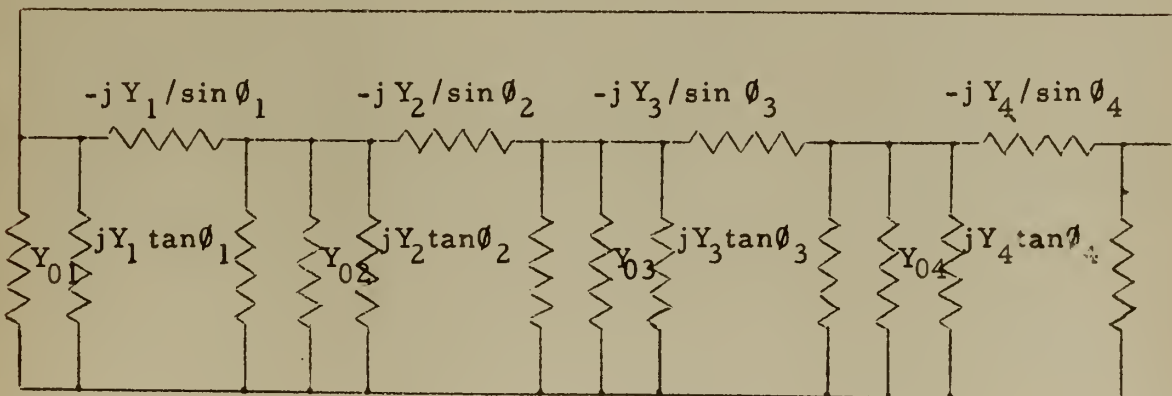
The hybrid junction may be employed over a wide frequency range if a slight deterioration in performance may be accepted. This appendix is a limited quantitative investigation into the effect of varying frequency on the characteristics of the shunt hybrid junction.

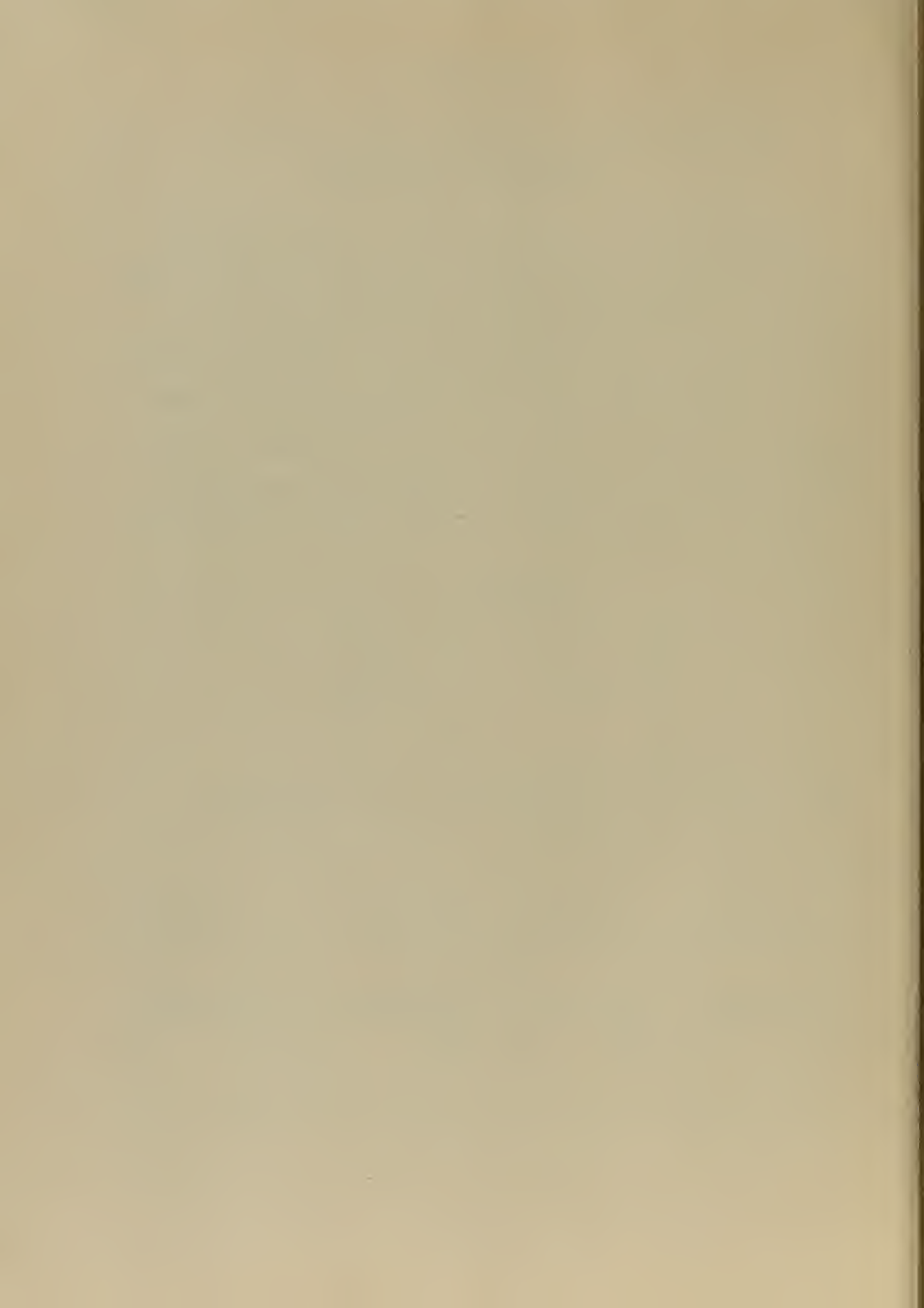
The analysis of this appendix is similar in procedure to the analyses of Chapter IV. Here a single general equivalent circuit will be drawn to cover all types of junctions at all frequencies.

The general pi equivalent circuit for a length of transmission line is:



This leads to the general hybrid junction equivalent circuit:





From the equivalent circuit the following determinant may be written:

$$\Delta = \begin{vmatrix} y_{11} & y_{12} & 0 & y_{14} \\ y_{21} & y_{22} & y_{23} & 0 \\ 0 & y_{32} & y_{33} & y_{34} \\ y_{41} & 0 & y_{43} & y_{44} \end{vmatrix}$$

where:

$$y_{11} = Y_{01} + j[Y_1(\tan \phi_1/2 - 1/\sin \phi_1) + Y_4(\tan \phi_4/2 - 1/\sin \phi_4)]$$

$$y_{22} = Y_{02} + j[Y_1(\tan \phi_1/2 - 1/\sin \phi_1) + Y_2(\tan \phi_2/2 - 1/\sin \phi_2)]$$

$$y_{33} = Y_{03} + j[Y_2(\tan \phi_2/2 - 1/\sin \phi_2) + Y_3(\tan \phi_3/2 - 1/\sin \phi_3)]$$

$$y_{44} = Y_{04} + j[Y_3(\tan \phi_3/2 - 1/\sin \phi_3) + Y_4(\tan \phi_4/2 - 1/\sin \phi_4)]$$

$$y_{12} = y_{21} = jY_1/\sin \phi_1$$

$$y_{23} = y_{32} = jY_2/\sin \phi_2$$

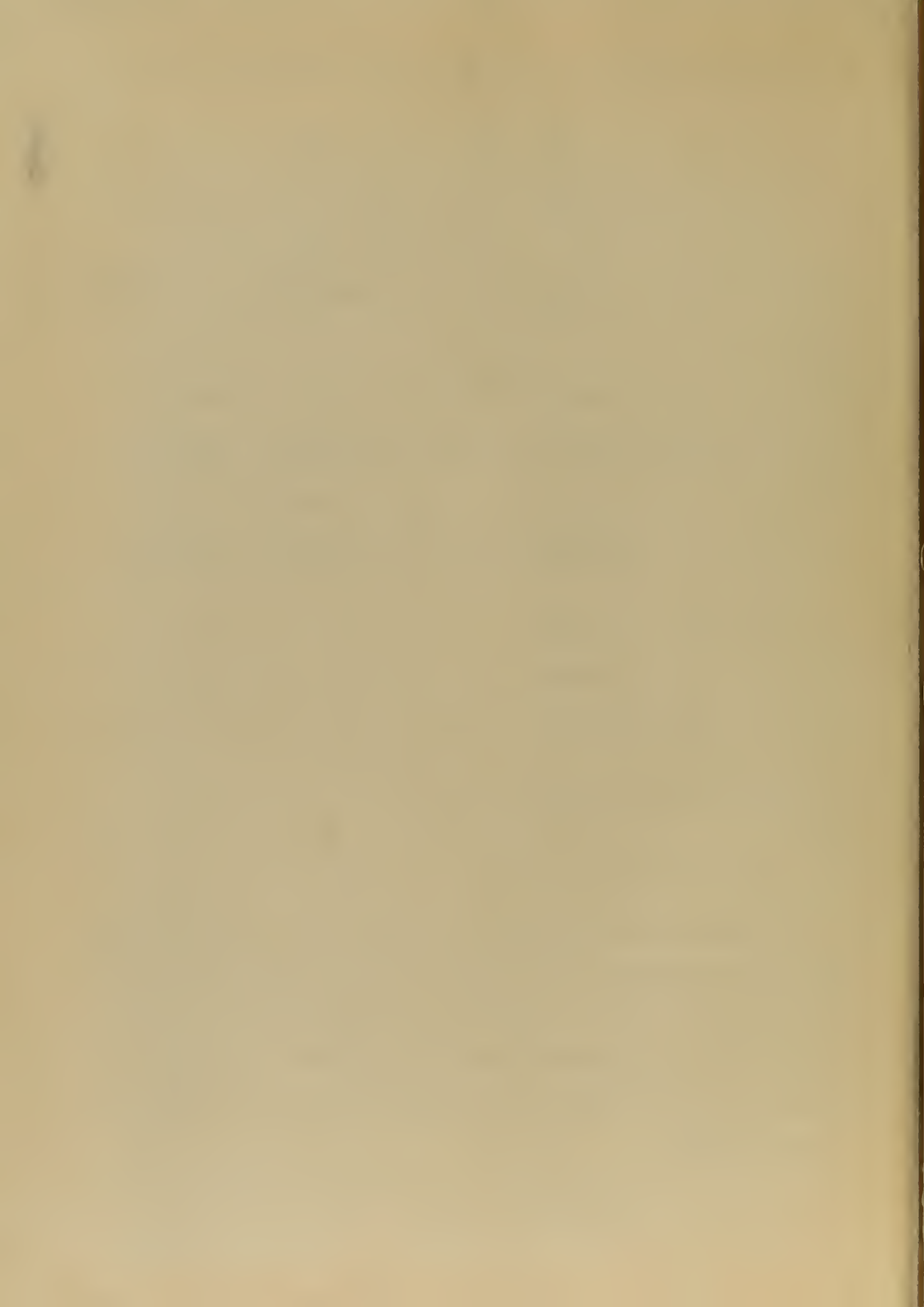
$$y_{34} = y_{43} = jY_3/\sin \phi_3$$

$$y_{14} = y_{41} = jY_4/\sin \phi_4$$

and

$$\phi_n = [2\pi f/c]L_n$$

The determinant may now be solved for specific values of Y_n , Y_{0n} , L_n , and f , to determine the characteristics of any shunt hybrid junction at any frequency. This calculation is quite tedious with a slide rule, but results of reasonable accuracy may be obtained. The author performed the calculations with a Computer Research Co., Model 102A Digital Computer.

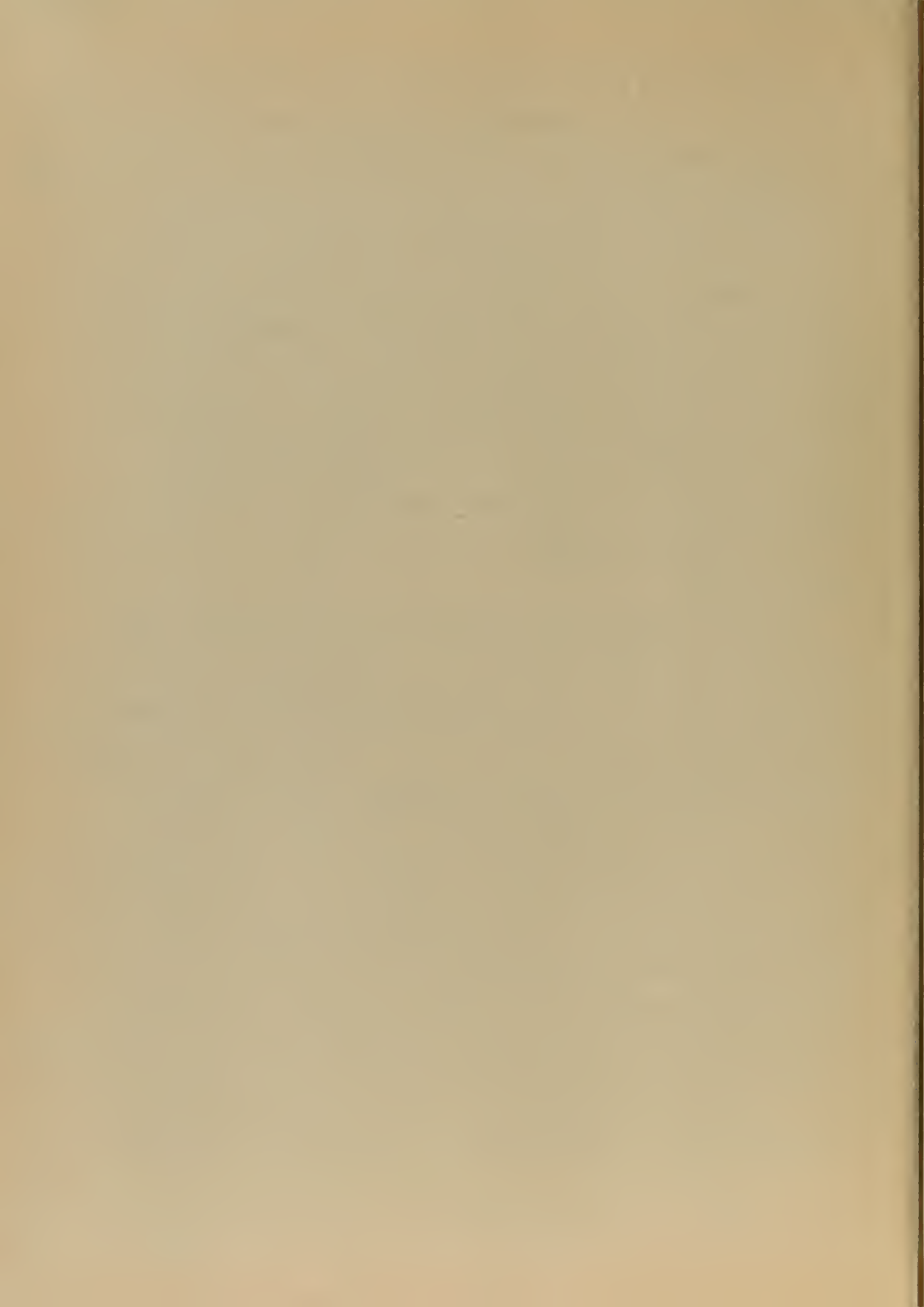


The results, as plotted by the computer, are shown in figures D-1 through D-7. The classification of the types of junctions is in accordance with the definitions in Chapter IV. The validity of the calculations is confirmed by the agreement of the measured and calculated data. The test arrangement for obtaining the measured data for figures D-1 and D-4 is shown in figure 55. The center frequency of the measured data for figure D-6 was shifted ten percent from the design center to correspond with the apparent actual operating center frequency. The design center frequency is located at 0.880 on the relative frequency scale. All measurements were performed at the Airborne Instruments Laboratory. The center frequency was in the C band.

CONCLUSIONS

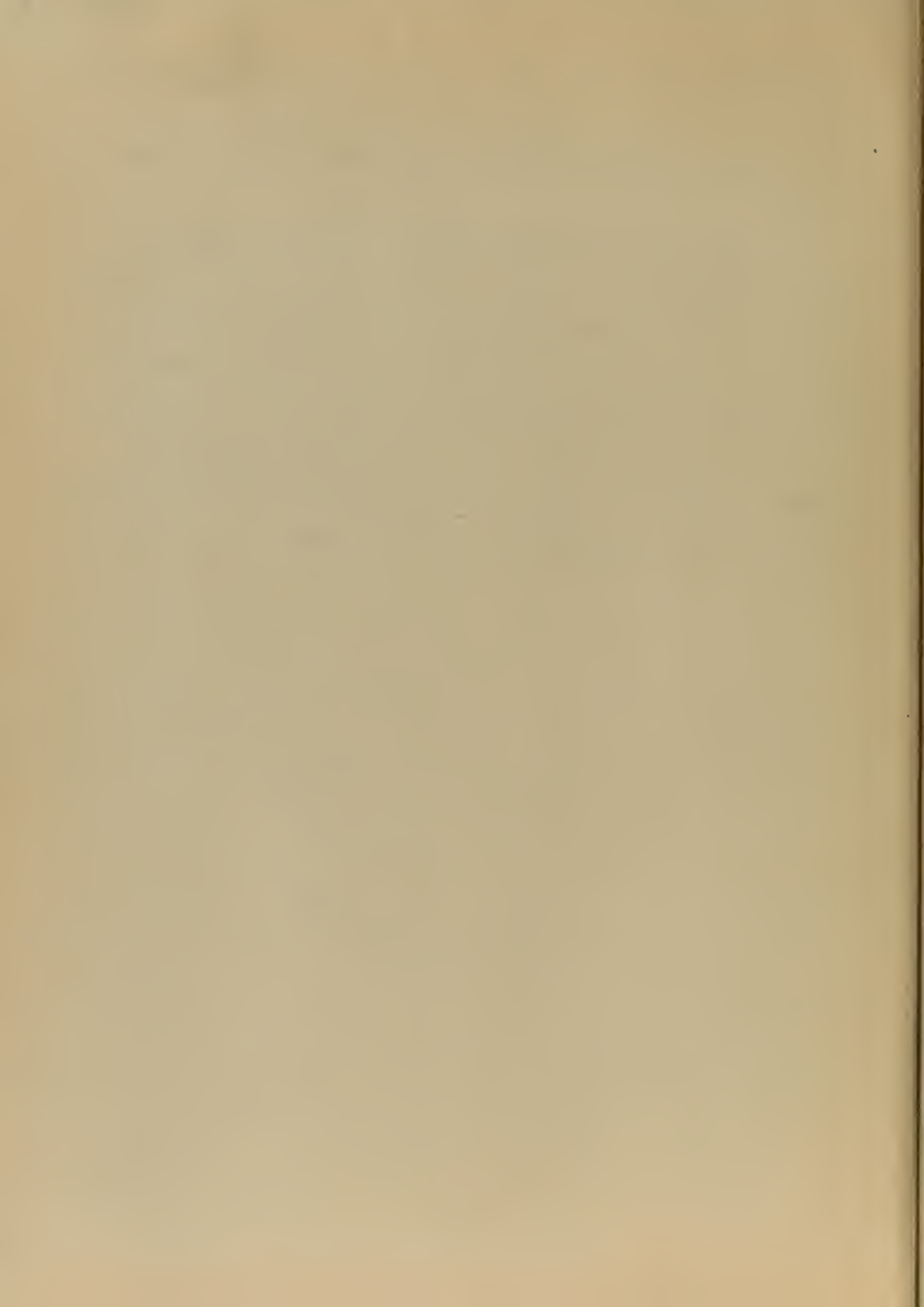
The hybrid junction may be utilized over a wide frequency range if the slight deterioration in performance, due to off center frequency operation, may be allowed consistant with other circuit considerations. Quantitatively the Case I or $1/4, 1/4, 1/4, 3/4$ wave junction maintains the balance of the magnitude difference between arms two and four within one DB over a thirty percent band width (fifteen percent on either side of the center frequency), while the phase difference varies linearly from 190° to 170° . The isolation between arms one and three is greater than 20 DB within the band width. It is interesting to note that the 48 DB isolation measured with the stripline hybrid junction is identical with that measured with a waveguide hybrid junction [9].

The Case II or $1/4, 1/4, 1/4, 1/4$ wave junction has essentially the same magnitude balance as Case I. Less than one DB difference



within a thirty percent band width. The phase difference of arms two and three remained within the range of 275° to 265° throughout the band. The isolation of arms one and four was greater than 36 DB within the band.

The author regrets that this appendix could not be presented in a more complete manner. The extreme length of time required to develop the program due to initial unfamiliarity with digital computation techniques and repeated computer and plotter failures while attempting to make the final calculations exhausted the time available for this phase of the work. The completed program and associated punched cards are on file with the Chairman of the Engineering Electronics Department awaiting the continuation of this work at a later date.



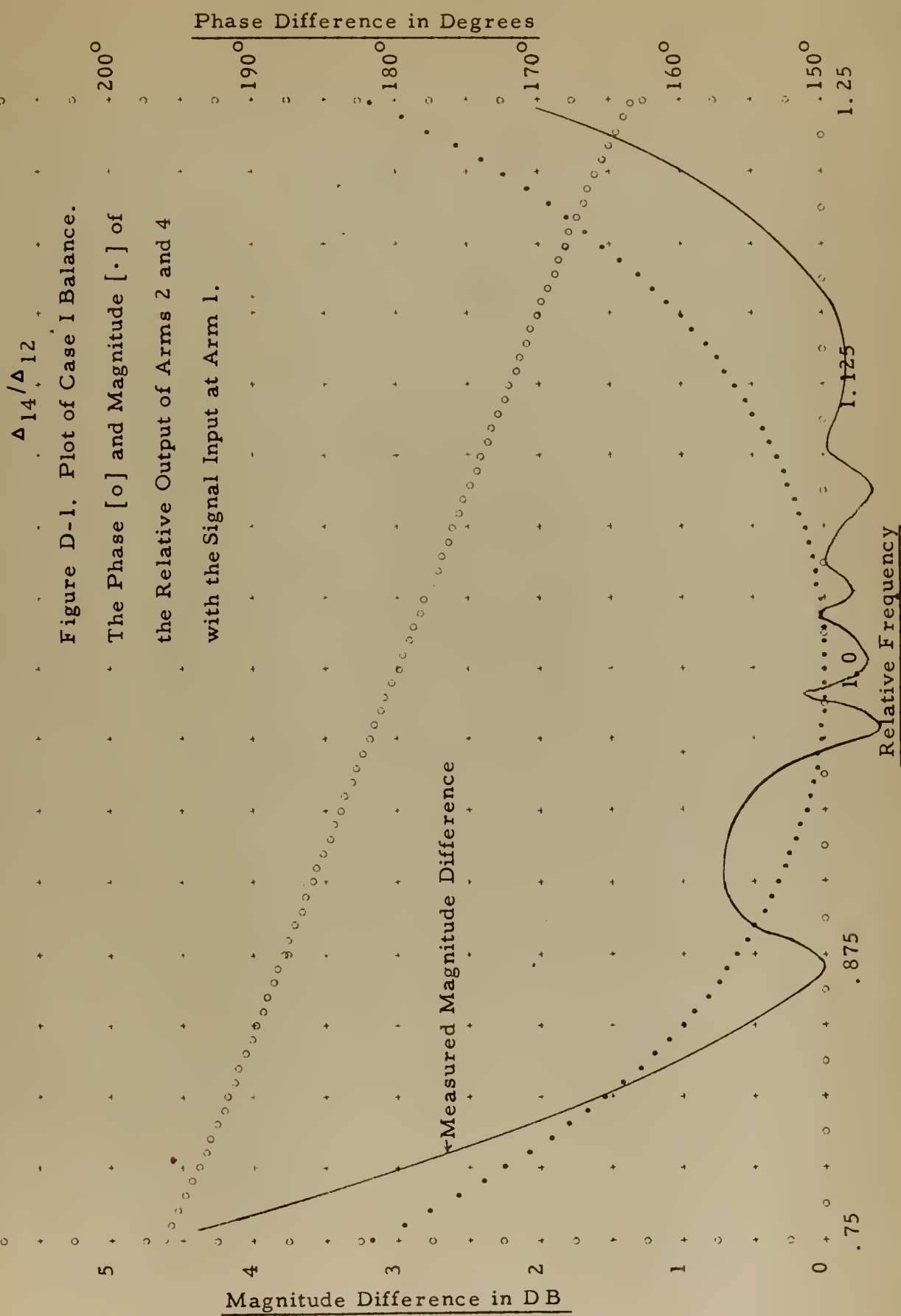
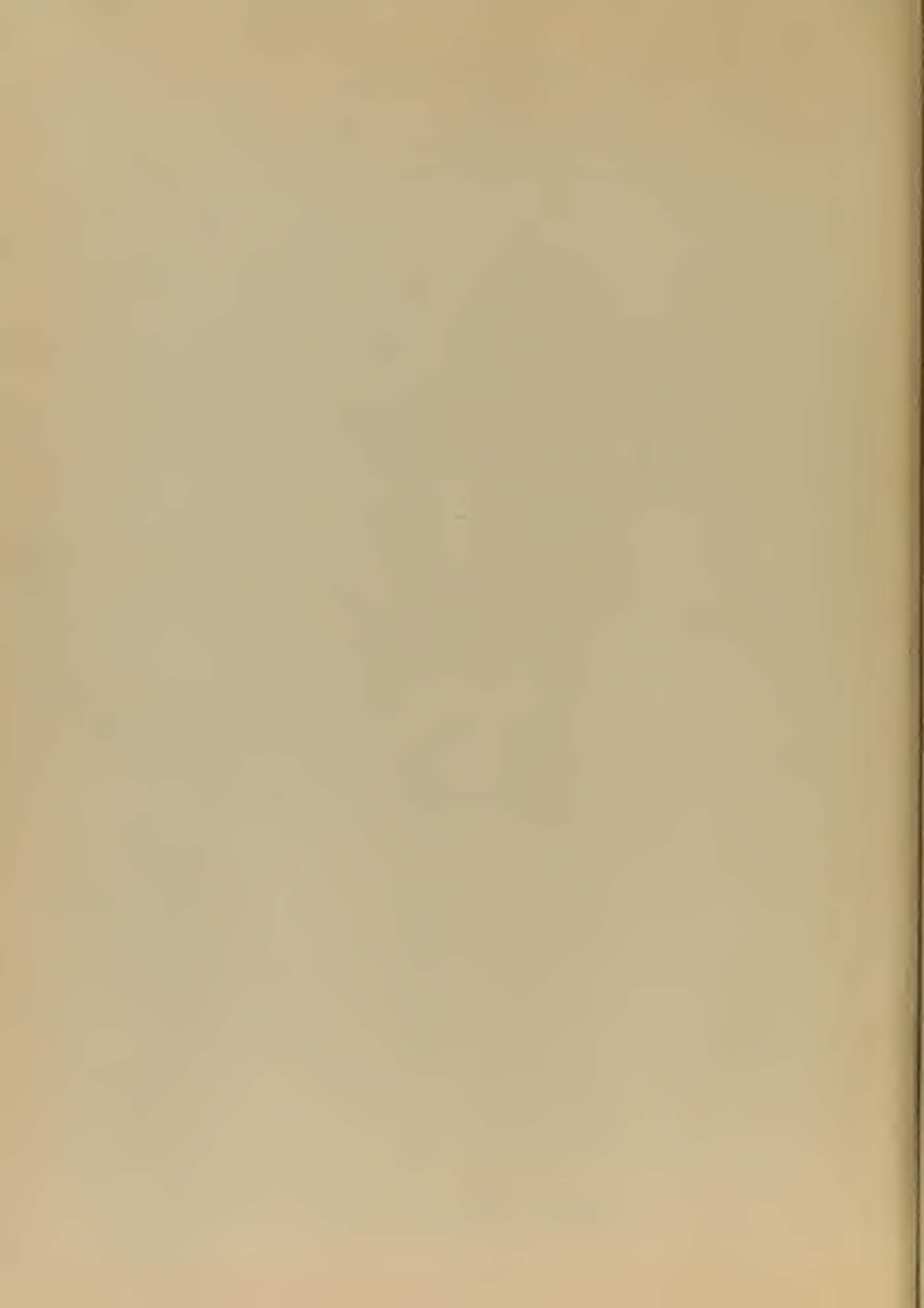
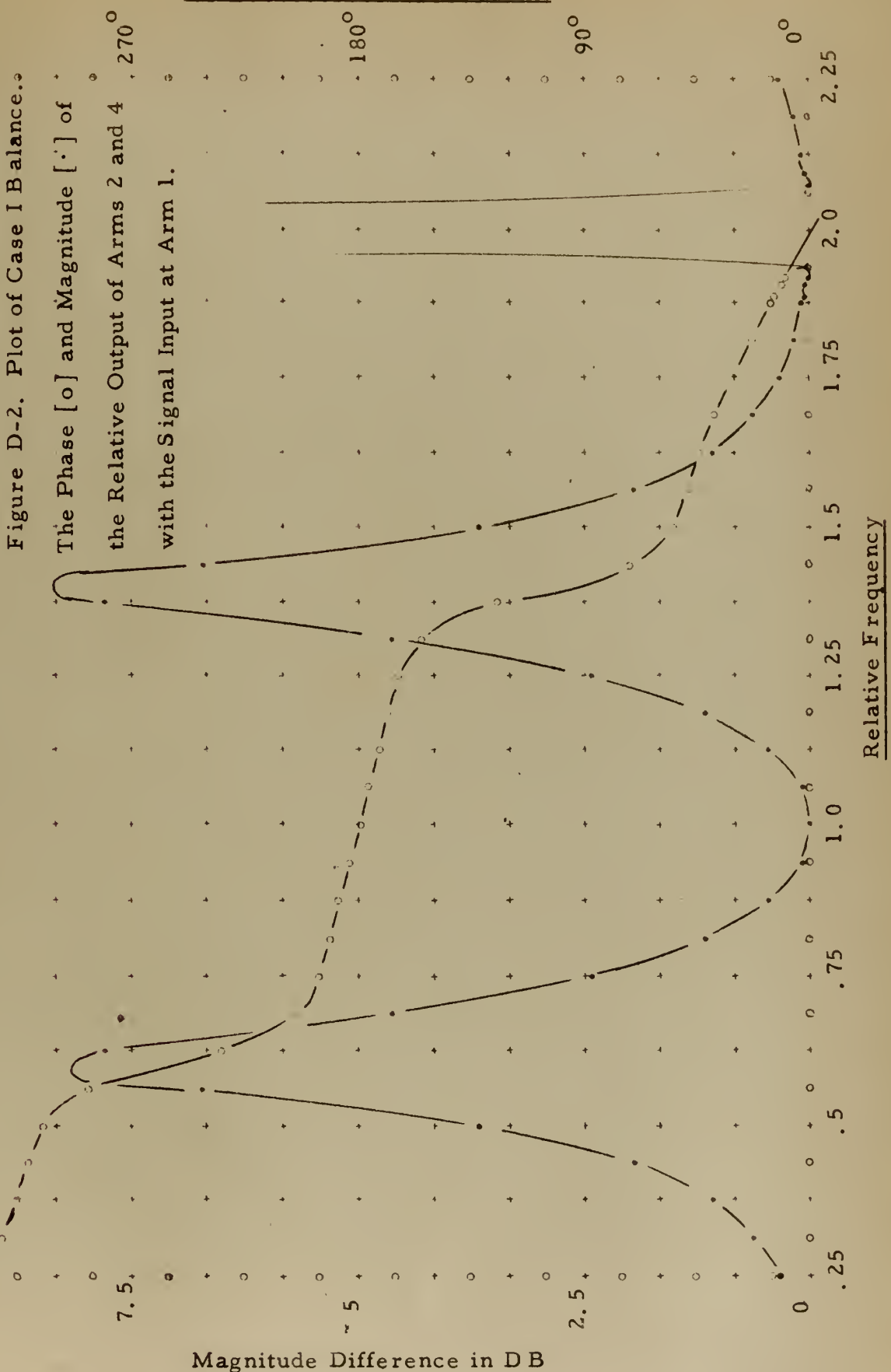


Figure D-1. Plot of Case I Balance.

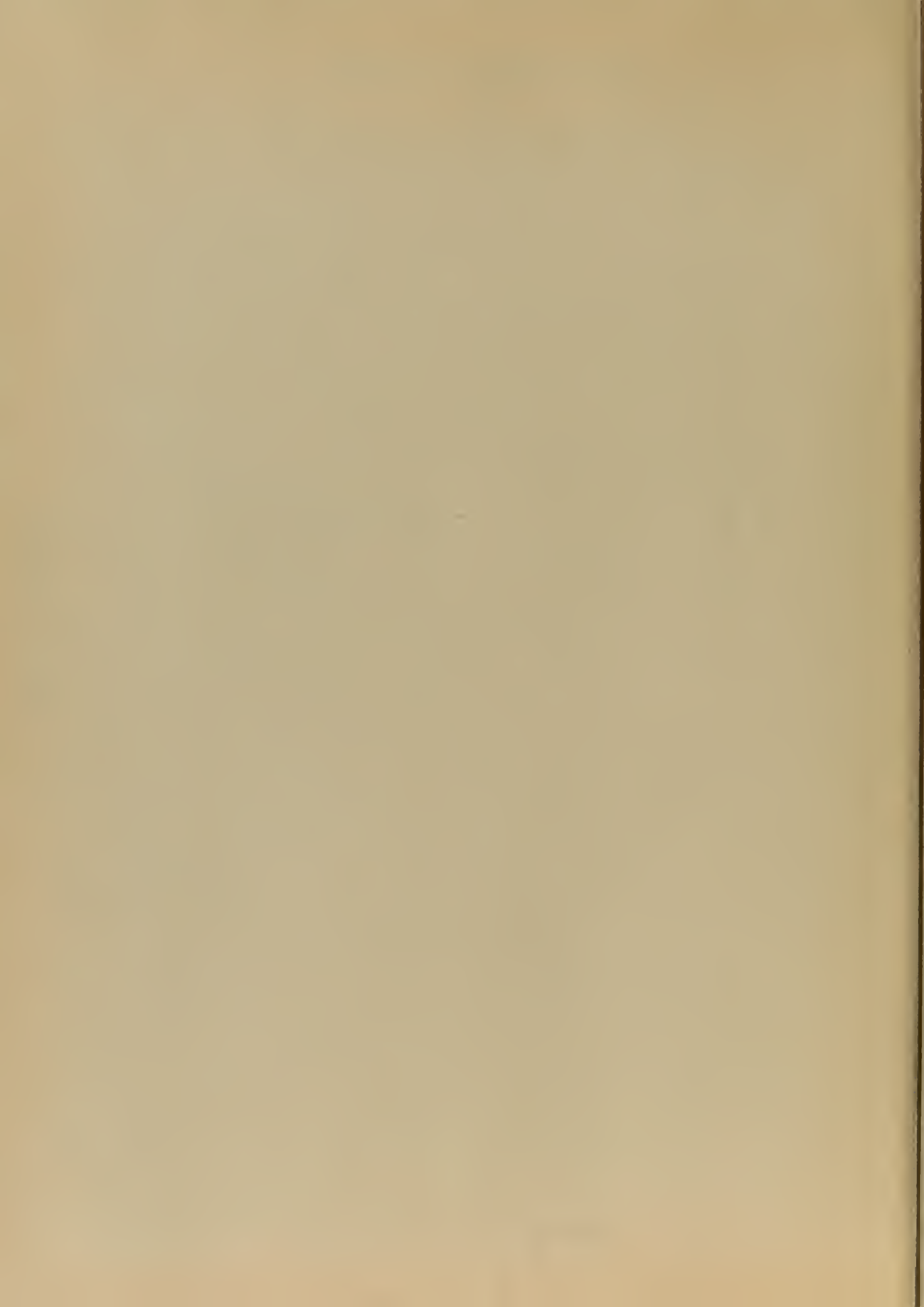
The Phase [o] and Magnitude [•] of the Relative Output of Arms 2 and 4 with the Signal Input at Arm 1.



Phase Difference in Degrees



Magnitude Difference in DB



Phase Difference in Degrees

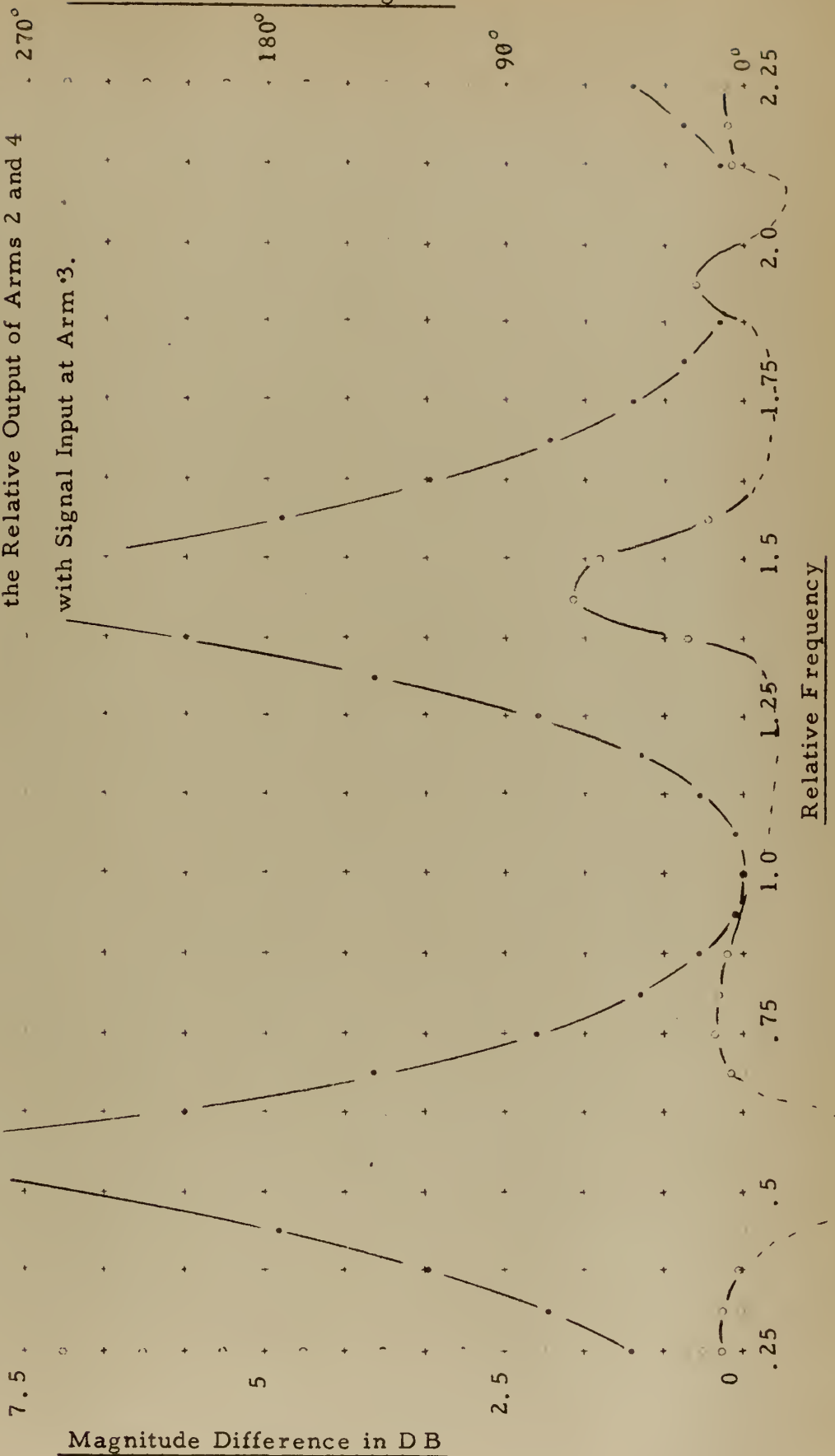


Figure D-3. Plot of Case I Balance.
The Phase [o] and Magnitude [·] of
the Relative Output of Arms 2 and 4
with Signal Input at Arm 3.

Phase Difference in Degrees

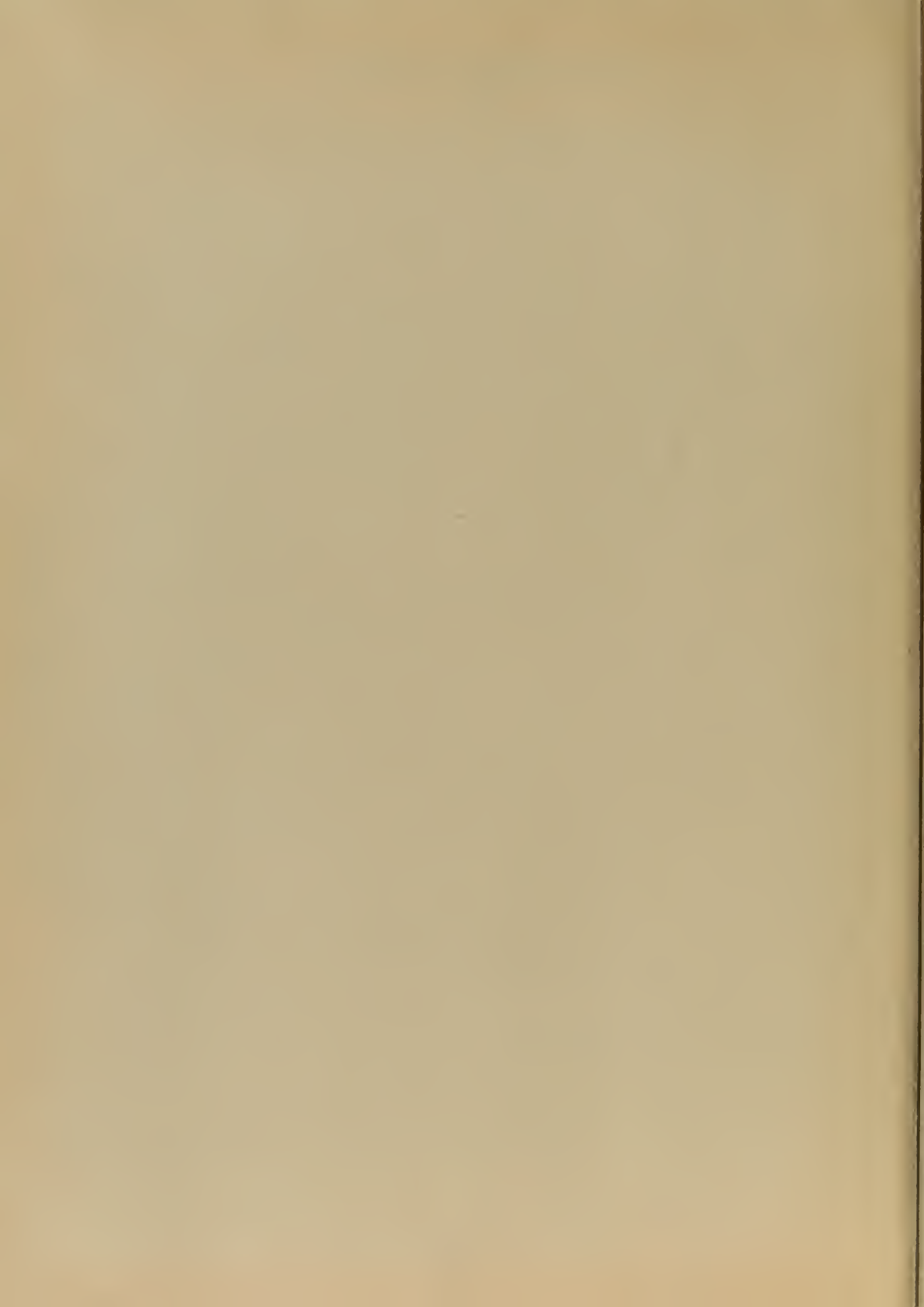
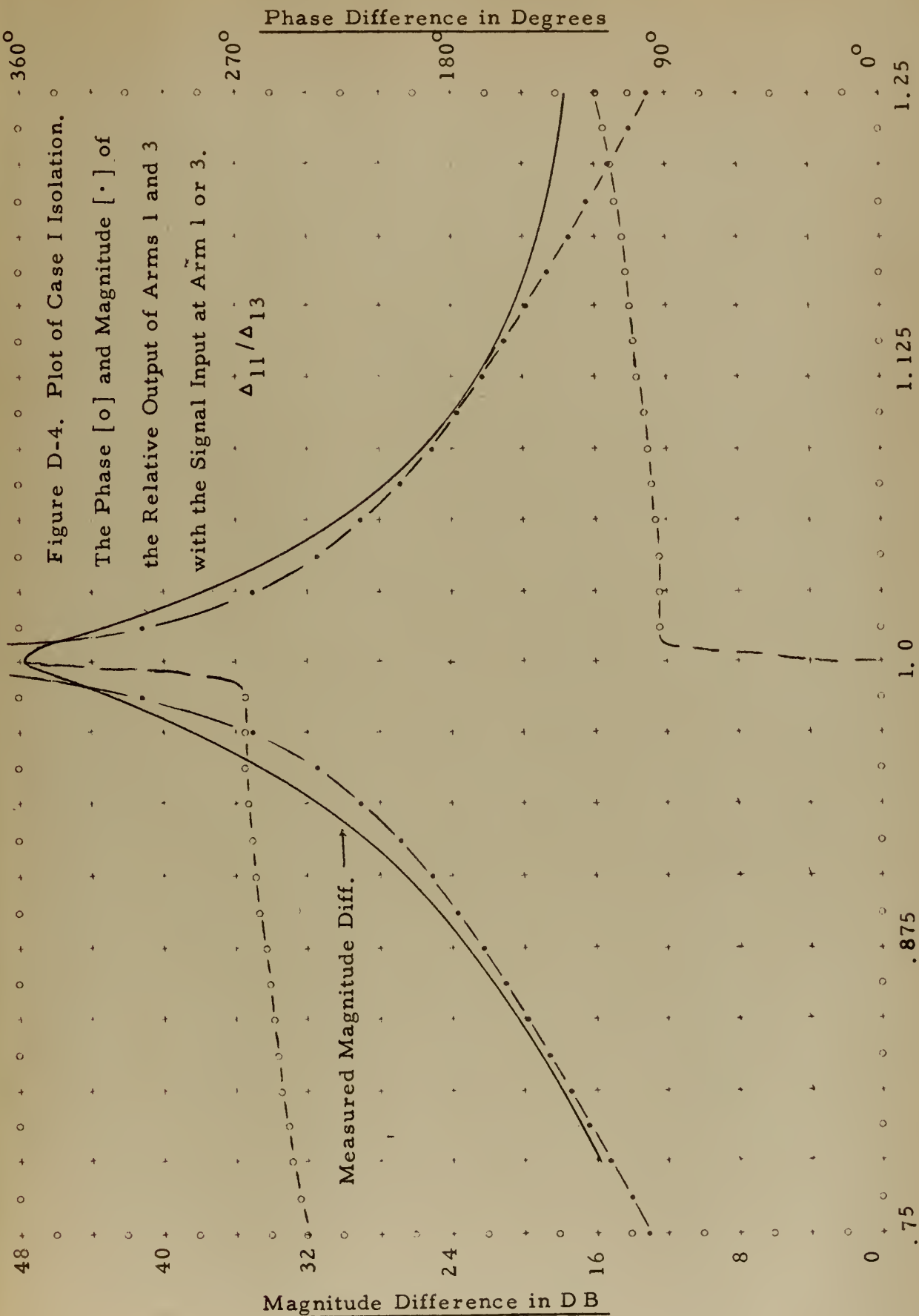
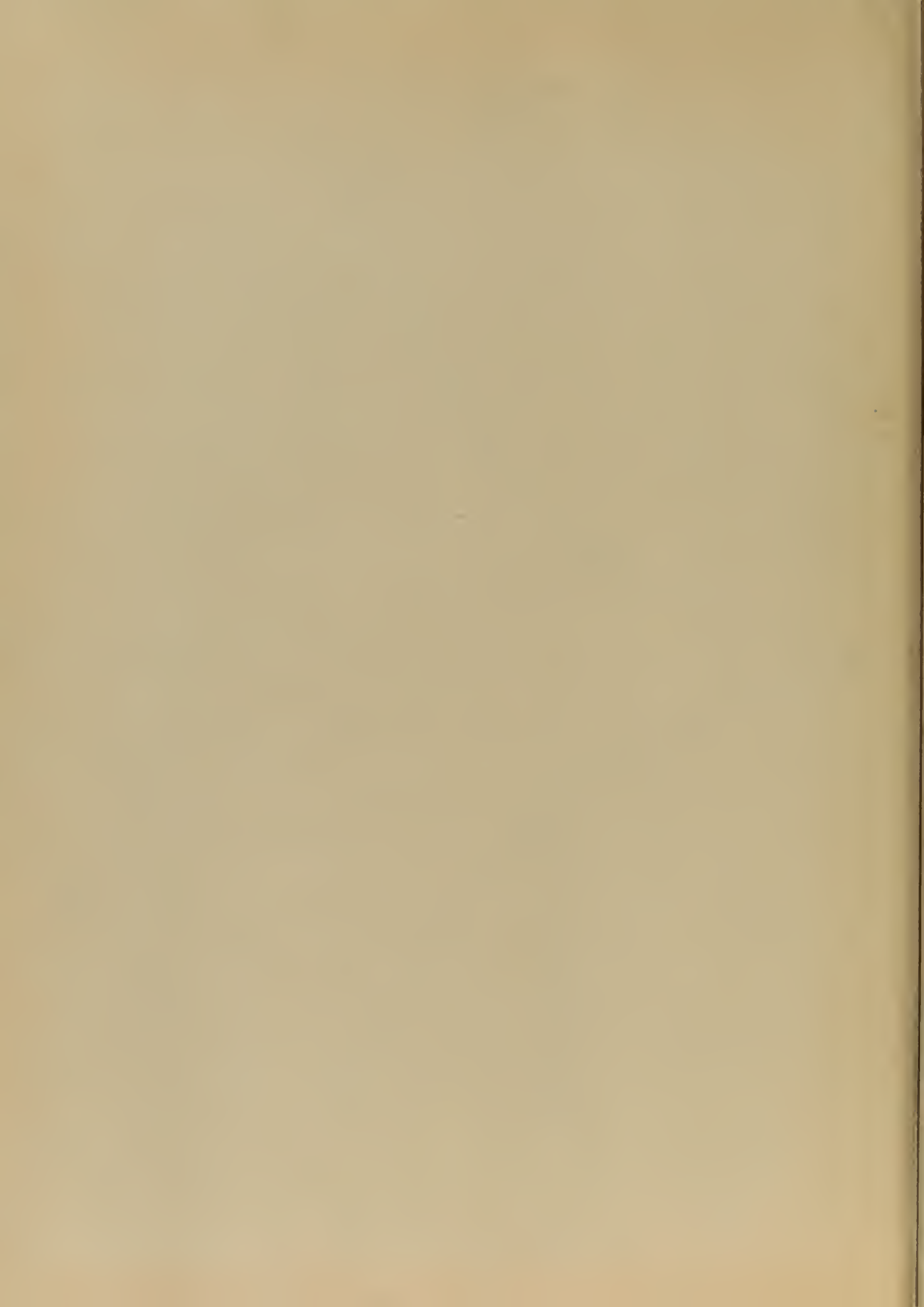
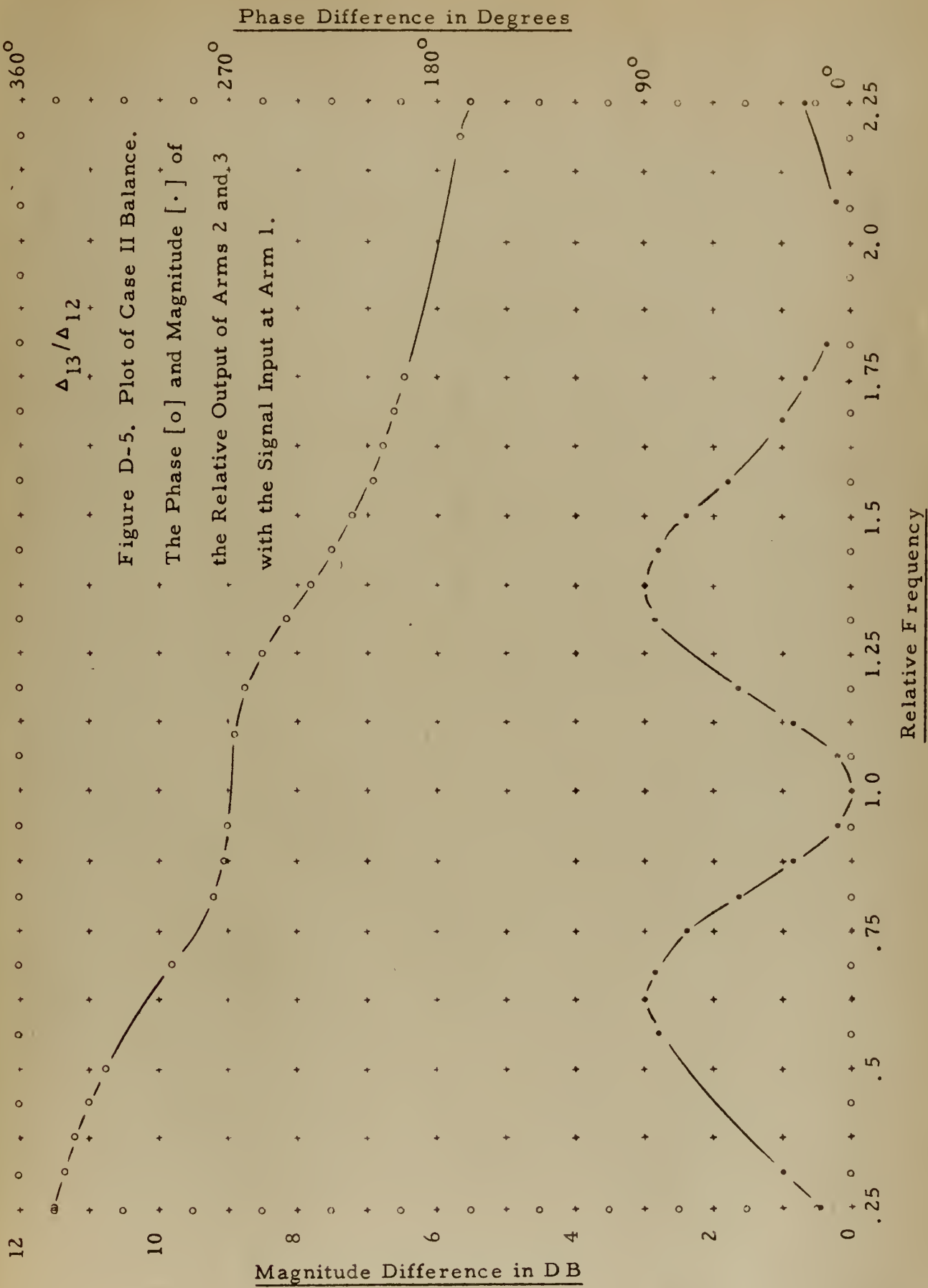


Figure D-4. Plot of Case I Isolation.

The Phase [o] and Magnitude [•] of the Relative Output of Arms 1 and 3 with the Signal Input at Arm 1 or 3.







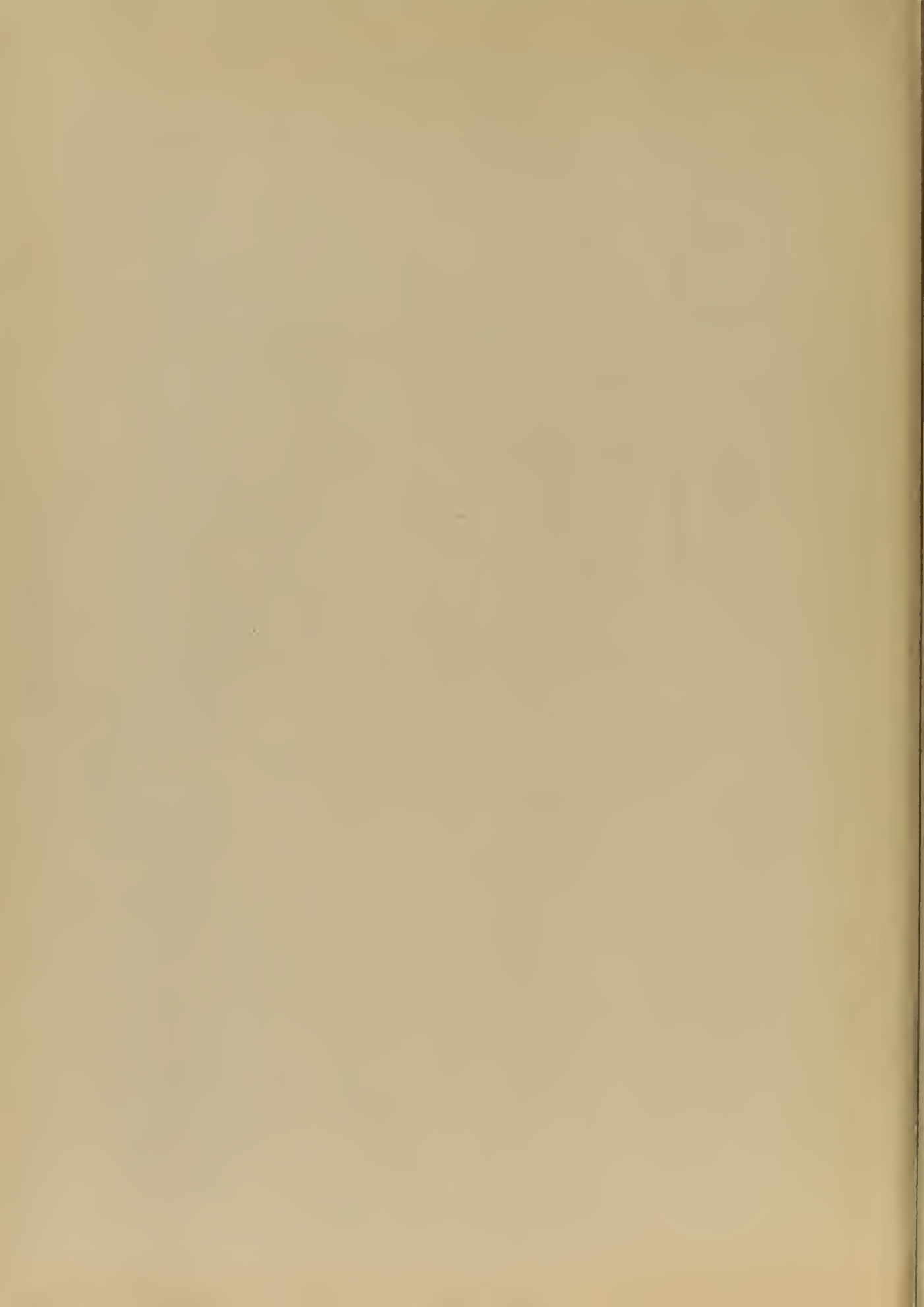
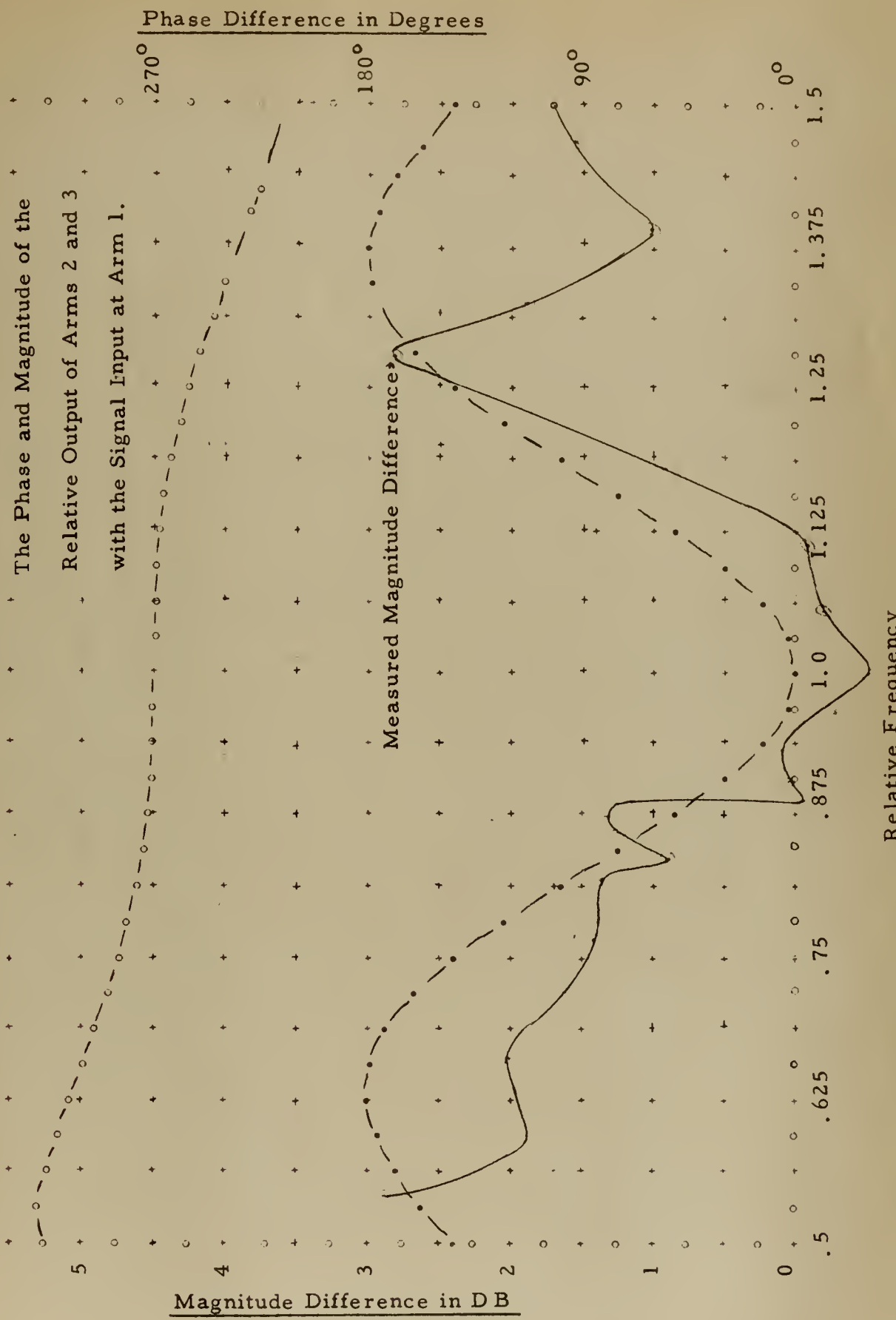
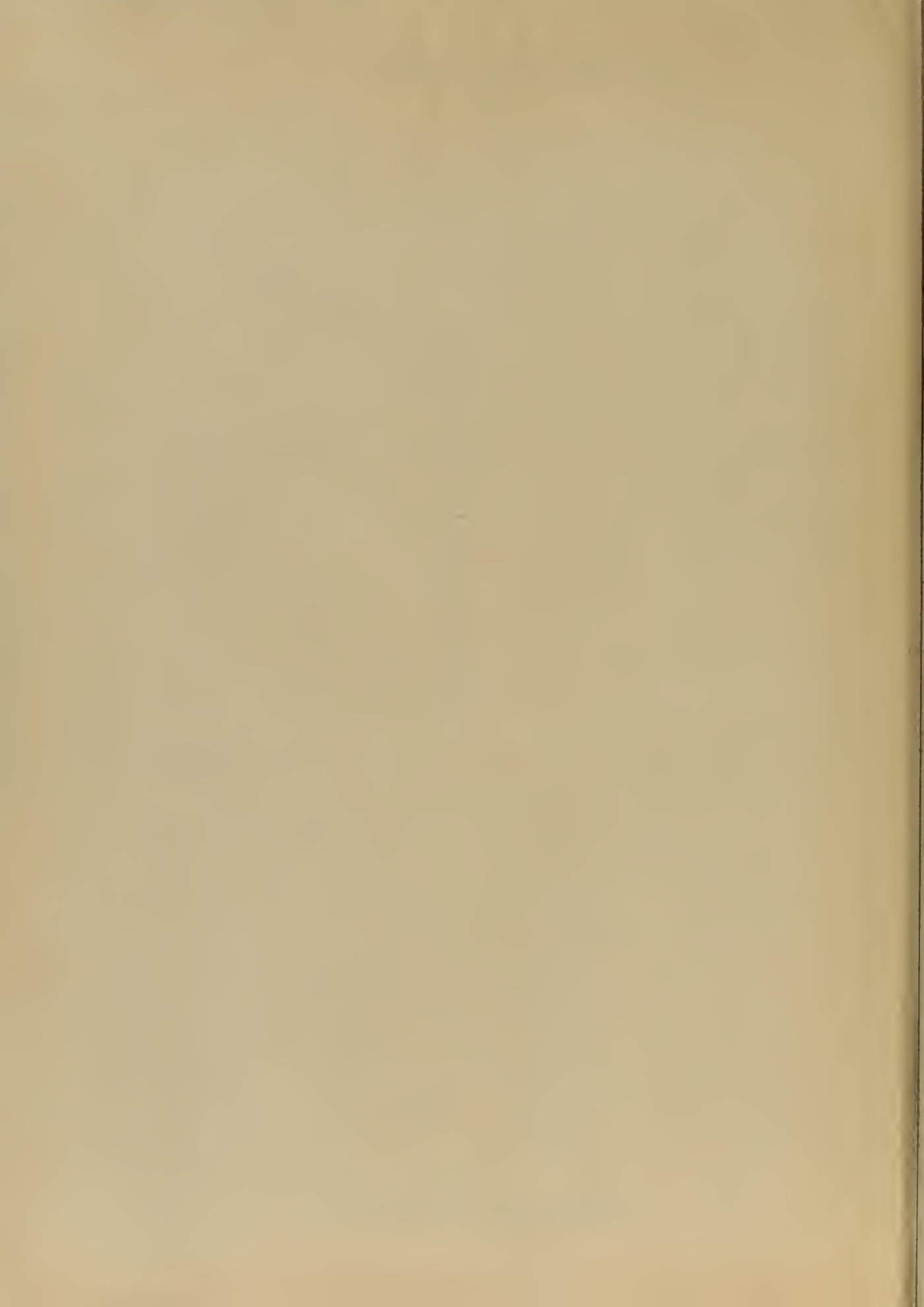


Figure D-6. Plot of Case II Balance.





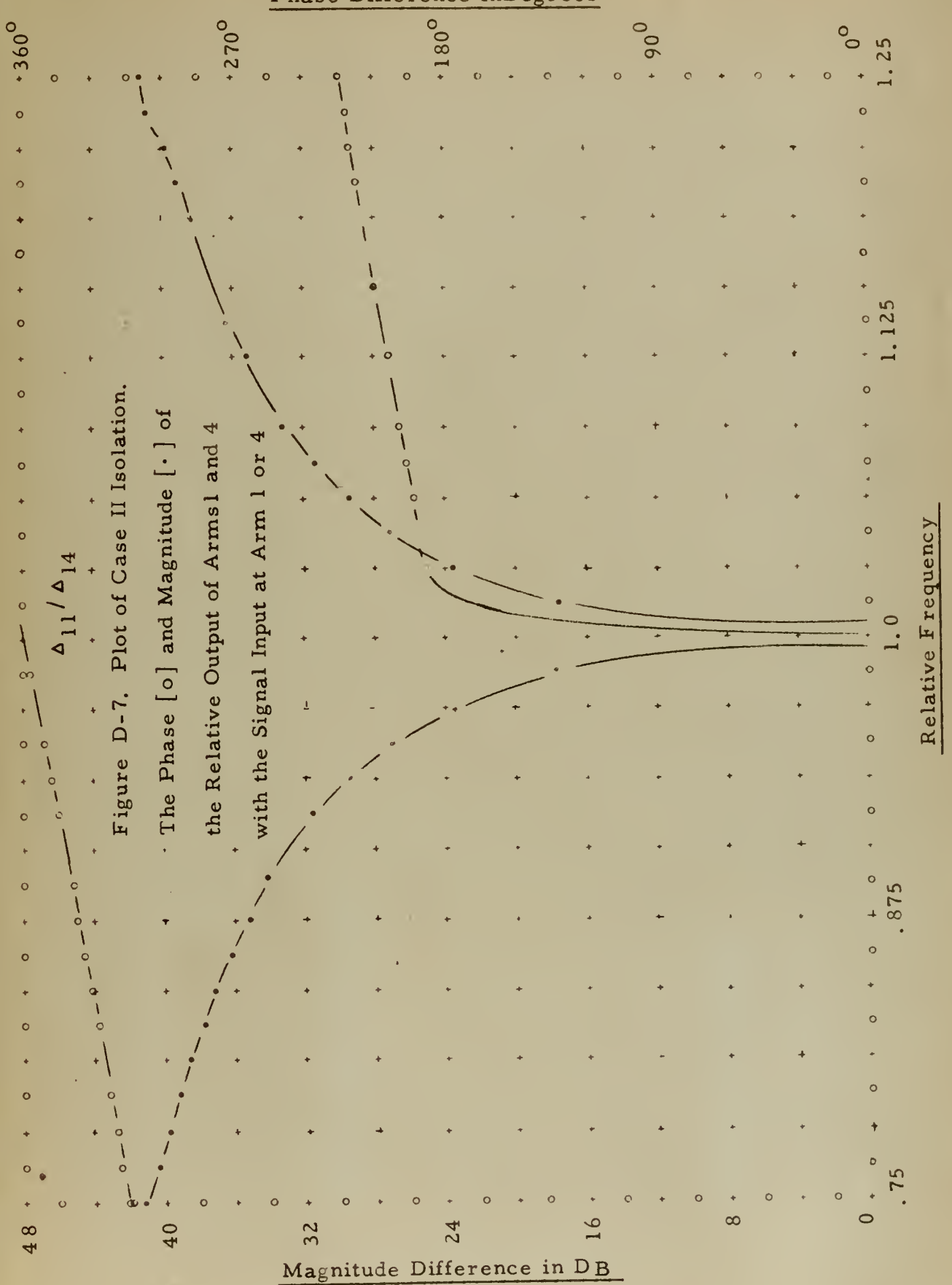


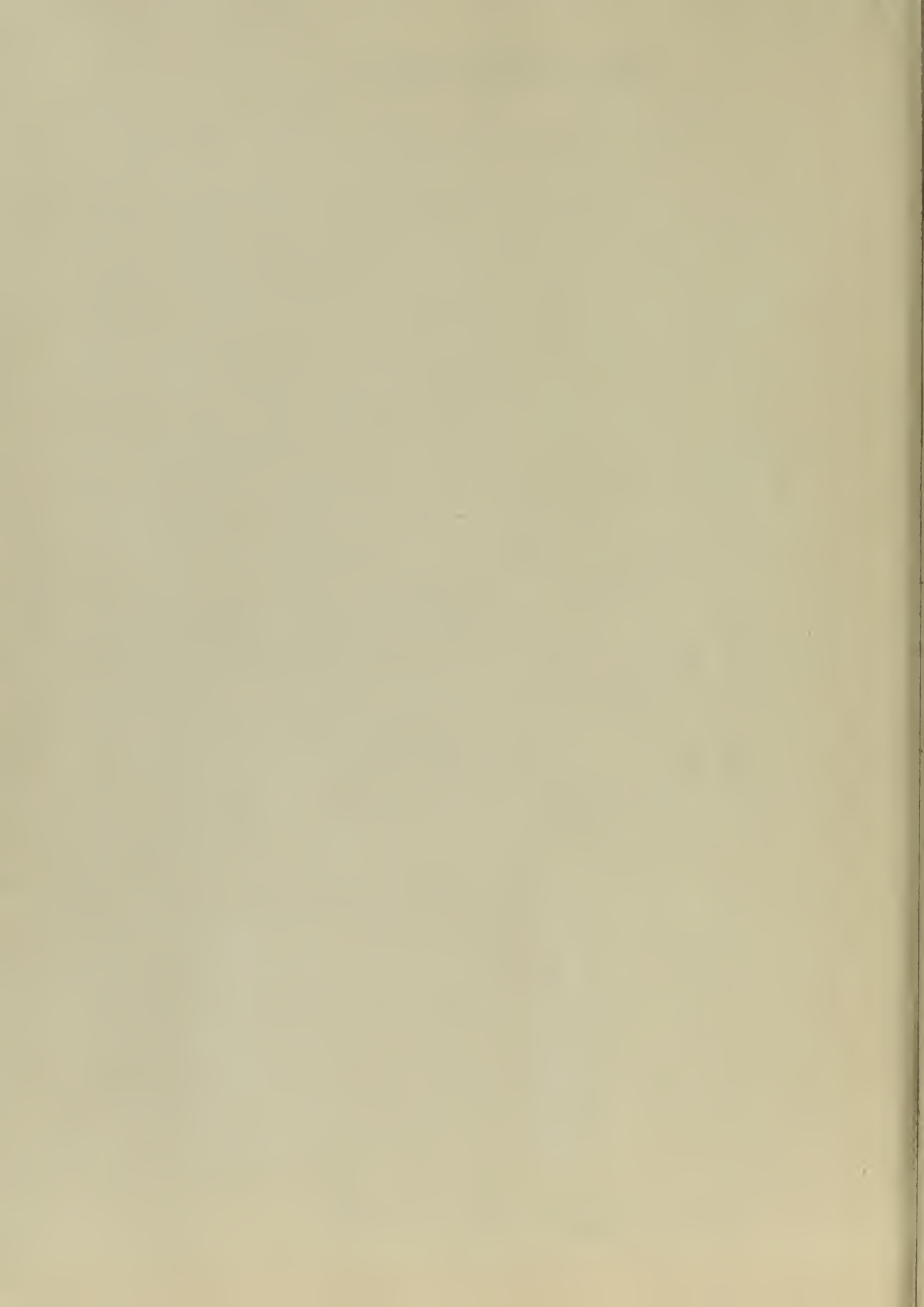
Figure D-7. Plot of Case II Isolation.

$\Delta_{11} / \Delta_{14}$

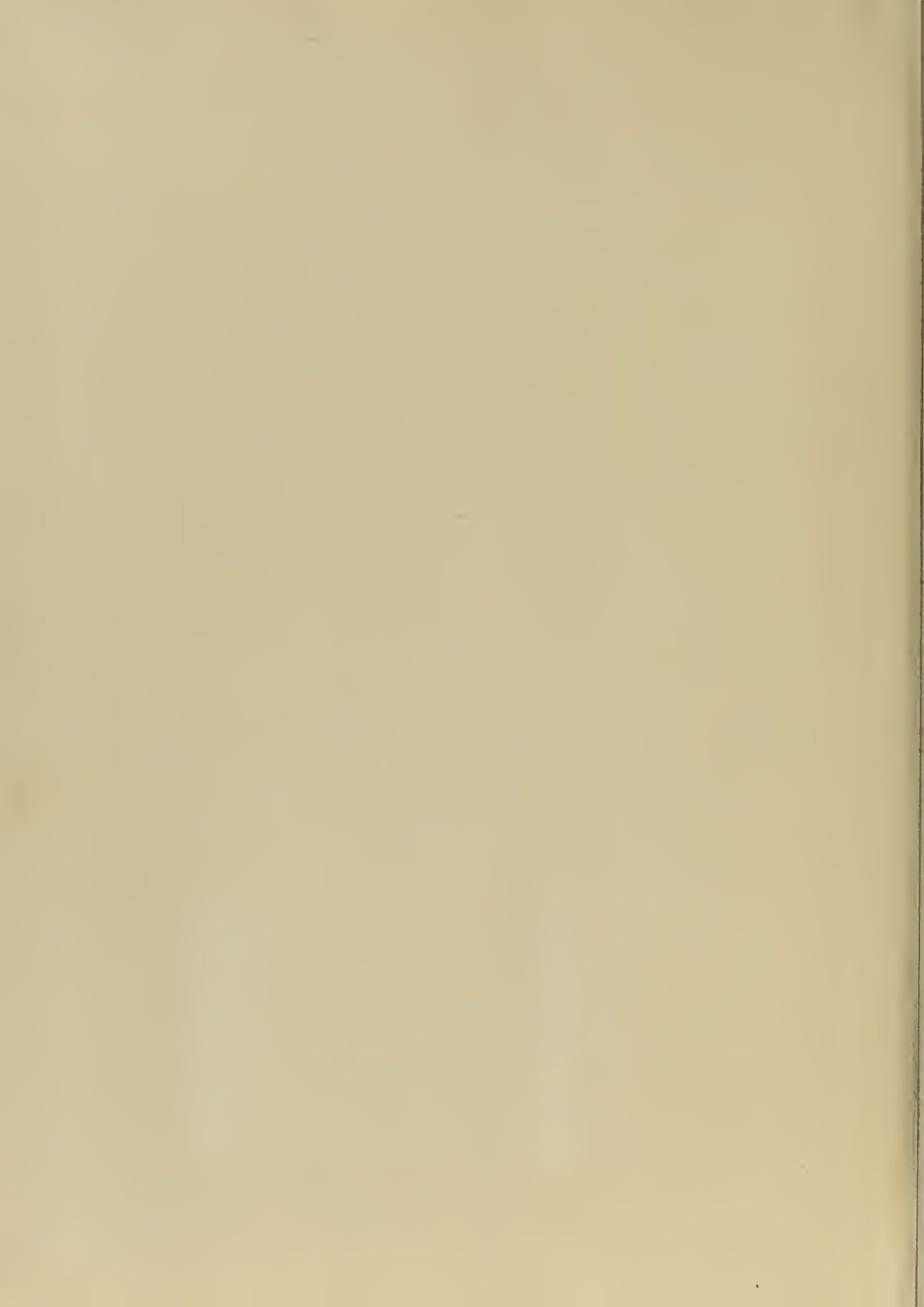
48
40
32
24
16
8
0

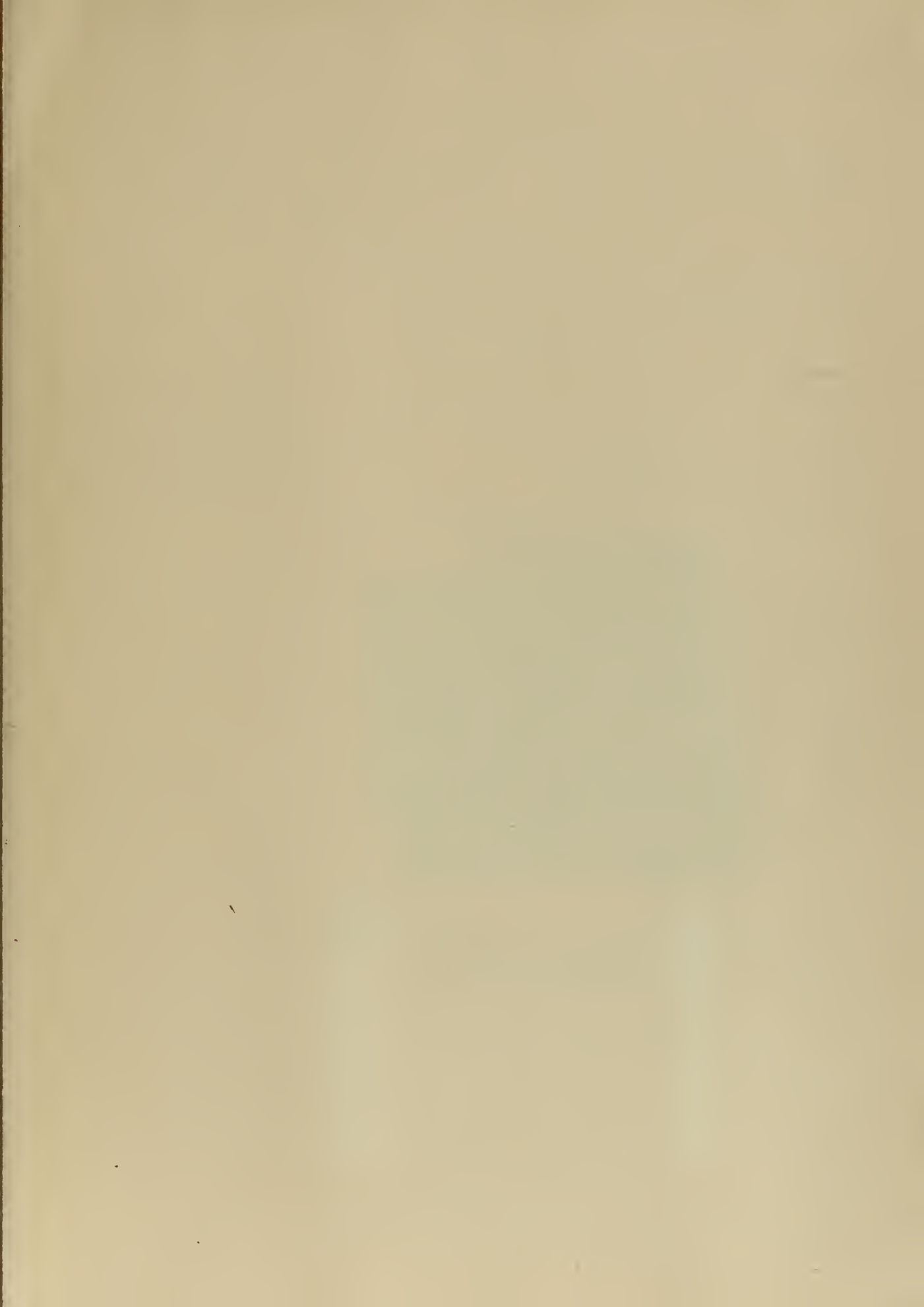
The Phase [o] and Magnitude [•] of the Relative Output of Arms I and II with the Signal Input at Arm 1 or 4

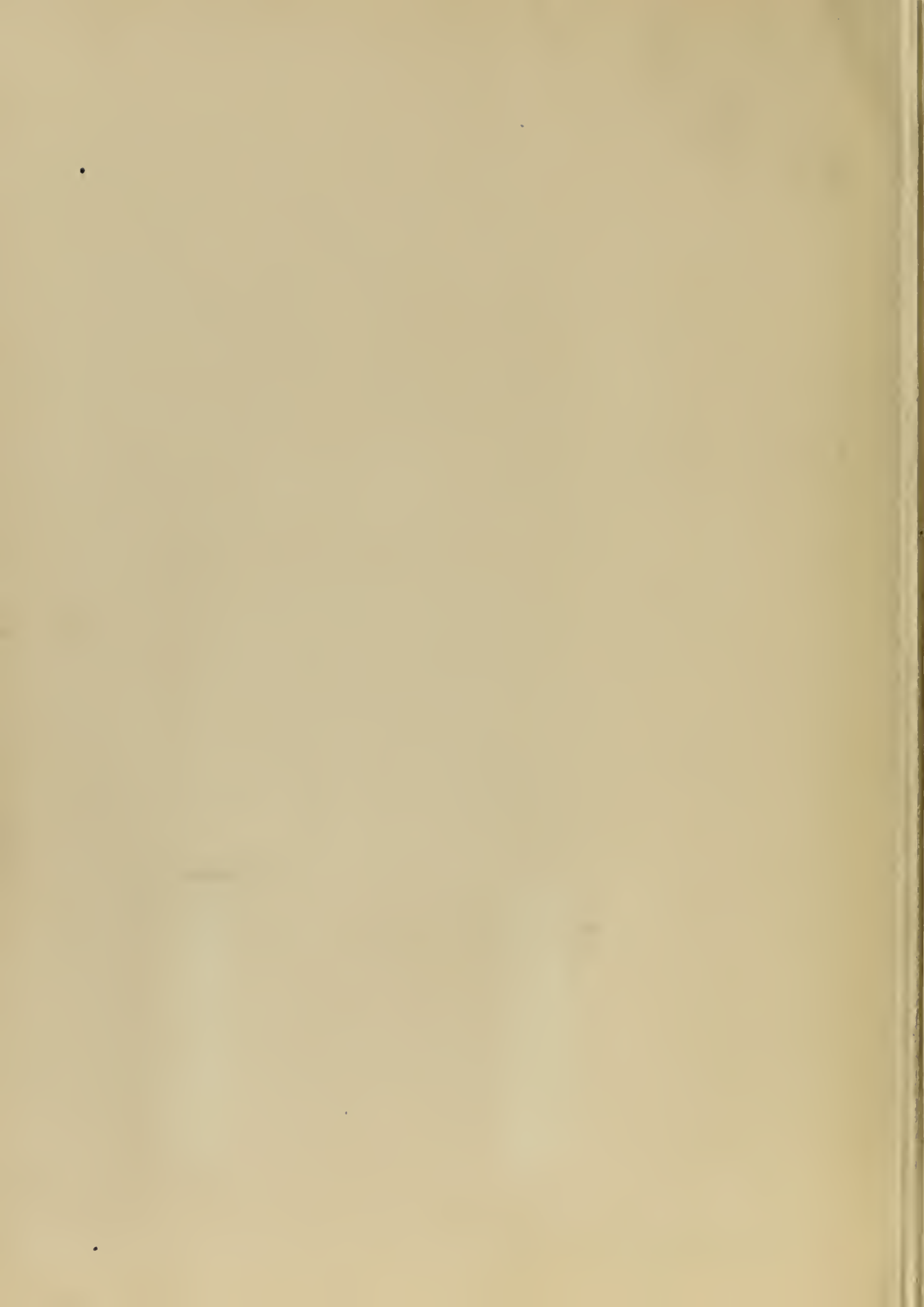
360°
270°
180°
90°
0°











Loan Requirement: (Action taken by Naval Postgraduate School)

No restriction is placed on loans of this thesis. However, all loans to non-Defense Department organizations are to be reported to

DR. E. G. Fubini, Director
R + E Division

Airborne Instruments Laboratory
160 Old Country Road
Mineola, N.Y.

The above note
no longer in effect.
R. Lyle Nov. 1962

DEC 21 1962

INTERLIB
Otis Elevator Co.
Brooklyn, N.Y.

17 Mar '64 INTERLIBRARY LOAN
(Goddard, Maryland)

1 Oct '65 28482

Thesis
B946 Butler
Design of strip transmission line systems and antennas.

DEC 21 1962

INTERLIB
Otis Elevator Co.
Brooklyn, N.Y.

17 Mar '64 INTERLIBRARY LOAN
(Goddard, Maryland)

1 Oct '65 [AVCO Corp - RAD Div.
Wilmington, Mass]

28482

B946 Thesis
Butler
Design of strip transmission line systems and antennas.

thesB946
Design of strip transmission line system



3 2768 002 08849 4
DUDLEY KNOX LIBRARY